VOLUME 41 SECOND SERIES NUMBER 2

Copy 2

JUL 25 1932

THE PHYSICAL REVIEW

A JOURNAL OF EXPERIMENTAL AND THEORETICAL PHYSICS

CONDUCTED BY

THE

AMERICAN PHYSICAL SOCIETY

BOARD OF EDITORS

Managing Editor, JOHN T. TATE, University of Minnesota, Minneapolis

Assistant Editor, J. W. BUCHTA, University of Minnesota, Minneapolis

K. F. HERZFELD, A. W. HULL, F. W. LOOMIS, A. J. DEMPSTER, DAVID M. DENNISON, J. C. SLATER, R. C. GIBBS, E. O. LAWRENCE, J. H. VAN VLECK

JULY 15, 1932

Diurnal Variation of Cosmic Rays - R. D. BENNETT, J. C. STEARNS, AND A. H. COMPTON 119

Diffuse Scattering of X-Rays from Sodium Fluoride - G. E. M. JAUNCEY AND P. S. WILLIAMS 127

Very Soft X-Ray Spectra of Heavy Elements - - - - - - - - C. DEL ROSARIO 136

On the Relative Abundances of the Nitrogen and Oxygen Isotopes - - - - - - - - - - - - - - - GEORGE M. MURPHY AND HAROLD C. UREY 142

Mass-Spectrograph Study of the Ionization and Dissociation by Electron Impact of Benzene and Carbon Bisulfide - - - - - - - - - - - ERNEST G. LINDER 149

Elastic Electron Scattering in Helium - A. L. HUGHES, J. H. McMILLEN AND G. M. WEBB 154

Infrared Dispersion of Carbon Dioxide - - - - - - HUGH M. SMALLWOOD 164

Band Spectrum of Sulphur Monoxide - - - - - - - EMMETT V. MARTIN 167

Influence of Crystalline Fields on the Susceptibilities of Salts of Paramagnetic Ions. I. The Rare Earths, especially Pr and Nd - - - WILLIAM G. PENNEY AND ROBERT SCHLAPP [illegible]

Theory of the Variations in Paramagnetic Anisotropy Among Different Salts of the Iron Group - - - - - - - - - - - - - - J. H. VAN VLECK [illegible]

Investigations in the Field of the Ultra-short Electromagnetic Waves. IV. On the Dependence of the Ultra-short Electromagnetic Waves upon the [illegible] Current and upon the Amplitude of the Oscillations - - - - - - - - - - G. POTAPENKO [illegible]

Hall Effect with Audiofrequency Currents - - - - - - LAWRENCE A. WOOD 231

Some Thermo- and Galvanomagnetic Properties of a Bismuth Crystal - - H. E. BANTA [illegible]

Does Nickel Show a Positive Elongation in the Joule Magnetostrictive Effect? - S. R. WILLIAMS 251

Letters to the Editor - - - - - - - - - - - - - - - - - [illegible]

Electronic Structure of the a-X Band System of N_2 - - - - - - E. T. S. APPLEYARD [illegible]

Deposition of Chromium on Glass - - - - - - - - - - ROBLEY C. WILLIAMS [illegible]

Note on Molecular Structure - - - - - - - - - - - JOHN C. SLATER [illegible]

Book Reviews - - - - - - - - - - - - - - - - - - - [illegible]

Proceedings of the American Physical Society: - - - - - - - - - - [illegible]

PULLMAN MEETING, June 17-18, 1932; Minutes and Abstracts 1-15, Author Index

Current Literature of Physics

PUBLISHED BY THE AMERICAN PHYSICAL SOCIETY

[illegible]

THE AMERICAN PHYSICAL SOCIETY

OFFICERS OF THE SOCIETY

President:	W. F. G. Swann	Bartol Research Foundation, Philadelphia, Pa.
Vice-President:	Paul D. Foote	The Gulf Companies, Pittsburgh, Pa.
Secretary:	W. L. Severinghaus	Columbia University, New York City
Treasurer:	G. B. Pegram	Columbia University, New York City
Editor:	John T. Tate	University of Minnesota, Minneapolis, Minn.
Local Secretary for the Pacific Coast:	L. B. Loeb	University of California, Berkeley, Calif.

THE PHYSICAL REVIEW

Published by the American Physical Society. Editor's office: University of Minnesota, Minneapolis, Minn. Four volumes annually, six issues per volume.

First series. From July 1, 1893, to January 1, 1913, the Review was conducted by Edward L. Nichols, Ernest Merritt and Frederick Bedell, with the financial support of Cornell University. The first four volumes were issued annually; subsequent volumes, semi-annually; thirty-five volumes in all.

Second series. On January 1, 1913, the Review was transferred to the American Physical Society as announced on the first page of the new series which was then begun. Since then it has been conducted by a Board of Editors elected by the Society. Volumes 1-38 are semi-annual, beginning in January and July of each year from 1913 to 1931. Volumes 1-33 contain six issues each. Volumes 34-38 twelve issues. Beginning with Volume 39 there will be four volumes per year of six issues each.

Contributors are referred to page 2 of the advertisements for further information.

Annual subscription, throughout the Postal Union, $12.00 in advance.

General index, 1893-1920, $4.00 in advance.

Back Volumes. Volumes 1-38, $9.00 per volume; Volume 39, $4.50; Back Numbers, $1.50 per copy for issues prior to July 1, 1929 (Vols. 1-33), $.75 per copy for issues subsequent thereto. Postage is free if remittance accompanies order; otherwise postage is extra. No bound volumes can be supplied. The Review offers to purchase a limited number of First Series, Vol. 1, No. 1 (at $2.00 each); Second Series, Vol. 7, No. 1, January 1916; Vol. 7, No. 2, February 1916; Vol. 7, No. 4, April 1916; and Vol. 7, No. 5, May 1916 (at $2.00 each).

Advertisements. Rates will be supplied by the Editor on request. Copy for each number must be received at Minneapolis two weeks prior to the dates of issue; old copy is used until new copy is received. Send electrotypes direct to printers, George Banta Publishing Co., Menasha, Wis.

Discount of ten percent is allowed to members of the American Physical Society on purchase of back numbers.

Changes of Address and Complaints of failure to receive the Review, in the case of members of the Physical Society, should be addressed to the Treasurer; in the case of other subscribers, to the Editorial Secretary. New copies can be sent free in response to complaints of non-delivery only if notice of non-delivery is received within three months of date of issue.

Manuscripts for publication should be submitted to the Editor, Physical Review, University of Minnesota, Minneapolis, Minn.

Proof and all correspondence concerning papers in process of publication should be addressed to the Editorial Secretary, American Institute of Physics, 11 East 38th Street, New York, New York.

Subscriptions, renewals, and orders for back numbers should be addressed to the Editorial Secretary, American Institute of Physics, 11 East 38th Street, New York, New York.

Entered at the post office at Menasha, Wis., as second class matter.
Acceptance for mailing at special rate of postage provided for in section 1103, Act of October 3, 1917, authorized September 6, 1924.

Second Series *July 15, 1932* *Vol. 41, No. 2*

THE

PHYSICAL REVIEW

Diurnal Variation of Cosmic Rays

By R. D. BENNETT, J. C. STEARNS AND A. H. COMPTON

Massachusetts Institute of Technology, University of Denver and University of Chicago

(Received April 9, 1932)

The intensity of cosmic rays at an altitude of 3900 meters was measured hourly over a consecutive period of 240 hours. The procedure eliminated the effects due to the variations of the temperature and possible variations of pressure of the gas in the chamber. The ionization was about 1.5 ± 0.25 percent more between 8 A.M. and 4 P.M. than between 8 P.M. and 4 A.M. If the variation is due to the soft component of the cosmic rays, these results are in satisfactory agreement with the results of other observers. Analysis of the data suggests that the portion of the space in the neighborhood of the sun may emit cosmic rays more copiously than the remote regions. This makes doubtful the inference that the energy in the universe in the form of cosmic rays is comparable with that in the form of light.

SOME of the earlier investigators of cosmic rays reported considerable variations in the intensity of these rays as measured at different times of day. More extensive observations have indicated that these variations were probably statistical fluctuations which did not indicate any significant changes in the intensity of the cosmic rays. There have, however, recently been found very small but consistent differences between day and night.[1] In previous papers[2] we have reported the discovery that the ionization in a pressure ionization chamber increases with increasing temperature. A review of the recent experiments showed that although in some of them the temperature of the apparatus was held constant, in others diurnal temperature changes might have affected the observed ionizations. We have therefore carried through a new series of measurements of cosmic rays over a period of 240 consecutive hours, in such a way that changes of ionization with temperature cannot influence our results. The suggestion has been made that the more absorbable portion of the cosmic rays shows the greater diurnal variation. This more absorbable component is however almost completely absent at sea level. Our work was accordingly done at a much higher altitude (3900 m) than any previous long series of observations.

[1] A good summary of this work is given by G. Hoffmann, Zeits. f. Physik **69**, 703 (1931).

[2] A. H. Compton, J. C. Stearns, and R. D. Bennett, Phys. Rev. **38**, 1565 (1931); **39**, 873 (1932).

Apparatus and Procedure

A diagram of the apparatus employed is shown partly in section, in Fig. 1. The ionization chamber is a steel sphere, approximately 10 cm internal diameter, filled with air at 30 atmospheres pressure. The ionization current is measured by a Lindemann electrometer, operating at about 50 divisions per volt. By applying an arbitrary potential to the grounding key, the sensitivity of the electrometer can be determined, and the needle can be made to move over any desired portion of the scale. The ionization current was approximately saturated when 144 volts from a dry battery were applied to the chamber. Surrounding the ionization chamber may be placed cylindrical shells of 2.5 cm of copper, and 5 successive layers of lead, each 2.5 cm thick,

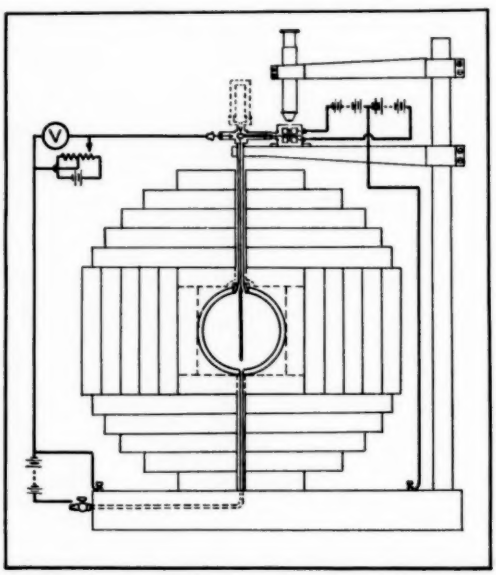

Fig. 1. Cross section of ionization chamber with shield.

a total mass of about 800 kg. The equipment was housed in a motor bus which had a wooden roof too thin to absorb any appreciable cosmic radiation.

The readings consisted in comparing the time required for the electrometer needle to move 10 microscope scale divisions when cosmic rays alone were used with the time when a tube of 0.941 milligrams of radium enclosed in 1 cm of lead, was brought to standard position at about 22 cm from the center of the chamber. All measurements were made with 2.5 cm of copper and 5 cm of lead surrounding the chamber. Auxiliary tests showed that when the radium was removed, the ionization due to the local radiation traversing this shield was less than 3 percent of that due to the cosmic rays. Thus the ratio of the readings is a measure of the cosmic rays in terms of the gamma rays from the radium standard.

In our previous paper we showed that the ratio of gamma ray to cosmic ray ionization is independent of pressure. According to the theory of the effect of temperature on ionization developed there, the ratio of the ionizations

must thus be independent also of the temperature. Thus neither gas leaks nor temperature changes should affect our measurements of the radium equivalent of the cosmic rays.

Evidence for a Diurnal Variation

The results of the measurements are summarized in Table I and are shown in detail in Fig. 2. In Table I the values of $i_c/i_{c+\gamma}$ are the averages, over 10 days for the hours indicated, of the observed ratios of the ionization due to cosmic rays alone and due to cosmic rays plus the gamma-rays, measured as described above. The values of $I = i_c/i_\gamma$ are calculated from the observed values of $i_c/i_{c+\gamma}$ from the algebraic relation,

$$\frac{a}{b} = \frac{a}{a+b} \Big/ \left(1 - \frac{a}{a+b}\right).$$

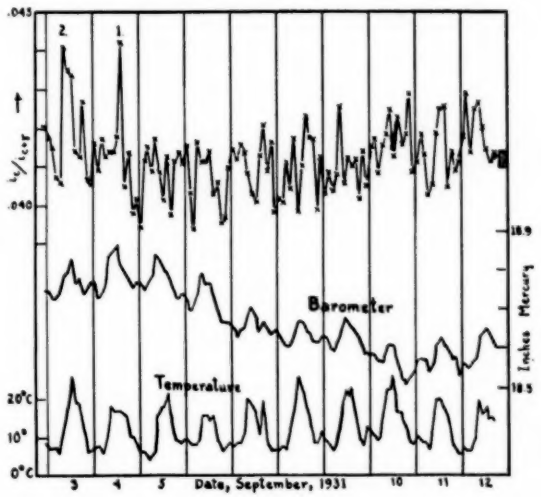

Fig. 2.

Table I. *Diurnal variation of cosmic rays at 3900 meters, 39°N 106°W, September 2–12, 1931.*

Hour	$i_c/i_{c+\gamma}$	$I = i_c/i_\gamma$	Temp. °C	Bar., inch	δI_T	δI_P	Chauvenet	I_0
6– 8A	0.04113	0.04289	9.0	18.663	−0.00002	−0.00024	—	0.04263
8–10	.04184	.04366	17.2	18.704	−.00024	+.00003	−0.00025	.04320
10–12	.04140	.04319	19.4	18.717	−.00013	+.00011	—	.04317
12– 2P	.04140	.04319	20.0	18.718	−.00010	+.00011	—	.04320
2– 4	.04179	.04361	17.7	18.687	−.00003	−.00008	−.00032	.04318
4– 6	.04106	.04282	15.4	18.673	.00000	−.00017	—	.04265
6– 8	.04119	.04296	9.8	18.657	+.00016	−.00027	—	.04285
8–10	.04092	.04267	7.8	18.651	+.00009	−.00031	—	.04245
10–12	.04082	.04256	8.4	18.663	+.00004	−.00024	—	.04236
12– 2A	.04106	.04282	8.4	18.666	+.00006	−.00022	—	.04266
2– 4	.04126	.04303	7.9	18.645	+.00007	−.00035	—	.04275
4– 6A	.04098	.04273	7.3	18.649	+.00008	−.00032	—	.04249

Probable error of bi-hourly mean value of $I = \pm 0.00019$.
Probable error of bi-hourly mean value of $I_0 = \pm 0.00014$.
Mean value of $I_0 = 0.04280 \pm 0.00005 = 85$ ions per cc per sec. at 30 atmospheres.

The ratio I is thus a measure of the ionization due to the cosmic rays in terms of the ionization due to the γ-rays as unity. The temperature and barometric pressure are likewise ten day averages taken over the hours indicated.

Corrections for Temperature and Pressure Variations

These values of I are subject to a small correction due to the variation of the battery voltage with the temperature; for a change of the potential applied to the ionization chamber induces a charge on the collecting electrode. It was found that a change of potential of 2.5 volts on the ionization chamber was sufficient to move the electrometer needle over the 10 scale divisions used in taking the readings. Thus if δV_T is the change in the battery potential during the reading, the correction to be applied is

$$\delta I_T = I\delta V_T/2.5.$$

The fluctuations δV_T during a single 10 minute reading were too small to be measured (of the order of 1 part in 30,000) with our field apparatus. They could be calculated, however, from the observed rate of temperature change and measurements of the electromotive force at different temperatures. These measurements were made on another dry battery of similar construction, using the Lindemann electrometer as an electrostatic voltmeter. When a battery potential of about 80 volts was applied to the plates of the electrometer, changes as small as 0.01 volt could be detected.

It was found that two types of voltage changes occur. The first is an increase of e.m.f. of about 0.015 percent per degree Centigrade, which follows closely the changes of the battery temperature. The second is a slow change, requiring more than 12 hours to come to equilibrium. This is an increase at the rate of about 0.003 percent per hour per degree change in temperature. The corrections to be applied due to these voltage changes are indicated in Table I by δI_T.

The rate at which the cosmic-ray intensity varies with the barometric pressure can be calculated from data showing the intensity at different altitudes. Using the values given by Millikan and Cameron[3] for the ionization inside lead screens, observed at different altitudes under conditions closely similar to ours, we find for barometric pressure of 18.7 inches, $(1/I)(dI/dP) = -0.147$ per inch of mercury. This enables us to standardize our intensity values by reducing them to 18.7 inches pressure. The appropriate corrections are indicated in Table I as δI_p.

The probable error of each bi-hourly value of I was calculated from the variations between the 10 daily readings which make up the average. The mean value of the 12 probable errors thus calculated is $r = \pm 0.00019$. With this probable error, it is found by applying Chauvenet's criterion that it is improbable that in 120 data there should be departures from the mean as great as those shown in Fig. 2 as points (1) and (2). By neglecting these data we thus get more reliable mean bi-hourly values, whose probable error is now reduced to $r_c = \pm 0.00018$.

[3] R. A. Millikan and G. H. Cameron, Phys. Rev. **37**, 242 (1931).

Changes in barometric pressure on successive days introduce a fluctuation in the bi-hourly values of I of $r_p = \pm 0.00011$. Similarly, due to the difference in the temperature changes on successive days, there is a fluctuation of $r_t = \pm 0.00002$. When the intensity is corrected for pressure and temperature changes, the probable error of the mean I_0 values thus becomes

$$r_0 = (r_c^2 - r_t^2 - r_p^2)^{1/2} = \pm 0.00015.$$

It will be noted from Table I and Fig. 3 that the variations in the bi-hourly values of I are hardly more than is to be expected from the probable error. On the basis of this evidence, we stated in a preliminary report of this work[4] that our readings "showed no variations in intensity greater than were to be expected from purely statistical considerations." However, when the

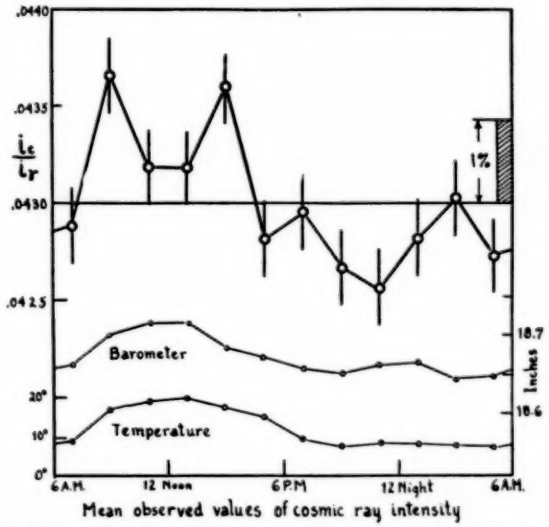

Fig. 3. Mean observed values of cosmic-ray intensity.

corrections due to the daily changes in barometric pressure are applied, there appears a marked difference between the intensity of the rays in the daytime and at night. During these experiments, the ionization was about 1.5 ± 0.25 percent more intense between 8 A.M. and 4 P.M. than between 8 P.M. and 4 A.M. There is only one chance in about 10^4 that this variation of 6 times the probable error should result from statistical fluctuations.

The existence of this diurnal variation, as well as the effect on the data of changes in the barometer, are shown graphically in Figs. 3 and 4. In Fig. 4, the dotted circles are calculated including the datum points (1) and (2) of Fig. 2 in calculating the average. In these figures the probable error of the data is represented by the length of the line drawn through each datum point. It will be noted that whereas before correction for barometric changes, 7 of the 12 points lie within the probable error of the mean position, after this correction only 3 of the 12 points lie within the probable error of the mean. In

[4] R. D. Bennett, J. C. Stearns and A. H. Compton, Phys. Rev. **38,** 1566 (1931).

Fig. 2 the "barometer effect" shows itself by the gradual rise of the mean intensity of the cosmic rays as the daily average of the barometer readings falls.

Diurnal variations similar to that here reported have been noted by other observers. Recently Lindholm[5] and Hess[6] have shown that an analysis of the data taken by Hoffmann and Lindholm[7] at 2450 m shows a diurnal change larger than the probable error, and about 0.5 percent of the whole cosmic-ray intensity. Likewise Hess and Pforte[8] from their own data at 100 m elevation find an intensity which is on the average 0.33 percent greater during the day than at night. This is precisely the magnitude of the effect reported by Millikan[9] in his most recent sea level measurements, though Millikan doubts whether the difference he observed was greater than the experimental error. Hoffmann[10] also notes an effect (at about sea level) "due to the sun" of the same order of magnitude as Millikan's, but of questionable reality.

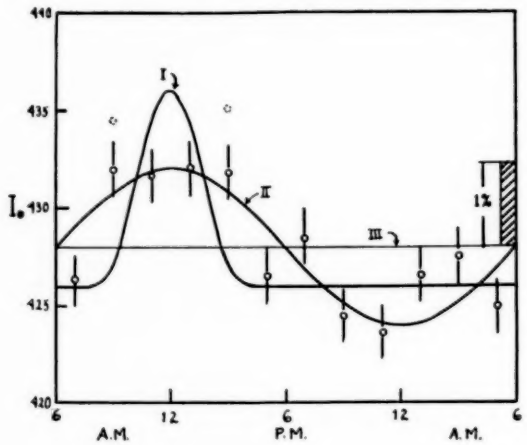

Fig. 4. Cosmic-ray ionization as function of time of day. Corrected for effects of temperature and pressure variations.

A possible explanation of the greater magnitude of the diurnal variation which we have found is that the variation occurs only in the soft component of the cosmic rays ($\mu =$ *ca.* 0.8 per meter of water). At 3900 m this constitutes about 65 percent of the whole cosmic radiation, whereas at sea level it amounts to only 8 percent. Thus our average difference of 1.0 percent between the 12 daylight hours and the 12 night hours would correspond to a difference of 0.12 percent at sea level or 0.7 per cent at 2450 meters. These values are in reasonably satisfactory agreement with those cited above.

[5] F. Lindholm, Gerlands Beitrage zur Geophysik **22,** 141 (1929).
[6] V. F. Hess, Naturwiss **18,** 1094 (1930).
[7] G. Hoffmann and F. Lindholm, Gerlands Beitrage zur Geophysik **20,** 12 (1928).
[8] V. F. Hesse and W. S. Pforte, Zeits. f. Physik **71,** 171 (1931).
[9] R. A. Millikan, Phys. Rev. **39,** 391 (1932).
[10] G. Hoffmann, reference 1.

Significance of the Diurnal Variation

Two alternative types of diurnal variations may be anticipated. The first would be due to rays coming directly from the sun. In this case the intensity of the "solar component" would be a maximum at noon, falling gradually to zero at sunset as the rays penetrate greater and greater thickness of the atmosphere. Curve I of Fig. 4 is calculated on this hypothesis, assuming that the solar component has the same absorption coefficient (*ca.* 0.8 per meter of water) as the soft component of the cosmic rays. The calculation is made for latitude 39°36′N, and sun's declination of 5°30′N.

The second alternative would be that cosmic rays are emitted more abundantly from the portions of space in the neighborhood of the sun than at remote distances. This would give rise to a gradual change, with a maximum at noon and a minimum at midnight, following approximately a sine curve, as indicated by curve II of Fig. 3.

If we represent by 1 the mean square departure of the data from the true value as calculated from the probable error, the mean square departure from curve I is found to be 1.9, from II is 0.8 and from III is 2.5. That is, curve II is much more probable than curve I or the straight line III, and agrees satisfactorily with the experimental data. It should be added that if a curve similar to I is calculated assuming the absorption of the solar component to be the same as of the total cosmic-ray beam it agrees considerably better with the experiments than does the curve I as here drawn. Such an assumption seems however to be ruled out by the fact noted above that at low altitudes the diurnal variation is much less prominent than at high altitudes.

Thus the evidence favors the view that the diurnal variation follows approximately a sine curve, with the maximum at noon and minimum at midnight. Unless this effect is due to some obscure atmospheric phenomenon, it suggests that the portion of space in the neighborhood of the sun emits cosmic rays more copiously than the more remote regions. It can be simply shown that the effective radius of the region from which the rays come should be approximately,

$$r = 2a/\delta$$

where a is the radius of the earth's orbit, and $\delta = (I \text{ noon} - I \text{ midnight})/I$. Thus if δ for the soft component of the cosmic rays is 0.02, r becomes 100 times the radius of the earth's orbit, or about twice the radius of the orbit of Pluto.

Millikan and Cameron have shown that the energy received by the earth as cosmic rays is comparable with that received as star-light. If the cosmic rays which we receive are a fair sample of those existing in interstellar space, this means that the energy in the universe in the form of cosmic rays is of the same order as that in the form of light. Curve II which these experiments confirm is however based on the assumption that the part of space near the sun emits cosmic rays more copiously than the more remote regions. That is, these experiments support the view that we do not receive a fair sample of the cosmic rays. This makes it difficult to form any reliable estimate of the energy of cosmic rays in interstellar space.

Without the cooperation of Messrs. V. J. Andrew, A. A. Compton, J. A. Longman, P. J. Mills, and L. N. Ridenour, Jr. of Chicago, and of P. Barth, C. Hedberg and W. Overbeck of Denver, the long series of readings required to obtain these results could not have been secured. We are indebted also to Mr. J. W. Ailinger, Superintendent of the Department of Mountain Parks, and to Mr. Donald Keim of the Chamber of Commerce of the City of Denver for facilitating our work on Mt. Evans in every possible way. Part of the equipment was purchased with a grant from the Rumford Committee.

Diffuse Scattering of X-Rays from Sodium Fluoride

By G. E. M. JAUNCEY* AND P. S. WILLIAMS
Washington University, St. Louis

(Received May 27, 1931)

S(class) values have been obtained for the monatomic gases argon and neon by Wollan, and for the simple cubic crystals sylvine and rocksalt by Harvey, and Jauncey and May. *F* values for the average $\frac{1}{2}(K^+ + Cl^-)$ and $\frac{1}{2}(Na^+ + Cl^-)$ atoms have been obtained by James and Brindley, and James and Firth. By means of the formulas for gases and crystals developed by Compton, and by Jauncey and Harvey, the above have yielded comparisons between *S*(class) and f' values for argon and the average sylvine atoms, and for the average $\frac{1}{2}$(A+Ne) atoms and the average rocksalt atoms. The agreement on the whole has been excellent. The object of the present research was to make similar comparisons of the above results for neon with those for $\frac{1}{2}(Na^+ + F^-)$, by using Havighurst's *F* values for this average atom. The methods of experiment and calculation were similar to those of Jauncey and May, as modified by Harvey, except that Woo's form of the crystal formula was used to take account of the incoherent scattering. Unlike the case of argon and sylvine, we found that the f' values for the crystal of NaF are definitely lower than those for the gas neon. This implies that for weak nuclear fields the electron distribution in an atom of a crystal is perceptibly more diffuse than that in an atom of the corresponding gas. We also calculated *B* values and found that the second hump in the *B* curve which is barely indicated by Wollan's values for neon is definitely present. A Fourier analysis will therefore give a *U* curve which shows a hump for the *K* electrons of NaF.

I. INTRODUCTION

CONSIDER the case of a beam of unpolarized x-rays of intensity I_0 per unit area of the beam falling upon a speck of matter containing n molecules, where n is so small that the loss due to absorption of the x-rays in the speck may be neglected and yet so large that the intensity of the x-rays scattered by the speck per unit solid angle in a direction ϕ with the primary beam is proportional to n and to I_0, the primary intensity. We may then say that the intensity of these scattered rays is $I_{M\phi}nI_0$, where $I_{M\phi}$ is a proportionality constant for a given value of ϕ. It is possible to measure $I_{M\phi}nI_0$ experimentally, whence upon dividing by nI_0 the value of $I_{M\phi}$ may be found. We shall call $I_{M\phi}$ the scattered intensity per unit solid angle per molecule per unit primary intensity in the direction ϕ.

On the simple Thomson[1] theory of x-ray scattering, the scattered intensity from a molecule containing Z electrons is given by

$$I_{M\phi} = (Ze^4/m^2c^4)\cdot(1 + \cos^2\phi)/2 \qquad (1)$$

since each of the electrons in a molecule scatters independently. However, it is found that the experimental values of $I_{M\phi}$ are not in general given by the

* The senior author was aided in part by a grant from the Rockefeller Foundation to Washington University for research in science.

[1] J. J. Thomson, The Conduction of Electricity through Gases, 2nd Ed., p. 325.

right side of (1). Barkla and Ayers[2] found that at small angles the experimental values of $I_{M\phi}$ are greater than the right side of (1) and it has now become customary to multiply the right side of (1) by a factor S, so that

$$I_{M\phi} = (SZe^4/m^2c^4)(1 + \cos^2\phi)/2 \tag{2}$$

We shall call S the scattering factor per electron or simply the scattering factor. The value of S depends upon the electron distribution in each molecule of the speck and upon the arrangement of the molecules in the speck. The value of S may be found experimentally in all cases, but can only be calculated theoretically in particular cases. In 1930 Compton,[3] using the principles of the classical theory, showed that for the case of scattering from a monatomic gas

$$S = 1 + (Z - 1)f'^2/Z^2 \tag{3}$$

where Z is the number of electrons in an atom of the gas and f' is related to the true atomic structure factor f in a manner discussed by Jauncey[4] and Herzog.[5] In 1931 Jauncey[6] showed that for the case of scattering from a solid consisting of atoms of one kind

$$S = 1 + (Z - 1)f'^2/Z^2 + (F^2/nZ)X \tag{4}$$

where F is the atomic structure factor including the effect of thermal agitation and X is a certain double summation. Jauncey and Harvey[7] have shown that for the case of a simple cubic crystal $X = -n$, where n is the number of atoms in a speck of the crystal. Hence, for a simple cubic crystal consisting of atoms of one kind Eq. (4) becomes

$$S = 1 + (Z - 1)f'^2/Z^2 - F^2/Z. \tag{5}$$

Eqs. (3), (4) and (5) are derived from the principles of the classical theory and do not take account of the Compton effect. Wentzel[8] has applied the principles of wave mechanics to the theory of the Compton effect, and Woo[9] by extending Wentzel's arguments has arrived at a formula for S of the form

$$S = S_1 + S_2/(1 + \alpha \operatorname{vers}\phi)^3 \tag{6}$$

where $\alpha = h/mc\lambda$. For both the case of a monatomic gas and the case of a simple cubic crystal consisting of atoms of one kind, Woo gives

$$S_2 = 1 - f'^2/Z^2 \tag{7}$$

For a monatomic gas, Woo gives

$$S_1 = f'^2/Z \tag{8}$$

and, for a crystal,

$$S_1 = (f'^2 - F^2)/Z. \tag{9}$$

[2] C. G. Barkla and T. Ayers, Phil. Mag. **21**, 275 (1911).
[3] A. H. Compton, Phys. Rev. **35**, 925 (1930).
[4] G. E. M. Jauncey, Phys. Rev. **38**, 1 (1931).
[5] G. Herzog, Zeits. f. Physik **69**, 207 (1931).
[6] G. E. M. Jauncey, Phys. Rev. **37**, 1193 (1931).
[7] G. E. M. Jauncey and G. G. Harvey, Phys. Rev. **37**, 1203 (1931).
[8] G. Wentzel, Zeits. f. Physik **43**, 1 and 779 (1927).
[9] Y. H. Woo, Phys. Rev. **38**, 6 (1931).

We shall call S_1 and S_2 the coherent and incoherent scattering factors, respectively. It should be noted that from Eq. (6)

$$S = S_1 + S_2 \tag{10}$$

when $\alpha = 0$. In this case, using Eqs. (7) and (8), it is seen that the right side of Eq. (10) reduces to the right side of Eq. (3); also, using Eqs. (7) and (9), the right side of Eq. (10) reduces to the right side of Eq. (5). Since Eqs. (3) and (5) were derived by means of the classical theory, we may say that the sum of the coherent and incoherent scattering factors equals the classical scattering factor.

Jauncey and Harvey[10] have noted that, if the f' values for a monatomic gas are the same as those for a crystal consisting of the same kind of atoms as the gas, f' may be eliminated from Eqs. (3) and (5), giving

$$S_{\text{gas}} = (S + F^2/Z)_{\text{cryst}}. \tag{11}$$

This relation is also valid if Woo's Eqs. (6), (7), (8) and (9) represent the true state of affairs. Since the atoms of sylvine are argon-like, the relation expressed by Eq. (11) should hold for argon and sylvine. Using the experimental S values for argon and sylvine obtained by Wollan[11] and Harvey[12] respectively, and the F values for sylvine obtained by James and Brindley,[13] Jauncey and Harvey[10] have shown that the relation expressed by Eq. (11) holds very closely for argon and sylvine.

The purpose of the present research was to test the accuracy of the relation expressed by Eq. (11) for neon and sodium fluoride. Since S values for neon and F values for sodium fluoride have already been obtained by Wollan[11] and Havighurst[14] respectively, it remained for us to determine the S values for sodium fluoride.

II. Experimental Method

The experimental method was essentially that used by Jauncey and May[15] and modified by Harvey.[12] Unpolarized x-rays from a tungsten target tube were used. The rays were made effectively homogeneous by placing 1.65 mm of aluminum in the primary beam of x-rays. This beam was scattered by a slab of sodium fluoride crystal into an ionization chamber. With the ionization chamber placed at an angle ϕ with the primary beam, the crystal was set at various positions, so that θ, the angle between the normal to the crystal slab and the primary rays, passed through the value $\phi/2$. At $\theta = \phi/2$, which is the Crowther[16] position, a Laue spot was reflected into the chamber. Readings on both sides of the Laue spot were made and an interpolated reading at the position of the Laue spot was calculated as described in the papers of Jauncey and May[15] and Harvey.[12] The ionization chamber was filled with

[10] G. E. M. Jauncey and G. G. Harvey, Phys. Rev. **38,** 1071 (1931).
[11] E. O. Wollan, Phys. Rev. **37,** 862 (1931).
[12] G. G. Harvey, Phys. Rev. **38,** 593 (1931).
[13] R. W. James and G. W. Brindley, Proc. Roy. Soc. **A121,** 155 (1928).
[14] R. J. Havighurst, Phys. Rev. **29,** 1 (1927).
[15] G. E. M. Jauncey and H. L. May, Phys. Rev. **23,** 128 (1924).
[16] J. A. Crowther, Proc. Roy. Soc. **A86,** 478 (1912).

air saturated with ethyl bromide at a temperature of 22°C, at which temperature the vapor pressure of the bromide[17] is 415 mm of mercury. The length of the ionization chamber was 43 cm. The effective wave-length of the x-rays passing through the aluminum filter and the crystal in the Crowther position was found by observing the absorption in further sheets of aluminum. The effective wave-length was 0.39A when the x-ray tube was operated at about 65 k.v. peak and 10 m.a.

Instead of comparing the intensity of the x-rays scattered at an angle ϕ from the crystal with those of the rays scattered from the crystal at some standard angle such as 60° as in Harvey's experiment, we compared the intensity of the rays scattered from the crystal in a direction ϕ with that of the rays scattered from a slab of carbon at a constant angle of 40°. Not only were the intensity of the scattered rays compared but also the intensities of the transmitted rays. Then, later, the intensity of the rays scattered from the carbon slab were compared with that of the rays scattered from a slab of paraffin at 90°, and also the intensities of the transmitted rays were compared. We were therefore able to calculate the ratio of the intensity of the x-rays scattered by the crystal at an angle ϕ to that of the rays scattered by paraffin at 90°, and also the ratio of the intensity of the primary beam transmitted through the crystal when in the Crowther position corresponding to a scattering angle ϕ to that of the primary beam transmitted through the paraffin when in the Crowther position corresponding to a scattering angle of 90°. We shall call these two ratios the scattering ratio and the transmitted ratio, respectively.

It must be noted that the ratios actually observed are ratios of ionization currents and not ratios of intensities. This difference comes in because the length of the ionization chamber is not sufficient for the complete absorption of the x-rays entering the chamber. The values of the ratios are shown in Table I.

TABLE I. *Experimental ratios. Sodium fluoride to paraffin.*

$(\sin \frac{1}{2}\phi)/\lambda$	Scattering	Transmission
0.109	0.26	1.333
.218	2.47	1.333
.327	3.02	1.331
.434	3.16	1.327
.540	3.20	1.317
.647	3.14	1.310
.855	2.77	1.282
1.057	2.46	1.243
1.250	2.19	1.196
1.447	1.91	1.140
1.631	1.73	1.072
1.812	1.59	1.000

The surface density of the crystal was 1.443 gm/cm² while that of the paraffin was 0.701 gm/cm².

III. INTERPRETATION OF THE RESULTS

Crowther's formula[16] for the intensity of the x-rays scattered in a direction ϕ from a slab of material whose thickness is t is

[17] International Critical Tables, III, p. 217.

$$I_\phi = (AIt/R^2 \cos \tfrac{1}{2}\phi) \cdot s \tag{12}$$

where I is the intensity per unit area of the rays transmitted through the slab when held in the Crowther position, A is the area of the ionization chamber window, R is the distance of the window from the slab, and s is the linear spatial scattering coefficient per unit solid angle in a direction ϕ. At the time Eq. (2) was derived by Crowther, the Compton effect was unknown. Jauncey and Defoe[17] have considered the effect of the division of the scattered rays into coherent and incoherent rays and have shown that the simple Crowther formula must be replaced by

$$I_\phi = (AIt/R^2 \cos \tfrac{1}{2}\phi)(s_1 + s_2 T) \tag{13}$$

where s_1 and s_2 are respectively the coherent and incoherent linear spatial scattering coefficients per unit solid angle in a direction ϕ, and where T is a complicated expression involving the absorption coefficients of the coherent and incoherent scattered x-rays in the slab, in the air between the slab and in the aluminum window of the chamber. T is a function of the scattering angle ϕ. We shall write

$$I_\phi = I_{\phi 1} + I_{\phi 2} \tag{14}$$

where $I_{\phi 1}$ and $I_{\phi 2}$ are the intensities of the coherent and incoherent rays respectively. From Eq. (13),

$$I_{\phi 1} = (AIt/R^2 \cos \tfrac{1}{2}\phi) \cdot s_1 \tag{15}$$

and

$$I_{\phi 2} = \frac{AIt}{R^2 \cos \tfrac{1}{2}\phi} s_2 T. \tag{16}$$

Let the fractions of $I_{\phi 1}$ and $I_{\phi 2}$ which are absorbed in the ethyl bromide of the ionization chamber be K_0 and K_ϕ respectively. Then, if $C_{\phi 1}$ and $C_{\phi 2}$ are the respective ionization currents produced, we have

$$C_{\phi 1} = K_0 I_{\phi 1} \tag{17}$$

$$C_{\phi 2} = K_\phi I_{\phi 2}. \tag{18}$$

Also, if C is the ionization current produced by the transmitted rays,

$$C = K_0 I. \tag{19}$$

Hence, replacing the I's in Eq. (14) by the C's and taking account of Eqs. (15) and (16), we obtain, after rearranging and putting $C_\phi = C_{\phi 1} + C_{\phi 2}$,

$$C_\phi = \frac{ACt}{R^2 \cos \tfrac{1}{2}\phi} \left\{ s_1 + \frac{K_\phi T}{K_0} s_2 \right\} \tag{20}$$

C_ϕ is the actual measured ionization current. The relation between s_1 and S_1 is

$$s_1 = S_1 (NZ\rho/W) \cdot (e^4/m^2c^4) \cdot (1 + \cos^2 \phi)/2 \tag{21}$$

while that between s_2 and S_2 is

$$s_2 = S_2 \frac{(NZ\rho/W) \cdot (e^4/m^2c^4)}{(1 + \alpha \operatorname{vers} \phi)^3} \cdot \frac{(1 + \cos^2 \phi)}{2} \tag{22}$$

where ρ is the density of the slab, N is Avogadro's number, Z is the number of electrons in a molecule, and W is the molecular weight of the slab. If the scattering is from a slab of crystal, we use the values of S_1 and S_2 as given by Woo's Eqs. (7) and (9).

According to Harvey,[12] when x-rays of wave-length 0.39A are scattered at 90° from paraffin, the scattered rays are almost entirely incoherent, so that for this case, we may take $S_1 = 0$ and $S_2 = 1$. Hence, for scattering from paraffin at 90° we obtain an equation similar to Eq. (20), but with $s_1 = 0$ and s_2 given by Eq. (22) when $S_2 = 1$. In this equation for the scattering of paraffin, let us represent the ionization currents by P's. Dividing Eq. (20) by this equation for paraffin, we obtain after rearranging and taking account of Eqs. (7) and (9) for a crystal

$$K_0(f'^2 - F^2)/Z_C + K_\phi T_C \cdot \frac{1 - f'^2/Z_C^2}{(1 + \alpha \operatorname{vers} \phi)^3} = \frac{K_{90}{}^\circ T_P}{1 + \cos^2 \phi} \cdot \frac{\cos \tfrac{1}{2}\phi}{\cos 45^\circ} \cdot \frac{\rho_P t_P}{\rho_C t_C} \cdot (W/Z)_C \cdot (Z/W)_P \cdot C_\phi / P_{90} \cdot P/C \cdot 1/(1+\alpha)^3. \tag{23}$$

Quantities with the subscript C refer to the crystal of sodium fluoride, while those with the subscript P refer to the paraffin. In the present case the changes of absorption due to change of wave-length in the air between the scattering slab and the ionization chamber and in the aluminum chamber window are negligible, so that T reduces to

$$T = (1 - e^{-g})/g \tag{24}$$

where

$$g = (\mu_2 - \mu_1)t/\cos \tfrac{1}{2}\phi. \tag{25}$$

The quantities μ_2 and μ_1 are the linear absorption coefficients of the incoherent and coherent scattered rays in the scattering slab.

All quantities in Eq. (23) except f' are either known, can be calculated, or can be measured. Eq. (23) therefore enables us to find f'. These values of f' are shown in Table II. Values of F^2/Z as given by Havighurst[14] are also shown in this table. Knowing f' we can find S_1 and S_2 by means of Eqs. (9) and (7) and hence also S(class), where

$$S(\text{class}) = S_1 + S_2. \tag{26}$$

The values of S_1, S_2 and S(class) are also shown in Table II.

TABLE II. *f' and S values for sodium fluoride.*

$(\sin \frac{1}{2}\phi)/\lambda$	F^2/Z	f'	S_1	S_2	S(class)	B
0.109	8.65	9.27	—	0.141	0.141	2.53
.218	4.95	7.20	0.240	.482	.722	3.94
.327	2.37	5.00	0.130	.750	.880	4.10
.434	.99	3.23	0.053	.895	.948	3.52
.540	.45	2.21	0.038	.951	.989	3.05
.647	.20	1.51	0.028	.977	.995	2.45
.855	.05	.74	0.005	.994	.999	1.59
1.057	.00	.17	0.003	1.000	1.003	.45
1.250	.00	.55	0.030	.997	1.027	1.72
1.447	.00	.48	0.023	.998	1.021	1.74
1.631	.00	.46	0.021	.998	1.019	1.87
1.812	.00	.00	0.000	1.000	1.000	.00

Compton has introduced a quantity B which is given by

$$BZ = 8\pi f'(\sin \phi/2)/\lambda. \tag{27}$$

The values of B are shown in the seventh column of Table II. This quantity is used in Compton's Fourier analysis method of obtaining the electron distribution within an atom.

IV. Comparison with the Scattering from Neon

Wollan's S(class) values for neon, our S(class) values for sodium fluoride and Havighurst's F^2/Z values for sodium fluoride are shown by curves I, II and III respectively, of Fig. 1. Curve IV shows the values of S(class) $+ F^2/Z$ for sodium fluoride. It is seen that, unlike the case of sylvine and argon, the

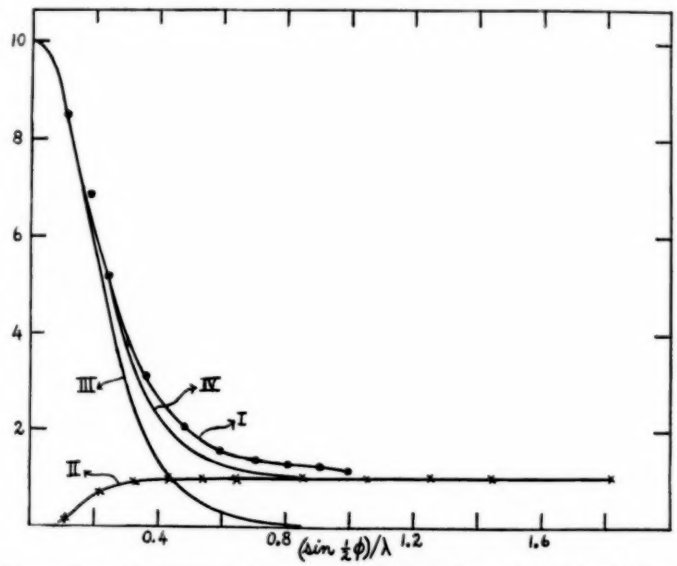

Fig. 1. Comparison of scattering from neon and NaF. Curve I—S(class) for neon (Wollan); Curve II—S(class) for NaF; Curve III—F^2/Z for NaF (Havighurst); Curve IV—S(class) $+ F^2/Z$ for NaF.

(S(class) $+ F^2/Z$) curve for sodium fluoride falls definitely below the S(class) curve for neon. Wollan's f' values for neon and our f' values for sodium fluoride are shown by curves I and II respectively, in Fig. 2. Comparing these curves, we note that the f' values for sodium fluoride are definitely below those for neon, so that the electron distribution for the average atom in a crystal of NaF is more diffuse than that for an atom of the gas neon. It is reasonable to expect that, when the atoms of a gas are concentrated into a crystal, there should be a distortion of the electron distribution of the atoms. This distortion explains the difference between the f' values for NaF and those for neon and it also explains the difference between the curves I and IV of Fig. 1. We might expect the distortion to be greater in the case of NaF than in the case of KCl, since the nuclear field of an atom in NaF is much weaker than that of an atom in KCl. This explains why there is such good

agreement between argon and sylvine but not such good agreement between neon and sodium fluoride.

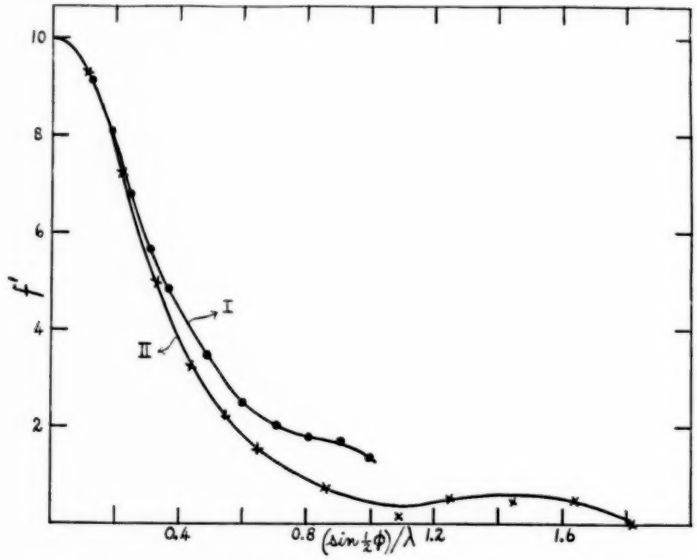

Fig. 2. Comparison of f' values. Curve I—Neon (Wollan); Curve II —NaF (Jauncey and Williams).

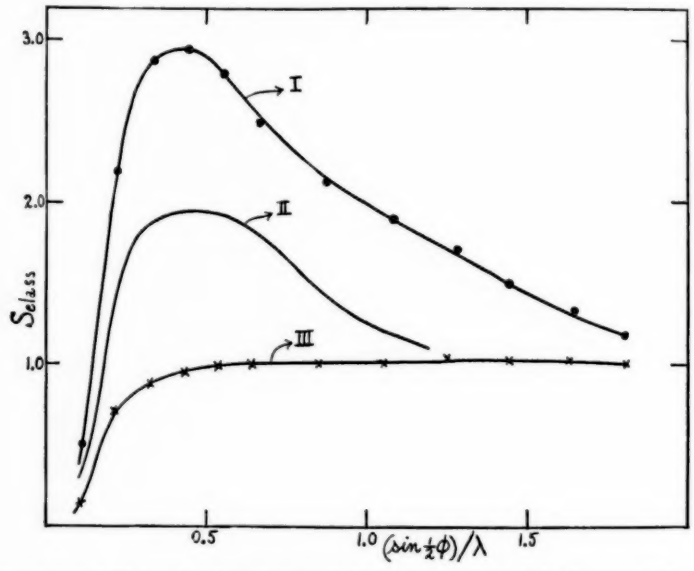

Fig. 3. Comparison of S(class) values for crystals. Curve I—sylvine (Harvey); Curve II—rock-salt (Jauncey and May); Curve III—NaF.

By referring to the seventh column of Table II, it is seen that our B values indicate two humps in the B curve in agreement with the B curve for neon which Wollan gives. It is the presence of the second hump which, according to

Wollan, causes the separation of the K electrons in the Fourier analysis of neon. We may say then that our B values support qualitatively Wollan's finding of a hump for the K electrons of neon in the U curve which he obtains by means of a Fourier analysis of his B curve for neon.

In this connection, the senior author wishes to remark that, as he[4] has already pointed out, the Compton Fourier analysis method in its present form is applicable only if $f'=f$. The senior author is not at present willing to admit that $f'=f$. Indeed, Woo has recently shown that the experimental evidence is rather in favor of $f'\neq f$. Jauncey[4] has shown that $f'<f$ if

$$\left(\sum_r E_r\right)^2 < Z\sum_r E_r^2 \tag{28}$$

which is always the case unless all the E's are equal. All the E's can be equal only if the individual electrons of an atom are indistinguishable from one another as far as the scattering of x-rays is concerned. The senior author is not at present willing to admit that the electrons in an atom are indistinguishable from one another.

V. Comparison with Sylvine and Rocksalt

An interesting comparison of the S curves for sylvine,[12] rocksalt[7] and sodium fluoride is shown by curves I, II, and III respectively of Fig. 3. It is seen that as the average atomic number decreases the hump of the S curve diminishes until in the case of NaF the presence of a hump is by no means obvious.

In conclusion it should be pointed out that we found it necessary to use Woo's formula for the diffuse scattering from crystals in preference to Jauncey and Harvey's formula. For sylvine the scattered radiation is principally coherent so that the classical formula of Jauncey and Harvey is sufficiently approximate. However, in the case of sodium fluoride it is necessary to take account of the fact that a considerable portion of the scattered radiation is incoherent. Woo's separation of the scattered radiation into coherent and incoherent radiation has enabled us to allow for the difference in the absorption of the two kinds of radiation in the ionization chamber, and also for the extra absorption of the incoherent radiation in the crystal itself.

We wish to thank Professor H. M. Randall of the University of Michigan for supplying the crystal of sodium fluoride.

Very Soft X-Ray Spectra of Heavy Elements

By C. DEL ROSARIO
University of Pennsylvania

(Received May 31, 1932)

Absolute wave-length measurements by photographic methods with plane gratings (280 and 1180 lines per mm) have been made on very soft x-ray lines of Th, Pb, Hg, Au, Ir, W and Ta. The wave-lengths range from 43.6A to 104.8A. For Hg, Au, Ir, W and Ta doublets were observed whose probable origins are transitions within the N shell, i.e., $\Delta n = 0$. These doublets fall on a smooth Moseley curve of small curvature.

INTRODUCTION

IN A recent work[1] on very soft x-rays, Thibaud measured the wave-lengths of several emission lines of the N and O series of some elements of high atomic numbers. He showed that, from the ordinary x-ray selection rules and with the energy-level values computed by Bohr and Coster, no electron transition could be selected that could predict accurately the wave-lengths of several lines he obtained by experiment. He suggested the possibility of an electron transition from one orbit to another in the same shell, and he showed a good agreement between the energy changes following such *forbidden* transitions and those experimentally observed. On account of the fundamental character of the principles and facts involved, it was thought desirable to confirm and extend Thibaud's determinations with hope of obtaining additional information on the structure of the outer part of the heavy atoms.

EXPERIMENTAL METHODS

The high absorbability of the radiation to be investigated requires the experiments to be done in vacuo. In the present work photographs of the

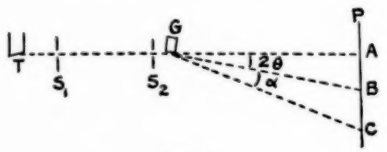

Fig. 1.

x-ray lines were taken with the aid of two vacuum spectrographs of a design resembling in general principles those used by Thibaud[2] and other investigators[3] in soft x-rays. Several variations in details were made, however, with the end in view of possible improvements or simplifications. Fig. 1 shows

[1] Thibaud, Comptes Rendus **188**, 1394 (1929).

[2] Thibaud, Jour. de Physique **8**, 447 (1927).

[3] For instance see: Hunt, Phys. Rev. **30**, 227 (1927); Weatherby, Phys. Rev. **32**, 707 (1928); Howe, Phys. Rev. **35**, 717 (1930); Soderman, Zeits. f. Physik **65**, 656 (1930).

schematically the principle involved in the wave-length measurements. X-rays from the target T pass through the limiting slits S_1 and S_2. Part of the narrow beam thus formed falls on a glass line grating G which reflects and diffracts it, while the rest passes by the grating and falls on a photographic plate P at A. The reflected and diffracted beams fall on the plate at B and C respectively.

The wave-lengths of the lines were calculated from the ordinary diffraction relation

$$n\lambda = D[\cos\theta - \cos(\theta + \alpha)]$$

using the modified form $n\lambda = 2D \sin[(2\theta+\alpha)/2] \sin \alpha/2$ where n denotes the order of the spectrum, λ, the wave-length and D the grating constant. To determine the glancing angle θ, it is necessary to know the position on the photographic plate of that part of the x-ray beam which was reflected and diffracted. This was accomplished by giving to the position of the image of the undeviated beam such correction as to make the wave-lengths of the different orders of a line—e.g., the O $K\alpha$—agree among themselves. This correction was always small. Most of the wave-length measurements were made with the nearest order of this line for comparison.

The glass gratings used in this work have spacing constants of 4.000×10^{-4} cm and 8.476×10^{-5} cm determined with the aid of the 5461A line of mercury. The grating was mounted on a carefully made holder which, by fine screws, can give it rotation about three mutually perpendicular axes besides a horizontal translation perpendicular to the x-ray beam without disturbing the orientation of the grating.

The limiting slits have beveled jaws with fine screws for width adjustment and horizontal displacement perpendicular to the x-ray beam. In addition, both slits can be rotated independently about an axis parallel to the x-ray beam to put them in the same vertical plane.

The photographic plate is held perpendicular to the x-ray beam in a light-tight box with the emulsion side pressed against a rigid metal surface in the box, obviating the necessity of measuring the thickness of the glass backing of every plate to get the grating-to-plate distance. The box is provided with a trap door in the front end which can be opened and closed at will by a magnet outside the spectrograph. One of the boxes used was so constructed that two parallel plates at different distances from the grating could be exposed at the same time. This offered a way to check up the measured distance, grating to plate, the distance between the plates being known. Five inch plates were used in the big spectrograph at about 50 cm from the grating, and lines as far as 10 cm from the undeviated line could be measured. The positions of these lines were obtained from densitometer measurements.

Fogging of the plates due to stray visible light from the hot filament, which gave trouble to some previous investigators, was effectively eliminated by three circular disks. They were bolted to the optical bench, which also carried the slits and grating holder. Two of these disks, each with an opening 1.5×0.2 cm, were placed one in front of each slit; while the third, which had a rectangular opening, part of which was covered with aluminum foils of suitable thickness to cut down the intensities of the undeviated beam and the

reflected beam, was in front of the plate box. The undesirable broadening of the images of the direct and reflected beams was prevented by the aluminum foils.

Figs. 2 and 3 show the construction of the two types of x-ray tubes employed. Copper, iron, lead, bismuth, iridium and gold targets were used, the last four in the form of buttons imbedded in copper. The electron source was a spiral filament of pure tungsten, thoriated tungsten or tantalum. It can

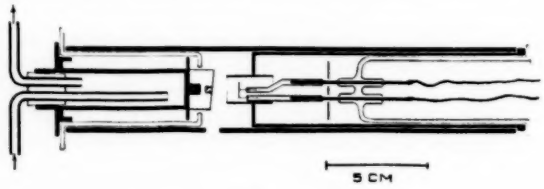

Fig. 2.

be seen that the target can easily be removed from the tube for cleaning or replacement, and put back in its original position. The filament can also be replaced readily. Its position and that of a focussing tube were adjusted by a series of trials to make the focal spot of the most satisfactory size. The wide flange at the outer end of the glass insulator for the target in the metal x-ray tube increases greatly the sparking distance, while the turned-in edges at the inside end keep the inner surface of the insulator free from sputtered metal.

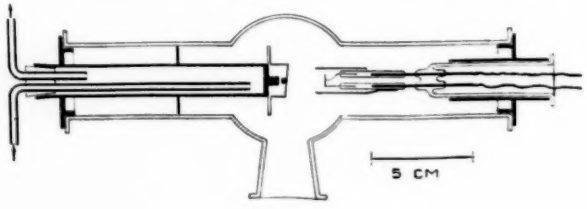

Fig. 3.

The vacuum in the spectrograph and in the x-ray tube was obtained with a Kurth two-stage mercury vapor pump backed by a Cenco Megapump. Voltages ranging from 2500 to 7500 volts were supplied to the x-ray tube by a transformer-rectifier-condenser set connected for full wave rectification. The current through the tube ranged from 30×10^{-3} to 100×10^{-3} ampere, but in no case was the power used more than 300 watts.

Experimental Results

Table I gives the wave-lengths of the observed lines, the corresponding values for ν/R and the probable transitions giving rise to these lines. For comparison, Thibaud's wave-lengths are also listed as well as computed values of ν/R based on Bohr and Coster's table of energy levels.

Discussion of Results

The agreement between the wave-lengths here obtained and those of Thibaud for the same lines is very satisfactory. The two observed lines each

of tantalum, tungsten, gold and mercury seem to form regular or relativity doublets of about 3A separation. The transitions assigned to these lines are identical for these elements but are forbidden by the selection rules, since

TABLE I. *Wave-length of observed lines.*

Element atomic number	Wave-length Present work	Thibaud's value	Probable origin	Present work	Bohr and Coster
Tantalum	58.3A	58.3A	$N_{iv}-N_{vi}$	15.6	15.6
73	61.3	61.4	$N_{v}-N_{vi-vii}$	14.8	14.4
Tungsten	56.0	56.0	$N_{iv}-N_{vi}$	16.2	15.9
74	59.0	59.1	$N_{v}-N_{vi-vii}$	15.4	15.6
Iridium	53.0	—	$N_{v}-N_{vi-vii}$	17.2	—
77					
Gold	46.2	46.8	$N_{iv}-N_{vi}$	19.7	20.0
79	48.9	49.4	$N_{v}-N_{vi-vii}$	18.6	18.6
Mercury	43.6	—	$N_{iv}-N_{vi}$	20.8	—
80	46.4	—	$N_{v}-N_{vi-vii}$	19.6	—
Lead	84.2	—	$N_{vi}-O_{iv}$	10.8	10.0
82	102.3	—	$O_{i}-P_{ii}$	8.9	—
	104.8	—	$O_{i}-P_{iii}$	8.7	—
Thorium	50.4	50.3	$N_{vii}-O_{v}$	18.1	18.4
90	64.5	64.5	$O_{ii}-P_{i}$	14.1	—
	68.3	68.1	$O_{iii}-P_{i}$	13.3	—

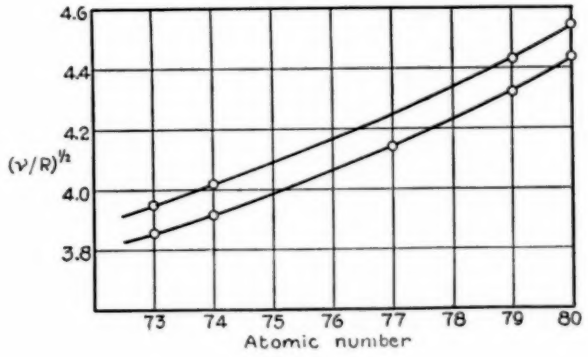

Fig. 4.

here the total quantum number does not change. The nearest values for changes in ν/R allowed by the rules are 1.9 to 2.6 or 9.5 to 17.6 percent smaller than those corresponding to the observed lines which, by the way, are the only ones found for these elements. Fig. 4 shows how closely these doublets follow Moseley's law.

No spectrum line has so far been observed characteristic of bismuth. This is not surprising since its low melting point and poor heat conductivity made it impossible to use a fair amount of power in the x-ray tube and to use a reasonably small focal spot. The lines obtained for iridium, mercury and lead

are believed to have been measured for the first time. There is some doubt about the justification of assigning to mercury the lines at 43.6A and 46.4A. The assignment was made on the basis of known facts for the doublets of tantalum, tungsten and gold. First, the two lines have about the same separation as the other doublets; second, the component of greater wave-length is of greater intensity; third, the plotted points fall close to the Moseley curve for the other elements if the atomic number for mercury is used. The line at 53.0A is probably the more intense line of the doublet for iridium. Why corresponding doublets did not appear in the spectra of lead and thorium is not yet understood; however, a further extension of this work may shed light on this question.

In conclusion I wish to express my thanks to Professor C. B. Bazzoni for his encouragement and suggestions during the progress of the work.

On the Relative Abundances of the Nitrogen and Oxygen Isotopes

By GEORGE M. MURPHY AND HAROLD C. UREY
Department of Chemistry, Columbia University

(Received June 9, 1932)

The absorption spectra of samples of nitric oxide were investigated for the purpose of obtaining the relative abundance of the nitrogen and oxygen isotopes. Nitrogen from four different sources was investigated: air nitrogen, obtained from the Haber and Birkeland-Eyde processes; nitrogen from Pennsylvania coal and from Chili saltpeter. One sample of oxygen was obtained from a Pre-Cambrian magnetite. A method has been described for converting the nitrogen and oxygen from these different sources into nitric oxide. A method of photographic photometry has been applied to the spectra obtained. The procedure for obtaining the relative abundance of the isotopes is discussed together with the possible sources of error. The average of 32 measurements gives for the ratio of $N^{15}O^{16}/N^{14}O^{18}$ the result $0.549 \pm 0.007 : 1$. This gives the value 346:1 for the ratio N^{14}/N^{15}. The isotopic composition of the four samples of nitrogen and two samples of oxygen is constant within approximately 10 percent.

THE relative abundances of isotopes that are present only in small amounts such as those of carbon, nitrogen, oxygen and hydrogen are of great importance for several reasons. Because of the fact that oxygen is chosen as the standard for atomic weight determinations, the relative abundance of its isotopes is required as precisely as possible in order to convert from the chemical scale to the mass spectrograph scale. Recent discussions[1] as to other possible standards for atomic weights, also point out that it is very important to discover whether rare isotopes such as those of oxygen are constant in abundance with respect to samples of oxygen from different sources. Although the constancy of the more common isotopes is fairly well established both for terrestrial elements and for some from meteoric sources, no experiments of this sort have been made for the rarer isotopes mentioned above.[2]

Moreover, spectroscopic determinations of King and Birge[3] on the relative abundance of C^{13} indicate an apparent dependence of this quantity on the method of excitation of the spectra. Three typical sources such as arc, furnace and *N*-type stars, the effective temperatures of which probably decrease in this order, show that the abundance of C^{13} relative to C^{12} increases in the same order.

The detection of rare isotopes in molecular emission spectra seems to be particularly difficult. King and Birge failed to find C^{13} and $C^{13}N^{14}$ in arc spec-

[1] R. T. Birge and D. H. Menzel, Phys. Rev. **37**, 1669 (1931); R. Mecke, Phys. Zeits. **33**, 49 (1932); S. Meyer, Phys. Zeits. **33**, 301 (1932).

[2] Charles A. Bradley, Jr. and Harold C. Urey have investigated the relative abundance of the H^1 and H^2 isotopes in hydrogen samples from different sources and find that any variation in relative abundances is not large. Phys. Rev. **40**, 889 (1932).

[3] A. S. King and R. T. Birge, Astrophys. J. **72**, 251 (1930).

tra. Watson and Parker[4] were not able to observe the oxygen isotopes in the BeO emission spectra and Estey[5] failed to find any indication of the O^{17}, O^{18} or C^{13} atoms in the fourth positive emission bands of CO. Almy and Rahrer[6] failed to find bands due to $O^{18}H$ in the OH spectrum. On account of these as yet unexplained difficulties, it seems that the most reliable determination of the relative abundance can be made from absorption spectra.

The discovery of an isotope of nitrogen of mass 15 and the determination of its abundance relative to N^{14} is due to Naudé[7] who investigated the γ bands of nitric oxide. He redetermined the abundance of O^{16} relative to O^{18}, obtaining $1075 \pm 110:1$. He then determined the ratio of the nitrogen isotopes from the relative intensities of the $N^{15}O^{16}\,{}^{O}P_{12}$ and the $N^{14}O^{18}\,{}^{P}Q_{12}+P_2$ branches of the $(v', v'') = (1, 0)$ band, which he states have nearly the same intensities. Our own investigation shows that this is not the case (see Fig. 1). The results of Naudé are also open to objection because even if these heads were of the same intensity, the $N^{14}O^{18}\,{}^{P}Q_{12}+P_2$ branch is superimposed on the $N^{15}O^{16}\,{}^{O}P_{12}$ branch, so that it is difficult or impossible to determine what part of the absorption is due to each molecule. The determination of Naudé has also been criticized by Mecke and Childs.[8] Using the values of Mecke and Childs for the relative abundance of O^{16}/O^{18}, Naudé's result for N^{14}/N^{15} becomes 409 ± 20 percent. Birge and Menzel have calculated from atomic weight considerations that this figure should be 320.

Because of these considerations, we have thought it worth while to redetermine the relative abundance of the nitrogen isotopes by the methods of photographic photometry. Moreover, we have worked with samples of nitrogen and oxygen from different sources as follows: Nitrogen: (1) from the air by the Haber process; (2) from the air by the Birkeland-Eyde process; (3) from Chili salt-peter; (4) from Pennsylvania coal. Oxygen: (5) from Pre-Cambrian magnetite.

The various samples of nitrogen were selected with the objects (1) of search for any variation of relative abundances of nitrogen isotopes in natural nitrogen samples, and (2) of finding whether any variation might be produced by the electric arc used in the Birkeland-Eyde process. The latter possibility seemed worth testing because of the general failure to observe these rare isotopes in emission spectra. The oxygen sample comes from the Pre-Cambrian magnetite of New York State and has not been a part of the atmosphere of the earth since the time the crust of the earth formed according to the best judgment of geologists.

Preparation of Nitric Oxide

Because of the variety of samples used, the method of preparation of the NO was different in each case. The Haber process nitrogen[9] was in the form

[4] W. W. Watson and A. E. Parker, Phys. Rev. **37,** 167 (1931).
[5] R. S. Estey, Phys. Rev. **35,** 309 (1930).
[6] G. M. Almy and G. D. Rahrer, Phys. Rev. **38,** 1816 (1931).
[7] S. M. Naudé, Phys. Rev. **34,** 1498 (1929); **35,** 130; **36,** 333 (1930).
[8] R. Mecke and W. H. J. Childs, Zeits. f. Physik **68,** 376 (1931).
[9] Kindly furnished by The Grasselli Chemical Company.

of 60 percent nitric acid and presented little difficulty. The gas generating apparatus was part of an all-glass system that also contained the absorption cell which was mounted directly in front of the slit of the spectrograph. This apparatus was first thoroughly swept out with nitrogen. The nitric acid was then allowed to drop into a solution of ferrous sulfate and concentrated sulfuric acid. By gently heating this mixture, the NO gas was evolved and after passing through several traps containing a solid CO_2-alcohol mixture was collected in a trap immersed in liquid air. After all the gas had been collected, this last container was closed from the generator by means of a stopcock and both it and the absorption cell were evacuated. Nitric oxide was admitted into the absorption cell by partially removing the liquid air and allowing it to distill slowly until the desired pressure as read on a manometer attached, was reached. Gas pressures ranging from 1 to 10 cm were used, the most convenient pressure being about 4 cm.

Sample 2 was in the form of "nitrate of lime."[10] This was dissolved in hot water, and Na_2CO_3 solution was then added to convert the calcium nitrate to sodium nitrate. The insoluble material was filtered off and the concentrated solution of sodium nitrate was added to the $FeSO_4$–H_2SO_4 mixture in the same way as described above.

Sample 3 was simply dissolved in H_2O, filtered and then added to the $FeSO_4$–H_2SO_4 mixture.

Sample 4 caused more difficulty as it was furnished to us in the form of ammonium sulfate.[11] Ammonia was liberated by adding NaOH solution. Oxygen was bubbled through this solution and then over an electrically heated platinum spiral where it was converted into oxides of nitrogen. The gases, NO and NO_2, were collected in a trap immersed in liquid air. These gases were then passed into the H_2SO_4–$FeSO_4$ solution by means of a stream of nitrogen and the NO gas collected as before in a liquid air trap.

The method for sample 5 was similar to that for sample 4. The magnetite[12] was first broken into small pieces and the oxygen was removed in the form of H_2O by passing hydrogen over the mineral at about 450°C. The H_2O was collected in a trap placed in a solid CO_2-alcohol mixture. After the addition of about 10 percent of H_2SO_4 it was electrolyzed in a small cell. The gases evolved were collected by displacement of oil from two chambers that had a volume ratio of 2:1 so that the hydrogen and oxygen gases were kept at the same pressure. After the electrolysis was finished, the oxygen was mixed with

[10] We wish to thank the Department of Chemistry of the College of the City of New York for supplying us with the sample of Birkeland-Eyde nitrogen.

[11] The ammonium sulfate was made from coal from the Pittsburgh seam mined in Washington County, Pennsylvania. The coal comes from two mines Vesta No. 4 and No. 5. These two mines are very close to one another but differ slightly in chemical analysis. It was kindly sent to us by Mr. M. W. St. John of the Jones and Laughlin Steel Corporation, Pittsburgh, Penna., whom we would like to thank in this place.

[12] The magnetite was a sample of Pre-Cambrian origin from Fort Henry, New York and came from the collection of the Geology Department of this University through the kindness of Professor Charles P. Berkey.

nitrogen and ammonia and the mixture was passed over the platinum spiral. From this point on the procedure was the same as for sample 4.[13]

Experimental Method

The absorption cell was 50 cm long and 4 cm in diameter and was fitted with two crystal-quartz windows stuck on with deKhotinsky cement.

A hydrogen discharge tube* was used as a continuous source of ultraviolet light. This tube carried about 2 amperes at 2500 volts and was constant in intensity within about 1 percent during an exposure. This was determined by means of a Moll surface thermopile placed at the back window of the tube. The deflections of a galvanometer connected to the thermopile were read continually during the time that was required to put the density marks on the plates. Two crystal-quartz lenses were used, one between the discharge tube and the absorption cell which gave a parallel beam of light through the cell and the second lens brought this light to a focus on the slit of the spectrograph. With this arrangement of lenses, a good exposure of the (1, 0) band could be obtained in one minute while the (2, 0) band at 2051A could be photographed in about five minutes. The Hilger E1 quartz spectrograph was used.

Various kinds of photographic plates were used. At first we sensitized Eastman 33 plates with vaseline or oil dissolved in petroleum ether. We then obtained an ultraviolet sensitizing solution from the Eastman Kodak Company and used this on Eastman 33 plates. These proved quite satisfactory and most of the results in this paper were obtained with them. More recently, we have secured Eastman U.V. spectroscopic plates.[13a] These have been even more convenient than the ones that we sensitized ourselves.

Calibration of Plates

We used two methods of putting density marks on our plates. At first we used a quartz wedge[14] with five steps of sputtered platinum and one clear step. It was calibrated directly on the spectrograph by means of the hydrogen tube and the method of variation of the width of the slit. Because of the irregularities on the surface of the sputtered steps and the uncertainties of the calibration of the wedge for a wave-length so far in the ultraviolet, we thought it desirable to use some other method of obtaining density marks.

We therefore made a set of neutral wire screens.[15] These screens were prepared as described by Harrison and were arranged so that they were kept in motion during use by means of a motor. Screens of this sort must be covered with CuO in order to give them a black surface. The usual method of oxidiz-

* This tube will be described in another place.

[13] We wish to thank Miss Pilar de Madariaga and Mr. S. H. Manian for their aid in working out the method and the preparation of the gas from sample 5.

[13a] C. E. K. Mees, J. Opt. Soc. Am. **21**, 753 (1931).

[14] The method of making these wedges has been investigated by Professor H. W. Webb of the Physics Department of this University. The wedge that we used was very kindly prepared for us by Professor Webb with our assistance.

[15] G. R. Harrison, J.O.S.A. and R.S.I. **18**, 492 (1929).

ing the surface by heating is not very satisfactory since the coat of CuO so formed is not adherent. We have found that the following method gives a good dull surface that is very permanent. The screens were first cleaned by dipping into a so-called mat solution which is used for producing a dull surface on articles that are to be electroplated. They were washed quickly and dipped into a boiling solution containing 1 percent potassium persulfate and 5 percent sodium hydroxide.* After the surface was black enough, they were washed and dried.

We had four screens, combinations of which would give 10 density marks. They were calibrated by means of the thermopile mentioned above and also by means of a photoelectric cell with a large tungsten lamp running on a constant source of alternating current. The results from the two methods of calibration are given in Table I.

TABLE I. *Transmission of screens.*

Screen	Photoelectric cell	Thermopile	Average
1	73.4	74.5	74.0
2	45.5	45.7	45.6
1+2	34.5	34.6	34.6
3	32.5	32.1	32.3
1+3	24.2	24.3	24.2
4	17.8	17.5	17.6
2+3	16.6	16.9	16.8
1+4	14.6	14.8	14.7
2+4	8.6	8.1	8.4
3+4	6.5	5.9	6.2

A Moll recording microphotometer was used to determine the density of the calibration marks on the plates and of the two isotopic band heads. Since the transmission of the wedge or screens was known, a curve of log i *vs.* d could be plotted by means of the relation

$$\log_{10} O = d = \log F_0/F \tag{1}$$

where O is the opacity, d is the density and F_0 and F are intensities of light transmitted by the unexposed and exposed parts of the plate respectively. Moreover

$$d = \log g_0/g \tag{2}$$

where g_0 and g are the throws of the galvanometer for an unexposed part of the plate and for one of the density marks, put on through a screen whose transmission was known.

The intensity of the isotopic bands could be determined by means of Beer's law

$$\log i_x - \log I = - kcx \tag{3}$$

where i_x and I are the intensities of the light transmitted by a layer of gas of thickness x and the incident radiation respectively; k is the molecular absorption coefficient and c is the molecular concentration.

* See: Electro-Deposition of Metals, 9th Edition, Langbein-Brannt, p. 278, 629, New York: Henry Carey Baird and Co., 1924.

The situation in the actual case is somewhat more involved because of the fact that bands are sometimes superimposed and that other absorbing molecules may be present, such as NO_2, for example. Then Eq. (3) must be replaced by

$$\log (i/I) = - (k_1 c + k_2)x \tag{4}$$

where k_1 is the molecular absorption coefficient and k_2 is the absorption coefficient due to other molecules which may be present. We assume that k_1 is the same for the same branches of the different isotopic molecules. But we cannot determine the value of I, since we do not have any point on the plate, where we are certain that there is no absorption due to extraneous molecules or superimposed bands. To avoid this difficulty we extrapolate the microphotometer curves as shown by the broken lines of Fig. 1. This gives an estimate of $\log i/I$, if k_1 were zero. Then we have

$$\log (i/I) - \log (i_0/I) = - (k_1 c + k_2)x + k_2 x = - k_1 c x \tag{5}$$

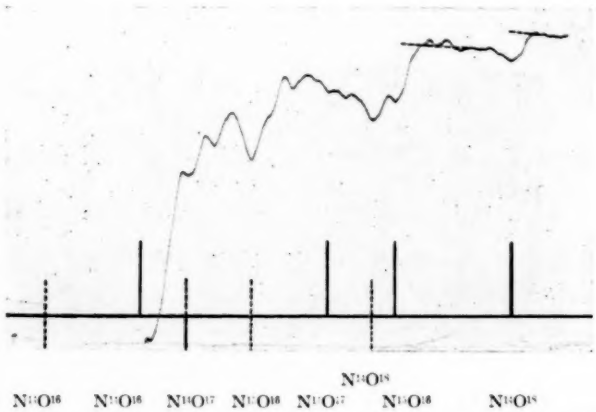

Fig. 1. A typical microphotometer curve of the (1, 0) γ-band of nitric oxide. The heads due to the different isotopic molecules are indicated. The full lines are the ${}^{O}P_{12}$ heads and the broken lines are the $({}^{P}Q_{12}+P_{12})$ heads.

where i_0 is the intensity (extrapolated) of the light which would have been transmitted if the band were not present. This equation reduces to

$$\log (i/i_0) = - k_1 c x \tag{6}$$

which is identical in form with Eq. (3).

Since k_1 and x are the same for the isotopic molecules

$$\log (i'/i'_0) - \log (i''/i_0'') = c'/c'' \tag{7}$$

where the primes refer to the quantities for the first and second molecules respectively.

These quantities are related to throws of the galvanometer by the relation

$$d = \log g_0 - \log g = f(\log i) \tag{8}$$

where g_0 is again the throw at a clear part of the plate and g is now the galvanometer throw at a band head or the estimated throw if the band were not present. In all cases our densities fell on the straight line portion of the d *vs.* $\log i$ curve and for this region

$$d = \gamma \log i + a. \tag{9}$$

A typical calibration curve is shown in Fig. 2. By using Eq. (9), we have

$$\gamma \log (i'/i_0') = d' - d_0' \tag{10a}$$

and

$$\gamma \log (i''/i_0'') = d'' - d_0'' \tag{10b}$$

where d and d_0 refer respectively to the density at the band head and the extrapolated density and the primes and double primes refer to the light and heavy isotopic molecules, respectively. These four points are indicated for a typical case on Fig. 2.

Taking the ratio, we secure the ratio of concentrations

$$\frac{\log i'/i_0'}{\log i''/i_0''} = \frac{d' - d_0'}{d'' - d_0''} = c'/c''. \tag{11}$$

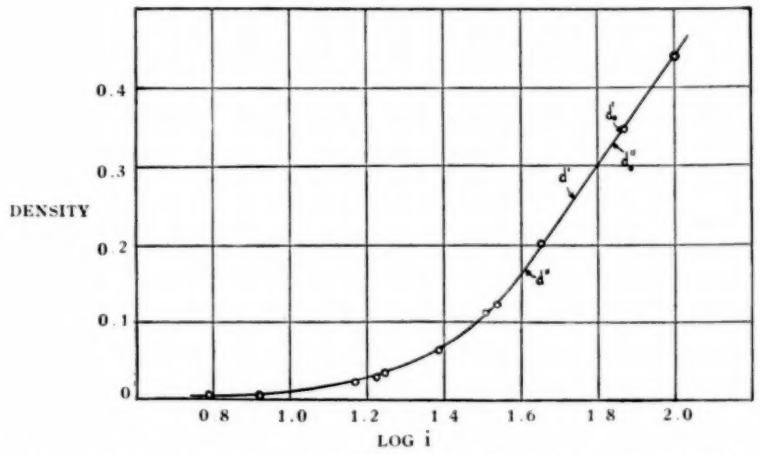

Fig. 2. A typical log i *vs.* density curve. The points indicated with arrows are those obtained from the microphotometer curves of the spectra and used for determining the ratio.

In this way we have compared the relative intensities of the ${}^{O}P_{12}$ branches of $N^{14}O^{18}$ and $N^{15}O^{16}$. Although the $N^{15}O^{16}$ ${}^{O}P_{12}$ branch is superimposed on the $N^{14}O^{18}$ ${}^{O}P_{12}$ branch, they are well separated by the spectrograph and it is therefore possible to estimate the contribution of each molecule to the absorption. A typical microphotometer curve is shown in Fig. 1, where the eight band heads due to the two branches and the four molecules are in-

TABLE II.

Source of sample	Number of microphotometer curves	Ratio $N^{15}O^{16}/N^{14}O^{18}$
Haber process	17(a)	0.54 ± 0.05
Coal	9(a)	0.56 ± 0.08
Birkeland-Eyde	4(b)	0.52 ± 0.08
Chili salt-peter	4(b)	0.56 ± 0.09
Haber	8(b)	0.58 ± 0.06
Pre-Cambrian	6(a)	0.54 ± 0.06

(a) Plates calibrated by means of screens.
(b) Plates calibrated by means of wedge.

dicated. The results from the four samples of nitrogen and the sample of oxygen are given in Table II.

Source of Error

The error given which is the root mean square represents only the error, if no systematic error is present. The possible errors are:

(1) The lines at the head of these bands may not give a true continuous absorption so that Beer's law may not hold. We have used gas pressures up to 10 cm of NO hoping that the lines would be somewhat broadened in this way. We have also added N_2 up to one atmosphere total pressure for the same purpose but in neither case was there any essential difference in the appearance of the microphotometer curves.

(2) It is not certain that there are no superimposed bands of $N^{14}O^{16}$. We had thought to eliminate this difficulty by working with the (2, 0) band but unfortunately a Si emission line from our hydrogen tube falls almost on top of the $N^{14}O^{18}$ $^{O}P_{12}$ band head. Moreover, the $^{O}P_{12}$ and $^{P}Q_{12}+P_2$ branches overlap here so we cannot allow for the continuous background.

Our most reliable determinations are those marked *a* in Table II since we have more confidence in the results from plates that were calibrated with the wire screens. The average from these thirty-two microphotometer curves is 0.549 ± 0.007 for the ratio of $N^{15}O^{16}:N^{14}O^{18}$. Because of the difficulties mentioned above, this result may be in error by more than the probable error quoted. But it seems certain that the possible source of error mentioned under 2 would be the same from sample to sample. Therefore, a change in the relative abundance of the isotopes of oxygen or nitrogen would have been detected. We feel safe in concluding that the isotopic composition of nitrogen and oxygen in the samples investigated is constant within approximately ± 10 percent.

Using Mecke and Child's[8] value for the ratio of $O^{16}:O^{18}=630:1$, we get for the ratio of N^{14} to N^{15}, the value 346:1 in satisfactory agreement with the ratio of 320:1 required by Birge and Menzel. This means that Aston's value for the atomic weight of N^{14} on the basis of $O^{16}=16.0000$ is consistent with the chemical value.

We wish to thank the Physics Department of this University and Professor H. W. Webb in particular for the use of the quartz spectrograph used in this investigation. We are also indebted to the Chemistry Department of New York University and to Mr. R. L. Garman in particular for the microphotometer curves.

Note added in proof. Herzberg (Zeits. f. physik. Chem. **B9,** 43 (1930)) has determined 800:1 for the ratio of N^{14} to N^{15} from the relative exposure times for the second positive nitrogen bands obtained in emission in an electrodeless discharge. This result differs from ours in the same direction as that of other workers for emission spectra compared with absorption spectra. Until this peculiarity is explained, relative abundances of isotopes obtained from absorption measurements seem more certain in view of the fact that the results in absorption make the values of Aston more consistent with the chemical results.

Mass-Spectrograph Study of the Ionization and Dissociation by Electron Impact of Benzene and Carbon Bisulfide

By ERNEST G. LINDER*
Cornell University, Ithaca, N. Y.
(Received June 9, 1932)

Benzene (C_6H_6) and carbon bisulfide (CS_2) have been analyzed by a mass-spectrograph designed especially for use with large molecules. In the case of benzene, ions have been found containing carbon in amounts from C_1 to C_6 with various amounts of hydrogen attached. The principal ion for electrons of 120 e-volts is $C_6H_6^+$. No negative ions and no H^+ ions were detected. Impacts of positive ions in the ionization chamber detach H atoms from the carbon ring, but the carbon content of all observed ions seems to be unaffected by such collisions. The carbon-to-carbon bonds appear to be more stable than in the straight-chain hydrocarbons. Carbon bisulfide was used principally to calibrate the mass scale, and no extensive work done on it. At a pressure of 9.7×10^{-3} mm Hg and impacts of 120 e-volts, the ions observed were CS_2^+, CS^+, S^+, and C^+.

THE only work which appears to have been done with the mass-spectrograph on large hydrocarbon molecules is that of Stewart and Olson,[1] who studied the straight-chain paraffins, propane (C_3H_8) and butane (C_4H_{10}). The present work on benzene (C_6H_6) was undertaken for the purpose of determining the behavior of a typical member of another important class of hydrocarbons, the aromatics, which are built up of rings of six carbon atoms, instead of straight chains, and therefore might be expected to exhibit a different sort of behavior in regard to dissociation by electron impact. The question was of interest to the writer in connection with studies of chemical reactions in electrical discharges, and that particular application of the data will be published in some chemical journal.

Apparatus and Procedure

Large molecules introduce additional difficulties to mass-spectrograph technique. High resolving power at large molecular weights is necessary, which requires the use of strong electric and magnetic fields, and slits as narrow as possible. The intensity is usually low because of the narrowness of the slits, and also because the ions are spread out over a large number of peaks. Furthermore, thermal dissociation at the filament must be eliminated, this problem being more acute with large molecules since they are in general more readily decomposed by heat.

Mass-spectrographs designed to eliminate thermal effects have been described by Stewart and Olson,[1] and Smyth and Stueckelberg.[2] In both these

* Detroit Edison Research Associate. The work described in this article is a part of an investigation of the fundamentals of the disintegration of organic dielectrics. It is supported by a fund provided by the Detroit Edison Company.

[1] Stewart and Olson, J.A.C.S. **53**, 1236 (1931).

[2] Smyth and Stueckelberg, Phys. Rev. **36**, 472 (1930).

apparatuses differential pumping was employed, the gas to be analyzed being introduced into the ionization chamber through a capillary and pumped out through two narrow slits, one opening into the magnet chamber and the other into the filament chamber. High speed pumps kept the pressures in these latter two chambers extremely low. Thus high pressure gradients at the slits were maintained, against which it seems very unlikely that any dissociation products formed at the filament could diffuse back into the ionization chamber. Thermal effects were decreased also by the use of low temperature, oxide-coated filaments.

Stewart and Olson give data indicating that thermal dissociation products were thus eliminated from the ionization chamber of their apparatus. The writer's mass-spectrograph was closely modelled after theirs, and the slit dimensions and pressure ranges employed were the same. It is therefore unlikely that thermal dissociation has appreciably affected the data given here. The similarity of the two apparatuses also renders comparison between the results more reliable.

For all of the data reported here a potential of 53 volts was used for drawing the ions out of the ionization chamber, the accelerating potential was about 515 volts. The radius of the ion path in the magnet chamber was 6.95 cm. The pressure in the magnet chamber was of the order of 10^{-5} mm Hg, while that in the ionization chamber was varied over the range from 10^{-3} to 80×10^{-3} mm Hg. This latter variation was effected, sometimes by changing the size of the capillary through which the gas was admitted, and sometimes by placing cooling baths of different temperatures around the bulb of liquid from which the vapor was drawn.

The benzene was purified as follows. Kahlbaum's thiophene free benzene was shaken six times with concentrated sulfuric acid. It was then washed with concentrated sodium hydroxide, with dilute sodium hydroxide, and finally with water until the wash water was neutral to litmus. It was dried over metallic sodium for 48 hours, and then distilled from the sodium. Then it was distilled three times, the middle fraction being taken each time. After being placed in the mass-spectrograph it was distilled twice in vacuum to remove dissolved gases. The carbon bisulfide used was Eimer and Amend's C. P. It was not treated in any manner before use.

In making the runs, the magnetic field was varied rather than the accelerating potential, on account of the unusually great mass range to be explored. The procedure was followed of starting with zero magnetic field and going up to the maximum necessary without reversals. This was done in order to get a more uniform mass scale. Reversals would introduce irregularities due to hysteresis and residual magnetism. At best however, it was found extremely difficult to avoid small accidental reversals due principally to heating of the rheostats and magnet coils. The field also appeared to vary appreciably with the temperature of the magnet core. Hence in general, the mass scale is not quite uniform. However all uncertainty in regard to the masses corresponding to the great majority of the peaks is removed by the calibration of the scale by means of the carbon bisulfide peaks.

Data and Discussion

A typical curve showing the various ions found is given in Fig. 1. For this run the energy of the impacting electrons was 120 e-volts, the pressure in the ionization chamber was 3×10^{-3} mm Hg, and that in the magnet chamber, 2.7×10^{-3}. Each peak is labeled with the formula of the ion to which it corresponds. No negative ions and no H^+ ions were observed, in agreement with the results of Stewart and Olson[1] on propane and butane, and that of Hogness and Kvalnes[3] on methane.

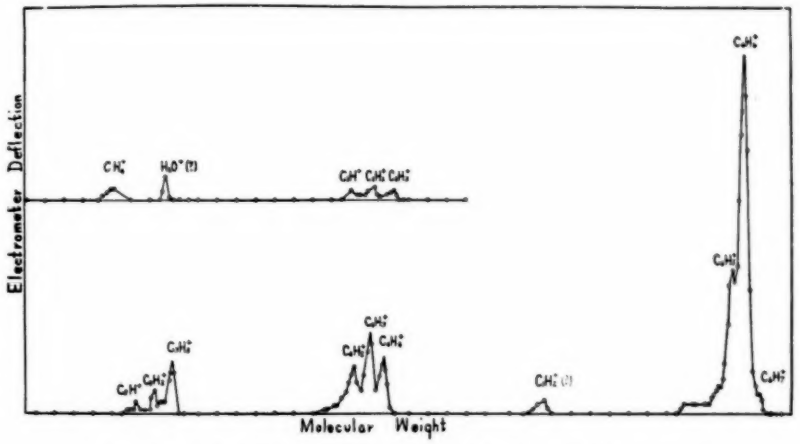

Fig. 1. Ions formed in benzene (C_6H_6) by 120 e-volt electrons.

In Table I is given the variation of ion percentage with pressure in the ionization chamber. A considerable number of runs were made in which measurements were taken only on the three largest groups of ions, i.e., the

Table I. *Percentages of ion groups formed by electron impacts in benzene at various pressures.*

Ion Group	Pressure (mm Hg$\times10^3$)			
	3.0	3.8	4.3	31.0
6C	71.5%	85.2%	57.0%	58.7%
5C	1.9	1.0	4.8	6.8
4C	16.1	9.9	21.6	23.7
3C	6.5	3.9	7.4	7.0
2C	3.3	0.0	4.4	1.8
1C	0.7	0.0	4.8	2.0

6C, 4C and 3C groups. The ion percentages for these three groups only (on the basis of 100 percent for the three groups only) are plotted in Fig. 2. These ion percentages were all determined by measuring the areas under the peaks with a planimeter, and correcting for the nonlinearity of the mass scale.

The scattering of the points in Fig. 2 is due principally to the difficulty of maintaining constant experimental conditions during the approximately two-hour period required to explore the large mass range. In spite of this scatter-

[3] Hogness and Kvalness, Phys. Rev. **32**, 942 (1929).

ing it is quite evident that the carbon content of these ions does not vary markedly with pressure. Likewise the hydrogen content was found not to vary, with the exception of the 6C group.

The variation of the shape of the 6C group with pressure is shown in Fig. 3. It will be observed that the structure on the left side of the peak increases with increasing pressure. This indicates that impacts made by the ions in the ionization chamber cause H atoms to be stripped from the carbon ring. The small peak corresponding to the molecular weight 79, which appeared in all the runs, is likely due to the attachment of a hydrogen atom to the $C_6H_6^+$ ion.

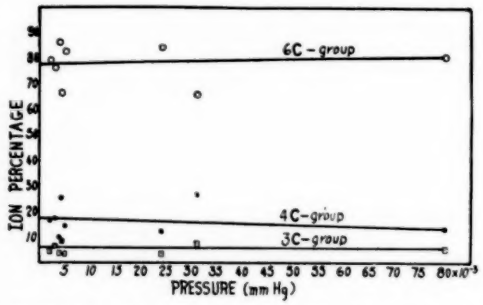

Fig. 2. Variation of ion percentage with pressure for benzene.

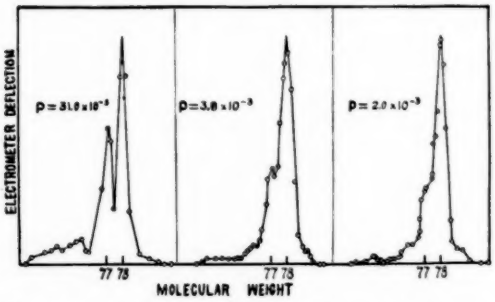

Fig. 3. Variation of 6C peak shape with pressure.

Attempts to determine critical potentials were unsuccessful due to low intensity. All that can definitely be concluded is that the appearance potential for the 6C peak is less than 40 volts.

In contradistinction to the results of Stewart and Olson[1] on normal paraffin hydrocarbons, the principal ion for benzene is a complete benzene molecule. For the paraffins, these authors found a very extensive dissociation into almost all possible lighter hydrocarbons, the ion corresponding to the entire original molecule being but a small percent of the total ions formed. Unfortunately they do not state the impacting energy of their electrons, but preliminary results of the writer's on octane, another straight-chain hydrocarbon, with 120 e-volt electrons, also show this extensive breaking up of the molecule. Thus it appears that straight carbon chains break up under electron bombardment more readily than does the six carbon ring.

This stability of the benzene ring may be partially due to the fact that in

order to divide a ring into two parts it is necessary to break it in *two* places, whereas to divide a straight chain into two portions it is necessary to break it in only *one* place. However the stability of benzene is doubtlessly due to other factors than this, since there are other six carbon ring compounds, e.g., cyclohexane, which are known from chemical evidence not to be nearly so stable as benzene.

A similar stability of the benzene ring in comparison with the paraffins has long been known in chemical reactions induced by heat,[4] and in various types of electrical discharges.[5] The reactions of benzene induced by these agents consist principally of polymerization and condensation, i.e., of the building up of more complex compounds by the adding together of benzene ring units with or without the evolution of a small amount of hydrogen. On the other hand, it is known that the normal paraffins under similar experi-

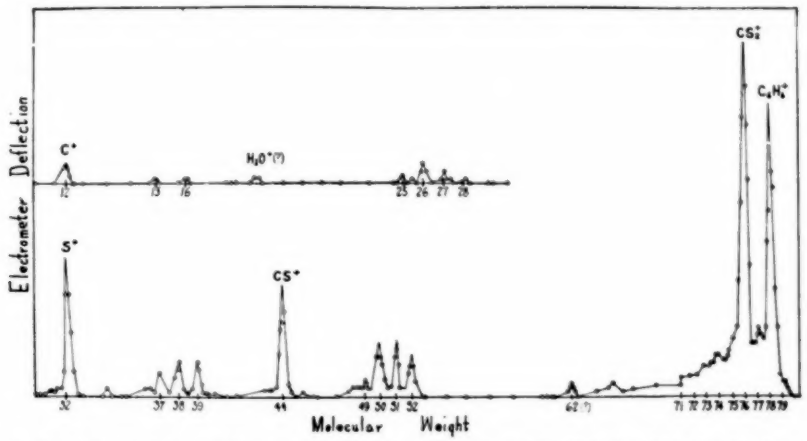

Fig. 4. Ions formed in a mixture of benzene and carbon bisulfide by 120 e-volt electrons.

mental circumstances suffer much more dissociation, and a much larger portion of the products are of a gaseous nature than in the case of benzene; see, for example, the work of Linder and Davis.[5]

The purpose of the runs with carbon bisulfide was to calibrate the mass scale and thus indentify the benzene peaks. However, since this compound seems not to have been investigated previously the data are of interest in themselves. The peaks observed are shown in Fig. 4 along with the benzene peaks. For this run the pressure was 9.7×10^{-3} mm Hg. The principal ion is CS_2^+, but peaks for S^+, CS^+, and C^+ are also present.

In conclusion the author wishes to express his thanks to the Cornell Physics Department for the laboratory facilities provided, and to Professor Vladimir Karapetoff, who is in general charge of the above-mentioned research program on dielectrics. He wishes especially to acknowledge his indebtedness to the President of the Detroit Edison Company, Mr. Alex Dow, and the Chief of Research, Mr. C. F. Hirshfeld, for the financial support of the above work and for permission to publish the results.

[4] Hurd, Pyrolysis of Carbon Compounds, Amer. Chem. Soc. Monograph No. 50.

[5] Linder and Davis, Jour. Phys. Chem. **35**, 3649 (1931).

Elastic Electron Scattering in Helium

By A. L. HUGHES,* J. H. MCMILLEN AND G. M. WEBB
Washington University, St. Louis

(Received June 4, 1932)

The scattering of electrons by helium atoms was measured experimentally over an angular range from 15° to 150° for electrons varying in speed from 25 to 700 volts. The scattering curves all fall steeply with angle, especially so for the smaller angles, provided that the speed is above 100 volts. For speeds below 100 volts, the steep fall at small angles is followed by a gentle rise beginning near 90°. Within the range cited, no maxima in the angular scattering curves were found. The theory of Mott accounted for the 700 and 500 volt curves accurately over the whole range, and for the 350 volt curve, over the range 20° to 100°. Below 20° the experimental curve was steeper than the Mott curve, and above 100° the experimental curve was flatter than the Mott curve. As we go to lower energies, the departures from the Mott curve increase progressively. For small angles the theoretical curve is not steep enough and for large angles it is too steep. The results were also compared with the theory developed by Massey and Mohr taking into account certain factors omitted by Mott. While the newer theory accounts qualitatively for the upturn in the angular scattering curve, it fails to give its correct shape. It is shown how atomic structure factors, or F values, which are employed in the theory of x-ray scattering, can be inferred from these experiments in electron scattering.

THE scattering of electrons by helium atoms has been investigated by a number of physicists. Dymond and Watson,[1] who studied the angle distribution of 210 volt electrons between 5° and 60°, established the fact that the scattering curves for elastic collisions were considerably less steep than they would have been had the scattering been due solely to the attraction of the nucleus of the atom for the electron passing by it. Results of the same general type were obtained by Harnwell,[2] who investigated the scattering of electrons at three angles, 0°, 8°, and 16°, with electron energies varying between 75 and 300 volts. McMillen[3] obtained curves for the scattering of electrons by helium atoms, the angle range being from 7° to 60° and the electron energies varied from 50 to 150 volts. According to his results, the scattering curves fall off more steeply with the angle the higher the energy of the electrons. A discussion of the results obtained by McMillen, Harnwell, and by Dymond and Watson, and their connection with the theories put forward by Sommerfeld, Mott and Mitchell, will be found on page 1043 of McMillen's paper. Investigations of the scattering of electrons at a fixed angle (90°), as the energy of the electrons was varied, have been made by Kollath[4] and by

* This work was made possible by assistance to the senior author from a grant made by the Rockefeller Foundation to Washington University for research in science.

[1] E. C. Dymond and E. E. Watson, Proc. Roy. Soc. **A22,** 571 (1929).
[2] G. P. Harnwell, Phys. Rev. **33,** 559 (1929).
[3] J. H. McMillen, Phys. Rev. **36,** 1034 (1930).
[4] R. Kollath, Ann. d. Physik **87,** 259 (1928).

Werner.[5] Kollath's measurements and Werner's measurements were for the ranges 1 to 36 volts, and 40 to 300 volts, respectively. A considerable extension in the angular range was effected by Bullard and Massey[6] who studied the elastic scattering of electrons by helium, between 20° and 140° for energies varying from 4 to 50 volts. The new features in the scattering curves found by them are that, when the electrons have energies between 20 and 50 volts, the curves become practically flat between 90° and 140°, and that, when the energies are reduced below 10 volts, there is a decided rise in the curves from about 70° to 140°. Ramsauer and Kollath[7] made very extensive measurements of the scattering over a range extending from 15° to 167° for slow electrons (1.8 to 19.2 volts). In marked contrast to the scattering for faster electrons (e.g., above 50 volts), they found but little scattering at small angles (0° to 30°), then a gradual rise to a maximum (at 90° for 19 volt-electrons, and at 110° for 1.8 volt electrons) and after that a slow decrease. The theoretical papers which we have found useful in discussing our experimental results are those of Mott[8] and of Massey and Mohr.[9]

Mott's theory leads to the result that the number of electrons scattered elastically at any angle should decrease monotonically with increasing angle. However, Arnot[10] found that in many cases this was not true; the scattering curves fall steeply as the angle is increased to somewhere between 70° and 100°, but for larger angles the curves often pass through well-marked maxima and minima. These maxima and minima fade out as the speed of the electrons is increased. Now the speed at which these maxima and minima fade out appears to be higher, the greater the atomic number of the atom under investigation. It would appear therefore that the maxima and minima should vanish at comparatively low electron energies when helium is used to scatter the electrons. As Arnot did not include helium in his comprehensive study of electron scattering in gases and as Bullard and Massey did not use electrons of energy higher than 50 volts, it appeared to be very desirable to make a study of electron scattering in helium over a wide range of energies and angles.

Experimental Method

The method of measuring the scattering of electrons by helium was very much the same as that employed by us in our studies of scattering in argon[11] and in hydrogen.[12] However, a new apparatus was constructed in which the analyzer and the collision chamber were made small enough to allow both of them to be put inside a glass tube 4.25 inches in diameter, so that they could be well outgassed if necessary. The new apparatus was designed chiefly to allow us to investigate another aspect of the general problem of scattering,

[5] S. Werner, Proc. Roy. Soc. **A134,** 202 (1931).
[6] E. C. Bullard and H. S. W. Massey, Proc. Roy. Soc. **A133,** 637 (1931).
[7] C. Ramsauer and R. Kollath, Ann. d. Physik **9,** 756 (1931); **12,** 529 (1932).
[8] N. F. Mott, Proc. Roy. Soc. **A127,** 658 (1930).
[9] H. S. W. Massey and C. B. O. Mohr, Proc. Roy. Soc. **A132,** 605 (1931); **A136,** 289 (1932).
[10] F. L. Arnot, Proc. Roy. Soc. **A133,** 615 (1931).
[11] A. L. Hughes and J. H. McMillen, Phys. Rev. **39,** 585 (1932).
[12] A. L. Hughes and J. H. McMillen, Phys. Rev. **41,** 39 (1932).

but it happened also to be very suitable for investigation of elastic scattering in helium. A detailed description of the apparatus is postponed to a later paper. Pure helium was prepared by passing helium from a tank through charcoal in liquid air into a reservoir. From the reservoir the helium passed through a fine capillary tube and then through another tube of charcoal in liquid air into the apparatus, from which it was pumped out continuously. It was possible to use pressures as high as 0.02 mm because of the two factors which worked together, (1) the small dimensions of the apparatus and (2) the long mean free path of electrons in helium.

The experimentally-measured scattering coefficients are given in Table I. By the scattering coefficient we mean, as in our previous papers, the number of electrons scattered in a direction θ from that of the original beam, through unit solid angle, per unit length of path of the original beam, per single electron in the beam, per single atom in unit volume.

TABLE I. *Scattering coefficients* $\times 10^{+20}$.

700 volts		500 volts		350 volts		200 volts	
7°	1597.0	9.5°	1195.0	11°	2088.0	11°	3192.0
9.5°	1307.0	12°	1047.0	16°	1183.0	13.5°	2367.0
12°	914.0	22°	467.0	21°	717.0	16°	1930.0
17°	541.0	27°	284.5	26°	469.0	21°	1285.0
22°	272.0	37°	148.2	31°	334.0	26°	728.0
27°	182.0	47°	60.5	41°	160.0	31°	624.0
37°	65.8	57°	30.76	51°	90.1	41°	292.3
47°	30.7	67°	15.88	61°	53.1	51°	176.6
57°	15.5	77°	11.41	71°	36.7	61°	113.9
72°	8.12	87°	6.14	81°	23.4	71°	82.0
87°	5.10	107°	5.56	91°	27.1	81°	55.85
102°	3.97	127°	4.36	106°	8.3	91°	50.4
117°	3.56	137°	2.87	136°	7.4	101°	39.45
132°	3.44	147°	1.51	151°	8.4	111°	31.65
147°	1.54					121°	29.00
						131°	28.50
						141°	27.9
						151°	25.8

100 volts		75 volts		50 volts		25 volts	
14°	3121.0	17°	3010.0	12°	3570.0	15°	2430.0
19°	2097.0	22°	2145.0	17°	2505.0	20°	1852.0
24°	1550.0	27°	1547.0	22°	1732.0	25°	1325.0
29°	1055.0	37°	844.2	27°	1320.0	35°	1012.0
39°	660.2	47°	557.0	37°	827.0	45°	791.0
49°	451.0	57°	402.0	47°	615.0	55°	693.0
59°	307.5	67°	301.0	57°	410.2	65°	588.0
69°	201.5	77°	233.0	67°	347.5	75°	560.0
74°	169.7	87°	189.0	77°	280.2	85°	513.0
79°	159.7	97°	159.2	87°	242.0	95°	513.0
89°	116.8	117°	160.5	97°	208.0	105°	523.0
99°	103.2	127°	161.0	107°	205.0	115°	545.0
109°	100.2	137°	162.0	117°	205.0	125°	576.0
119°	86.0	142°	159.5	127°	214.5	135°	609.0
129°	85.4	147°	174.0	137°	222.2		
139°	83.7			142°	210.7		
149°	74.8						

The results are also shown graphically in Figs. 1 and 2. Two diagrams are necessary to avoid undesirable crowding of the curves. The heavy black lines

are the smoothed experimental curves and the experimental points through which they were drawn are indicated in an appropriate manner. When the heavy line is continuous it means that the experimental curve coincides with Mott's theoretical curve. When the heavy line is broken, it indicates that Mott's theoretical curve and the experimental curve no longer coincide. In this case the theoretical curve is shown as a *light continuous* line. Finally, where comparison is possible with the recent theoretical curves of Massey and Mohr,[13] these theoretical curves are indicated by a *light broken* line. The Mott curves are given by the formula

$$\alpha(\theta, v) = [(e^2/2mv^2)(Z - F)\ \mathrm{cosec}^2\,\theta/2]^2$$

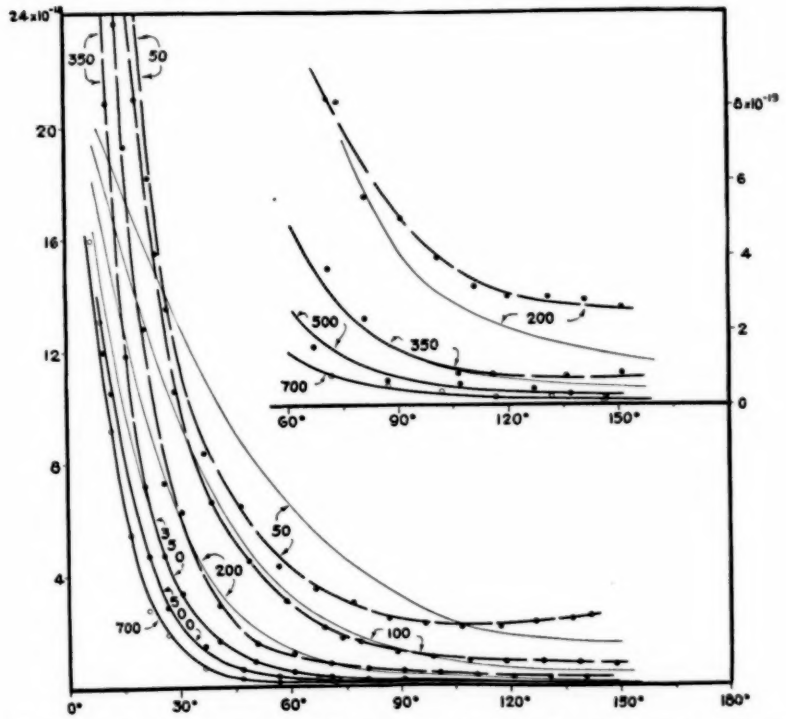

Fig. 1. Scattering of electrons by helium atoms. Angular distributions for 700 to 50 volt electrons. *Heavy continuous* lines: for experimental curves coinciding with Mott's theoretical curves. *Heavy broken* lines: for experimental curves not coinciding with Mott's theoretical curves. *Light continuous* lines: Mott's theoretical curves. *Inset:* Magnified diagram for the range 60 to 150 degrees.

where e, m, v are the charge, mass, and velocity of the electron, Z the atomic number of helium, θ the angle of scattering and F the atomic structure factor. F values for use in computing the formula were kindly supplied to us by Mr. Mott. Since then, they have been published in a paper by James and Brindley.[14] It was found that the 700 and 500 volt experimental curves fitted

[13] H. S. W. Massey and C. B. O. Mohr, Proc. Roy. Soc. **A132,** 605 (1931); **A136,** 289 (1932).

[14] R. W. James and G. W. Brindley, Phil. Mag. **12,** 81 (1931). The F values above 1.1μ were obtained by extrapolation according to the method outlined by D. K. Froman (Phys. Rev. **36,** 1339 (1930)).

Mott's formula exactly over the whole range. It will be seen that there is a slight departure from Mott's formula for the 350 volt curve at small angles and at large angles. For angles between 20° and 100° the coincidence is good. As we go to lower energies, the departure from the Mott formula becomes more and more marked. We do not show the Mott curve for the smallest electron energies, because the disagreement becomes too great to allow us to regard the theory as more than a very rough approximation to the experimental facts.

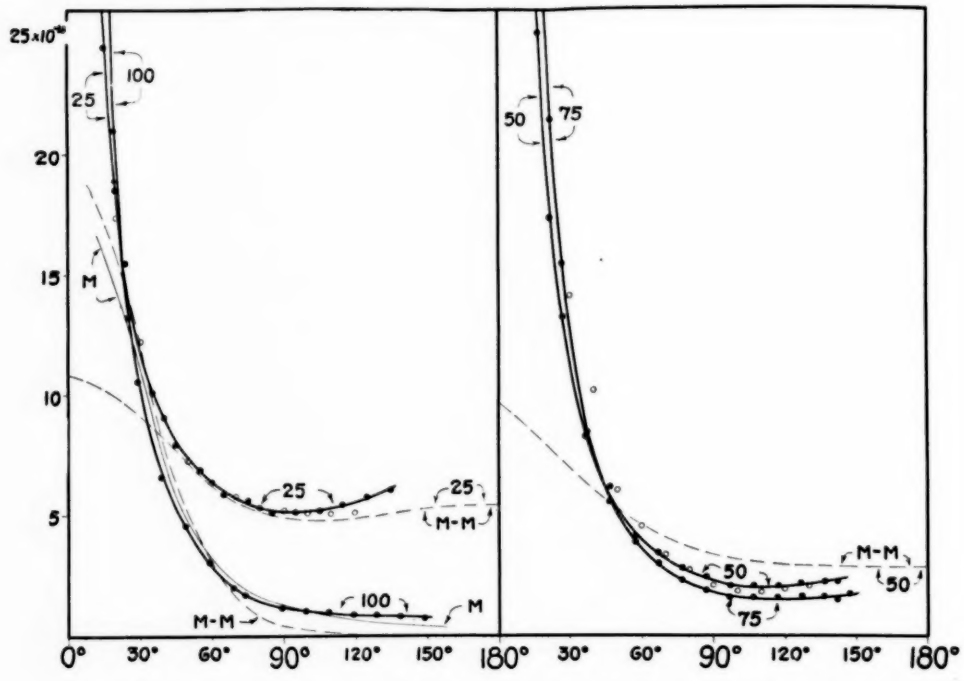

Fig. 2. Scattering of electrons by helium atoms. Angular distributions for 100 to 25 volt electrons. *Heavy continuous* lines: experimental curves. *Dots*: our experimental points. *Circles*: Bullard and Massey's experimental points (for the 50 and 25 volt curves only). *Light continuous* line: Mott's theoretical curve (for 100 volts). *Light broken* lines: Massey and Mohr's theoretical curve (for 25, 50 and 100 volts).

It should be emphasized that all the experimental curves and all the Mott curves shown in Figs. 1 and 2 are accurately drawn to the same scale. There was but one arbitrary adjustment (since our experimental arrangement did not give us accurate *absolute* values) and that was to make the 700 volt experimental curve fit the corresponding Mott curve. (The scattering coefficients, given in Table I, are obtained in this way.) When this was done it was found that the 500 volt curves fitted each other and that a departure from a perfect fit began to be discernable for 350 volts. The character of the departure of the experimental curves from the Mott curves is always of the same kind (at least down to 50 volts): the experimental curve is always steeper at small angles and always flatter at large angles. Moreover, the

experimental and theoretical curves cut each other twice as is evident from the diagrams; alternatively, at two points for each electron speed the Mott formula happens to give just the right value for the scattering.

In Fig. 1, an enlargement of the curves, for the region above 60°, is shown in the inset. In Fig. 2 we have assembled the experimental results and the theoretical curves for the lower electron energies. The 50 volt theoretical curve is taken from the more recent paper of Massey and Mohr[13] and the 25 volt theoretical curve is an interpolation between the curves they give for 20 and 30 volts. The 100 volt theoretical curve attributed to Massey and Mohr is taken from their earlier paper, as they do not give a 100 volt curve in their later paper. This procedure is of course open to question, since they believe that the method of calculation developed in the second paper is more dependable than the one used earlier.

In view of the fact that theoretical physicists are continually improving their methods of calculating electron scattering, it is therefore desirable to discuss briefly the accuracy of the experimental curves. The work of Bullard and Massey[15] overlaps our work in the region between 25 and 50 volts. We have therefore superposed their values on the corresponding curves in Fig. 2. It is clear that the agreement is very satisfactory. When one considers how different their experimental arrangements were from ours, one may now feel confident in assuming that both sets of results are free from serious error arising in some way or another from the peculiarities of the apparatus. Although we did not investigate the scattering for electrons moving with speeds less than 25 volts, it is possible to make the same sort of comparison between the results of Ramsauer and Kollath and those of Bullard and Massey in the region below 20 volts. Both investigations agree well as to the shapes of the 10 and 20 volt curves. However, there is no agreement between their 4 volt curves; all we can find in common between them is an upward trend as we go from 50° to 120°. The final conclusion to be drawn from the comparisons discussed in this paragraph is that, over the range 10 to 50 volts, the experimental angular distribution curves now available may be regarded as fairly exact, and free from systematic errors due to the particular type of apparatus used. This conclusion is based on the significant fact that there is very satisfactory agreement between the final results, where they overlap, although each investigation was carried out with an entirely different type of apparatus from that used in the other two investigations.

Our results were compared with those of Werner.[16] It will be remembered that Werner measured the scattering of electrons by helium, at a fixed angle 90°, and varied the energy of impact of the electrons. To effect a comparison, we measured the number of electrons scattered, at a fixed angle 37°, as the electron energy was varied from 25 to 700 volts. (This, incidentally, was the method whereby the relative magnitudes of the experimental curves in Figs. 1 and 2 were determined.) Then, using our experimental curves shown in Figs. 1 and 2, we calculated the relative scattering, at 90°, of electrons having

[15] E. C. Bullard and H. S. W. Massey, Proc. Roy. Soc. **A133,** 637 (1931).
[16] S. Werner, Proc. Roy. Soc. **A134,** 202 (1931).

speeds ranging from 25 to 700 volts. The results were in very satisfactory accord with those given by Werner.

Werner concluded that Mott's theory held for electron scattering by helium atoms so long as the electron energy was above 100 volts. This is true for the angle at which he worked, *viz.*, 90°, but an examination of Fig. 1 suggests that the conclusion has no particular significance, for it so happens that, at 90°, for 100 volt-electrons, the experimental curve and the Mott curve cross each other. Had any other angle been chosen the conclusion would have been such as to exclude 100 volt electrons from the generalization. From the curves shown in Fig. 1, we should be entitled to conclude that Mott's theory adequately describes the scattering of electrons at 90° so long as their energy exceeds an amount somewhere between 200 and 350 volts.

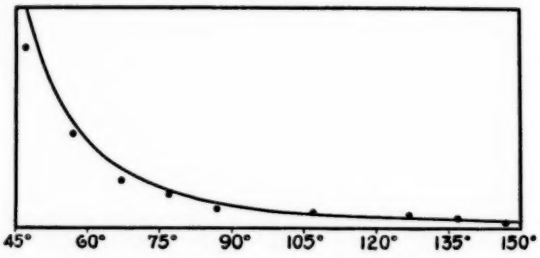

Fig. 3. Comparison of experimental scattering coefficient with values for a pure inverse square law scattering. *Continuous* line: graph of cosec $^4\theta/2$. *Dots*: experimental points for 500 volt electrons.

Mott's formula for electron scattering by atoms may be expressed in terms of μ, or in terms of v and θ, as follows,

$$\alpha(v, \theta) = [e^2/2mv^2(Z - F) \operatorname{cosec}^2 \theta/2\,]^2 \tag{1}$$

or,

$$\alpha(\mu) = [(e^2m/2h^2)(Z - F)(1/\mu^2)\,]^2 \tag{2}$$

where

$$\mu = [\sin(\theta/2)\,]/\lambda, \text{ and } \lambda = h/mv.$$

If the electrons within the atom contribute nothing at all to the scattering, the atomic structure factor F would be zero and the formula would then describe the scattering by a bare nucleus (Rutherford scattering, nuclear scattering, or inverse square law scattering). Now F is a function of μ which diminishes as μ increases, so that above a certain value of μ, F is negligible in comparison with Z. Evidently the larger μ is, (or, the larger θ is for a given electron speed), the more closely does the scattering approach Rutherford scattering. This is well illustrated in Fig. 3, which shows how closely the experimental points for 500 volt-electrons fit a $\operatorname{cosec}^4 \theta/2$ curve (Rutherford scattering), so long as the angles are greater than about 70°. Below this angle, it is necessary to use the Mott theory to describe the experimental results. This means that we can no longer neglect F in comparison with Z in the formula.

We may here recall the parallelism between Mott's theory of electron scattering and the theory of x-ray scattering. Eq. (2) can be resolved into two factors, $[(e^2m/2h^2)(1/\mu^2)]^2$ which measures the scattering by the nucleus per unit nuclear charge, and $(Z-F)^2$ which gives the effective nuclear charge. Here Ze is the total nuclear charge, whose full effect is diminished by the presence of the electrons within the atom by an amount which is measured by F, the atomic structure factor. F depends on the number of electrons within the atom and the way in which they are distributed. The formula for the scattering of x-rays by gaseous atoms is

$$\alpha(\theta, \lambda) = \left(F^2 + \frac{Z^2 - F^2}{Z}\right)\left(\frac{e^2}{mc^2}\right)^2\left(\frac{1 + \cos^2\theta}{2}\right). \tag{3}$$

If we retain only that part associated with coherent scattering, that is, the part most directly comparable with the elastic scattering of electrons, we have left

$$\alpha(\theta, \lambda) = (F^2)(e^2/mc^2)^2(1 + \cos^2\theta)/2. \tag{4}$$

Here the factor $(e^2/mc^2)^2(1+\cos^2\theta)/2$ denotes the Thomson scattering per single free electron, and the factor F^2 may be regarded as the effective number of electrons in the atom. Thus, in both x-ray scattering and electron scattering, the way in which the electrons are distributed in the atom leads us to the notion of an effective number of electrons which is measured by F the atomic structure factor. If all the electrons were concentrated at the nucleus, F would equal Z the total number of electrons within the atom, but because they are distributed over a finite volume the phase differences between the scattered waves for each electron lead to a value of F necessarily smaller than Z.

It is instructive to change Eq. (2) into

$$\mu^2[\alpha(\mu)]^{1/2}(2h^2/e^2m) = (Z - F). \tag{3}$$

If we replace the theoretical scattering coefficient $\alpha(\mu)$ by the experimental values I_{exp}, and then plot $\mu^2[I_{\text{exp}}]^{1/2}(2h^2/e^2m)$ against μ, we ought to get a graphical representation of $Z-F$. This is done in Fig. 4. If the F were always negligible in comparison with Z, then of course the graph would be a horizontal line parallel to the x-axis, whose height would be given by Z. The fact that it is not, indicates that F is, over a large range of μ's, of the same order of magnitude as Z. Indeed, we could say that the *points* plotted in Fig. 4 determine the atomic structure factor for helium atoms by means of electron scattering data. The *heavy continuous* line in Fig. 4 is a plot of $(Z-F)$ using the F values calculated by James and Brindley. (The *light continuous* line is a plot of F values obtained from x-ray data by Wollan[17] and Herzog[18].) The ordinates of the F curve and the $Z-F$ curve add up to Z as they should. The coincidence of the experimental points with the continuous line, over the range $\mu=0$ to $\mu=1.1$, of course shows that the Mott formula, in conjunction

[17] E. O. Wollan, Rev. Mod. Phys. **4**, 205 (1932).
[18] G. Herzog, Zeits. f. Physik **70**, 590 (1931).

with James and Brindley's F values, is adequate to describe electron scattering by helium atoms when the electron energy is not too low. It will be noticed that the experimental points for μ greater than about 1.1 are very irregularly distributed. This comes about from the peculiar way in which Fig. 4 involves the experimental results. Where the experimentally-measured quantities are small and difficult to measure accurately, the corresponding ordinates in the figure are large, but where they are large and easy to determine with precision the corresponding ordinates are small. Figs. 1 and 3 afford a fairer test of the relative accuracy of the results over the whole range of angle than does Fig. 4, but of course they do not bring out in so explicit a manner the shape of the curve showing the atomic structure factor as a function of μ.

The failure of Mott's theory to account for the experimental results when the electron energies are low has been attributed to the neglect of certain factors in the theory which are important only when the energies are relatively

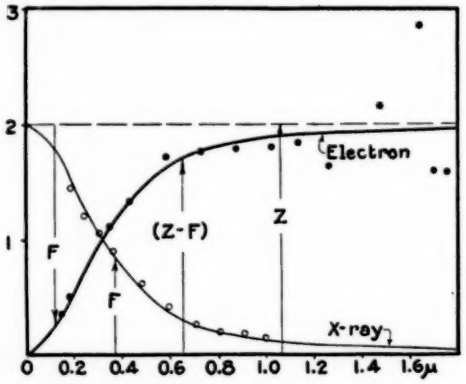

Fig. 4. Atomic structure factor for helium from electron scattering data. *Heavy continuous* line: From Mott's theory. Dots are experimental points. *Light continuous* line: F values according to Wollan.

low. Such factors are the distortion of the electron wave by the atom it passes over, electron exchange, and polarization of the atom by the electron. Massey and Mohr,[9] in the second of the papers referred to, computed the scattering when electron exchange and the distortion of the electron wave are taken into account. The calculations are difficult, and certain approximations have to be made in order to arrive at results. In Fig. 2 we show their 25 and 50 volt curves along with our experimental curves. It must be admitted that the agreement between theory and experiment is far from satisfactory. The upturn in the 25 volt curve is accounted for qualitatively by theory, but not the one in the 50 volt curve. There is also a serious difference at small angles (below about 50°) where the experimental curve is far steeper than the theoretical. In Fig. 2 we show the experimental curve for 100 volt-electrons, the Mott curve and the Massey and Mohr curve. (The Massey and Mohr curve for 100 volts is taken from their *earlier* paper in which they consider electron exchange effects, but not distortion of the electron wave. They do not give a 100 volt curve in their later paper.) It seems that, for 100 volt-electrons, the

original Mott theory gives a somewhat better agreement with experiment than does the theory of Massey and Mohr, although the latter theory takes into account the exchange effect which was supposed to be a cause of the deviation between the Mott theory and experiment.

It will be noticed that nowhere do we find a maximum in the scattering curves, although it is possible that one may be found at an angle greater than 150° for the low velocities. This is in qualitative accord with the results of Arnot, which indicate that the maxima in the scattering curves at large angles were more marked the greater the atomic number of the scattering atom.

We should like to thank Professor G. E. M. Jauncey and Dr. G. G. Harvey for information they have supplied to us in connection with the atomic structure factors.

The Infrared Dispersion of Carbon Dioxide

By HUGH M. SMALLWOOD
Mallinckrodt Chemical Laboratory, Harvard

(Received May 31, 1932)

The term in the dispersion equation of carbon dioxide corresponding to the bending vibration ($\lambda = 14.91\mu$) has been calculated from the assumption that this dispersion is due to interaction of the electric vector of the light wave and the permanent dipole moments associated with the carbon-oxygen valence bonds. The calculation indicates a magnitude of 1.17×10^{-18} e.s.u. for these dipoles, which is shown to be in agreement with the value to be expected from the measured moment of acetone.

THE experimental data on the refractive index of carbon dioxide, comprising a range from 1800A to 13μ, have been collected by Fuchs[1] and represented by a four-term dispersion equation, corresponding to the two ultraviolet and two infrared absorptions of the molecule. The term which takes account of the far infrared absorption is found by Fuchs to equal $8.1742 \times 10^{21}/(\nu_0^2 - \nu^2)$. When this empirical value is equated to the usual expression for dispersion ($Ne^2f/2\pi\bar{m}$), it is found that one must assume a value for the effective number of dispersion electrons f equal to 0.121. This result indicates the desirability of expressing the phenomenon in a somewhat different manner.

The properties of carbon dioxide have been shown to be best represented by the assumption of a symmetrical linear molecule.[2] The normal mode of vibration of this model, to which the far infrared absorption is ascribed, is a motion of the nuclei perpendicular to the line of symmetry (Fig. 1). Since this frequency is optically active, and since the resultant electric moment of the molecule is zero, it must be supposed that there is a permanent moment associated with each of the valence bonds, as shown by the heavy arrows in Fig. 1. This is, of course, also to be expected from the results of numerous

Fig. 1.

measurements of dipole moments of organic molecules. When placed in an oscillating electric field, this molecule will execute forced vibrations due to the couples exerted upon the dipoles. These forced vibrations result in a distortion of the molecule such that there is an average induced moment in the direction of the electric field. According to the present interpretation, it is this induced moment which is responsible for the infrared dispersion.

[1] O. Fuchs, Zeits. f. Physik **46**, 519 (1928).

[2] See, for example, K. W. F. Kohlrausch, *Der Smekal-Raman-Effekt*, p. 178, Berlin, 1931.

Consider a set of axes fixed in the molecule so that the carbon nucleus is stationary and at the origin, and the Y axis coincides with the line defined by the oxygen nuclei when at rest. The free vibration may then be compounded from one in the XY plane one in the YZ plane. Since the displacements are assumed to be small, the equations of motion for these component vibrations are

$$\left.\begin{aligned} \bar{m}\ddot{x} + 4\pi^2\nu_0^2\bar{m}x &= 0 \\ \bar{m}\ddot{z} + 4\pi^2\nu_0^2\bar{m}x &= 0 \end{aligned}\right\} \tag{1}$$

where $\bar{m}$ is the relative mass $(2m_om_c/2m_o+m_c)$ and ν_0 is the normal frequency of this mode of vibration. Let the molecule be subjected to the action of a beam of plane polarized light arbitrarily directed so that the direction cosines of the electric vector (at $t=0$) are α, β, γ. Then

$$\left.\begin{aligned} \mathbf{E} &= \alpha E, \beta E, \gamma E \\ E &= E_0 \exp\,[2\pi i\nu(t - r/w). \end{aligned}\right\} \tag{2}$$

The electrostatic potential energy of the molecule is

$$\epsilon = -(\boldsymbol{\mu}_1\mathbf{E}) - (\boldsymbol{\mu}_2\mathbf{E}). \tag{3}$$

Since it is assumed that $\boldsymbol{\mu}_1$ and $\boldsymbol{\mu}_2$ are directed along the lines joining the carbon nucleus with the two oxygen nuclei, and since $\boldsymbol{\mu}_1$ and $\boldsymbol{\mu}_2$ are assumed to have the same magnitude (μ),

$$\left.\begin{aligned} \boldsymbol{\mu}_1 &= -\mu x/d, \; -\mu(1 - x/d - z/d), \; -\mu z/d \\ \boldsymbol{\mu}_2 &= -\mu x/d, \quad \mu(1 - x/d - z/d), \; -\mu z/d \end{aligned}\right\} \tag{4}$$

where x and z are the displacements of the oxygen nuclei in the X and Z directions, respectively, and d is the carbon oxygen internuclear distance. Substituting Eqs. (2) and (4) in (3), it follows that

$$\epsilon = 2\mu E(\alpha x + \gamma z)/d. \tag{5}$$

From this equation may be obtained the X and Z components of the impressed force leading to the following equations for the forced vibration:

$$\left.\begin{aligned} \bar{m}\ddot{x} + 4\pi^2\nu_0^2\bar{m}x &= -2\mu E\alpha/d \\ \bar{m}\ddot{z} + 4\pi^2\nu_0^2\bar{m}z &= -2\mu E\gamma/d; \end{aligned}\right\} \tag{6}$$

$$\left.\begin{aligned} x &= -2\mu E\alpha/4\pi^2\bar{m}d(\nu_0^2 - \nu^2) \\ z &= -2\mu E\gamma/4\pi^2\bar{m}d(\nu_0^2 - \nu^2). \end{aligned}\right\} \tag{7}$$

The moment induced in the direction of the field is

$$\mu_i = \frac{1}{E}[(\boldsymbol{\mu}_1\mathbf{E}) + (\boldsymbol{\mu}_2\mathbf{E})]. \tag{8}$$

Upon substituting Eqs. (2), (4) and (7) in Eq. (8), it is found that

$$\mu_i = \frac{\mu^2 E}{\pi^2\bar{m}d^2(\nu_0^2 - \nu^2)}\{\alpha^2 + \gamma^2\}. \tag{9}$$

This expression must be averaged over all possible directions of $\mathbf{E}$, that is,

over all possible values of α and γ. Since the average of the square of the cosine is $\frac{1}{3}$, the polarizability per molecule is

$$\frac{\tilde{\mu}_i}{E} = \frac{2\mu^2}{3\pi^2 \bar{m} d^2 (\nu_0^2 - \nu^2)} . \tag{10}$$

The dispersion follows at once from the familiar expression

$$n - 1 = 2\pi N \tilde{\mu}_i / E \tag{11}$$

where n is the refractive index and N the number of molecules per cc. From Eqs. (10) and (11) it follows that the coefficient of $1/(\nu_0^2 - \nu^2)$ appropriate to this type of polarization is

$$C = 4N\mu^2 / 3\pi \bar{m} d^2 . \tag{12}$$

All of the quantities appearing in the expression for C are known with the exception of μ, the moment of the C=O bond in CO_2. Setting C equal to 8.17×10^{21} (Fuchs' value) and solving for μ, one obtains[3] 1.17×10^{-18}. This value is about what one would expect for the moment of the double bond uniting carbon and oxygen. The simplest molecule available for the measurement of the C=O moment is acetone,

$$\begin{matrix} H_3C \\ H_3C \end{matrix} \!\!\diagdown\!\!\diagup C = O,$$

the resultant moment of which is[4] 2.80×10^{-18}.

There is some uncertainty in the magnitude of the moment to be ascribed to the CH bond, but this quantity is probably not far from 0.5×10^{-18}. Since this moment is directed from carbon to hydrogen, and since the C=O moment is directed from oxygen to carbon, the latter dipole must equal 2.2×10^{-18}, if one assumes the group moments to be directed along the tetrahedral valence bonds. This value cannot, however, be compared directly with the moment in CO_2 for two reasons. In the first place, the figure 2.2×10^{-18} includes the moment induced in the two CC bonds of acetone by the CH and CO moments. This induced moment has the same direction as the CO moment so that the latter quantity must be less than 2.2×10^{-18}. Secondly, in CO_2 the two dipoles are so oriented that each lessens the other by induction. The extent of these two effects cannot be calculated for these molecules, but the results obtained for some substances that can be treated[5] indicate that the decrease due to each effect should be about $0.4 - 0.5 \times 10^{-18}$. Taking into account the induced moments, therefore, leads to the conclusion that the C=O moment calculated from the infrared dispersion is about what one would expect from the measured moment of acetone.

In conclusion, I wish to express my thanks to Professor K. F. Herzfeld for pointing out the opportunity for this calculation, and to Professor Linus Pauling for a suggestion which has proven valuable in the procedure used.

[3] d has been set equal to 1.15A, cf. W. V. Houston and C. M. Lewis, Phys. Rev. **37**, 227 (1931).

[4] C. P. Smyth, *Dielectric Constant and Molecular Structure*, p. 193, Chemical Catalog Co., 1931.

[5] H. M. Smallwood and K. F. Herzfeld, J. Am. Chem. Soc. **52**, 1919 (1930).

The Band Spectrum of Sulphur Monoxide

By EMMETT V. MARTIN
University of California, Berkeley, California

(Received May 16, 1932)

The spectrum of SO, which lies in the region 2400–4000A, has been photographed in the 2nd order of a 21-foot grating. The wave-numbers of the lines of the seven bands, (0,4), (0,5), (0,6), (0,7), (0,8), (0,9), and (1,4), are tabulated.

Rotational structure.—The analysis of the rotational structure leads to the assignment of the band system to a $^3\Sigma$, $^3\Sigma$ electronic transition, and yields the following values of the constants:

$r_e' = 1.769\times10^{-8}$ cm	$r_e'' = 1.489\times10^{-8}$ cm	$D_e' = -1.280\times10^{-6}$ cm^{-1}
$I_e' = 55.10\times10^{-40}$ gr. cm^2	$I_e'' = 39.02\times10^{-40}$ gr. cm^2	$\beta' = -3.56\times10^{-9}$ cm^{-1}
$B_e' = 0.5020\pm0.0005$ cm^{-1}	$B_e'' = 0.70894\pm0.00009$ cm^{-1}	$D_e'' = -1.129\times10^{-6}$ cm^{-1}
$\alpha_e' = 0.0062$ cm^{-1}	$\alpha_e'' = 0.00562\pm0.000013$ cm^{-1}	$\beta'' = -3.20\times10^{-10}$ cm^{-1}

Spin fine-structure. The triplets are resolved for $K>30$ and for $K<13$. However, due to overlapping of the different branches, the resolution for $K<13$ could be observed well in the (0,8) band only. It was found that, in order to represent adequately the observed separations of the triplets, it was necessary to modify somewhat the equations in Kramers' theory of spin tripling in $^3\Sigma$ states. The equations which best respresent the data are:

$$\Delta_{2-1} = A - B/(2K+3) - (\gamma'-\gamma'')(K+1)$$
$$\Delta_{2-3} = A + B/(2K-1) + (\gamma'-\gamma'')K$$

where, for the (0,8) band, $A=-2.11$, $B=-10.83$, and $(\gamma'-\gamma'')=+0.0150$. Of these three constants, A is the only one which is different for different bands; it ranges from -1.97 for the (0,4) band to -2.19 for the (0.9) band. We cannot determine which one, if either, of the two terms, A and B, represents the value of $3(\epsilon'-\epsilon'')$ in Kramers' theory. The values of $\Delta_2F_1(K)$ and $\Delta_2F_3(K)$ indicate that $\gamma'\sim+0.017$ and that $\gamma''\sim-0.003$.

Predissociation and perturbations. Bands with $v'=0$, 1, 2, and 3 are observed to break off at $K'=66$, 53, 39, and 6, respectively. No bands with $v'>3$ are observed. This effect is explained as predissociation, and is assumed to be caused by a $^3\Pi$ state. Not only do the rotational levels for different v' end at different values of K', but also the term value at which the break occurs decreases with increasing v'. If the potential energy curve for the $^3\Pi$ state is assumed to have a shallow minimum, a satisfactory explanation of the effect of rotation on predissociation is obtained by an application of Oldenberg's theory of dissociation by rotation. A further indication that the $^3\Pi$ potential energy curve has a shallow minimum is given by the observed perturbations of the rotational levels of the upper $^3\Sigma$ state. According to our interpretation, the term value at which the rotational levels for $v'=3$ terminate corresponds to dissociation of the normal state of the SO molecule. The energy of dissociation of this state, measured from the $v''=0$ vibrational level, is calculated to be 5.053 ± 0.001 volts.

Vibrational structure. The origins of several bands of the $v'=0$ progression are calculated, and the vibrational constants of the lower state determined from them. Since the bands with $v'>1$ are too much perturbed to permit an analysis of their rotational structure, it was necessary to use measurements of band heads to determine the vibrational constants of the upper state. The constants obtained are: $\omega_e''=1123.73\pm0.24$ cm^{-1}, $x_e''\omega_e''=6.116\pm0.017$ cm^{-1}, $\omega_e'=628.7$ cm^{-1}, and $x_e'\omega_e'=5.65$ cm^{-1}.

I. Introduction

THE sulphur monoxide band spectrum, which appears in the region 4000 to 2400A, was first described in 1906 by Miss Lowater.[1] A more complete study of this spectrum was made in 1924 by Johnson and Cameron,[2] who arranged the bands in series. In 1929, Henri and Wolff[3] photographed this system with a quartz-prism Littrow spectrograph, made the vibrational analysis, and assigned the spectrum to the molecule SO. As shown below, there is good evidence that their assignment of vibrational quantum numbers is correct; hence it has been used in this work. Because of insufficient dispersion, however, they were able to make only a partial analysis of the rotational structure. From the average second differences of the frequencies of the unresolved P and R series in a number of bands with $v'=0$, they evaluated the constant α'', which is defined by the relation:[3a]

$$B_v'' = B_e'' - \alpha''(v'' + \tfrac{1}{2}). \tag{1}$$

In order to determine B_e'', they then substituted α'' into the equation:

$$\alpha''\omega_e'' = 6B_e''^2 \tag{2}$$

where ω_e'' is the frequency of vibration for infinitesimal amplitude; ω_e'' was known from the analysis of the vibrational structure of the system.

Eq. (2) results from a special form[4] of the function assumed by Kratzer[5] for the potential energy of a diatomic molecule. This function can be written:

$$U = 2k(\tfrac{1}{2} - 1/\rho + 1/2\rho^2 - c_3\xi^3 - c_4\xi^4), \tag{3}$$

where $\rho = r/r_e$, $\xi = \rho - 1$, and k, c_3, and c_4 are constants. It can be shown that[4]

$$c_3 = \tfrac{1}{2}(\alpha\omega_e/6B_e^2 - 1), \text{ and } c_4 = (x_e\omega_e/3B_e - 1) - \tfrac{1}{2}5c_3(c_3 + 2), \tag{4}$$

where $x_e\omega_e$ is the coefficient of the second degree term in the expression for the vibrational term values. If c_3 and c_4 are set equal to zero, Eq. (2) follows. Birge[6] has calculated the values of c_3 and c_4 for the electronic states of a number of different molecules, and has found that, if they are neglected as in Eq. (2), values of B_e are obtained which are in some cases in error by as much as 50 percent. Therefore, it seemed likely that the value of B_e'' given by Henri and Wolff represented only the order of magnitude of the correct value.

Henri and Wolff concluded that the band structure consisted of a Q branch only, the lines of which were narrow multiplets. This type of structure appeared to be in marked contrast with that of the known band systems

[1] Frances Lowater, Ast. Jour. **23,** 324 (1906).

[2] R. C. Johnson and W. H. B. Cameron, Proc. Roy. Soc. **A106,** 195 (1924).

[3] V. Henri and F. Wolff, Jour. Phys. Rad. **10,** 81 (1929).

[3a] The notation used in this paper is that agreed upon by leading spectroscopists, as reported by R. S. Mulliken, Phys. Rev. **36,** 611 (1930).

[4] W. Weizel, Handbuch der Experimentalphysik, Ergänzungswerk, Band I, (1931). A.E Ruark and H. C. Urey, *Atoms, Molecules, and Quanta* (1930).

[5] A. Kratzer, Zeits. f. Physik **3,** 289 (1920).

[6] R. T. Birge, Unpublished work.

of O_2[7,8] and S_2[9] which lie in the same spectral region as the SO bands. Since these systems of O_2 and S_2 are quite similar, in that both result from the same type of electronic transition, it was expected that this system of SO would also have similar characteristics. In view of these uncertainties, it was considered to be of value to obtain new spectrograms under higher dispersion in an attempt to obtain unambiguous values of the molecular constants, and to clarify the apparently anomalous rotational structure.

II. Experimental Procedure

In the investigation by Henri and Wolff, the spectrum was excited by passing a spark discharge between small aluminum rods in a quartz bulb containing SO_2 at a pressure of 30–40 mm. A quartz window was placed close to the spark to avoid the absorption by SO_2 which occurs in the same spectral region as the SO bands. This method had the disadvantages that an exposure

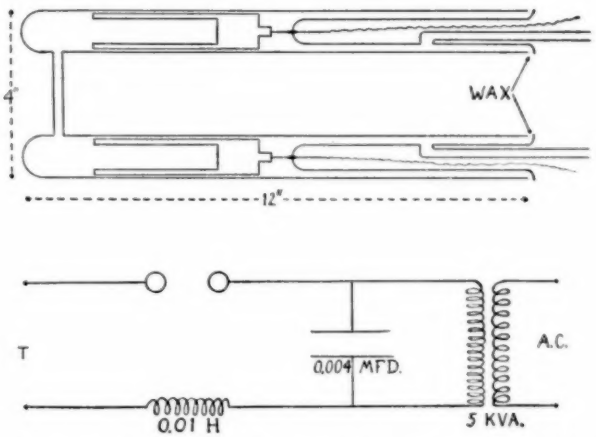

Fig. 1. Upper; diagram of the quartz discharge tube. The light was taken from the side of the constricted ($\frac{1}{4}$'' diameter) portion of the tube. Lower, schematic diagram of the electrical circuit. The leads marked *T* connect to the discharge tube.

of several hours was required even with a quartz spectrograph, and that it was necessary to interrupt exposure frequently in order to remove deposits of sulphur from the window and to allow the tube to cool.

A diagram of a discharge tube which does not have these disadvantages is shown in Fig. 1. This tube was constructed entirely of quartz, and was connected to the glass system by means of the wax seals shown. These seals were far enough removed from the discharge so that they were not overheated. The electrodes were heavy aluminum cylinders. A P_2O_5 drying tube, a liquid-air trap, and a two-liter flask comprised the remainder of the system. SO_2 was taken from a tank and frozen in the liquid-air trap; the system was then evacuated and allowed to fill with SO_2 to a pressure of about 20 mm. The two liter flask was necessary as a reservoir, because, even with this much volume.

[7] W. Ossenbrüggen, Zeits. f. Physik **49**, 167 (1928).
[8] W. Lochte-Holtgreven and G. H. Dieke, Ann. d. Physik **3**, 937 (1929).
[9] S. M. Naude and A. Christy, Phys. Rev. **37**, 490 (1931).

the pressure in the system would fall several millimeters in an hour, due to the removal of SO_2 by the deposition of sulphur on the walls of the tube and to the oxidation of the electrodes. The SO_2 could then be replenished from the liquid-air trap supply.

If the light was taken from the side of the constricted portion ($\frac{1}{4}''$ diameter) of the tube, there was no appreciable absorption by SO_2, and the heat produced by the discharge itself prevented the deposition of sulphur on this constricted part. Previous trials had shown the impossibility of using a tube of the "end-on" type, with which these difficulties could not be avoided.

The tube adopted therefore required no interruption of exposure to be cooled or cleaned, and, when excited with a heavy current, produced a comparatively high intensity of the spectrum.

The electrical circuit also is shown in Fig. 1. The transformer was actuated by a potential of 220 volts, and had an open-circuit secondary voltage of 10 kilovolts and a capacity of 5 k.v.a. The condenser consisted of two Leyden jars in parallel, and the self-inductance coil was constructed by winding No. 24 D.C.C. copper wire in a single layer on a long paper cylinder. Henri and Wolff showed that this type of circuit was practically necessary for the production of the spectrum with any intensity. An ordinary uncondensed discharge produces the band spectrum, but most of the energy goes into the production of a continuous spectrum in the same spectral region. On the other hand, a condensed discharge produces the line spectrum only. The optimum values of capacity and inductance are indicated in Fig. 1; they could not be changed from these values by a factor of more than about five without a change in the spectrum becoming noticeable.

The intensity of the spectrum was also dependent upon the pressure in the tube; it increased with increasing pressure up to about 2 cm, but appeared to remain practically constant for pressures above this value. The power applied to the tube was controlled by regulating the primary voltage of the transformer. To obtain the maximum intensity, the power was adjusted to the maximum value at which the tube could operate continuously. This value is estimated to be about 2 k.w.

The spectrograms used for measurement were taken on Eastman Speedway plates in the first and second orders of a 21-foot grating which has a dispersion in the second order of about 1.3 A/mm. The exposure time required was six hours. The lines were measured with a Société Genévoise comparator reading to 0.001 mm. The lines of an iron arc in air were used as comparison standards. The wave-lengths used were taken from the "Transactions of the International Astronomical Union"[10] and the "Publications of the Allegheny Observatory of the University of Pittsburgh."[11] The former gives values for the arc in air, the latter for the arc in vacuum. Unfortunately, no International standard wave-lengths are available for the region below 3370A. However, the two sources agreed very closely for the wave-lengths which they both give; hence it was assumed that there was no appreciable error intro-

[10] Transactions of the International Astronomical Union, Vol. III, (1929).

[11] Publications of the Allegheny Observatory of the University of Pittsburgh, Vol. VI (1929).

duced by using for some of the standards the wave-lengths of the lines of the vacuum iron arc. The deviations of these lines from a smooth dispersion curve indicated that the SO band lines were measured with an absolute accuracy of about 0.01A, while combination relations showed for the sharper lines a relative accuracy within a band of about 0.003A.

III. Rotational Structure

The general appearance of the spectrum is shown in Fig. 2, a and b. The progression with $v'=0$ is predominant, and its most intense members, namely the (0, 4) to (0, 9) bands inclusive, are almost entirely free from overlapping by other bands of the system. These bands were therefore most suitable for the determination of the molecular constants. The constants of the lower states having $v''=4$ to 9, and of the upper state having $v'=0$, could be accurately determined from these bands, while for the upper state having $v'=1$, the (1, 4) band was found to be most suitable. No bands with $v'>1$ could be used for this purpose; those with $v'=2$ were too much perturbed to permit an analysis of their structure, while those with $v'=3$ were extremely narrow, an effect which is explained below as due to predissociation. No bands with $v'>3$ are observed, also because of predissociation.

The structure of the bands with $v'=0$ is illustrated in Fig. 2, d and f, which show enlargements of the (0, 7) and (0, 5) bands respectively. These bands show one R and one P branch, each of which consists of narrow triplets. The two high-frequency components (to left in Fig. 2) of the triplets have a frequency separation which is dependent on the value of K, while the separation of the low-frequency member from the mean of the two high-frequency members is nearly independent of K. The absence of any noticeable Q branches indicates that the transition is one for which $\Delta\Lambda=0$. Furthermore, because of the considerable intensity of the system, the possibility of an intersystem transition ($\Delta S\neq 0$) can be ruled out. Since no Λ-type doubling is observed, both states must have $\Lambda=0$. The presence of triplet R and P branches shows that the electronic states involved belong to a triplet system. These facts point quite definitely to the conclusion that this band system is produced by a $^3\Sigma$, $^3\Sigma$ transition, as is the case for the analogous systems of O_2[7,8] and S_2[9] lying in the same spectral region. Since the final $^3\Sigma$ states for these systems of O_2 and S_2 are the normal states of these molecules, the final $^3\Sigma$ state for this system of SO is probably also the normal state.

The complete resolution of the spin tripling is one of the most interesting features of the SO bands. In the corresponding bands of O_2, the tripling is much smaller, and the components arising from F_1 and F_3 terms are barely resolved at the highest observed K values. In S_2, although the triplet separations are as large as in SO, overlapping is so serious that the data are irregular and incomplete.

The rotational levels of a Σ state are given by[12]

$$F_i(K) = B_vK(K+1) + f_i(K, J-K) + D_vK^2(K+1)^2 + \cdots \qquad (5)$$

[12] For details, see R. S. Mulliken, Rev. Mod. Phys. **2**, 105 (1931). The factor $\overline{G^2}$ has been omitted from Eq. (5).

where K is the quantum number of the angular momentum exclusive of spin, J is the quantum number of the total angular momentum and takes the values $J=K+S$, $K+S-1$, $\cdots$, $K-S$, and S is the resultant spin. For a triplet state, $S=1$; hence, for this case, $J=K+1$, K, and $K-1$. Since the difference in energy for different orientations of spin is small for Σ states (Hund's case (b)), there will be, in this case, three rather closely spaced en-

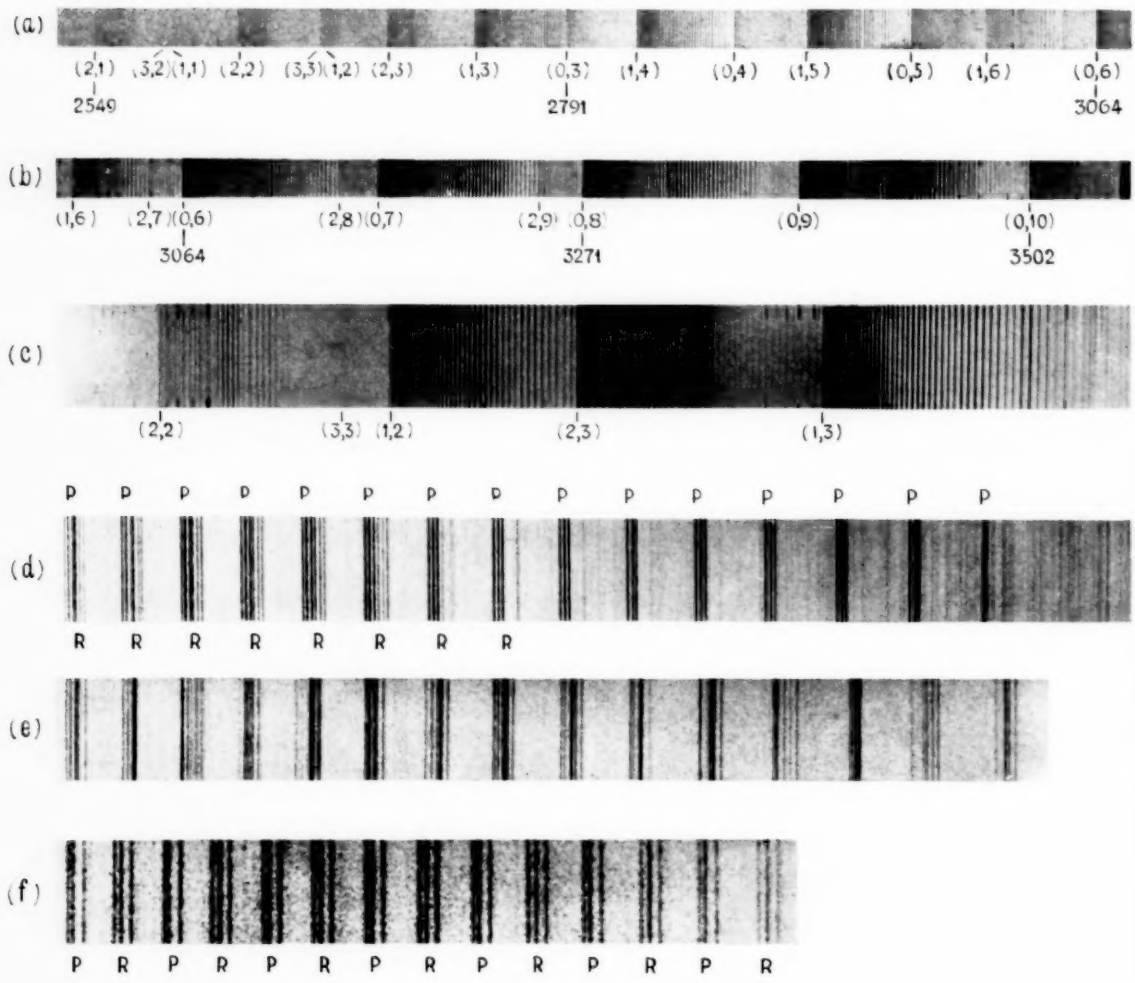

Fig. 2. Reproduction of the major parts of the SO emission spectrum, photographed with a 21-foot grating. (a) and (b). Contact prints of the region λ2500A to λ3550A, which contains most of the stronger bands. (c). Enlargement of the short wave-length end of the spectrum to show the abrupt termination of the bands with $v'=2$ and $v'=3$. This is especially well illustrated by the 2,2 band. The 3,3 band is probably too faint to show in the reproduction, but actually is only about 1 mm wide. (d). Enlargement of the end of the 0,7 band showing the abrupt ending of the R and P branches. (e). Enlargement of part of the 1,4 band illustrating the perturbations in the rotational structure. (f). Enlargement of part of the 0,5 band. The complete resolution of the triplets and their different relative spacing for adjacent lines, $R(K)$ and $P(K-6)$, are apparent.

ergy states for each value of K. These energy states are designated $F_i = F_1$, F_2, and F_3, where F_1 corresponds to $J = K+1$, F_2 to $J = K$, and F_3 to $J = K-1$.

Kramers[13] has shown that $f_i(K, J-K)$ for $^3\Sigma$ states is made up of two parts, one of which is due to the interaction of the resultant electron spin $S^*(=(S(S+1))^{\frac{1}{2}})$ and the magnetic field generated by the rotation of the nuclei, while the other is due to the interaction of the individual spins of the electrons. For the three values of J, $f_i(K, J-K)$ is given by

$$J = K+1 \qquad f_1 = -\epsilon + 3\epsilon/(2K+3) + \gamma K \tag{6}$$
$$J = K-1 \qquad f_3 = -\epsilon - 3\epsilon/(2K-1) - \gamma(K+1) \tag{7}$$
$$J = K \qquad f_2 = +2\epsilon - \gamma. \tag{8}$$

In these equations, terms containing γ arise from the interaction of the resultant spin and the magnetic field generated by the nuclear rotation, and those containing ϵ arise from the interaction of the individual spins.

The lines of the R and P branches are defined by the relations:

$$R_i(K) = \nu_0 + F_i'(K+1) - F_i''(K) \tag{9}$$
$$P_i(K) = \nu_0 + F_i'(K-1) - F_i''(K) \tag{10}$$

where ν_0 is the wave-number of the origin of the band under consideration.

In the analysis of a $^3\Sigma$, $^3\Sigma$ band system, it is impossible to determine the signs of the γ's and ϵ's. This fact prevents an unambiguous assignment of all three R (or P) branches to the series R_1, R_2, and R_3 (or P_1, P_2, and P_3). From the fact that f_2 is independent of K, we can identify the R_2 (or P_2) branch at once, but we cannot determine which of the other two R (or P) branches is R_1 (or P_1). In the present case, the low-frequency branch is R_2 (or P_2), while the high-frequency branch (for $K>18$) has been arbitrarily designated as R_1 (or P_1), by analogy with the corresponding convention used for S_2[9]. Table I gives the wave-numbers of the lines of the seven bands investigated. The lines indicated by asterisks are unresolved R_1 and R_3 (or P_1 and P_3) lines. The order in which the three branches are given in the table is, reading downward: R_1, R_3, R_2 (or P_1, P_3, P_2). This order is maintained for all of the bands with $v'=0$, and also for the (1,4) band up to $K=25$. For $K>25$, however, the (1,4) band is so much perturbed that it was impossible to arrange the R (or P) branches into three distinct series. The wave-length in I.A. of the head of each band is given at the top of the appropriate columns.

The correct designation of the lines by the values of K'' was obtained by the application of the combination principle. After a few preliminary trials, assignments were reached which yielded, for all bands with a common upper vibrational state, complete agreement in the term differences

$$\Delta_2 F_i'(K) = R_i(K) - P_i(K) = F_i'(K+1) - F_i'(K-1).$$

For the three components of the triplet, these differences should be given by:[14]

$$\Delta_2 F_1'(K) = 4B_v'(K+\tfrac{1}{2}) + 8D_v'(K+\tfrac{1}{2})^3 - 12\epsilon'/(2K+5)(2K+1) + 2\gamma' \tag{11}$$
$$\Delta_2 F_3'(K) = 4B_v'(K+\tfrac{1}{2}) + 8D_v'(K+\tfrac{1}{2})^3 + 12\epsilon'/(2K-3)(2K+1) - 2\gamma' \tag{12}$$
$$\Delta_2 F_2'(K) = 4B_v'(K+\tfrac{1}{2}) + 8D_v'(K+\tfrac{1}{2})^3. \tag{13}$$

[13] H. A. Kramers, Zeits. f. Physik **53**, 422 (1929).

[14] The omission of a term $+6D_v(K+\frac{1}{2})$ from these equations introduces no appreciable error, since $6D_v$ is entirely negligible in comparison with $4B_v$.

TABLE I. *Wave numbers of the lines of the (1, 4), (0, 4), (0, 5), (0, 6), (0, 7), (0, 8), and (0, 9) bands.*

K''	(1, 4) λ2827.395		(0, 4) λ2877.643		(0, 5) λ2968.470	
	R	P	R	P	R	P
7	—	35336.56*	—	34719.20*	—	33657.37*
	—	335.55	—	—	—	—
8	—	—	—	715.47*	—	653.36*
	—	331.38	—	—	—	—
9	—	—	—	711.20*	—	649.70*
	—	326.94	—	—	—	—
10	—	323.35*	—	706.57*	—	645.18*
	—	322.05	—	—	—	—
11	—	318.10*	34724.59*	701.61*	—	640.54*
	—	316.50	722.67	—	—	637.58
12	35337.35*	312.77*	721.13*	696.25*	—	634.53*
	335.55	310.86	719.20	694.13	—	632.18
13	333.28*	306.76*	717.41*	690.48*	33655.71*	628.84*
	331.38	304.84	715.47	688.41	653.85	626.79
14	328.99*	300.40*	713.10*	684.20*	651.74*	623.07*
	326.94	298.38	711.20	682.19	649.70	620.80
15	324.27*	293.73*	708.60*	677.68*	647.39*	616.51*
	322.05	291.72	706.57	675.64	645.18	614.49
16	319.12*	286.66*	703.60*	670.78*	642.67*	609.80*
	317.12	284.64	701.61	668.71	640.54	607.79
17	313.66*	279.16*	698.32*	663.47*	637.58*	602.68*
	311.65	277.16	696.25	661.44	635.52	600.61
18	307.69*	271.33*	692.66*	655.80*	632.18*	595.25*
	305.71	269.34	690.48	653.76	630.06	593.23
19	301.46*	262.96*	686.61*	647.76*	626.32*	587.42*
	299.54	261.07	684.56	645.81	624.33	585.39
20	294.94*	253.59*	680.21*	639.41*	620.07*	579.28*
	292.86	252.50	678.22	637.42	618.08	577.25
21	287.86*	245.31*	673.42*	630.62*	613.54*	570.69*
	285.86	243.52	671.45	628.64	611.47	568.66
22	280.41*	236.28*	666.33*	621.45*	606.65*	561.84*
	278.28	234.16	664.33	619.54	604.57	559.86
23	35272.64*	35226.26*	34658.75*	34612.00*	33599.32*	33552.57*
	270.05	224.31	656.74	610.01	597.26	550.54
24	264.36*	215.97*	650.83*	602.13*	591.74*	543.01*
	262.96	214.15	648.90	600.13	589.69	541.00
25	255.48*	205.77*	642.58*	591.88*	583.81*	533.07*
	254.36	203.06	640.59	589.83	581.75	531.00
26	247.66*	194.79*	633.95*	581.30*	575.45*	522.71*
	245.31	193.14	632.11	579.32	573.52	520.71
27	238.04	185.36	625.23	570.29*	567.02	512.03*
	—	183.20	624.73		466.48	
	235.78	181.94	623.01	568.25	564.71	510.01
28	228.54	172.52	615.82	559.16	557.92	501.03*
	—	—	615.34	558.72	557.43	
	226.26	170.16	613.60	557.07	555.68	499.18
29	218.16	160.35	606.07	547.51	548.57	489.68*
	—	—	605.54	547.02	548.02	
	214.15	158.05	603.86	545.30	546.23	487.65
30	207.42	148.12	596.06	535.41	538.76	478.16
	—	—	595.38	534.87	538.23	477.69
	206.61	145.56	593.64	533.16	537.42	475.90
31	197.37	135.03	585.48	523.04	528.63	466.04
	196.66	—	584.89	522.47	528.01	465.46
	194.79	132.58	583.17	520.70	526.35	463.78
32	185.97	121.73	574.64	510.15	518.16	453.62
	185.36	—	573.99	509.54	517.54	453.04
	181.94	120.67	572.32	507.86	515.79	451.33
33	175.13	108.65	563.41	497.00	507.34	440.78
	173.08	108.06	562.72	496.36	506.75	440.22
	171.66	106.21	561.10	494.58	504.97	438.49

TABLE I. (*Cont.*).

K''	(1, 4)		(0, 4)		(0, 5)	
	R	P	R	P	R	P
	160.35	094.35	551.85	483.39	496.10	427.60
34	—	—	551.10	482.72	495.45	427.00
	—	090.84	549.44	481.05	493.66	425.27
	150.33	081.18	539.87	469.44	484.49	414.12
35	149.74	079.14	539.08	468.70	483.76	413.45
	148.12	077.78	537.46	467.16	482.11	411.75
	137.48	063.82	527.56	455.16	472.56	400.21
36	136.84	—	526.85	454.45	471.88	399.57
	135.03	—	525.08	452.76	470.18	397.85
	35123.69	35050.98	34514.85	34440.49	33460.32	33385.93
37	—	050.34	514.03	439.76	459.48	385.34
	121.73	048.67	512.35	438.10	457.84	383.56
	110.91	035.47	501.69	425.47	447.63	371.37
38	109.96	034.81	500.86	424.78	446.80	370.63
	108.65	033.15	499.21	423.03	445.14	368.87
	097.02	018.98	488.24	410.07	434.58	356.44
39	095.82	—	487.37	409.21	433.71	355.56
	094.35	017.26	485.77	407.58	432.10	353.96
	082.60	003.44	474.41	394.20	421.21	341.05
40	—	002.58	473.43	393.44	420.26	340.21
	080.39	001.27	471.95	391.82	418.71	338.56
	067.23	34986.83	460.12	378.00	407.39	325.41
41	—	985.74	459.25	377.22	406.52	324.47
	065.26	984.32	457.70	375.59	404.93	322.86
	050.98	969.78	445.57	361.54	393.36	309.27
42	—	—	444.61	360.69	392.38	308.32
	049.31	967.56	443.13	359.10	390.80	306.77
	037.51	951.70	430.65	344.54	378.92	292.86
43	036.95	—	429.60	343.64	377.86	291.97
	036.27	949.81	428.13	342.13	376.29	290.47
	022.67	932.77	415.28	327.45	364.06	276.11
44	021.22	—	414.22	326.43	362.99	275.12
	019.85	931.14	412.75	324.87	361.45	273.52
	005.98	916.71	399.58	309.78	348.85	258.97
45	004.97	—	398.48	308.77	347.78	257.95
	003.44	915.78	397.05	307.27	346.23	256.43
	34989.33	899.14	383.47	291.88	333.25	241.52
46	988.48	897.66	382.36	290.62	332.16	240.46
	986.83	896.25	380.89	288.98	330.61	238.92
	972.23	879.65	367.01	—	317.31	223.60
47	971.44	878.76	365.90	—	316.15	222.50
	969.78	877.18	364.46	—	314.71	221.06
	955.06	860.41	350.20	—	301.04	205.42
48	—	859.53	349.01	—	299.88	204.25
	952.47	857.83	347.56	—	298.36	202.81
	936.91	840.66	333.06	—	284.49	186.83
49	936.08	839.82	331.75	—	283.14	185.67
	934.24	838.12	330.36	—	281.70	184.12
	35917.95	34820.77	34315.41	—	33267.36	33167.87
50	—	—	314.23	—	266.06	166.72
	916.71	818.20	312.72	—	264.67	165.24
	902.81	799.92	297.47	—	249.98	148.63
51	—	799.00	296.18	—	248.74	147.37
	899.98	797.32	294.71	—	247.25	145.99
	—	778.34	—	—	232.27	—
52	—	—	—	—	230.96	—
	881.98	777.30	—	—	229.38	—
	—	760.42	—	—	214.10	—
53	—	—	—	—	212.80	—
	—	757.64	—	—	211.41	—
	—	—	—	—	195.69	—
54	—	—	—	—	194.25	—
	—	—	—	—	192.85	—
	—	—	—	—	176.78	—
55	—	—	—	—	175.44	—
	—	—	—	—	174.02	—
	—	—	—	—	157.60	—
56	—	—	—	—	156.22	—
	—	—	—	—	154.62	—

TABLE I. (*Cont.*).

K''	(0, 6) λ3064.059		(0, 7) λ3164.761		(0, 8) λ3270.958		(0, 9) λ3383.114	
	R	P	R	P	R	P	R	P
5	—	—	—	—	30559.65	—	—	—
	—	—	—	—	560.89	—	—	—
	—	—	—	—	—	—	—	—
6	32624.35*	32611.17*	—	31572.68*	559.07	—	—	29533.82
			—		560.21	—	—	—
	—	—	—	—	—	—	—	531.72
7	622.85*	607.86*	—	569.22*	558.23	30543.42	29544.76	529.72
			—		559.65	—	546.24	—
	—	605.32	—	—	—	541.82	—	528.63
8	620.97*	604.17*	—	565.56*	556.90	540.00	543.59	526.35
			—		557.93	541.14	544.76	526.94
	—	601.71	—	563.53	555.28	538.31	541.38	524.95
9	618.45*	599.74*	—	561.51*	555.28	536.19	541.99	522.63
			—		555.93	537.08	542.73	522.91
	—	597.64	—	559.52	553.33	534.44	539.78	520.81
10	32616.05*	32595.05*	—	31557.18*	30553.07	30532.06	29539.78	29518.69*
			—		553.52	532.75	540.62	
	—	593.08	—	555.21	550.99	530.20	538.04	517.15
11	613.14*	590.20*	31575.36*	552.48*	550.42	527.53	537.40	514.36*
					550.99	528.13	538.04	
	611.17	588.20	573.57	550.52	548.54	525.60	536.23	512.70
12	610.09*	585.04*	572.68*	547.46*	547.88*	522.59	534.65	509.69*
						523.05	535.53	
	607.86	583.00	570.55	545.49	545.66	520.67	532.78	507.92
13	606.54*	579.56*	569.22*	542.01*	544.55*	517.40	531.72	504.67*
						517.77	532.11	
	604.17	577.49	567.22	540.10	542.48	515.50	529.72	502.84
14	602.63*	573.67*	565.56*	536.39*	540.92*	511.89	528.63*	499.36*
						512.21		
	600.53	571.64	563.53	534.64	538.92	509.95	526.35	497.50
15	598.39*	567.49*	561.51*	530.73*	537.08*	506.34*	524.95*	493.89*
	596.29	565.65	559.52	528.57	535.04	504.16	522.63	491.71
16	593.82*	560.92*	557.18*	524.32*	532.99*	500.06*	520.81*	487.96*
	591.82	559.02	555.21	522.18	530.83	497.96	518.69	485.80
17	588.87*	554.04*	552.48*	517.63*	528.40*	493.56*	516.47*	481.68*
	586.86	552.05	550.51	515.49	526.28	491.41	514.36	479.46
18	583.68*	546.78*	547.46*	510.54*	623.54*	486.73*	511.86*	475.07*
	581.59	544.79	545.49	508.50	621.42	484.55	509.69	472.81
19	578.09*	539.21*	542.01*	503.15*	518.36*	479.55*	506.86*	468.09*
	576.04	537.03	540.10	501.08	516.18	477.42	504.67	465.86
20	572.08*	531.29*	536.39*	495.51*	512.87*	472.09*	501.57*	460.74*
	570.04	529.02	534.19	493.48	510.72	469.96	499.36	458.51
21	565.65*	523.07*	530.24*	487.45*	507.04*	464.28*	496.04*	453.14*
	563.71	520.86	528.17	485.41	504.88	462.11	493.89	450.95
22	559.02*	514.31*	523.87*	479.09*	500.92*	456.12*	490.08*	445.23*
	557.07	512.18	521.72	477.04	498.76	453.97	487.96	443.06
23	552.05*	505.36*	517.01*	470.35*	494.39*	447.66*	483.93*	437.07*
	550.15	503.09	514.98	468.28	492.28	445.49	481.68	434.89
24	32544.79*	32496.01*	31509.89*	31461.33*	30487.60*	30438.85*	29477.32*	29428.56*
	542.72	493.69	507.87	459.21	485.48	436.69	475.07	426.37
25	537.03*	486.32*	502.53*	451.94*	480.56	429.76*	470.52*	419.76*
					480 25			
	535.00	484.25	500.44	449.84	478.33	427.57	468.09	417.52
26	529.02*	476.27*	494.85*	442.17*	473.12	420.39	463.42	410.61*
					472.83	420.18	463.12	
	527.11	474.26	492.91	440.06	470.96	418.14	461.23	408.41
27	520.40*	465.89*	487.01	432.12*	465.36	410.66	455.93	401.15*
			486.65		464.97	410.36	455.59	
	518.54	463.83	484.65	429.99	463.10	408.38	453.57	398.92
28	511.67*	455.11*	478.58	421.75*	457.30	400.60	448.18	391.52
			478.19		456.89	400.27	447.76	391.19
	509.80	453.15	476.22	419.74	454.95	398.41	445.79	389.19
29	502.59*	444.08*	469.86	411.20	448.89	390.21	440.07	381.53
			469.38	410.79	448.38	389.82	439.65	381.10
	500.70	442.05	467.45	408.79	446.55	387.89	437.72	379.06

TABLE I. (*Cont.*).

	(0, 6)		(0, 7)		(0, 8)		(0, 9)	
K''	*R*	*P*	*R*	*P*	*R*	*P*	*R*	*P*
	493.17*	432.70*	460.72	400.19	440.15	379.58	431.73	371.03
30			460.24	399.72	439.61	379.06	431.16	370.65
	491.22	430.64	458.34	397.77	437.74	377.16	429.26	368.72
	483.73	420.96*	451.29	388.73	431.04	368.46	422.95	360.34
31	483.27		450.77	388.27	430.52	367.98	422.40	359.89
	481.44	418.86	448.90	386.38	428.59	366.10	420.47	357.93
	473.69	409.04	441.55	377.02	421.62	357.07	413.91	349.28
32	473.11	408.54	440.98	376.51	421.04	356.57	413.32	348.83
	471.30	406.74	439.13	374.60	419.24	354.69	411.42	346.91
	463.24	396.66	431.45	365.00	411.95	345.41	404.59	337.95
33	462.62	396.04	430.83	364.38	411.31	344.85	403.94	337.45
	460.76	394.25	429.03	362.61	409.47	342.93	402.03	335.56
	452.39	383.84	420.97	352.53	401.90	333.47	394.87	326.41
34	451.68	383.25	420.34	351.96	401.22	332.81	394.20	325.82
	449.94	381.45	418.56	350.20	399.38	330.95	392.33	323.90
	441.22	370.72	410.20	339.80	391.50	321.23	384.89	314.47
35	440.43	370.10	409.54	339.18	390.80	320.47	384.20	313.82
	438.70	368.35	407.79	337.38	388.97	318.58	382.31	311.92
	32429.69	32357.29	31399.11	31326.73	30380.77	30308.50	29374.56	29302.18
36	429.19	356.59	398.50	326.02	380.11	307.74	373.93	301.53
	427.20	354.82	396.64	324.26	378.26	305.88	371.97	299.63
	417.89	343.35	387.70	313.27	369.72	295.49	363.99	289.56
37	417.05	342.73	386.83	312.57	368.95	294.74	363.21	288.91
	415.27	341.01	385.12	310.78	367.14	292.89	361.31	287.02
	405.48	329.26	375.80	299.54	358.33	282.14	352.95	276.72
38	404.72	328.55	374.97	298.83	357.52	281.48	352.22	276.02
	403.10	326.80	373.24	296.92	355.72	279.49	350.32	274.08
	392.94	314.77	363.68	285.46	346.60	268.47	341.71	263.51
39	392.09	313.96	362.85	284.63	345.79	267.71	340.92	262.76
	390.41	312.23	361.13	282.87	344.08	265.84	338.99	260.87
	380.03	299.87	351.15	271.00	334.55	254.42	330.08	249.89
40	379.09	299.03	350.20	270.20	333.62	253.69	329.25	249.16
	377.49	297.31	348.58	268.44	331.94	251.83	327.42	247.30
	366.69	284.63	338.32	256.20	322.16	240.08	318.15	236.09
41	365.81	283.80	337.38	255.33	321.23	239.35	317.34	235.33
	364.17	282.09	335.80	253.68	319.58	237.59	315.47	233.43
	353.12	268.99	325.21	241.15	309.57	225.43	306.01	221.96
42	352.14	268.15	324.26	240.25	308.50	224.61	305.10	221.12
	350.48	266.49	322.59	238.55	306.86	222.90	303.26	219.32
	339.13	253.09	311.72	225.59	296.52	210.39	293.46	207.44
43	338.11	252.22	310.78	224.77	295.49	209.65	292.52	206.62
	336.52	250.67	309.06	223.10	293.88	207.94	290.77	204.82
	324.78	236.83	297.84	209.91	283.16	195.13	280.56	192.70
44	323.72	235.91	296.92	209.02	282.14	194.36	279.60	191.77
	322.16	234.26	295.21	207.28	280.48	192.63	277.83	189.98
	310.10	220.23	283.65	193.79	269.48	179.60	267.43	177.58
45	309.01	219.23	282.66	192.79	268.47	178.68	266.39	176.59
	307.47	217.65	280.98	191.25	266.80	177.00	264.67	174.88
	295.04	203.26	269.15	177.32	255.46	163.66	253.93	162.14
46	293.96	202.20	268.10	176.30	254.42	162.68	252.86	161.11
	292.40	200.68	266.44	174.76	252.76	161.01	251.06	159.42
	279.64	185.98	254.27	160.49	241.18	147.52	240.15	146.49
47	278.49	184.87	253.18	159.48	240.08	146.42	239.04	145.41
	276.96	183.30	251.55	157.85	238.40	144.77	237.31	143.69
	263.87	168.27	239.07	143.37	226.50	130.89	225.98	130.40
48	262.72	167.13	237.93	142.34	225.43	129.80	225.41	129.33
	261.16	165.60	236.36	140.66	223.73	128.16	223.20	127.54
	247.84	150.21	223.56	125.94	211.52	113.97	211.61	114.01
49	246.57	149.07	222.33	124.79	210.39	112.86	210.39	112.91
	245.10	147.52	220.81	123.12	208.72	111.17	208.71	111.34
	32231.35	32131.85	31207.55	31108.10	30196.15	30096.68	—	—
50	230.04	130.73	206.38	106.97	195.13	095.74	—	—
	228.62	129.17	204.85	105.37	193.35	093.93	—	—
	214.54	113.20	191.25	090.09	180.51	079.13	—	—
51	213.27	111.93	190.15	088.85	179.28	078.06	—	—
	211.84	110.42	188.53	087.28	177.68	076.33	—	—

TABLE I. (*Cont.*).

K''	(0, 6) R	(0, 6) P	(0, 7) R	(0, 7) P	(0, 8) R	(0, 8) P	(0, 9) R	(0, 9) P
	197.44	094.07	174.76	071.50	164.61	061.20	—	—
52	196.01	092.76	173.54	070.32	163.27	060.10	—	—
	194.41	091.31	171.84	068.76	161.51	058.53	—	—
	179.80	074.63	157.85	052.64	148.22	043.08	—	—
53	178.51	073.40	156.55	051.42	146.92	041.83	—	—
	177.06	071.93	155.05	049.89	145.37	040.25	—	—
	161.97	054.93	140.66	033.53	131.62	024.60	—	—
54	160.61	053.60	139.26	032.24	130.26	023.14	—	—
	159.17	051.96	137.79	030.53	128.74	021.39	—	—
	143.74	034.73	123.12	013.99	114.61	005.62	—	—
55	142.40	033.43	121.69	012.70	113.26	004.23	—	—
	140.92	031.98	120.15	011.17	111.71	002.70	—	—
	125.19	014.28	105.16	30994.16	30097.25	29986.33	—	—
56	123.70	012.92	103.65	992.79	095.74	984.88	—	—
	122.34	011.50	102.19	991.26	094.35	983.39	—	—
	106.26	31993.45	086.80	974.03	079.62	966.76	—	—
57	104.76	992.04	085.35	972.64	078.06	965.31	—	—
	103.37	990.62	083.88	971.11	076.68	963.79	—	—
	086.96	972.26	068.17	953.48	061.65	946.81	—	—
58	085.43	970.85	066.70	952.08	060.10	945.38	—	—
	084.06	969.46	065.24	950.58	058.53	943.83	—	—
	067.34	950.76	049.16	932.61	043.08	926.64	—	—
59	065.86	949.27	047.71	931.14	041.83	925.26	—	—
	064.50	947.85	046.24	929.70	040.25	923.73	—	—
	047.40	928.83	029.90	911.37	024.60	906.13	—	—
60	045.63	927.34	028.20	909.91	023.14	904.69	—	—
	044.69	925.98	027.08	908.46	021.91	903.17	—	—
	027.05	906.57	010.25	889.89	005.62	885.23	—	—
61	025.38	905.13	008.62	888.36	004.23	883.82	—	—
	024.07	903.69	007.22	886.91	002.70	882.26	—	—
	006.25	884.04	30990.20	868.01	29986.33	864.10	—	—
62	004.66	882.40	988.55	866.31	984.88	862.43	—	—
	003.32	881.31	987.19	865.26	983.39	861.35	—	—
	31985.20	31861.10	30969.87	30845.81	29966.76	29842.60	—	—
63	983.61	859.54	968.19	844.22	965.31	841.00	—	—
	982.22	858.14	966.80	842.79	963.79	839.55	—	—
	963.82	837.81	949.14	823.20	946.81	820.69	—	—
64	—	836.14	947.53	821.55	945.38	819.06	—	—
	960.81	834.86	946.07	820.18	943.84	817.67	—	—
	941.95	814.11	928.08	800.27	926.29	798.54	—	—
65	—	812.49	—	798.67	924.70	796.96	—	—
	938.64	811.08	925.52	797.27	923.17	795.44	—	—
	—	790.10	—	776.95	—	776.05	—	—
66	—	788.55	—	775.40	—	774.46	—	—
	916.99	787.13	—	773.90	902.63	772.97	—	—
	—	765.72	—	753.37	—	753.14	—	—
67	—	764.27	—	—	—	—	—	—
	—	762.40	—	750.81	—	749.92	—	—
	—	—	—	—	—	—	—	—
68	—	—	—	—	—	—	—	—
	—	—	—	—	—	726.91	—	—

* These lines are made up of unresolved R_1 and R_2 (or P_1 and P_2) lines. The order in which the R branches are given is, reading downward, R_1, R_2, R_2. The same is true of the P branches.

The combination differences,

$$\Delta_2 F_i''(K) = R_i(K-1) - P_i(K+1) = F_i''(K+1) - F_i''(K-1)$$

for the lower electronic state have the same form as Eqs. (11), (12), and (13), except that the (′) is replaced by the (″). Because of lack of space, the numerical values of the combination differences are not given here. However, they can be obtained directly from the data in Table I. The values for a given

interval obtained from different bands agree, on the average, to about 0.06 cm^{-1}. The values of $\Delta_2F_2(K)$, which are not a function of ϵ or γ, were used to determine the value of B_v. Graphs of $\Delta_2F_2(K)/(K+\frac{1}{2})$ as ordinate with K as abscissa were made for all bands investigated. The ordinate at $K=-\frac{1}{2}$ is an approximate value of $4B_v$. Since

$$B_v = B_e - \alpha(v+\tfrac{1}{2}), \tag{14}$$

the difference between the values of B_v and B_{v+1} obtained from these graphs gave a preliminary value of α. The value of B_e was then calculated from Eq. (14) and substituted in the relation $D_e=-4B_e^3/\omega_e^2$ to obtain the value of D_e. D_v is given by the relation $D_v=D_e+\beta(v+\frac{1}{2})$, where $\beta=\alpha^2/6\omega_e+(20\alpha B_e^2-32x_eB_e^3)/\omega_e^2$. The value of D_v thus obtained can be used to calculate $8D_v(K+\frac{1}{2})^3$, which, when added to the observed values of $\Delta_2F_2(K)$, yields a set of values $\Delta_2F_2{}^*(K)$ which are practically linear in $(K+\frac{1}{2})$. $\Delta_2F_2{}^*(K)$ is represented by

$$\Delta_2F_2{}^*(K) = \Delta_2F_2(K) - 8D_v(K+\tfrac{1}{2})^3 = 4B_v(K+\tfrac{1}{2}). \tag{15}$$

The least squares solution of this equation gives an accurate value of $4B_v$. The values of $4B_v$ thus obtained were fitted to Eq. (14) by the least squares method to obtain B_e and α.

The values of the molecular constants obtained from the data given above are listed in Table II.

TABLE II. *Constants of the rotational structure.*[15]

v'	B_v'	Constants	v''	B_v''	Constants
0	0.4989	$B_e'=0.5020\pm0.0005$ cm^{-1}	4	0.68367	$B_e''=0.70894\pm0.00009$ cm^{-1}
1	0.4927	$\alpha_e'=0.0062$ cm^{-1}	5	0.67793	$\alpha_e''=0.005622\pm0.000013$ cm^{-1}
		$I_e'=55.10\times10^{-40}$ gr. cm^2	6	0.67248	$I_e''=39.02\times10^{-40}$ gr. cm^2
		$r_e'=1.769\times10^{-8}$ cm	7	0.66674	$r_e''=1.489\times10^{-8}$ cm
		$D_e'=-1.280\times10^{-6}$ cm^{-1}	8	0.66124	$D_e''=-1.129\times10^{-6}$ cm^{-1}
		$\beta'=-3.56\times10^{-9}$ cm^{-1}	9	0.65548	$\beta''=-3.20\times10^{-10}$ cm^{-1}

Band	A	B	$\gamma'-\gamma''$
(0,4)	−1.97	−10.83	+0.0150
(0,5)	−2.02	"	"
(0,6)	−2.06	"	"
(0,7)	−2.09	"	"
(0,8)	-2.11 ± 0.01	" ±0.01	" ±0.0005
(0,9)	−2.19	"	"
	$\gamma'\backsim+0.017$	$\gamma''\backsim-0.003$	

Note: As mentioned later in the text, the signs of γ', γ'', and $(\gamma'-\gamma'')$ are somewhat arbitrarily chosen.

IV. Spin Fine Structure of the Rotational Levels

As pointed out above, the existence of three energy levels for each value of K is to be attributed to the mutual interaction of the individual spins com-

[15] The constants A, B, and γ are discussed in the following section. The values of r_e are calculated for the molecule $S^{32}O^{16}$, since these are by far the most abundant of the isotopes of these elements.

bined with the interaction of the resultant spin S^* and the magnetic field generated by nuclear rotation. The separations of these levels from the energy given by $B_vK(K+1)+D_vK^2(K+1)^2+\cdots$ are represented by Eqs. (6), (7) and (8). The rotational term differences are expressed by Eqs. (11), (12), and (13). If the terms in ϵ in these equations are neglected, as they may be except at low K, then

$$\Delta_2F_1(K) - \Delta_2F_3(K) = 4\gamma. \tag{16}$$

The value of 4γ is, in the present case, less than the experimental error; hence, for any one value of K, Eq. (16) does not give even an approximate value of γ, and the average for a large number of K values gives only a rough approximation. The values of γ' and γ'' were determined from each of the six bands with $v'=0$ by averaging all the available differences $\Delta_2F_1(K)$ $-\Delta_2F_3(K)$ for $K>25$. The values of γ' thus obtained ranged from $+0.025$ to $+0.011$ with an average $+0.017$. The values of γ'' ranged from -0.006 to -0.0006 with an average -0.003. No consistent variation of γ'' with v'' was observed. Although these values of γ' and γ'' represent only the order of magnitude of the correct values, they appear to be definitely of opposite sign. However, the above data alone are insufficient to determine whether γ'' is negative or positive, since we do not know which of the two high-frequency R (or P) branches is the theoretical R_1 (or P_1) branch.

It has been shown that the value of γ''[16] for the normal $^3\Sigma_g^-$ state of the O_2 molecule is negative,[13] and that the value of γ' for the excited $^3\Sigma_u^-$ state for the Schumann-Runge bands of O_2 also is negative.[8] For this reason, Naudé and Christy[9] have assumed that the values of γ for the normal $^3\Sigma_g^-$ and the excited $^3\Sigma_u^-$ states of S_2 also are both negative, since both have the same sign. A similar situation in SO, however, does not exist, since the sign of γ for the normal $^3\Sigma$ state is opposite to that for the excited $^3\Sigma$ state. If we assume that the sign of γ'' for SO is the same as that for the normal states of O_2 and S_2, then the designation of the high-frequency R (or P) branch as R_1 (or P_1) is correct.

The equations for the separations of the three components of the triplet in the R and P branches, obtained from Eqs. (9) and (10) are:

$$R_1 - R_3 = 6\epsilon'(2K+3)/(2K+5)(2K+1) - 6\epsilon''(2K+1)/(2K+3)(2K-1) + (\gamma'-\gamma'')(2K+1) + 2\gamma' \tag{17a}$$

$$R_2 - R_1 = 3(\epsilon'-\epsilon'') - 3\epsilon'/(2K+5) + 3\epsilon''/(2K+3) - (\gamma'-\gamma'')(K+1) - \gamma' \tag{18a}$$

$$R_2 - R_3 = 3(\epsilon'-\epsilon'') + 3\epsilon'/(2K+1) - 3\epsilon''/(2K-1) + (\gamma'-\gamma'')K + \gamma' \tag{19a}$$

$$P_1 - P_3 = 6\epsilon'(2K-1)/(2K+1)(2K-3) - 6\epsilon''(2K+1)/(2K+3)(2K-1) + (\gamma'-\gamma'')(2K+1) - 2\gamma' \tag{17b}$$

$$P_2 - P_1 = 3(\epsilon'-\epsilon'') - 3\epsilon'/(2K+1) + 3\epsilon''/(2K+3) - (\gamma'-\gamma'')(K+1) + \gamma' \tag{18b}$$

$$P_2 - P_3 = 3(\epsilon'-\epsilon'') + 3\epsilon'/(2K-3) - 3\epsilon''/(2K-1) + (\gamma'-\gamma'')K - \gamma' \tag{19b}$$

[16] The γ used here corresponds to $(-B)$ in Kramers' terminology (cf. reference 13) and to $(-D)$ in that of Lochte-Holtgreven and Dieke (cf. reference 8).

For $K \geqq 5$, the average of Eqs. (18a) and (18b) is:[17]

$$\Delta_{2-1} = 3(\epsilon' - \epsilon'') - 3(\epsilon' - \epsilon'')/(2K + 3) - (\gamma' - \gamma'')(K + 1) \quad (20)$$

and the average of Eqs. (19a) and (19b) is:[17]

$$\Delta_{2-3} = 3(\epsilon' - \epsilon'') + 3(\epsilon' - \epsilon'')/(2K - 1) + (\gamma' - \gamma'')K. \quad (21)$$

The interval between R_2 and the mean of R_1 and R_3, for K greater than about 5,[17] is:

$$\Delta_{2-1,3} = 3(\epsilon' - \epsilon'') - \tfrac{1}{2}(\gamma' - \gamma''). \quad (22)$$

This interval is the same for the corresponding P branches.

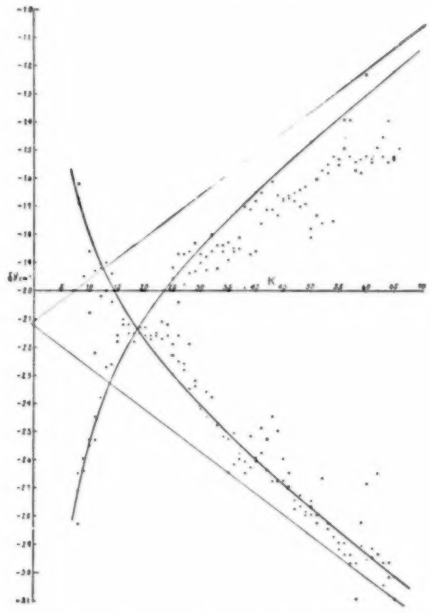

Fig. 3. Graphs showing the triplet separations in the 0,8 band. The ordinates for the circles and triangles represent, respectively, the observed separations of R_1 and R_3 from R_2, and of P_1 and P_3 from P_2. The curves are plotted according to Eqs. (23) and (24), where $A = -2.11$, $B = -10.83$, and $(\gamma' - \gamma'') = +0.0150$. These curves approach asymptotically the straight lines whose slopes are $\pm(\gamma' - \gamma'') = \pm 0.0150$.

The R_1 and R_3 (and P_1 and P_3) branches are resolved for $K > 30$, and, in some cases, for $K < 13$. The resolution for $K < 13$ was most satisfactorily observed in the (0,8) band, since this band showed very little overlapping of the different branches in the region of small K values. Accordingly, in order to determine the tripling constants as accurately as possible, the separations of the three components of the triplets of the (0,8) band were plotted on a large scale (Fig. 3). The circles and triangles represent, respectively, the wave-number separations of R_1 and R_3 from R_2, and P_1 and P_3 from P_2.

[17] These equations contain approximations of the type $(1/(2K+5))\,(1/(2K+1)) \sim (1/(2K+3))^2$, which are not very good for very low values of K.

According to Kramers' theory of spin tripling in $^3\Sigma$ states,[13] Eqs. (20) and (21) should represent the observed separations of the members of the triplets, at least for the smaller values of K. However, it was found that it was impossible to represent the data by using the same value of $3(\epsilon'-\epsilon'')$ in both of the first two terms of Eqs. (20) and (21). The equations which best represent the data for the (0,8) band, for low values of K, are:

$$\Delta_{2-1} = A - B/(2K+3) - (\gamma'-\gamma'')(K+1) \tag{23}$$

$$\Delta_{2-3} = A + B/(2K-1) + (\gamma'-\gamma'')K \tag{24}$$

where $A=-2.11$, $B=-10.83$, and $(\gamma'-\gamma'')=+0.0150$. Since there is at present no theoretical interpretation of this discrepancy, which also occurs in the $^3\Sigma_g^-$ normal state of O_2,[18] we cannot determine which one, if either, of two terms, A and B, represents the value of $3(\epsilon'-\epsilon'')$ in Kramers' theory.

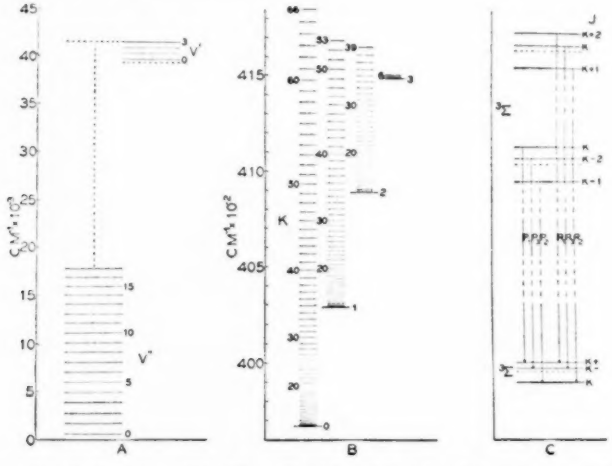

Fig. 4. Energy-level diagram. (A). The vibrational levels of the upper and lower $^3\Sigma$ states. No levels with $v'>3$ are observed. (B). The rotational levels of the upper state. This shows the values of K' at which the bands are observed to break off. (C). A schematic representation of the structure of the rotational levels of the two $^3\Sigma$ states. Only the levels associated with the lines $R(K)$ and $P(K)$ are shown. The separations of the actual levels from those which would exist if there were no spin are indicated qualitatively by the displacements of the full from the dashed lines.

The curves in Fig. 3 represent graphs of Eqs. (23) and (24) with the appropriate values of the constants A, B, and $(\gamma'-\gamma'')$. These curves approach asymptotically the straight lines whose slopes are $\pm(\gamma'-\gamma'')=\pm 0.0150$, and whose common intercept at $K=-\frac{1}{2}$ is $A-\frac{1}{2}(\gamma'-\gamma'')=-2.125$. The difference between the ordinates of the straight lines and of the corresponding curves represents the value of the terms containing K in the denominator in Eqs. (23) and (24). The data for low K values are represented well within experimental error, but for large K the data deviate considerably from sym-

[18] R. T. Birge and H. H. Nielsen, unpublished work on the atmospheric oxygen bands. The writer is indebted to Professor Birge for the methods used in the determination of the constants A, B, and $(\gamma'-\gamma'')$.

metry about the horizontal line $\delta\nu = -2.125$ cm^{-1}, due undoubtedly to the fact that the energy of interaction of S* and the magnetic field generated by the rotation of the molecule deviates appreciably from the linear form assumed in setting it equal to $\gamma(K^* \cdot S^*)$.[19]

The wave-number separations of the members of the triplets were plotted for all six bands with $v' = 0$, and the constants A, B, and $(\gamma' - \gamma'')$ were determined from them as accurately as possible. On account of the fact that overlapping prevented complete resolution of the branches at low K values for bands other than the (0,8), the constants obtained from these bands are undoubtedly less accurate than those obtained from the latter.

A schematic representation of the structure of the rotational levels is shown in Fig. 4c. Only the levels associated with the lines $R(K)$ and $P(K)$ are shown. The displacement of the actual levels from those which would exist if the spin were absent is indicated qualitatively by the displacements of the full from the dotted lines.

V. Predissociation and Perturbations

An unusual feature of the bands under consideration, and one which has considerable theoretical significance, is the abrupt termination of the band system at a certain definite value of the initial vibrational quantum number, namely $v' = 3$. It will be evident from the matrix diagram of Fig. 8 that no bands with $v' > 3$ are observed. The phenomenon is analogous to that found in the emission bands of S_2[9] and P_2,[20] and has been shown to be the result of predissociation. Furthermore, the rotational structure of the individual bands is found in all of the SO bands to break off suddenly at a particular value of K', the rotational quantum number in the upper state. This value is large for bands with $v' = 0$, but decreases with increasing v', and is very small for $v' = 3$.

The abrupt termination of the rotational structure of the (0,7) band is shown in Fig. 2d, while similar effects in the (2,2), (2,3), and (3,3) bands can be seen in Fig. 2c. The (3,3) band is extremely narrow, and so faint that it is difficult to observe on the enlargement, although it was easily visible on the original plates. Two other bands with $v' = 3$, which also present the same appearance, can also be seen on the original plates.

It has been shown by Bonhoeffer and Farkas,[21] and by Kronig,[22] that, if the discrete energy levels of an electronic state lie above the dissociation limit of another electronic state, there is, according to the quantum mechanics, a certain probability that a molecule in one of these levels will undergo a radiationless transition to the other electronic state, and dissociate spontaneously. This transition must obey certain selection rules derived by Kronig, and, if the conditions of the Franck-Condon principle are fulfilled, the probability

[19] R. S. Mulliken, Rev. Mod. Phys. **2,** 105 (1930) and references given there, especially J. H. Van Vleck, Phys. Rev. **33,** 467 (1929).

[20] G. Herzberg, Nature **126,** 239 (1930).

[21] K. F. Bonhoeffer and L. Farkas, Zeits. f. Physik Chem. **(A)134,** 337 (1927).

[22] R. de L. Kronig, Zeits. f. Physik **50,** 347 (1928); **62,** 300 (1930).

that such a transition will occur may be very great. In this case, the lifetime of the molecule in the discrete levels can become comparable with, or smaller than, the period of nuclear rotation. Accordingly, if these levels belong to the upper electronic state, the lines involving them will be diffuse in absorption, and either faint or absent in emission. This phenomenon is known as predissociation.[23]

Since the vibrational levels are spaced on a larger scale than the rotational levels, predissociation usually shows itself in absorption by the fact that the bands of the v' progressions become diffuse at a certain value of v', as was first observed in the S_2[24] spectrum. In emission, the same band progressions will terminate abruptly at this value of v'. The energy of this critical level represents, in some cases, the dissociation limit of the state which is causing the predissociation, and hence the phenomenon permits an evaluation of the heat of dissociation of the molecule. When the rotational structure is well resolved, as in the present case, observations on the exact value of the rotational quantum number at which the break occurs may lead to a very precise value of the heat of dissociation, and also give information of a new type concerning the mechanism of the process. The only case of this kind which has heretofore been studied is that of P_2,[20] where the resolution is less complete, and the details have not yet been published.

The K' values[25] of the last lines of the bands with $v'=0$, and $v'=1$, were found by application of the combination principle to be 66 and 53 respectively. However, the rotational levels for $v'=2$ were too much perturbed, and those for $v'=3$ too few, to permit an analysis of the rotational structure of bands involving these levels. Accordingly , the K' values of the last lines of these bands were determined from the wave-number difference between the head and last line of the band in question by means of Eq. (10), where B_v' and B_v'' were obtained from Eq. (14). These values of K' were found to be 39 for $v'=2$, and 6 for $v'=3$, but may be in error by one or two units.

The observed energy levels of the SO molecule are shown in Fig. 4; (A) shows the vibrational levels of both states, and (B) shows the rotational levels of the upper state. The rotational levels for different values of v' break off not only at different K values, but also at different energy values, and the energy at which the break occurs decreases with increasing v'. According to the interpretation of this effect given below, the term value at which the $v'=3$ levels break off (41,520 cm^{-1}) probably corresponds to dissociation of the lower electronic state. Linear extrapolation of the vibrational levels of the lower state gives 51,620 cm^{-1} as the term value corresponding to dissociation. However, it is well known that this extrapolation practically always leads to values which are considerably too large.[26]

[23] For a general discussion of predissociation, see G. Herzberg, Erg. exakt. Naturwiss. **10,** 207 (1931).

[24] V. Henri, Jour. Phys. Rad. **3,** 181 (1922); Structure of Molecules (1925).

[25] The use of K, instead of J, is justified by the fact that the three energy levels for a given K are much closer together than those with the same J.

[26] R. T. Birge, Nat'l. Research Council Bulletin on Molecular Spectra, (1926).

The oxygen atom and the sulphur atom each have a ^3P normal state and a ^1D first excited state. The energy of excitation of this ^1D state of oxygen is given by Frerichs[27] as 1.95 volts, and that of sulphur is estimated by Christy and Naudé[28] as 1.60 volts. Linear extrapolation of the vibrational levels of the excited state of SO leads to 56,840 cm^{-1} as the term value corresponding to dissociation of this state. If the convergence limit 41,520 cm^{-1} is subtracted from this limit at 56,840 cm^{-1}, we have 1.89 volts as the energy of atomic excitation. Although linear extrapolation of the levels of the excited state is especially untrustworthy in view of the fact that so few levels are observed, and that these levels may be perturbed, it seems probable that 1.89 volts is too high; therefore, we may assume that the sulphur atom is excited, and that 1.60 volts represents the energy of excitation. In this case, the dissocia-

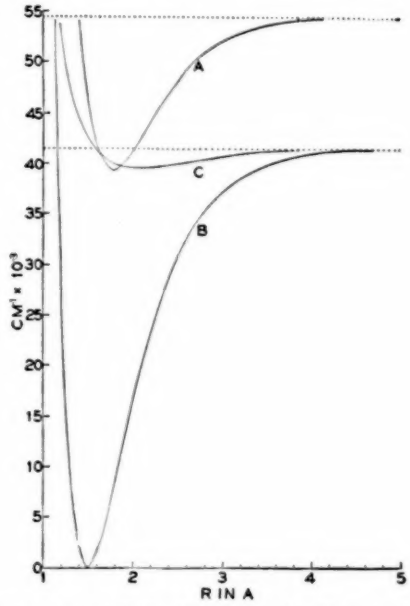

Fig. 5. Potential energy curves of the SO molecule. Curves *A* and *B* represent the two known $^3\Sigma$ states, and are plotted according to Morse's equation. Curve *C* ($^3\Pi$) has been assumed in order to account for predissociation.

tion limit of the excited $^3\Sigma$ state is at about 54,400 cm^{-1}, instead of 56,840 cm^{-1}, as obtained by linear extrapolation. Since this ^1D level is the first excited atomic state upon which the upper $^3\Sigma$ state of the molecule can be built, the dissociation limit at 41,520 cm^{-1} must represent dissociation into two normal ^3P atoms, and, therefore, dissociation of the normal state of the SO molecule.

Potential energy curves for the known states of the SO molecule are shown in Fig. 5; curves *A* and *B* represent the upper and lower $^3\Sigma$ states for

[27] R. Frerichs, Phys. Rev. **36,** 398 (1930).

[28] A. Christy and S. M. Naudé, Phys. Rev. **37,** 903 (1931), obtained the value for S by interpolation from the known values for O, Se, and Te atoms.

the observed bands, and are plotted according to Morse's[29] equation, while curve C must be assumed in order to account for predissocation. The electronic states represented by A and B are both $^3\Sigma$, and probably both $^3\Sigma^-$, since this is the case in O_2 and S_2. The molecule in state B is built of two ^3P atoms, and in state A of a ^3P and a ^1D atom. Since ^1D is the lowest excited atomic state, the molecule in state C, in order that C may cause predissociation, must also be built of two ^3P atoms. The possible electronic states of a molecule composed of two dissimilar ^3P atoms are:[30] two $^1\Sigma^+$, $^1\Sigma^-$, two $^1\Pi$, $^1\Delta$, two $^3\Sigma^+$, $^3\Sigma^-$, two $^3\Pi$, $^3\Delta$, two $^5\Sigma^+$, $^5\Sigma^-$, two $^5\Pi$, and $^5\Delta$. The selection rules for a radiationless transition of a molecule composed of two dissimilar atoms, as given by Kronig,[22] are: $\Delta\Lambda = 0, \pm 1$; $\Delta\Sigma$ and $\Delta S = 0$; $\Delta J = 0$; the transition can occur only between two rotational levels which are both positive or both negative. Accordingly, of the electronic states listed above, the only ones which can interact with the upper $^3\Sigma^-$ state are the $^3\Pi$ and the $^3\Sigma^-$ states. In addition to Kronig's selection rules, there is another requirement which must be fulfilled for two electronic states to be able to interact to any noticeable degree,[23] the potential energy curves of the two states must approach each other very closely. As shown in Fig. 5, the curves for the two $^3\Sigma^-$ states are everywhere well separated; hence these states cannot interact enough to cause predissociation. Therefore, the interacting state must be $^3\Pi$.

Herzberg[23] has suggested that the decrease with increasing v' of the term value at which the rotational levels break off, which was also observed in P_2,[23] is an effect of rotation of the molecule, and that an explanation is to be found by an application of the same principles which Oldenberg used to interpret the dissociation by rotation alone which occurs in the HgH bands.[31]

If we represent the potential energy of the molecule by $U(r)$, the force acting on the nuclei is given by $U'(r)$, the derivative of $U(r)$ with respect to the internuclear distance r. If the molecule is allowed to rotate, but not vibrate, it will expand to a new equilibrium position, such that the centrifugal force is equal to the attractive force; then $p^2/\mu r^3 = U'(r)$, where p is the angular momentum of the nuclei, and μ is their reduced mass. If the molecule then vibrates about this new position of equilibrium, with constant angular momentum, it will be acted upon by a restoring force $U'(r) - p^2/\mu r^3$. This force can be represented by the derivative with respect to r of the expression $U(r) + p^2/2\mu r^2$. The expression $p^2/2\mu r^2$ is equal to the kinetic energy of rotation of the molecule; or

$$T(r) = p^2/2\mu r^2 = BK(K+1) + DK^2(K+1)^2 + \cdots \tag{25}$$

Hence, with the assumption that the angular momentum is constant, $U(r) + T(r)$ is an "effective" potential energy, and has the same meaning for

[29] P. M. Morse, Phys. Rev. **34**, 57 (1929).

[30] R. de L. Kronig, Band Spectra and Molecular Structure (Cambridge), (1930); R. S. Mulliken, Rev. Mod. Phys. **4**, 1 (1932); E. Wigner and E. E. Witmer, Zeits. f. Physik **51**, 859 (1928).

[31] O. Oldenberg, Zeits. f. Physik **56**, 563 (1929). In the case of the HgH bands, the effect was due entirely to dissociation by rotation of the molecule in the lower electronic state, while in the present case, a radiationless electronic transition is involved.

a vibrating and rotating molecule that $U(r)$ has for a molecule which is vibrating, but not rotating.

As required by the Franck-Condon principle, $T(r)$ must be added to the $U(r)$ curve of each of the interacting states, and a radiationless transition can occur between only those $U(r)+T(r)$ curves which have the same $T(r)$ (i.e., same angular momentum). Accordingly, the shape of the $^3\Pi$ curve determines the intersections of its $U(r)+T(r)$ curves with those of the upper $^3\Sigma^-$ state, and, therefore, the term values at which the rotational levels break off. If the $^3\Pi$ state is assumed to be repulsive for all values of r, as Christy and Naudé[28] assumed for S_2, the decrease with increasing v' of the term value at which the rotational levels break off would be much greater than is observed. In order to satisfactorily explain the observed facts, it was necessary to assume a shallow minimum in the $^3\Pi$ curve, as shown in Fig. 5 (curve C).

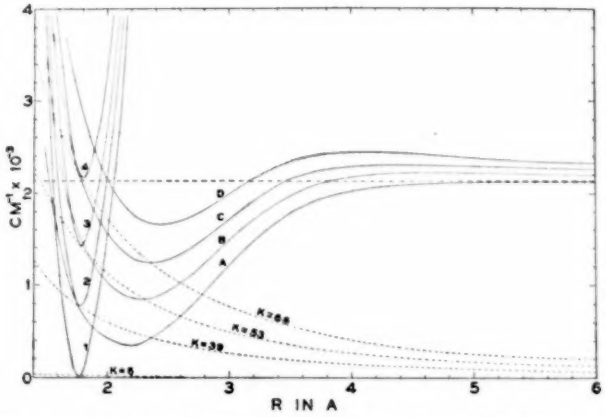

Fig. 6. *Effective* potential energy curves for the $^3\Pi$ and upper $^3\Sigma$ states for various amounts of rotation. The dashed curves represent the kinetic energy of rotation of the molecule, $T(r) = p^2/2\mu r^2$, for the K values indicated. Curves 2, 3, and 4 are obtained by adding the dashed curves to curve 1. Curves B, C, and D are obtained from A similarly. The horizontal dashed line, according to our interpretation, corresponds to the energy of dissociation of the $^3\Pi$ and lower $^3\Sigma$ states.

In Fig. 6, $U(r)+T(r)$ curves are plotted for states A (upper $^3\Sigma^-$) and $C(^3\Pi)$ of Fig. 5 for the four values of K' at which the rotational levels for the different values of v' are observed to break off. The dashed curved lines represent graphs of $T(r) = p^2/2\mu r^2$, where p, for a given K', has been evaluated from Eq. (26) by using B_e', D_e', and r_e'. Curves 1 and A of Fig. 6 correspond to curves A and C of Fig. 5 respectively, but are on a much larger scale. Curves 1 and A have also been taken to represent $U(r)+T(r)$ for $K=6$, since $T(r)$, in this case, is negligibly small for the values of r with which we are concerned here. Curves 2, 3, and 4 are obtained by adding the dashed curves $(T(r))$ to curve 1 $(U(r))$; curves B, C, and D are obtained from A similarly. The horizontal dashed line represents the term value at which the rotational levels for $v'=3$ are observed to break off.

If the molecule is in the upper $^3\Sigma^-$ state, and is rotating with $K=6$, its

potential energy is represented by curve 1, and, if in addition it is vibrating with $v'=3$, it has an energy corresponding to the horizontal dashed line. Accordingly, as the molecule vibrates along curve 1, it can undergo, at the points of intersection of 1 and A, an electronic transition, without any change of internuclear distance and momentum, from $^3\Sigma^-$ to $^3\Pi$, and begin vibrating along curve A. Since the molecule has sufficient energy, it vibrates along A to large r and dissociates. If $K'=66$, the molecule vibrates along curve 4, and can undergo a transition to curve D at the point of intersection. In this case, only the vibrational energy corresponding to $v'=0$ is required for the molecule to be able to pass the hump at large r in curve D and dissociate.

The Franck-Condon principle allows only the following transitions between the curves shown in Fig. 6: 1 to A, 2 to B, 3 to C, and 4 to D. These are the transitions which the molecule undergoes when it dissociates with $v'=3$, 2, 1, and 0, respectively. If the molecule has only the vibrational energy corresponding to $v'=0$, then, in order to dissociate, it must also have rotational energy corresponding to $K'=66$. For $K'>66$, the molecule can also dissociate, and, if the probability that this will occur is sufficiently great, spectrum lines involving these levels will not be observed in emission. A similar argument applies to the other vibrational levels.

The fact that the height of the hump at large r in the $U(r)+T(r)$ curves of the $^3\Pi$ state increases with increasing rotational energy requires the total (vibrational plus rotational) energy necessary for predissociation to increase with decreasing vibrational energy. Accordingly, the rotational levels for $v'=0$ break off at a term value greater than those for other v' levels by just the difference in the heights of the humps in the corresponding $U(r)+T(r)$ curves of the $^3\Pi$ state. If we assume that the $^3\Pi$ state has the $U(r)$ curve shown in the figures, the agreement between the heights of these humps and the term values at which the rotational levels for the various values of v' are observed to break off is quite satisfactory.

As mentioned above, the $^3\Pi$ state cannot be repulsive for all values of r, because its $U(r)+T(r)$ curves would then intersect those of the $^3\Sigma^-$ state with the same angular momentum considerably above the dissociation limit of the $^3\Pi$ state (except for small angular momentum), with the result that the decrease with increasing v' of the term value at which the rotational levels break off would be much greater than is observed. In order than an appreciable interaction between the $^3\Pi$ and upper $^3\Sigma^-$ states shall occur, the potential energy curves for these states must intersect.[23] Accordingly, the minimum in the $^3\Pi$ curve must occur at large r and be shallow, which means a low frequency of vibration. As drawn in the figures, the curve obeys the empirical rule of Morse:[29] $\omega_e r_e^3 \sim 3000\times10^{-24}$ cm^2.

A further indication that the $^3\Pi$ curve has a shallow minimum is given by the observed perturbations of the rotational levels of the upper $^3\Sigma^-$ state. Since perturbations of the type observed in the present case are the result of interaction of two electronic states which have discrete levels of nearly the same energy, they indicate, as shown below, that the $^3\Pi$ state cannot be repulsive for all values of r.

Only a few of the rotational levels for $v'=0$ are perturbed; these perturbations consist of displacements of only a single level from its expected position. The only noticeable perturbations occur at $K'=53$ and 61, where the F_2 levels only are displaced from their expected positions. The perturbation at $K'=61$ can be seen in Fig. 2d; it occurs in the P_2 branch in the sixth member from the right of the figure, and in the R_2 branch in the second member from the left. This type of perturbation indicates that the levels of the perturbing state are spaced quite differently than those of the perturbed $^3\Sigma^-$ state.

The rotational levels for $v'=1$, however, are considerably perturbed. Fig. 2e, is an enlargement of part of the (1,4) band, and shows very clearly the irregularities of the rotational structure. As can be seen in the figure, the lines occur in distinct groups, where each group is composed of the lines $P(K)$ and $R(K+5)$. The difference in appearance of successive groups is so great, however, that it is impossible to distinguish the R from the P lines by inspection. The identification and proper numbering of the lines in terms of K'' were obtained from term differences for the lower electronic state.

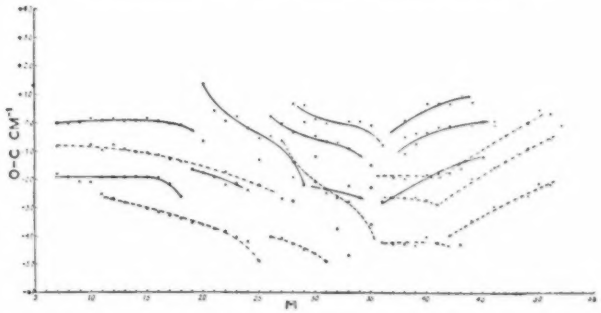

Fig. 7. Perturbations in the rotational structure of the 1,4 band. The ordinate represents the difference between the observed wave numbers of the lines and the wave numbers calculated from a formula of the type, $\nu=a+bM+cM^2+dM^3$. The circles and triangles refer to R and P lines, and the full and dashed curves represent the general course of the R and P branches, respectively. M is equal to K'' for the P branches, and to $K''-5$ for the R branches. The band is quite regular up to $K'=23$,but thereafter the perturbations are complex.

Any regularities which are present in the band can be discovered by fitting the edges of the groups to an equation of the type $\nu_M=a+bM+cM^2+dM^3$, where M is an integer. The differences between the observed wave numbers of the lines and the wave numbers calculated from this equation are shown in Fig. 7 as ordinate with M as abscissa. M is equal to K'' for the P branches (represented in the figure by dashed lines), and $K''-5$ for the R branches (solid lines). The similarity of the curves for the R and P branches is apparent. For $K''<23$, the band is fairly regular, but, for $K''>23$, the perturbations are large and complex. Because of this complexity, only the general course of the branches is represented by the curves in this region.

The rotational levels for $v'=2$ are so much perturbed that an analysis of the structure of bands involving these levels could not be made. Similarly, nothing can be said concerning perturbations of the levels for $v'=3$, since only about 6 rotational levels are present, and the bands are very weak.

Since the rules governing states which can interact to cause perturbations[22] are identical with those for predissociation, the only states which can perturb the upper $^3\Sigma^-$ state are the $^3\Pi$ and lower $^3\Sigma^-$ states, however, the potential energy curves of the $^3\Sigma^-$ states do not approach each other very closely; it therefore seems very improbable that these states could interact enough to cause perturbations of the magnitude observed. Hence the $^3\Pi$ state must be causing the perturbations. If this is the case, its potential energy curve, as stated above, must have a minimum. That the minimum is shallow is indicated by the fact that there are no perturbations of levels whose term values are less than that corresponding to $v'=1$, $K'=23$, while above this point there are many. It should be mentioned that it is possible, although it does not seem probable, that some other molecular state built on a normal and an excited atom is causing the perturbations.

Since both the perturbations and predissociation observed in the rotational structure require the $^3\Pi$ potential energy curve to have a shallow minimum, the curve must lie approximately as drawn in the figures. In this case, one would expect to observe discrete bands resulting from transitions from the $^3\Pi$ state to the lower $^3\Sigma^-$ state. However, the molecule in this $^3\Pi$ state would spend most of its time at large values of r; therefore, the most intense bands would occur at longer wave-lengths than those of the $^3\Sigma^-$, $^3\Sigma^-$ system. These bands have not been observed. Perhaps the continuum underlying the observed bands is an indication of the presence of this state.

Herzberg[23] has pointed out that the abruptness of the termination of the bands is an indication of the accuracy with which heats of dissociation can be determined by this method. If the bands terminate very abruptly, as in the present case, a very good value of the energy of dissociation can be obtained. According to the above interpretation of predissociation of the SO molecule, the term value at which the rotational levels for $v'=3$ break off corresponds to dissociation of the normal state. If the energy of dissociation is measured from the $v''=0$ vibrational level, it is calculated from the relation

$$D'' = \nu_e - G_0'' + G_0' + \Delta G_{3/2}' + \Delta G_{1/2}' + \Delta G_{2_2^1}' + F'_{v'=3}(6) \qquad (26)$$

to be 5.053 ± 0.001 volts. (See next section for the values of these terms, except $F_{v'=3}'(6)$, which is calculated from Eq. (5).) This result for D'' is considerably less than the value 6.42 volts obtained by Henri and Wolff by linear extrapolation of the vibrational levels. The uncertainty of 0.001 volt in our value is due principally to inaccuracy in the determination of the value of K' at which the rotational levels for $v'=3$ break off. Provided our interpretation of the phenomenon is correct, the accuracy of this value of the energy of dissociation of SO is equal to that of the most precise determination of energy of dissociation by any method, namely the spectroscopic value for I_2.[32]

If we assume that the excited $^3\Sigma^-$ state is built on a normal oxygen atom and a sulphur atom excited with 1.60 volts of energy, its energy of dissociation, measured from the $v'=0$ vibrational level, is 1.83 volts. The $^3\Pi$ state,

[32] W. G. Brown, Phys. Rev. **38**, 709 (1931).

according to our interpretation, has an energy of dissociation of the order of 0.2 volt.

VI. Vibrational Structure

The wave-lengths and estimated intensities of the band heads are given in the $v'v''$ diagram in Fig. 8. These values were taken from the work of Henri and Wolff.[3] The fact that the left and upper sides of this diagram are sharply bounded by fairly intense progressions is a good indication that this assignment of vibrational quantum numbers is correct, although the assignment of v' is more certain than that of v''. The solid curve is drawn through the most intense bands of the system, and thus indicates the observed most probable changes of the vibrational quantum number. The dashed curve represents the most probable changes predicted by an application of the Franck-Condon principle, using potential energy curves plotted according to Morse's equation. The agreement between the two curves is as good as could be expected,

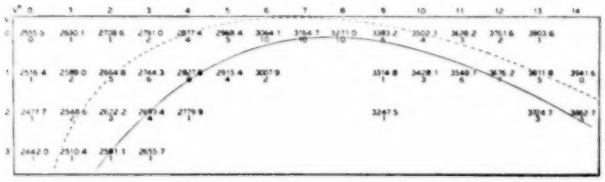

Fig. 8. This $v'v''$ matrix diagram gives the wave-lengths and estimated relative intensities of the heads of the bands of the SO spectrum. These values are taken from the work of Henri and Wolff. The solid curve is drawn through the most intense bands of the system, and thus indicates the observed most probable changes of the vibrational quantum number. The dashed curve indicates the most probable changes predicted by an application of the Franck-Condon principle, using potential energy curves plotted according to Morse's equation.

in view of the fact that the predicted values were determined from classical, instead of wave-mechanical, transition probabilities, and that the observed intensities are merely visual estimates of photographic density. The rapid decrease of plate sensitivity at the short wave-length end of the spectrum is probably responsible for the fact that, in this region, the observed curve lies below and to the right of the predicted curve.

Henri and Wolff obtained values of ω_e'', ω_e', and $x_e''\omega_e''$, but, due to inaccuracies of measurement, could not get the value of $x_e'\omega_e'$. In the present work, the origins of the six bands of the $v'=0$ progression which were measured were calculated by means of Eq. (9), using the R_2 branches. (In this calculation, the constant A of Eqs. (23) and (24) was arbitrarily taken to represent the value of $3(\epsilon'-\epsilon'')$.) From these origins, the values of ω_e'' and $x_e''\omega_e''$ were determined with much greater accuracy than is afforded by measurements of band heads only. The wave numbers of the origins and the vibrational term differences, $\Delta G_v''$, are given in Table III. The differences, $\Delta G_v''$ observed, were fitted to the equation:

$$\Delta G_v'' = \omega_e'' - 2x_e''\omega_e''(v'' + \tfrac{1}{2}), \tag{26}$$

using least squares formulas. The values thus obtained are: $\omega_e''=1123.73$

± 0.24 cm^{-1}, and $2x_e''\omega_e'' = 12.232 \pm 0.034$ cm^{-1}. The values of $\Delta G_v''$ calculated from Eq. (26) are recorded in Table III as $\Delta G_v''$ calc., and the differences between the observed and calculated values are given as $O-C$.

Due to perturbations of the rotational levels, it was not possible to determine accurately the origins of bands with $v' > 1$. Therefore, in order to ob- the values of ω_e' and $x_e'\omega_e'$, it was necessary to use measurements of band heads. Table III also gives the wave-lengths and wave-numbers of the heads of the bands used for this purpose, and the values of $\Delta G_v'$.

TABLE III. *Band heads, band origins, and vibrational term differences.*

Band	ν_0 cm^{-1}	$\Delta G_v''$ Obs.	$\Delta G_v''$ Calc.	$O-C$
(0, 4)	34736.31			
		1062.62	1062.57	+0.05
(0, 5)	33673.69			
		1050.20	1050.34	−0.14
(0, 6)	32623.49			
		1038.28	1038.10	+0.18
(0, 7)	31585.21			
		1025.74	1025.87	−0.13
(0, 8)	30559.47			
		1013.69	1013.64	+0.05
(0, 9)	29545.78			

Band	λ_h I.A.	ν_h cm^{-1}	$\Delta G_v'$	Band	λ_h I.A.	ν_h cm^{-1}	$\Delta G_v'$	Av. $\Delta G_v'$
(0, 3)	2791.33	35814.7		(0, 4)	2877.66	34740.4		
			617.5				617.3	617.4
(1, 3)	2744.02	36432.2		(1, 4)	2827.41	35357.7		
			606.3				605.6	606.1
(2, 3)	2699.10	37038.5		(2, 4)	2779.79	35963.3		
			606.1					
(3, 3)	2655.64	37644.6						

The fact that the values of $\Delta G_v'$ for the $v'' = 3$ progression are not linear shows that at least one of the upper state vibrational levels is perturbed. Since the $v' = 3$ level is very close to the dissociation limit of the lower state, it was considered as more likely to be perturbed than any of the others. Therefore, only the values of $\Delta G_v'$ obtained from the levels with $v' = 0$, 1, and 2 were used in the determination of the vibrational constants of the upper state. In getting the average $\Delta G_{1\frac{1}{2}}' = 606.1$, the value 606.3 was given greater weight than 605.6, since the position of the head of the (2,4) band was difficult to measure. The average $\Delta G_v'$ values thus obtained give $\omega_e' = 628.7$ cm^{-1}, and $2x_e'\omega_e' = 11.3$ cm^{-1}. Because of the fact that these were obtained from only two values of $\Delta G_v'$, no probable error for them can be given, although it seems quite likely that they may be in error by a few tenths of a wave number.

The vibrational term values of the upper state are given by:

$$G_v' = 628.7(v' + \tfrac{1}{2}) - 5.65(v' + \tfrac{1}{2})^2 \tag{27}$$

and those of the lower state by:

$$G_v'' = 1123.73(v'' + \tfrac{1}{2}) - 6.116(v'' + \tfrac{1}{2})^2. \tag{28}$$

The origin of the band system was calculated from the relation $\nu_e = \nu_0 + G_v'' - G_v'$, where ν_0 represents the origin of the (v', v'') band, and G_v' and G_v'' are obtained from Eqs. (27) and (28). The average ν_e obtained from the seven bands investigated is 39356.3 cm^{-1}.

The writer takes this opportunity to express his sincere appreciation of the invaluable suggestions given to him by Professor F. A. Jenkins, under whose supervision this investigation has been conducted.

The Influence of Crystalline Fields on the Susceptibilities of Salts of Paramagnetic Ions. I. The Rare Earths, Especially Pr and Nd

By WILLIAM G. PENNEY* AND ROBERT SCHLAPP
Department of Physics, University of Wisconsin

(Received May 28, 1932)

The paramagnetic susceptibilities of the salts of the rare earth elements Pr and Nd are considered on the assumption that it is permissible to represent the potential of the electric field of the atoms surrounding the metallic ion by a Taylor's expansion. This amounts to applying to the whole crystal the method of the "self-consistent field," and consequently neglects exchange effects between different crystal atoms. Hund has calculated the susceptibilities on the assumption that the ion can be regarded as free and that the multiplet intervals are so large compared with kT that only the lowest level need be considered. The introduction of an electric field causes a splitting of the levels and a redistribution of magnetic moment, with a consequent change in the susceptibility. The theoretical interpretation of the Curie-Weiss law $\chi=C/(T+\Delta)$ is considered. At temperatures so high that kT is large compared with the splitting produced by the crystal field, the susceptibility can be expanded in the form of a series of inverse powers of T. It is shown that the susceptibility of a crystal powder, or the average susceptibility over all directions in a single crystal is of the form $\chi=C/T+C_2/T^3+\cdots$ the term in $1/T^2$ vanishing rigorously. Thus at sufficiently high temperatures, the susceptibility of a crystal powder obeys the simple Curie law up to and including terms in $1/T^2$. However, the curious result emerges that at ordinary temperatures kT is of the same order as the energy separations produced by the crystal field, and the behaviour of the susceptibility actually simulates the Curie-Weiss law closely over a large range of temperatures. The hydrated sulphates of Pr and Nd are considered in detail. Excellent agreement is obtained with the experimental results of Gorter and de Haas for the variation of susceptibility with temperature on the assumption that the crystal field has cubic symmetry, and can be represented by a potential $D(x^4+y^4+z^4)$. In this connection the matrix elements of the squares and fourth powers of the coordinates for a many-electron system are given. The over-all splitting produced by this field in the hydrated sulphates is 389 cm^{-1} for Pr and 834 cm^{-1} for Nd, the detailed appearance of the energy spectrum being shown in Fig. 1. A comparison of the constant D in the two cases gives a value for Nd nearly four times that for Pr.

THE theory of paramagnetic susceptibilities as developed by Van Vleck[1] and others has been applied with considerable success to the calculation of the Curie constants of salts of the rare earth group on the assumption that it is legitimate to regard the metallic ion as free. At ordinary temperatures, the theory then leads to an expression for the susceptibility of the Curie form $\chi=C/T$. Experimentally the Curie-Weiss law

$$\chi = C/(T+\Delta), \tag{1}$$

where Δ is a constant over a wide range of temperature, frequently gives a good representation of the results. It very often happens that at extremely

* Commonwealth Fund Fellow.

[1] J. H. Van Vleck, Theory of Electric and Magnetic Susceptibilities, Oxford, 1932.

low temperatures, neither law will fit the experimental measurements. It has been suggested[2] that the deviations from the simple Curie law are due to the influence of the electric fields of the surrounding ions, which remove, wholly or partially, the spatial degeneracy of the energy levels of the free ion, thereby modifying both their positions and magnetic moments. Fields of this nature have already been postulated by Becquerel[3] and by Kramers,[4] in connection with the Zeeman effect and paramagnetic rotation in crystals, while Bethe[5] has worked out by group theory the energy spectrum of ions in fields of various symmetries. In an ionic crystal, such as nickel chloride, it seems likely that the crystal field will have the same symmetry as the crystal, but in a molecular crystal, such as hydrated $Pr_2(SO_4)_3$, there is no reason why this should any longer be true. In the absence of definite knowledge of the electric field to which an ion in a given crystal is subject, the only possible procedure is to find the simplest field which will give agreement with the experimental results.

Although considerable experimental material is available, it is not as complete as could be desired; in particular, accurate measurements at different temperatures on single crystals are lacking. From the calculations given below, there seems to be no doubt that the mechanism of crystal fields is competent to account for all the observed results. A summary of the results obtained for Pr, Nd, Ni, and Cu has been given in a Letter to the Editor.[6] In the present paper an attempt is made to calculate the magnitude of the electric fields necessary to account for the experimental variation with temperature of the susceptibility of the rare earth elements Pr and Nd. In a second communication we shall present the calculations for Ni, Co and Cr while those for Cu will be given by Mr. Jordahl. We have considered only crystals of high magnetic dilution. This is necessary in order that the influence of exchange may be neglected. It has been found possible in these cases to represent the variation of susceptibility over a wide range of temperature by an equation of the form (1) although as will be discussed more fully below, this arises in a peculiar way, and also to account for the deviations from (1) which occur at very low temperatures.

The majority of measurements have been made on crystal powders, so that the observed value of Δ represents an average over all the directions in a single crystal. In such cases, the simplest assumption is that of a cubically symmetric field, and this involves only a single parameter which must be chosen to fit the experimental average Δ. With Pr and Nd it proves that a cubic field is adequate to account for all the features which have been observed up to the present. It is possible to fit the experimental curves very

[2] Reference 1, Chap. IX.

[3] J. Becquerel, Zeits. f. Physik **58,** 205 (1929).

[4] H. A. Kramers, Proc. Amst. Acad. **32,** 1176 (1929).

[5] H. Bethe, Ann. d. Physik **3,** 133, (1929); Zeits. f. Physik **60,** 218, (1930).

[6] O. M. Jordahl, W. G. Penney and R. Schlapp, Phys. Rev. **40,** 637 (1932). The affix $+++$ for Pr and Nd, and $++$ for Ni, Co, Cu, is to be understood throughout where the symbol of the element refers to the ion.

well, but owing to a discrepancy of some 16 percent in the absolute magnitude of the susceptibility as measured by different observers,[7] more refined calculations seem out of place. However, when more detailed experimental data are available it may be necessary to introduce fields of lower symmetry to obtain agreement with experiment.

One may classify crystal fields as strong or weak according as they are able or unable to break down the coupling between the total orbital and spin angular momenta. It is assumed that the fields are never strong enough to break down the coupling between the individual orbital or individual spin angular momenta. Thus the crystal field is strong or weak according as it produces a splitting of energy levels which is large or small compared with the multiplet separation. The criterion that the ion can be considered as free is that the work required to turn over the ion against the influence of the crystal field should be small compared with kT. For the rare earths, it has been shown that the magneton numbers calculated on the assumption that the ions are perfectly free agree closely with the observed values, indicating that the crystal fields are weak. For the iron group, on the other hand, the fields are so strong that the contribution of the orbital angular momentum to the susceptibility is very much less than it would be for the free ion, although the spin may still contribute its full amount. This difference in the crystal fields is in harmony with the fact that in the rare earths the $4f$ electrons causing the paramagnetism are much more completely screened from outside influences than the $3d$ electrons of the iron group. Our quantitative results are in excellent accord with the theory of Van Vleck and it was at his suggestion that the detailed calculations given in this paper were made with the object of testing numerically the general predictions of the theory.

The Constant Δ for the Rare Earths

The fundamental expression for the susceptibility is

$$\chi = -\frac{N}{H}\sum\frac{\partial W}{\partial H}e^{-W/kT}/\sum e^{-W/kT}, \tag{2}$$

the summation extending over all levels. Here H is the magnetic field, N Avogadro's number, and W the energy levels in the presence of the magnetic field. Let us assume that a certain number of the levels form a group having a range of energy much smaller than kT, while the other levels are all so far distant that on account of the Boltzmann factor, their contribution to the susceptibility can be neglected. This state of affairs would presumably be realized in the rare earths at high temperatures, the "low-frequency" group comprising the components into which the lowest multiplet level is split by the crystal field, the components of the other multiplets being much higher. Let us take as origin the center of gravity of the low frequency group. Then,

[7] The magneton numbers for the salt $Nd_2(SO_4)_3 \cdot 8H_2O$ at room temperatures according to different observers are as follows: Cabrera 18.00, Gorter and de Haas 16.68, Zernicke and James 17.50. The susceptibility is proportional to the square of the magneton number.

if we neglect saturation, i.e., retain only the part of χ independent of H, we find

$$\chi = C/T + C_1/T^2 + \cdots$$

where

$$C = N\sum \frac{\partial W^2}{\partial H}\Big/ 2kH(2J+1), \quad C_1 = -N\sum \frac{\partial W^3}{\partial H}\Big/ 6H(2J+1)k$$

Thus to the approximation which neglects terms in $1/T^3$ and beyond, the constant Δ in the empirical formula (1) is given by

$$k\Delta = \tfrac{1}{3}\sum \frac{\partial W^3}{\partial H}\Big/ \sum \frac{\partial W^2}{\partial H}.$$

We shall now show that under the assumptions stated above the value of the constant C is independent of the direction of the magnetic field, and that the susceptibility averaged over three perpendicular directions follows the law $\chi = C/T + C_2/T^3 + \cdots$ the term in $1/T^2$ being absent. The Hamiltonian is of the form $\mathfrak{H} = \mathfrak{H}_0 + \mathfrak{H}' + H\mathfrak{H}_1$ where $\mathfrak{H}_0$ is the Hamiltonian of the free ion, $\mathfrak{H}'$ is the potential of the crystal field, and $\mathfrak{H}_1$ is the component of the magnetic moment $\beta(L+2S)$ in the direction of the magnetic field. Using the property of the invariance of the spur we have

$$\sum \partial W^2/\partial H = \mathrm{Sp}(\partial/\partial H)(\mathfrak{H}_0 + \mathfrak{H}' + H\mathfrak{H}_1)^2.$$

The spur of $(\mathfrak{H}_0+\mathfrak{H}')\mathfrak{H}_1$ vanishes, since the terms contributing to this spur have equal and opposite values for $\pm M$, so that the above expression is equal to $2H\mathrm{Sp}\mathfrak{H}_1^2$. Here Sp denotes summation over the elements diagonal in a given value of J and in all possible values of M. Since the multiplet width is large compared with kT we are concerned only with those elements of the magnetic moment $\mathfrak{H}_1$ which are of the low frequency type, i.e., diagonal in J, the contribution of the off-diagonal elements to the susceptibility being independent of the temperature. Now $\mathrm{Sp}\,\mathfrak{H}_1^2 = g^2\beta^2 J(J+1)(2J+1)/3$ so that the constant C has the Hund value $Ng^2\beta^2 J(J+1)/3k$ for all directions of the magnetic field.

The value of C_1 for a crystal powder is the average of the three values obtained when the magnetic field acts along the three axes x, y, z, respectively. By an argument similar to that just given, we can show that the average C_1 so defined vanishes. If we denote summation for three perpendicular directions of the magnetic field by $\sum_{xyz}$ the average is proportional to the term independent of H in $(1/H)\sum_{xyz}\sum \partial W^3/\partial H$ where the second summation extends over all the levels W in the lowest multiplet level. Using the property of the invariance of the spur, we have

$$\begin{aligned}\frac{1}{H}\sum_{xyz}\sum \frac{\partial W^3}{\partial H} &= \frac{1}{H}\sum_{xyz}\mathrm{Sp}\,\frac{\partial}{\partial H}(\mathfrak{H}_0 + \mathfrak{H}' + H\mathfrak{H}_1)^3 \\ &= 6\sum_{xyz}\mathrm{Sp}\,(\mathfrak{H}_0 + \mathfrak{H}')\mathfrak{H}_1^2 + \cdots \\ &= 6\,\mathrm{Sp}\left[(\mathfrak{H}_0 + \mathfrak{H}')\sum_{xyz}\mathfrak{H}_1^2\right].\end{aligned}$$

We may replace $\sum_{xyz} \mathfrak{H}_1^2$ by $(\mu_x^2+\mu_y^2+\mu_z^2)(J, M; J, M) = g^2\beta^2 J(J+1)(2J+1)$ where $\mu_x\mu_y\mu_z$ are the three components of the magnetic moment. Since this is independent of M, it may be taken outside the Sp sign, so that the mean value of C_1 is proportional to

$$6g^2\beta^2 J(J+1)(2J+1)\ \mathrm{Sp}\ (\mathfrak{H}_0 + \mathfrak{H}').$$

Since we have chosen the origin of energy at the mean centre of the unperturbed levels, Sp $(\mathfrak{H}_0+\mathfrak{H}')=0$, and therefore the average value of C_1 vanishes. Since we have shown that the value of C is independent of the direction of the magnetic field, and since $\Delta = -C_1/C$, this may be expressed by saying that Δ for a crystal powder vanishes, and hence, neglecting terms of order $1/T^3$, the susceptibility obeys the law $\chi = C/T$.[8] It must be borne in mind that in deducing this result we have assumed kT large compared with the splitting produced by the crystal field. However, from our calculations it appears that kT is of the same order as this splitting at ordinary temperatures. Under these conditions, it is no longer permissible to expand the exponentials as we have done, and on substituting the exact values, deviations from the law $\chi = C/T$ appear of such a kind that the susceptibility can be represented with considerable accuracy by a formula of the type $\chi = C/(T+\Delta)$, where Δ is appreciably constant over a wide range of temperature. It is to be hoped that experimenters, after having devoted so much attention to these mysterious Δ's will not be disappointed to find that in a sense they do not exist at all, at least for highly hydrated salts. At very low temperatures there are further deviations, and these will be discussed later.

The Potential of the Crystal Field

Each ion is supposed to be subject to an electric field of force represented by a potential V of the form

$$V = Ax^2 + By^2 + Cz^2 + 0(3) + 0(4) + \cdots$$

inasmuch as the first order terms vanish. If the field has cubic symmetry the first nonvanishing terms are of the fourth order; with rhombic symmetry the quadratic terms do not vanish and it is sufficient to consider these alone. The terms of any degree in the expansion of the potential V must satisfy Laplace's equation. For the quadratic terms this gives $C = -(A+B)$. For cubic symmetry, it is sufficient to write the potential

$$V = D(x^4 + y^4 + z^4)$$

since this can be made to satisfy Laplace's equation by adding a function of r^2 (*viz.* $-3Dr^4$). This corresponds to superposing a spherically symmetrical field, and merely shifts all levels equally.

[8] This point was first noticed in a particular case. We are indebted to Professor Van Vleck for the general proof. Sommerfeld, *Atombau und Spektrallinien* I (1931) p. 558, mentions that Bethe has shown in unpublished work that at all but very low temperatures the susceptibility of a crystal powder is the same as that of the free ion.

The Matrix Elements of the Crystal Field

We require the matrix elements of the squares and fourth powers of x, y and z, and shall retain only those elements which are diagonal in J. For a one-electron system they may be calculated by quadrature alone, using the usual form of the hydrogenic wave-function involving $P_J{}^M(\cos\theta)$. For our problem we shall however use the more general method given by Wigner,[9] in which the $2J+1$ wave functions $\psi_{J\,M}$, of the atom in the state J are expanded in the form $\psi_{J\,M}=\sum_\lambda D_{M\lambda}{}^J(\alpha, \beta, \gamma)\chi_\lambda{}^J(g)$, where $\chi_\lambda{}^J(g)$ depends only on the relative positions of the electrons, and $D_{M\lambda}{}^J(\alpha, \beta, \gamma)$ is the matrix element of the M-th row and λ-th column of the $(2J+1)$-dimensional representation of the rotation group. The arguments (α, β, γ) are Eulerian angles defining the spatial orientation of the atom. The coefficients $D_{M\lambda}{}^J$ satisfy certain recurrence relations,[9] by means of which it is possible, though somewhat laborious, to express the quantities $D_{M\lambda}{}^J\cos^2\beta$, $D_{M\lambda}{}^J\cos^4\beta$ etc., which occur in the integrands of the required matrix elements, as a linear combination of the quantities $D_{M'\lambda}{}^{J'}$. The integration over all orientations (α, β, γ) is readily effected by means of the orthogonal relations holding between the coefficients $D_{M\lambda}{}^J$ of a representation of the rotation group; the result is to give the matrix elements in the form of a factor involving M, multiplied by a factor depending on J and the χ's, with the possible addition of a constant independent of M. We find for the elements diagonal in J of the squares and fourth powers of the coordinates of the i-th electron the following values.

$$
\begin{aligned}
z_i{}^4(M, M) &= \gamma - \delta M^2 + \epsilon M^4 \\
x_i{}^4(M, M+4) &= y_i{}^4(M, M+4) \\
&= \epsilon[(J-M)!(J+M+4)!/(J+M)!(J-M-4)!]^{1/2}/16 \\
z_i{}^2(MM) &= \zeta + \eta M^2, \qquad (x_i{}^4 + y_i{}^4)(M, M \pm 2) = 0, \\
x_i{}^2(M, M+2) &= -\, y_i(M, M+2) \\
&= \eta[(J-M-1)(J-M)(J+M+1)(J+M+2)]^{1/2}/4.
\end{aligned}
$$

Here γ, ζ, ϵ, δ, η, are constants independent of M, γ and ζ being merely additive. To define the values of ϵ, δ, η, we introduce the following abbreviations

$$
\begin{aligned}
F &= [(J-1)J(J+1)(J+2)(2J-3)(2J-1)(2J+1)(2J+3)(2J+5)]^{-1}, \\
a &= 6J(J-1)(J+1)(J+2),\ b = -\,10(6J^2+6J-5), \\
c &= 70,\ d = a(2J^2+2J-5), \\
e &= -\,(72J^4+144J^3-132J^2-204J+190), \\
f &= a(2J-3)(2J+1)(2J+5)/3,\ g = -\,3f/J(J+1).
\end{aligned}
$$

[9] E. Wigner, Zeits. f. Physik **43**, 624, (1927) and correction in **45**, 601, (1927).

Then in terms of these

$$\epsilon = \sum_\lambda \int F(a + b\lambda^2 + c\lambda^4)\chi^2 r_i^4 dg,$$

$$\delta = \sum_\lambda \int F(d + c\lambda^2 - b\lambda^4)\chi^2 r_i^4 dg,$$

$$\eta = \sum_\lambda \int F(f + g\lambda^2)\chi^2 r_i^2 dg$$

where we have written χ^2 for $\chi_\lambda^J(g)\chi_\lambda^{J*}(g)$ in the integrals. The matrix elements so defined suffice to determine the elements $\Delta M = 0, \pm 2$ of $x_i^2 y_i^2 z_i^2$, and the elements $\Delta M = 0, \pm 4$ of $x_i^4 y_i^4 z_i^4$, which are all that we require, since x_i^4 and y_i^4 occur only in the combination $x_i^4 + y_i^4$ which has no elements $\Delta M = \pm 2$. From these we may pass to the matrix elements of $\sum_i x_i^2$, $\sum_i x_i^4$, etc., occurring in the Hamiltonian, by using relations of the form

$$\sum_i x_i^4(J, M; J'M') = n x_i^4(J, M; J'M')$$

assuming that the n electrons are all equivalent, which is the case in our problem. In this way we find for the matrix elements of $\sum_i(x_i^4 + y_i^4 + z_i^4)$

$$\begin{aligned} &\sum(x_i^4 + y_i^4 + z_i^4)(J, M; J, M) \\ &\qquad = K + pM^2\{7M^2 + 5 - 6J(J+1)\} \\ &\sum(x_i^4 + y_i^4 + z_i^4)(J, M; J, M \pm 4) \\ &\qquad = \tfrac{1}{2}p[(J \mp M)!(J \pm M + 4)!/(J \pm M)!(J \mp M - 4)!]^{1/2} \end{aligned} \tag{3}$$

where K and p are independent of M.

In order to obtain an idea of the relative magnitude of the constant D of the crystal field in different cases, it is necessary to examine the constants p and K in greater detail. Let us consider a two electron system such as Pr: the analysis can easily be modified for systems with a greater number of electrons. We will assume that $L(=5)$ and $S(=1)$ are good quantum numbers, these two combining to give the various multiplet levels $J(=4, 5, 6)$. We have

$$x^4 + y^4 + z^4 = \tfrac{1}{4}(7\sin^4\theta - 8\sin^2\theta + 4 + \sin^4\theta\cos 4\phi).$$

The term independent of ϕ gives the matrix elements diagonal in M, while the term dependent on ϕ gives elements $\Delta M = \pm 4$.

Consider the sum S for one of the permissible J values

$$S = \sum_M (x^4 + y^4 + z^4)(J, M; J, M) \tag{4}$$

where for brevity we have written x^4 for $\sum_i x_i^4$ etc. Since all the wave functions for a given L and S have the same radial factor, the summation over M involves averaging (4) over a sphere. The result is clearly

$$\begin{aligned} S &= n(2J+1)\int_0^{\pi/2} \tfrac{1}{4}(7\sin^4\theta - 8\sin^2\theta + 4)\sin\theta d\theta \int_0^\infty r^6 R^2(r) dr \\ &= 6I(2J+1)/5 \end{aligned}$$

with $I=\int_0^\infty r^6 R^2(r)dr$, n being the number of electrons, two in this case and $R(r)$ the radial wave function of one of the two equivalent electrons. The quantity I is independent of J, L, M, S but it does depend on the total quantum number and the effective nuclear charge. For elements so similar in structure as Pr and Nd a good approximation is to assume I the same for both. A better approximation is to take into account the small difference in the effective nuclear charges. From the relations (3) and (4) it is immediately possible to eliminate the constant k in the matrix elements and we obtain

$$(x^4+y^4+z^4)(J,M;J,M) = 6I/5 + p_J[7M^4+5M^2-6JM^2(J+1) + 3J(J-1)(J+1)(J+2)/5] \quad (5)$$

the subscript J on p being used to denote that p depends on J. Transforming from the J, M system to the M_L, M_S system, we have from the invariance of the spur in the two representations

$$\sum_J (x^4+y^4+z^4)(J,M;J,M) = \sum_{M_L} (x^4+y^4+z^4)(M_L,M_S;M_L,M_S), \quad (6)$$

with $M=M_L+M_S$, where the matrix elements on the right hand side of this equation can be obtained from (5) by replacing p_J by q, M by M_L and J by L. The quantity q depends on L, but since we are considering only one value of L there is no need to indicate this dependence.

If we take $M=6$, then $J=6$, $M_L=5$ and $M_S=1$; Eq. (6) then determines p_6 in terms of q. By taking in succession $M=5$, $M=4$, it is possible to find p_5 and p_4 in terms of q.

It remains now to determine q in terms of I. If we transform from the (L, S, M_L, M_S) system to the $(m_{l_1}, m_{l_2}, m_{s_1}, m_{s_2})$ system, we have another spur relation,

$$\sum_{LS}(x^4+y^4+z^4)(L,S,M_L,M_S;L,S,M_L,M_S) = \sum_{m_{l1}m_{l2}}[(x_1^4+y_1^4+z_1^4)(m_{l_1},m_{s_1};m_{l_1},m_{s_1}) + (x_2^4+y_2^4+z_2^4)(m_{l_2},m_{s_2};m_{l_2},m_{s_2})] \quad (7)$$

with $M_S=m_{s_1}+m_{s_2}$ and $M_L=m_{l_1}+m_{l_2}$. There is no need to include l_1, s_1, etc., since we are going to assume that these are always good quantum numbers. Let us take $M_S=1$; then we must have $m_{s_1}=1/2$, $m_{s_2}=1/2$. Furthermore, if we take $M_L=5$, the only possibility is $L=5$, just the value we require. Moreover, we can evaluate the matrix elements of $(x^4+y^4+z^4)(m_l;m_l)$ for a one-electron problem by quadrature alone. We find

$$(x^4+y^4+z^4)(m_l;m_l) = 3I\,\frac{7l^4+14l^3-23l^2-30l+18-6l^2m_l^2+5m_l^2-6lm_l^2+7m_l^4}{2(2l-1)(2l-3)(2l+3)(2l+5)}.$$

Using this relation and the spur relation (7) one can obtain q and hence p_4 in terms of I.

Performing the calculations, we find for Pr

$$p_6 = 14q/33, \qquad p_5 = 2q/3, \qquad p_4 = 21q/11, \quad (-q = I/10395) \tag{8}$$

and for Nd

$$p_{15/2} = 33q/91, \; p_{13/2} = 6q/13, \; p_{11/2} = 799q/1001, \; p_{9/2} = 2380q/1001, \quad (-q = I/32670) \tag{9}$$

These relations enable us to find the ratio of the magnitudes of the electric fields in similar salts of these two elements.

Praseodymium

The normal state of Pr is $^3H_4$; the multiplet separation between the levels $J=4$ and $J=5$ is about 2100 cm^{-1}, and hence in calculating the susceptibility the higher multiplet levels may be neglected. This corresponds to discarding off-diagonal elements in J in the magnetic moment and in the crystal field. Good experimental data have been given by Gorter and de Haas[10] for the variation of the susceptibility of a crystal powder of $Pr_2(SO_4)_3\ 8H_2O$.

As has already been explained, the simplest assumption is a cubically symmetrical field. The Hamiltonian is

$$D\sum_i (x_i^4 + y_i^4 + z_i^4) + H\beta\mu_z,$$

μ_z being the component of magnetic moment along the z-axis, which is also taken to be the direction of the magnetic field. The diagonal elements arising from the magnetic field are simply $g\beta HM$, where g is the Landé g-factor ($=4/5$ for Pr), M is the component of J along the axis and β is the Bohr magneton. Bethe[5] has shown that in the absence of a magnetic field the level $J=4$ splits up into a single level, a doubly degenerate level and two triply degenerate levels. In virtue of the selection rule obeyed by the Hamiltonian, the secular determinant factors into a cubic and three quadratics, two of the quadratics being identical since there is degeneracy as regards the sign of M. Hence at least one root of the cubic must be identical with one of the roots of the repeated quadratic, while another root must be the same as one of the roots of the remaining quadratic. Thus the determination of the levels in the absence of the magnetic field involves only the solution of quadratic equations. When the magnetic field is present the secular determinant still breaks up into a cubic and three quadratics, the factors being

$$\begin{vmatrix} 4G - 96a - W & s & 0 \\ s & -W & s \\ 0 & s & -4G - 96a - W \end{vmatrix}$$

$$\begin{vmatrix} \pm 3G - 936a - W & t \\ t & \pm G - 216a - W \end{vmatrix} \begin{vmatrix} 2G - 696a - W & 360a \\ 360a & -2G - 696a - W \end{vmatrix}$$

[10] C. J. Gorter and W. J. de Haas, Leiden Comm. 218b.

where

$$s = 24a(70)^{1/2},\quad t = 120a(7)^{1/2},\quad G = g\beta H$$

and $a = pD$, p being the coefficient in the matrix elements (3). Since the roots without the magnetic field are known there is no great difficulty in finding the roots in the presence of the field H as a power series in H. For convenience, we choose as origin of energy the centre of gravity of the unperturbed levels. Then the levels in the presence of the field are

$$W_1 = 672a + 5G^2/252a, \qquad W_2 = 336a + G/2 + 7G^2/3840a,$$
$$W_3 = 336a + 2G^2/105a, \qquad W_4 = 336a - G/2 + 7G^2/3840a,$$
$$W_5 = 96a + G^2/180a, \qquad W_6 = 96a - 180aG^2/,$$
$$W_7 = -624a + 5G/2 - 7G^2/3840a, \qquad W_8 = -624a - G^2/180a,$$
$$W_9 = -624a - 5G/2 - 7G^2/3840a.$$

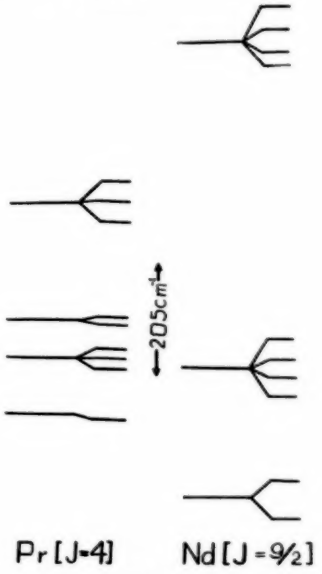

Fig. 1.

The susceptibility per gram atom is then

$$\chi = (2Ng^2\beta^2/a)\,[53e^{13\mu}/5760 + e^{-2\mu}/30 - 61e^{-7\mu}/2688 - 5e^{-14\mu}/252 + \mu(25e^{13\mu} + e^{-7\mu})/192] \div (3e^{13\mu} + 2e^{-2\mu} + 3e^{-7\mu} + e^{-14\mu}) \tag{10}$$

where $\mu = 48a/kT$. The constant a is chosen so that this formula gives the value of χ_0, the susceptibility at the absolute zero of temperature, extrapolated from the experimental data. This gives $\chi_0 = -10Ng^2\beta^2/a$, since a must be negative in order that χ_0 may be finite. From this we obtain the value $a = -0.293$ cm^{-1} which corresponds to an over-all splitting produced by the crystal field of 389 cm^{-1}. Fig. 1 gives the way in which the crystal field splits the lowest multiplet level of Pr. The same figure gives similar results for Nd, and the influence of the magnetic field in removing the degeneracy is also shown. The curve $1/\chi$ against T is given in Fig. 2 and on it are marked the ex-

perimental values for $Pr_2(SO_4)_3 \cdot 8H_2O$ as measured by Gorter and de Haas.[10] The agreement is extremely good. In order to show the sensitivity to variations in a we have plotted the curves (1) $a = -0.37$ cm^{-1} (2) $a = -0.293$ cm^{-1} (3) $a = -0.30$ cm^{-1}, while the straight line (4) through the origin gives the asymptote for all values of a at very high temperatures (but not high enough for the higher multiplet levels to count). This straight line represents the Hund formula for the susceptibility $\chi = N\beta^2 g^2 J(J+1)/3kT$, obtained on the assumption that the ion is perfectly free. It should be explained that the experimental values are given per gram ion. The molecular weight of $Pr_2(SO_4)_3 \cdot 8H_2O$ is 714, and since there are two Pr atoms it is necessary to divide χ as given by Eq. (10) by 357 in order to give the χ used by experimenters and employed in Fig. 2. In the temperature range 100°K to 300°K the experimental

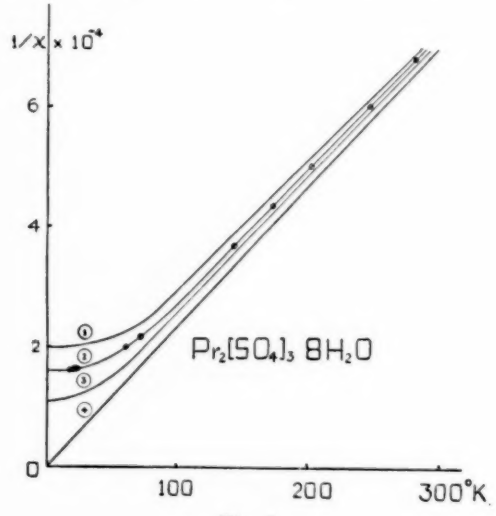

Fig. 2.

Δ is 32°, while the theoretical value is about 25°. The difference is too small to show in the figure. More will be said about the agreement with experiment when we have considered Nd.

Before it was realized that a field of cubic symmetry would give such a good account of the experimental results, a field of rhombic symmetry was tried, but with little success. A simple assumption in this case is that the potential of the field is of the form $A(x^2+y^2-2z^2)$. Since the measurements were made on crystal powders, it is necessary to average over all directions. This can be accomplished by first solving the problem where the magnetic field acts along the z-axis, the axis of symmetry, and then when it acts perpendicularly to the axis. The average susceptibility will be the average of these two, taken with the weights one and two respectively. The problem bears a formal resemblance to the problem of the symmetrical top; the group $J=4$ of energy levels are all doubly degenerate except one which is single and which must be taken as the lowest in order to fit the observed susceptibility at low temperatures. However the temperature dependence of the susceptibility calculated

on the assumption of a "symmetrical top" field bore very little resemblance to that observed and it was necessary to reject it. If data were available on single crystals one could tell immediately by comparing the three principal susceptibilities and Δ's how good an assumption a field of cubic symmetry is. If the three are equal, everything would be very satisfactory; if not, then one would have to introduce a small field of rhombic symmetry to account for the differences. The effect of introducing a field of rhombic symmetry would be to give three principal Curie constants and three principal Δ's, and the Δ's would not vanish even at high temperatures although the Curie constants would then all become equal and the mean Δ would vanish. Nothing further can be said until experiments have been made on single crystals.

Neodymium

The normal state of Nd is ${}^4K_{9/2}$ (K states have $L=6$). The multiplet separation between $J=9/2$ and $J=11/2$ is about 1800 cm^{-1} and at room temperatures one ought not to neglect the higher multiplet levels. We are indebted to Miss Frank for the information that the correction for the other multiplet levels is to add about three percent to the susceptibility at room temperatures.[11] However we make no attempt to apply this correction, since the discrepancy between different observers is considerably greater than this. Since the ground state has $J=9/2$, so that J is a half integer, the electric field, as shown by Kramers,[12] will be unable to remove all the spatial degeneracy of this state; each level will be at least doubly degenerate and will have a Zeeman effect of the first as well as of the second and higher orders. It is known from the work of Bethe[5] that in the absence of the magnetic field the ten components of $J=9/2$ fall into two coincident groups of five on account of the Kramers two-fold degeneracy, and each group of five levels will split up into a single level and two doubly degenerate levels. In the presence of the magnetic field, the factoring is into a quadratic and a cubic, given by

$$\begin{vmatrix} 9G/2 + 5Av - W & 6A & 0 \\ 6A & G/2 + 5Av - W & 10A \\ 0 & 10A & -7G/2 - 3Av - W \end{vmatrix}$$

$$\begin{vmatrix} 5G/2 + 2Av - W & 5Au \\ 5Au & -3G/2 - 2Av - W \end{vmatrix}$$

[11] Miss Frank has shown, Phys. Rev. **39**, 119 (1932), that it is very important to take into account the off-diagonal elements in J in the magnetic moments for Eu and Sm, since for these the separation between the two lowest multiplet levels is not small compared with kT. For Eu, the lowest level has $J=0$, the next lowest $J=1$ and neither of these breaks up under the action of a crystal field of cubic symmetry nor is their relative position altered to a first approximation; and since they belong to different representations of the cubic group, the field does not introduce elements of magnetic moment between them. From analogy with the conclusions given in the present paper, one would expect the crystal fields in the rare earths to have cubic symmetry. If this is so, Miss Frank's calculations for Eu still apply. For Sm, whose two lowest levels have $J=5/2$ and $J=7/2$ as normal states, it may be necessary to amend the results given in her paper. Further calculations will be made on this point.

[12] H. A. Kramers, Proc. Amst. Acad. **33**, 959 (1930).

where $u=(6)^{1/2}$, $v=(14)^{1/2}$, $G=g\beta H$ ($g=8/11$ for Nd) and $A=12a\overline{r^4}(14)^{1/2}$. The origin of energy has been chosen to make the spur of the quadratic zero, a device which greatly simplifies the algebra. The cubic and quadratic arising from the other quintic can be obtained from those above by changing the sign of G. The roots in the absence of the magnetic field can readily be obtained, since then the roots of the quadratic must also be roots of the cubic. Solving these equations up to terms in H^2, we find for the ten energy levels

$$W_1 = 20.95A + 1.833G + 0.3879G^2/A, \quad W_2 = 9.11A + 2.788G - 0.3411G^2/A,$$
$$W_3 = 9.11A - 0.542G + 0.1015G^2/A, \quad W_4 = -19.59A - 3.121G - .00468G^2/A$$
$$W_5 = -19.59A + 1.542G - 0.1015G^2/A.$$

and five more obtained from these by changing the sign of G.

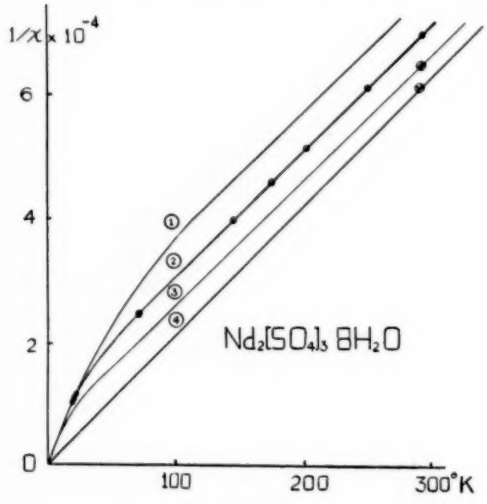

Fig. 3.

The expression for the susceptibility per gram atom is

$$\chi = (2g^2\beta^2N/A)\,[(0.1483e^{19.59\mu} + 0.2396e^{-9.11\mu} - 0.3879e^{-20.95\mu}) + \mu(6.065e^{19.59\mu} + 4.031e^{-9.11\mu} + 1.680e^{-20.95\mu})] \div [2e^{19.59\mu} + 2e^{-9.11\mu} + e^{-20.95\mu}],$$

where $\mu=A/kT$. To obtain the susceptibility per gram ion it is necessary to divide by 361. As with Pr, a is negative, and its value is about -0.458 cm^{-1} ($A=-20.6$ cm^{-1}), which gives an over-all splitting of 834 cm^{-1}. The splitting of the lowest multiplet level produced by the crystal field is shown in Fig. 1. Curve 2 in Fig. 3 gives the theoretical variation of $1/\chi$ with T, while on it are marked the experimental results of Gorter and de Haas.[10] The agreement is extremely good. Curves 1 and 2 in Fig. 3 show the sensitivity to A and are for the values $A=-36$ cm^{-1} and $A=-12$ cm^{-1} respectively, while the straight line 4 gives as before Hund's law. The measurements of Cabrera[13] at 290°K,

[13] B. Cabrera, C. R. **180**, 669 (1925).

and of Zernicke and James[14] at 293°K, and of St. Meyer,[15] which agree almost exactly with Zernicke and James, are also marked and are seen to fall considerably below those of Gorter and de Haas. If, on account of some error in calibration, it should prove necessary to reduce the experimental values by a constant factor, D can still be chosen to fit the results. Exactly the same discrepancies appear with Pr. Again, the susceptibility as measured by Cabrera is 11 percent higher, and that measured by Zernicke and James and also by St. Meyer is 2 percent higher, than that obtained by Gorter and de Haas, all at room temperature. The disagreement in this case is not quite so bad as with Nd.

Using the relations (8) and (9) we can compare immediately the values of the constants D of the crystal fields in the two salts $Pr_2(SO_4)_3 \cdot 8H_2O$ and $Nd_2(SO_4)_3 \cdot 8H_2O$, on the assumption that the integral I is the same in both cases. This is not quite accurate and rather favors Pr, but it is sufficiently close for our purpose. The constant D for Nd is found to be about 3.9 times that for Pr. One would expect the electric fields in two salts so similar in every way to be of about the same magnitude. It should be remembered, however, that we determine this magnitude from the difference between the observed magneton number and the Hund value, and a small change in the observed magneton number will make a considerable difference in the calculated field. For example, the difference between the magneton number of Nd as measured by Cabrera, and the Hund value, is 0.08, while Gorter and de Haas obtain 1.24. For Pr the corresponding figures are 0.17 and 0.76 respectively. The electric fields calculated from Cabrera's values are much less than those given here. More accurate data on the susceptibilities, even at one temperature, would allow this question to be settled satisfactorily.

In conclusion we desire to express our sincere thanks to Professor J. H. Van Vleck, whose advice and criticism during the course of this work have been invaluable.

[14] J. Zernicke and C. James, Jour. Am. Chem. Soc. **48,** 2827 (1926).
[15] Stefan Meyer, Phys. Zeits. **26,** 51, 478 (1925).

Theory of the Variations in Paramagnetic Anisotropy Among Different Salts of the Iron Group

By J. H. Van Vleck
University of Wisconsin

(Received June 6, 1932)

A theoretical explanation is given of why nickel salts are nearly isotropic magnetically, while those of cobalt exhibit over 25 percent anisotropy even though the Ni^{++} and Co^{++} ions are both in F states and are adjacent in the periodic table. The cause is an inversion of the levels in the crystalline Stark effect in passing from the configuration $d^8\ {}^3F$ (Ni^{++}) to $d^7\ {}^4F$ (Co^{++}). If the crystalline field has only rhombic symmetry, but with the deviations from cubic symmetry comparatively small, extension of the methods in Penney and Schlapp's preceding paper shows that a nearly isotropic level will be the ground level in Ni^{++}, but an anisotropic one in Co^{++}. It is to be particularly noted that the inversion exists purely in virtue of the difference between the configurations d^7 and d^8, and does not require different crystalline fields in Ni and Co compounds. The theory predicts that hydrated Ni salts conform closer to Curie's law than those of Co, and have a Curie constant more nearly equal to the "spin only" value $4NS(S+1)(he/4\pi mc)^2/3k$. This agrees with experiment. Other pairs of ions are cited in the iron group in which the inversion phenomenon is encountered, with attendant diversity in magnetic behavior. The nearly perfect magnetic isotropy of manganous salts is trivial, as the ground state of Mn^{++} is ${}^6S$; the slight anisotropy may be due to a small amount of incipient j-j coupling or to distortion of the constancy of orbital angular momentum by the crystalline field, so that the orbital magnetic moment does not vanish completely in S states.

NO ONE who has examined the measurements of the principal susceptibilities of salts of the iron group can fail to note how remarkably the amount of magnetic anisotropy varies with the nature of the cation. Typical determinations are, for instance, those by Rabi,[1] according to which the ammonosulphates of Mn, Co, Ni, and Cu exhibit anisotropies amounting respectively to 1, 30, $1\frac{1}{2}$, 20 percent.

The nearly perfect isotropy of the manganous salts is exactly what one expects inasmuch as the Mn^{++} ion has a ${}^6S$ ground state. Nearly complete symmetry should also be found in ferric salts, as Fe^{+++} and Mn^{++} have the same configuration, but adequate data on ferric compounds are wanting. The usual cause of magnetic anisotropy is the unsymmetrical partial freezing of orbital angular momentum by the lattice forces. The orbital magnetism is thus largely destroyed by these forces, but not completely. Particularly important is usually the coupling between the spin and the remains of the orbital angular momentum, which are not centro-symmetric and so destroy the equivalence of different spin orientations. In S states with perfect Russell-Saunders coupling there is no orbital angular momentum to congeal, and so the usual cause of anisotropy disappears in manganous salts. The ordinary explanation of the small residuum (about 1 percent) of anisotropy found in

[1] I. I. Rabi, Phys. Rev. **29**, 173 (1927).

manganous compounds is the magnetic spin-spin coupling, since the electrostatic exchange coupling is well known not to cause anisotropy. However, it seems doubtful whether the magnetic spin-spin forces could be great enough to cause even the 1 percent dissymmetry in manganous salts of high "magnetic dilution," such as e.g., hydrated sulphates, where the separation of the paramagnetic ions is great. Therefore we wish to suggest the possibility of a small amount of incipient j-j coupling, not enough to distort appreciably the g-factors from their Russell-Saunders values, but enough to impart a slight amount of orbital angular momentum to S states which would then behave anisotropically. Along with this is also, perhaps more important, the angular momentum which arises because the crystalline fields do not have complete central symmetry. In quantum mechanics the orbital angular momentum cannot be constant in time in noncentral fields[2] and so cannot vanish completely in the presence of the latter.

So much for the rather straightforward case of Mn. Much more puzzling is the great difference in isotropy between nickel and cobalt salts. The ions Co^{++} and Ni^{++} are adjacent in the periodic table, and both are in F states (respectively $d^7\,{}^4F$ and $d^8\,{}^3F$). Nevertheless Ni salts are nearly as isotropic as those of Mn, while Co salts are the least symmetrical of the whole group. Closer examination reveals that precisely this behavior is to be expected if the crystalline field possesses only rhombic symmetry, but with the departures from cubic symmetry relatively small. The development of the crystalline potential then takes the form

$$V = \sum_i [f(r_i) + Ax_i^2 + By_i^2 - (A + B)z_i^2 + D(x_i^4 + y_i^4 + z_i^4)], \quad (1)$$

provided we neglect the departures from cubic symmetry in the fourth but not the second order terms. The summation need be extended for our purposes only over the electrons not in closed shells, i.e., the d electrons in the ions of the iron group, inasmuch as completed shells exhibit no orientation effect and so contribute nothing interesting to (1). The reader is referred to the preceding paper by Penney and Schlapp and to reference 3 in case he desires further general exposition of the use of crystalline potentials in connection with magnetic problems.[3] That the rhombic or second order part of (1) is subordinate to the cubic or fourth order part is evidenced by the fact that paramagnetic salts are nearly isotropic in many cases, and especially by the success which has attended Penney and Schlapp's preceding calculation of the temperature dependence of the susceptibilities of rare earth salts involving Nd and Pr under the assumption that only the cubic portion of (4) need be considered. They have also tried calculations keeping only the rhombic part of (1), but the wrong temperature dependence is then obtained in the rare earths, as well as far too much anisotropy in Ni salts.

If the "cubic" or fourth-order part of (1) is the dominant noncentral term, then from Bethe's[4] group theory of levels in crystalline fields, one finds that

[2] Cf. J. H. Van Vleck, Phys. Rev. **31**, 600 (1928).

[3] J. H. Van Vleck, "The Theory of Electric and Magnetic Susceptibilities," section 73.

[4] H. Bethe, Ann. d. Physik **3**, 133 (1929); especially pp. 164–167, 196–199.

the Stark splitting is arranged either as in Fig. 1, or as in this figure turned upside down. The vertical lines represent the matrix elements of magnetic moment along some one principal direction, say x. The separation of the components of Γ_4 or of Γ_5 is due only to the rhombic terms, since Γ_4, Γ_5 (in Bethe's notation) are triply degenerate "Darstellungen" in strictly cubic fields.

If Fig. 1 is right side up, the orbital magnetic moment will be largely suppressed, and its "remains" will be nearly isotropic for the following reason. By perturbation theory,[5] the magnetic moment induced in the state a by application of a magnetic field H along x is given by the expression

$$2H \sum_k | \mu_x(ak) |^2 / h\nu(ka), \tag{2}$$

where the $\mu(ak)$ are the matrix elements of magnetic moment in the absence of H but in a system of representation which diagonalizes (1). The matrix μ

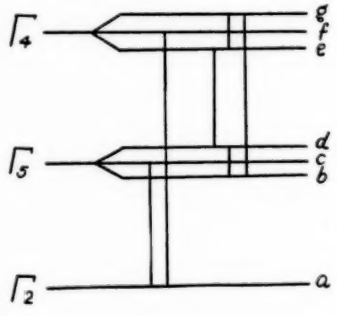

Fig. 1.
(upright in Ni^{++}, inverted in Co^{++})

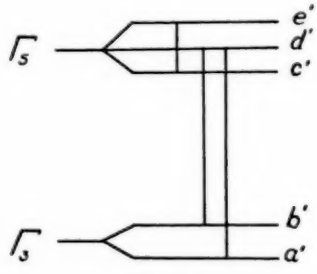

Fig. 2.
(upright in Cu^{++}, inverted in Fe^{++})

will contain no diagonal elements, because, as the writer has shown elsewhere,[3] crystalline fields of no more than rhombic symmetry suppress the diagonal elements of orbital angular momentum (neglecting perturbations by spin-orbit interaction, which restores some of the diagonal part in systems with an odd number of electrons). In the case shown in Fig. 1, the summation over k embraces only c and f, but if one changes the direction of H to another principal axis y or z, one encounters the matrix elements of μ_y, μ_z and these may join a to other components of Γ_4 and Γ_5 than c and f. One finds that the magnetic anisotropy of a exists only in virtue of the difference between the frequencies $\nu(ab)$, $\nu(ac)$, $\nu(ad)$ or between $\nu(ae)$, $\nu(af)$, $\nu(ag)$, and these percentage differences are small since the rhombic is small compared to the cubic separation.

Let us, however, turn Fig. 1 upside down, and suppose that the separations e-f-g, though small compared to a-e, etc., are nevertheless large compared to kT, making only g a normal state. The orbital magnetic moment will then be much less completely quenched than without the inversion, since

[5] See, for instance, p. 145 of reference 3.

the denominators $\nu(ge)$, $\nu(gf)$ will be involved in the formula analogous to (2). Furthermore there will be vastly more anisotropy than without the inversion. This will be true not merely because the percentage difference between $\nu(ge)$ and $\nu(gf)$ is greater than that between $\nu(ab)$ and $\nu(ac)$ or $\nu(ad)$ but also because the full symmetry of moment in the limiting case of perfectly cubic fields is achieved only with equal distribution of atoms among the three components of Γ_4 rather than concentration purely in one component g.

It is clear that one can understand the difference between Ni^{++} and Co^{++} if one can justify turning Fig. 1 upside down in passing from one of these ions to the other. Now it actually turns out that for a *fixed* sign of A, B, D in (1), precisely this behavior is to be expected theoretically. The argument is as follows. Let us consider matrix elements in the L, M_L system of representation rather than in the final system which diagonalizes (1). Then from the properties of the rotation group Penney and Schlapp find in the preceding paper that, regardless of the number n of electrons in the incomplete shell the matrix elements of $\sum(x_i^4+y_i^4+z_i^4)$ are of the form

$$\sum_i (x_i^4 + y_i^4 + z_i^4)(LM_L; LM_L) = Qf(L, M_L) + 3n\overline{r^4}/5, \tag{3}$$

where Q depends on L, S, n but not on M_L, and where

$$f(L, M_L) = M_L^2(7M_L^2 - 6L^2 - 6L + 5) + 3L(L^2 - 1)(L + 2)/5. \tag{4}$$

Besides (3) there are also elements of the form $\Delta M_L = \pm 4$ proportional to Q, as well as elements nondiagonal in L, but the explicit form of these does not concern us. Our interest is in the sign of the proportionality factor Q, which can be determined by the following adaptation of the Goudsmit-Slater method[6] of diagonal sums. For the configuration d^8, the only arrangement in m_l, m_s quantization consistent with $M_L = \sum m_l = 3$, $M_S = \sum m_s = 1$ is $m_l = 2$, $m_l = 1$, $m_l = 0$ each twice, $m_l = -1$, $m_l = -2$ each once. The spur invariant for $M_L = 3$, $M_S = 1$ thus consists of but a single term, which yields a ^3F state. Hence, since f is even in M_L,

$$Q(d^8\,{}^3F) \cdot f(3, 3) = Q(d^2D)\,[3f(2, 2) + 3f(2, 1) + 2f(2, 0)]. \tag{5}$$

Here $Q(d^8\,{}^3F)$ means the value of Q appropriate to the configuration $d^8\,{}^3F$, while $Q(d\,{}^2D)$ of course relates to a single isolated d electron. The term in $\overline{r^4}$ has been omitted since it is invariant of the vector addition involved in constructing the Russell-Saunders coupling. For the case $M_L = 3$, $M_S = 3/2$ of d^7, one has the same arrangement of m_l's as before, except that $m_l = 0$ is filled only once, and consequently

$$Q(d^7\,{}^4F)f(3, 3) = Q(d^2D)\,[3f(2, 2) + 3f(2, 1) + f(2, 0)]. \tag{6}$$

On comparing (5) and (6) and noting that

$$2f(2, 2) + 2f(2, 1) + f(2, 0) = 0, \tag{7}$$

one sees that $Q(d^8\,{}^3F)$ is the negative of $Q(d^7\,{}^4F)$. Of course the diagonal ele-

[6] S. Goudsmit, Phys. Rev. **31**, 945 (1928); J. C. Slater, *ibid.* **34**, 1293 (1929).

ments (3) are not the same as the characteristic values of $\sum(x_i^4+y_i^4+z_i^4)$, but except for the difference in Q, the matrix representing this expression in the L, M_L system is the same for $d^8\ ^3F$ as $d^7\ ^4F$ inasmuch as L is the same in both cases. Hence the characteristic values are obtained by the same canonical transformation and differ merely in the proportionality factor Q, which will thus cause inversion in the passage from Ni to Co. It is particularly gratifying that alteration of the sign of D in (1) is thus not necessary to invert the crystalline Stark effects. The crystals of Ni and Co hydrated sulphates, etc. have presumably so nearly the same structure and ionic arrangement that it would be illogical, to say the least, to postulate radically different fields in the two cases.

In the foregoing we have neglected entirely the spin in the interest of simplicity. Actually the spin is the main cause of the paramagnetism in Ni and Co, though not of its anisotropy. In point of fact, the spin-orbit interaction is comparable with the effect of the rhombic dissymmetry, but is subordinate to the "cubic" term, so that the inversion of cubic levels still comes into play. Inclusion of the spin-orbit interaction makes the remains of the orbital magnetic moment contribute to the part of the susceptibility which is inversely proportional to temperature, rather than merely a term such as (2) which is independent of temperature. When Fig. 1 is right side up, the spin interacts effectively with a smaller and more isotropic orbital moment than when Fig. 1 is inverted. The most potent elements of μ in the spin-orbit coupling, which is much looser than in the free gaseous state, can be shown[3] to be those whose associated frequencies $\nu(ij)$ are small. Hence the departures of the Curie constant C from the Stoner-Bose "spin only" value

$$C = 4NS(S+1)(he/4\pi mc)^2/3k \tag{8}$$

should be larger in Co than in Ni salts, and deviations from Curie's law in highly hydrated salts should appear at higher temperatures with a Co than with a Ni cation. (The hydration is to avoid exchange coupling between atoms.) This agrees with experiment. The deviation from (8) is about 30 percent in the nickel sulphates, as compared with 70 percent in those of cobalt. Further calculations by Schlapp and Penney, to appear shortly, predict that in hydrated nickel salts the deviations should become important only at temperatures near liquid helium. This is confirmed by Gorter, de Haas, and v. d. Handel's recent remeasurement[7] of $NiSO_4 \cdot 7H_2O$ at low temperatures (down to liquid hydrogen) which has obliterated Jackson's previous large negative Δ and restored Curie's law almost perfectly. On the other hand, $CoSO_4 \cdot 7H_2O$ apparently demands a Δ of about 14 in the Weiss-Curie formula $\chi = C/(T+\Delta)$, although it must be cautioned that here new measurements are not available.

By arguments very similar to the previous, one can show that the inversion phenomenon should also be found in the pair Fe^{++}, Cu^{++}, respectively $d^6\ ^5D$ and $d^9\ ^2D$, and also pairs of ions reciprocally related on the left and right sides of the group, such as (Cr^{+++}, Co^{++}) or (Ni^{++}, V^{+++}). We call ions re-

[7] C. J. Gorter, W. J. de Haas, and J. v. d. Handel, Leiden Comm. 218d.

ciprocally related if they have respectively x and $10-x$ d electrons, since then their ground states have the same L, S.

Adequate data are wanting on single crystals of Cr and V salts, but the Curie constant does have much more closely the Stoner-Bose value (8) for Cr^{+++} than for Co^{++}, as one should expect from the foregoing. In $Cr_2(SO_4)_2 K_2SO_4 \cdot 24H_2O$ the deviation from (8) is only about 2 percent.[8] The variation in the applicability of (8) is thus even more pronounced in the pair Cr^{+++}, Co^{++} (2 *vs.* 70 percent deviation) than in the pair Co^{++}, Ni^{++} (70 *vs.* 30). This is understandable on the ground that the multiplet structure and hence the spin-orbit interaction for the free ion are considerably smaller in Cr^{+++} than in Co^{++} or Ni^{++}. Of course the departures from (8) will be greater the larger this interaction, all other circumstances being equal. Consequently the alteration in free multiplet width and the inversion phenomenon reinforce each other in accentuating the deviations from (8) in Co^{++} as compared to Cr^{+++}.

The pair Fe^{++}, Cu^{++} require rather careful examination. Here we encounter D rather than F levels. Now Bethe[4] has proved that D terms split under the potential (1) in the fashion shown in Fig. 2, where the separation of the components of Γ_3 or of Γ_5 is due entirely to the deviations from cubic symmetry occasioned by the rhombic terms. The first thing to be remarked is that Fig. 2 is upright in Cu^{++} and inverted in Fe^{++} if Fig. 1 is upright in Ni^{++}. This follows from the fact that $Q(d^9\ ^2D)$ has the opposite sign from $Q(d^8\ ^3F)$ inasmuch as by the method of diagonal sums

$$Q(d^9\ ^2D)f(2,2) = Q(d^2D)[3f(2,2) + 4f(2,1) + 2f(2,0)] = -Q(d^2D)f(2,2), \quad (9)$$

and by (4) the bracketed sum in (9) has the value $-12/5$ as compared with $36/5$ for the corresponding bracketed sum in (5). Bethe[4] has shown that for a fixed sign of Q, as in a one electron system, the D level requires inversion of Fig. 2 if the F level requires an upright Fig. 1. When the sign of Q changes, there are thus two cancelling inversions which together leave Fig. 2 upright.

To be consistent with our interpretation of Ni and Co, it thus appears[9]

[8] W. J. de Haas and C. J. Gorter, Leiden Comm. 208c.

[9] At this juncture it is perhaps well to remark that the reversal of the sign of Q is perhaps a more general and certain phenomenon for the pairs Ni^{++}, Co^{++} and Fe^{++}, Cu^{++} than for the pair Ni^{++}, Cu^{++}. The reversal for the former pair is contingent only upon (7) and hence takes place for any potential whose diagonal elements vanish when summed over M_L except for an additive constant, such as $3nr^{-1}/5$ in (3), which is independent of the type of vector addition. That the additive constant is indeed independent of the vector compounding is shown by the theorem (cf. Niessen, Phys. Rev. **35,** 274 ff., 1929) that $\Sigma_{ML}F(n_1n_2 \cdots M_L;\ n_1n_2 \cdots M_L) = (2L+1) \times \overline{F}(n_1n_2 \cdots ;\ n_1n_2 \cdots)$ where the matrix elements relate to any function $F(r, \theta, \phi)$ of polar coordinates and $4\pi\overline{F} = \iint F \sin\theta d\theta d\phi$ .The function $\overline{F}$ is a purely radial one and consequently invariant of the vector addition involved in Russell-Saunders coupling etc. Hence the Ni^{++},Co^{++} inversion is surely found for other forms of potential besides (1), and the great diversity in anisotropy in this pair requires only that the crystal symmetry be dominantly but not completely cubic. On the other hand after Eq. (9) explicit use was made of the numerical form (4) of the matrix elements of the fourth degree part of (1) in proving the reversal in the sign of Q for the pair Ni^{++}, Cu^{++}. It is hence conceivable, though improbable, that if the cubic potential requires large sixth, eighth, etc. degree terms for its representation in addition to the fourth order terms, the reversal in the sign of Q may exist for the Ni^{++}, Co^{++} and Cu^{++}, Fe^{++} pairs, but not for Ni^{++}, Cu^{++}. Fig. 2 would then be upright in Fe^{++} and inverted in Cu^{++}.

necessary that Fig. 2 be upright in Cu^{++} and inverted in Fe^{++}. Now Bethe[4] has demonstrated that the portion Γ_3 of Fig. 2 is "nonmagnetic," and so μ consequently has no matrix elements of the form $\mu(a'b')$, whereas the elements inside Γ_5 do not all vanish. The expression analogous to (2) will consequently be much larger in Fe^{++}, where e' is a ground state, than in Cu^{++}, because of the existence of small denominators such as $\nu(e'c')$. Hence the remains of the orbital angular momentum will be larger in Fe^{++} than Cu^{++}, and, all other things being equal, the distortion from (8) with attendant magnetic anisotropy should be much more accentuated in Fe^{++} than in Cu^{++}. Actually the anisotropy of cupric salts (e.g., 26 percent in $CuK_2(SO_4)_2 \cdot (6H_2O)$ is usually greater than for ferrous ones (e.g., 16 percent in $FeK_2(SO_4)_2 \cdot 6H_2O$), while (8) holds no more closely for Cu^{++} than for Fe^{++}. About 20 percent deviations from (8) are found in both cases. Because of the somewhat greater anisotropy in the cupric case, it thus appears at first sight that the inversion of Fig. 2 comes at the wrong place. However, "all other things" are not equal. The free multiplet structure is wider for Cu than Fe, so that if there were no inversion the spin-orbit distortion would be bigger in Cu than in Fe. Also the spin quantum number has the small value 1/2 in Cu^{++}, compared with 2 in Fe^{++}, so that residual orbital angular momentum of given magnitude is relatively more important in Cu^{++} than in Fe^{++}. These two effects may more than counteract the fact that the denominators in the formula for the induced orbital moment are smaller in Fe^{++} than in Cu^{++}. One thing to be particularly emphasized in connection with the question of anisotropy is the following. The orbital moment induced in a' in Fig. 2 exists, to be sure, solely in virtue of the matrix element $\mu(a'c')$, $\mu(a'd')$, $\mu(a'e')$ rather than $\mu(a'b')$, and hence tends to be small because the frequencies $\nu(a'c')$ etc. are large. However, unlike the case of a in Fig. 1, this moment in a' does not owe its anisotropy purely to departures of the ratios $\kappa = \nu(a'c')/\nu(a'd')$ etc. from unity. Instead the full cubic isotropy of the induced moment in Γ_3 is achieved only when the two components of Γ_3 are equally populated, whereas we suppose the separation $a' - b'$ large compared to kT, so that only a' is inhabited. Consequently, the anisotropy in the induced orbital moment of a', Fig. 2 is of the order of magnitude unity, like that of g in Fig. 1 or e' in Fig. 2, whereas that in a, Fig. 1 is only of the order $\kappa - 1$. By an anisotropy of the order unity we mean that the differences between the x, y, z components are comparable with the components themselves. Of course the anisotropy is in any case diminished because the residual orbital angular momentum is overshadowed by the spin, but we can say that for given deviations from (8), the anistropies should be of the same order of magnitude regardless of whether or not Fig. 2 is inverted, and inversion accentuates the anisotropy only in so far as the deviation from (8) is enhanced, whereas we have seen that in the Fe^{++}, Cu^{++} pair there are other counteracting tendencies which forestall this enhancement. The effect of inversion on anisotropy is thus a different story for Fig. 2 than Fig. 1. It must be further remembered that Fe, Cu are not adjacent in the periodic table, and their salts' crystalline fields need not resemble each other as closely as those of Co, Ni, thus obscuring the

purity of the inversion phenomenon. The inversion becomes less important the more one increases the rhombic terms at the expense of the cubic ones.

In order to make Figs. 1, 2 upright at Ni^{++}, Cu^{++} respectively rather than Co^{++}, Fe^{++}, it is necessary that the constant D in (1) be positive. This follows since the quotient of the bracketed sum in Eq. (5) and f (3, 3) is positive, making Q have the same sign in Ni^{++} as for a one electron system, where Bethe[4] shows that Fig. 1 is upright if D is positive. The positive choice of D agrees with Penney and Schlapp's preceding calculations on the susceptibilities of the rare earths, but iron and rare earth salts are so widely different that it seems scarcely necessary that the sign of D be the same in both cases.

Detailed numerical calculations amplifying and testing quantitatively the foregoing ideas will be published by Schlapp and Penney and by Jordahl. The writer wishes to thank them for valuable discussions and comments.

Investigations in the Field of the Ultra-short Electromagnetic Waves. IV. On the Dependence of the Ultra-short Electromagnetic Waves upon the Heating Current and upon the Amplitude of the Oscillations*

By G. POTAPENKO**
Norman Bridge Laboratory of Physics,
California Institute of Technology

(Received May 31, 1932)

An investigation has been made of the dependence of the length of the ultra-short electromagnetic waves generated by vacuum tubes on the magnitude of the heating current. It is shown that the normal waves (i.e., waves the frequency of which corresponds to the frequency of the oscillations of the electrons about the grid of the tube) differ from the dwarf waves (i.e., waves with frequency exceeding several times the frequency of electronic oscillations) in their dependence on the heating current. The length of the normal waves increases, while the length of the dwarf waves of all orders decreases as the heating current is decreased. Therefore, as the heating current is decreased, there is a better agreement between the observed and computed values of wave-lengths of the normal and of the dwarf waves. At low heating currents the product $\lambda^2 E_g$ for dwarf waves of different orders is very close to the theoretical values

$$\lambda^2 E_g = \text{const.}_0 / n^2 \qquad n = 2, 3, 4, \cdots$$

where const.$_0$ corresponds to the value of the product $\lambda^2 E_g$ for normal waves. The results of the experiments are in agreement with the theory of P. S. Epstein, which explains the discrepancy between the calculated and the observed length of the normal and the dwarf waves being due to the influence of the alternating potentials appearing on the electrodes of the tube during oscillations. In the limit, at infinitely low amplitudes of these potentials, the ratio of the values of the products $\lambda^2 E_g$ for normal and for dwarf waves approaches the theoretical value within the limits of the experimental error. Neglecting these alternating potentials introduces the largest error in the results of the existing theories of the generation of ultra-short waves. At sufficiently intensive oscillations, this error exceeds all the others taken together, including the error introduced through the simplifying assumption of plane electrodes. The limiting value of const.$_0$ corresponding to infinitely low amplitudes of the alternating potentials, approaches very closely the value of the product $\lambda^2 E_g$ calculated from the formulas of H. Barkhausen and A. Scheibe. This shows that normal waves really do correspond to a complete period of oscillations of the electrons about the grid, i.e., to the time the electrons take to pass from the filament to the grid and back to the filament.

§1. INTRODUCTION

IN THE previous papers[1] it was shown that ultra-short waves of several kinds can be obtained when large positive potentials with respect to the filament and the plate are impressed on the grid of a vacuum tube. The wave-

* Reported at the Berkeley meeting of the American Physical Society, December 18, 1931.
** Carnegie Fellow.
[1] G. Potapenko, Phys. Rev. **39**, 625, 638, **40**, 988 (1932); these articles will be referred to as I, II and III.

length λ_0 of some of them is found to approximately correspond to the period of oscillations of the electrons about the grid of the tube, or in other words, to the time τ of the passage of the electrons from the filament of the tube to the plate and back to the filament; i.e.,

$$\lambda_0 = c_0\tau \text{ (normal waves)} \tag{1}$$

where c_0 is the velocity of light and the period τ can be approximately determined from the well-known formula:

$$\tau = d_a \times 10^{-7}/3(E_g)^{1/2} \tag{2}$$

where d_a is the diameter of the plate of the tube (in cm) and E_g is the constant positive potential (in volts) of the grid with respect to the filament and the plate. We called these waves normal or normal Barkhausen waves, since Eq. (1) is a fundamental equation of the theory proposed by Barkhausen. The lengths $\lambda_1, \lambda_2, \lambda_2, \cdots$ of the waves of the other kind are approximately 2, 3, 4, $\cdots$ times shorter than the length of the normal waves, calculated from Eq. (1), i.e.,

$$\begin{aligned} \lambda_1 &= c_0\tau/2 \text{ (dwarf waves of the 1st order)} \\ \lambda_2 &= c_0\tau/3 \text{ (“ “ “ “ 2nd “)} \\ \lambda_3 &= c_0\tau/4 \text{ (“ “ “ “ 3rd “)} \end{aligned} \tag{3}$$

We called these waves dwarf waves of the 1st, 2nd, 3rd etc. orders.

We have seen that Eqs. (3) are fairly well satisfied experimentally and that Eq. (1) gives values which differ systematically from the observed values by some 15 percent (II, §9).

While investigating the problem of the motion of the electrons within the tube, we have seen that the peculiarities of the character of this motion completely explain the causes of the generation of dwarf waves and lead us to expect waves with periods equal to integral multiples of the period of the oscillation of electrons about the grids of the tube (III, §3). In other words, the character of electronic motion permits us to expect waves satisfying Eqs. (1)–(3). These investigations gave no direct indications of the possibility of a systematic discrepancy between these equations and the observations.

Thus, so far, we do not know the causes of this discrepancy. Its systematic character shows, however, that it cannot be ascribed to experimental errors and must possess a definite physical meaning. The purpose of the present paper is to elucidate the causes of this discrepancy.

§2. The Relation between the Length of Normal and Dwarf Waves and the Magnitude of the Heating Current

All of the previously made observations refer to three tubes of the same type R5. First of all we must compare them with each other. Every one of these observations, as, for example, the measurement of the wave-length, or the determination of the amplitude of oscillations, refers to a certain length of oscillating circuits, to a certain grid voltage, etc. Therefore, unless all of

these factors are taken into account, a simple comparison of observations cannot be of any great value and will generally be avoided.

The measurements of the wave-lengths were made at such points of the working diagrams of the tubes (II, §3) which corresponded to the maximum current in the plate circuit of the generator (i.e., approximately corresponded to the maximum of the energy of oscillations). Moreover, observations were made at a constant heating current and only at such grid voltages which corresponded to the region of saturation current and were not in the neighborhood of the upper bend of the static characteristic of the tube. In this case the lengths of the normal and of the dwarf waves were satisfying Barkhausen's equation

$$\lambda^2 E_g = \text{const.} \tag{4}$$

An approximate estimate of the value of the constant could be made by means of Eqs. (1)–(3). If Eq. (4) holds true, we can compare the average values of the product $\lambda^2 E_g$ instead of comparing individual observations. This relieves us of the necessity of taking into a separate account the grid potentials as well as the lengths of the oscillating circuits. The latter follows from our having selected points of observation in such a manner that the length of the oscillating circuits already enters the value λ, in view of the definite relationship existing between these two magnitudes (II, §3).

Let us suppose that for the case of normal waves the observations give

$$\lambda_0^2 E_g = \text{const.}_0 \text{ (normal waves)} \tag{5}$$

If relations (1) and (3) hold true, we must have the following for the case of dwarf waves:

$$\begin{aligned} \lambda_1^2 E_g &= \text{const.}_1 = \text{const.}_0/4 \quad \text{(dwarf waves of the 1st order)} \\ \lambda_2^2 E_g &= \text{const.}_2 = \text{const.}_0/9 \quad (\text{ “ “ “ “ 2nd “ }) \\ \lambda_3^2 E_g &= \text{const.}_3 = \text{const.}_0/16 \ (\text{ “ “ “ “ 3rd “ }). \end{aligned} \tag{6}$$

A general form of Eqs. (5) and (6) can be written thus:

$$\lambda^2 E_g = \text{const.}_0/n^2 \tag{7}$$

where for normal waves $n=1$ and for dwarf waves of the 1st order, 2nd order, etc., we have $n=2$, $n=3$, $n=4$, etc. respectively.

If we know the average values of const.$_0$ for the tubes investigated, then by means of Eqs. (6) we can compute the corresponding values of const.$_1$, const.$_2$, const.$_3$, $\cdots$ and compare them with the observed values. Table I gives the results of these computations; the columns under the heading *Obs.* give the average values of the products $\lambda^2 E_g$ for dwarf waves of the first four orders, which we had obtained previously (II, §§10, 13). The table also gives the mean observed values of the product $\lambda^2 E_g$ for normal waves and the values of the emission current. From a comparison of the mean observed values of $\lambda^2 E_g$ it is easily seen that for the case of dwarf waves of the 1st, 2nd and 3rd orders the values of these products diminish systematically as the

heating of the filament is decreased. At the same time, for normal waves and for dwarf waves of the 4th order, the change in the value of $\lambda^2 E_g$ has no systematic character and is generally very small.

It must also be mentioned that Barkhausen's Eq. (4) was satisfied for all three tubes in spite of the fact that they were investigated at different absolute values of the heating current. Hence, it follows that under our conditions of observation the product $\lambda^2 E_g$ remains constant, regardless of the absolute value of the heating current.

TABLE I.

Tubes R5

	Tube No. 5 Const$_0$ = 5.81 × 10^5 I_e = 41 mA			Tube No. 20 Const$_0$ = 5.78 × 10^5 I_e = 19 mA			Tube No. 7 Const$_0$ = 5.85 × 10^5 I_e = 12 mA		
	Obs.	Calc.	$\frac{\text{Obs.}}{\text{Calc.}}$	Obs.	Calc.	$\frac{\text{Obs.}}{\text{Calc.}}$	Obs.	Calc.	$\frac{\text{Obs.}}{\text{Calc.}}$
Const.$_1$	2.01 × 10^5	1.45 × 10^5	1.39	1.97 × 10^5	1.45 × 10^5	1.36	1.90 × 10^5	1.46 × 10^5	1.30
Const.$_2$	0.856 "	0.646 "	1.33	0.846 "	0.642 "	1.32	0.800 "	0.650 "	1.23
Const.$_3$	0.495 "	0.363 "	1.36	0.481 "	0.361 "	1.33	0.466 "	0.366 "	1.27
Const.$_4$	0.303 "	0.232 "	1.31	0.300 "	0.231 "	1.30	0.300 "	0.234 "	1.28
		Average	1.35		Average	1.33		Average	1.27

The ratios of the mean observed values of $\lambda^2 E_g$ to those computed from Eq. (6), which are given in Table I, indicate a systematic discrepancy between them. The mean observed values of $\lambda^2 E_g$ are systematically exceeding the calculated values by approximately 30 percent. This is as should be expected, according to what we had before. It is very significant, that the average values of these ratios Obs./Calc. decrease appreciably as we pass to tubes which worked with a lower heating of the filament. A decrease in the ratios Obs./Calc. mean, evidently, a decrease in the discrepancy between the observed wave-lengths and those computed from Eqs. (1)–(3).

§3

As there could be a difference in the vacuum of the tubes and consequently in their working regime, it is necessary to test the validity of the above relationship between the value of the ratio Obs./Calc. and the heating of the tube and to see whether it might be due to a possible difference in the vacuum of the tubes.

The simplest way of avoiding the effect of a difference in the vacuum is to make observations using only one tube at different heating currents. Such observations were made with tube No. 5. As far as could be seen, this tube possesses the greatest symmetry in the arrangement of the electrodes, its dwarf waves had a greater intensity than those generated by the two other tubes; it was therefore used for these tests. The tests were made by selecting some point on the lines of maxima of the working diagram (II, §3) and measduring the corresponding wave-length, intensity of oscillation, etc., at different heating currents I_h beginning with the largest possible values and ending with those at which the intensity of oscillations was very low and measurements were becoming uncertain. Each time the grid voltage was selected according to the maximum current I_a in the plate circuit of the generator.

The selection of the points of observations was made so as to obtain monochromatic oscillations. This circumstance was very important, since the intensity of waves of different length varies differently as the heating current is changed. Therefore, it frequently happens that waves, which at large heating currents play the role merely of an "admixture," become relatively intensive at low heating, thus completely distorting the results obtained.

As the intensity of dwarf waves of the 4th order was generally low and as the precision of the measurements of their wave-length fell off rapidly with decreasing heating current, it was decided not to include them in the tests, making observations for normal waves and dwarf waves of the first three orders only.

TABLE II. *Tube R5 (No. 5).*

I_k (Amp.)	E_g (volt)	I_a (mA)	λ (cm)	$\lambda^2 E_g$
		normal waves; $L=23$ cm		
0.701	162	4.40	60.0	5.83×10^6
0.684	161	3.75	60.6	5.91 "
0.662	160	2.90	61.0	5.95 "
0.651	161	2.25	61.3	6.05 "
0.640	162	1.75	61.6	6.15 "
0.632	165	1.30	61.8	6.30 "
0.625	167	0.90	62.0	6.42 "
0.610	169	0.30	62.4	6.58 "
		dwarf waves, 1st order; $L=13$ cm		
0.701	152	2.70	36.6	2.04×10^5
0.684	146	2.20	37.0	2.00 "
0.662	138	1.80	37.3	1.92 "
0.651	136	1.30	37.2	1.88 "
0.640	133	0.85	37.0	1.82 "
0.625	127	0.30	36.8	1.72 "
		dwarf waves, 2nd ord.; $L=6$ cm		
0.701	240	2.00	18.85	0.852×10^5
0.684	234	1.60	18.9	0.836 "
0.662	228	0.80	18.8	0.806 "
0.651	224	0.50	18.7	0.783 "
0.640	221	0.20	18.55	0.760 "
0.625	217	0.02	18.4	0.735 "
		dwarf waves, 3rd ord.; $L=8$ cm		
0.701	305	0.95	12.7	0.492×10^5
0.684	300	0.65	12.55	0.473 "
0.674	288	0.35	12.5	0.450 "
0.662	278	0.10	12.5	0.434 "

The results of the measurements[2] are presented in Table II. Figs. 1 and 2 show the relation between the wave-length and the heating current, and also the relation between the value of the grid potentials, corresponding to a maximum plate current, and the heating current. As to the normal waves, their length increases very appreciably with decreasing heating current. At

[2] In Table II the observed values are rounded off to 0.1 cm for normal waves and dwarf waves of the 1st order. They are rounded off to 0.05 cm for dwarf waves of the 2nd and 3rd orders, as the accuracy of the measurements was somewhat greater for shorter waves.

the same time, the value of the grid voltage corresponding to a maximum plate current passes through a small minimum and increases rapidly, as the heating current is further diminished. In connection with this, there is, in the

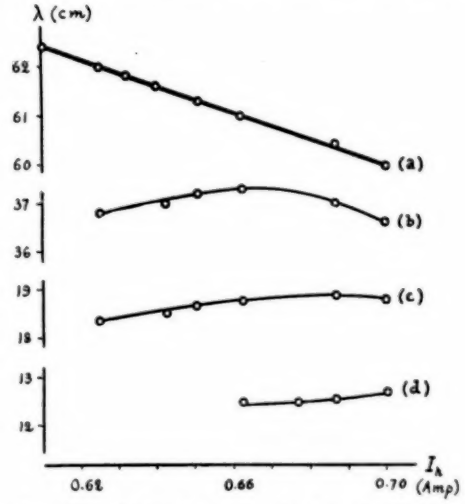

Fig. 1. Curves showing the relation between the length of the normal and dwarf waves and the heating current of the tube. Curve (a)—normal waves; curves (b), (c), (d)—dwarf waves of the 1st, 2nd and 3rd orders (E_g-variable).

case of normal waves, a rapid increase in the value of the product $\lambda^2 E_g$ as the heating current is decreased. This agrees well with the observations of W. Wechsung.[3]

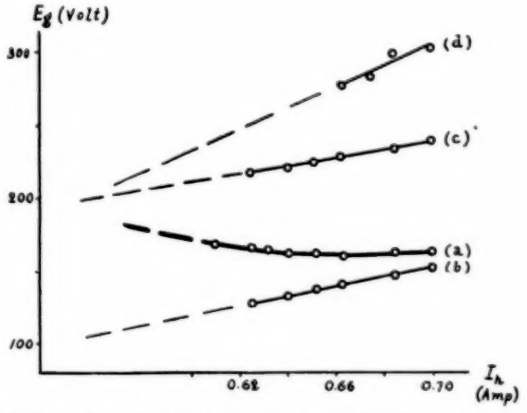

Fig. 2. Curves showing the relation between the grid voltage, corresponding to the maximum amplitude of oscillations, and the heating current. Curve (a)—normal waves; curves (b), (c), (d)—dwarf waves of the 1st, 2nd and 3rd orders.

A comparison of the results obtained for normal and for dwarf waves leads to an unexpected conclusion. It shows that *the normal waves depend on the heating current in a different way than the dwarf waves*. This is especially

[3] W. Wechsung, Zeits. f. Hochfr. **32**, 64 (1928).

clearly seen from the curves of Figs. 1 and 2 which show that the grid voltage corresponding to a maximum plate current, and also the length of the dwarf waves decrease as the heating current is decreased. As a result, in the case of dwarf waves the product $\lambda^2 E_g$ decreases as the heating current is decreased, i.e., it varies in a manner quite opposite to that of normal waves.

Table III gives a comparison of the values of const.$_1$, const.$_2$ and const.$_3$ calculated from Eq. (6) with those obtained from direct observations. For the sake of brevity the table gives the results of computation only for three values of the heating current. It is seen from Table III that the value of

TABLE III. *Tube R5 (No. 5).*

	I_h = 0.701 amp. Const.$_0$ = 5.83 × 10^5 I_e = 36 mA			I_h = 0.684 amp. Const.$_0$ = 5.91 × 10^5 I_e = 28 mA			I_h = 0.662 amp. Const.$_0$ = 5.95 × 10^5 I_e = 18 mA		
	Obs.	Calc.	$\frac{\text{Obs.}}{\text{Calc.}}$	Obs.	Calc.	$\frac{\text{Obs.}}{\text{Calc.}}$	Obs.	Calc.	$\frac{\text{Obs.}}{\text{Calc.}}$
Const.$_1$	2.04 × 10^5	1.46 × 10^5	1.40	2.00 × 10^5	1.48 × 10^5	1.35	1.92 × 10^5	1.49 × 10^5	1.29
Const.$_2$	0.852 "	0.648 "	1.32	0.836 "	0.657 "	1.27	0.806 "	0.661 "	1.22
Const.$_3$	0.492 "	0.364 "	1.35	0.473 "	0.370 "	1.28	0.434 "	0.372 "	1.17
		Average	1.36		Average	1.30		Average	1.23

the ratio Obs./Calc. decreases as the heating and emission current is decreased, exactly in the same manner as we have seen from Table I. Hence it follows that *the magnitude of the discrepancy between the observed wave-lengths and those calculated from Eqs. (1)–(3) does really depend on the heating current* and that there is no reason to ascribe it to a difference in the degree of vacuum of the tubes. Of course the mere fact that the magnitude of the discrepancy depends on the heating current, is not an explanation of the cause of these discrepancies. It indicates, however, a way of discovering this explanation. This question will be treated later.

From Table III it is seen also, hat the product $\lambda^2 E_g$ varies quite uniformly as the heating current is varied. Therefore, when the heating current is still lower, the divergence between the observed and calculated values must be

TABLE IV. *Tube R5 (No. 5).*

I_h (Amp.)	$\frac{\text{Const.}_0}{\text{Const.}_1}$	$\frac{\text{Const.}_0}{\text{Const.}_2}$	$\frac{\text{Const.}_0}{\text{Const.}_3}$
0.701	2.86	6.84	11.8
0.684	2.96	7.07	12.5
0.662	3.10	7.38	13.7
0.651	3.22	7.73	—
0.640	3.32	8.09	—
0.625	3.73	8.73	—

even smaller than it is seen from Table III. Without giving any detailed computations we shall determine the values of the ratios const.$_0$/const.$_1$, const.$_0$/const.$_2$ and const.$_0$/const.$_3$. Theoretically, according to Eqs. (5) and (6) these ratios must be equal to 4, 9 and 16. Table IV gives the values of these ratios calculated from the data of Table II. It is seen from the Table IV that as the heating current is decreased these ratios increase and rather closely approach

the theoretical values. A poorer agreement is obtained for the third ratio which cannot be calculated for the low heating current in view of the low intensity of the dwarf waves of the 3rd order.

As we said before, when measuring the wave-length at different heating currents, the grid voltage was selected in such a way as to have a maximum plate current. However, a change in E_g must affect the length of the waves. Therefore, in determining the relation between the wave-length and the heating current, for the sake of greater accuracy we should have kept E_g constand and the maximum values of the plate current should have been selected by varying the length of the oscillating circuits. We have chosen the first method because of its convenience. Furthermore, the results obtained by this method permit easily to determine the results obtainable by the second method. Figs. 1 and 2 show that as the heating current is decreased the length of the normal waves increases, at the same time there is an increase in the grid voltage corresponding to the maximum plate current. Since increasing the grid voltage produces a decrease in the wave-length (see article II Tables III and VI) it is clear that, if the grid voltage had been kept constant, we would have a still more pronounced increase in the wave-length of the normal waves as the heating current was decreased. It is also easily seen that, if the grid voltage had been kept constant, decreasing the heating current would produce even a more noticeable decrease in the wave-length of the dwarf waves than it is seen from Fig. 1.

§4. On the Influence of the Amplitude of the Alternating Potentials

The data of the last three tables confirm the existence of a definite dependence of the magnitude of the discrepancy between the observed and the calculated wave-lengths (or the values of $\lambda^2 E_g$) on the heating current. The data give also a fairly complete idea as to the character of this relationship. With these data it is possible to attempt an elucidation of the causes of this relationship.

The changes in the heating current and the consequent changes in the emission current can be accompanied by the following three phenomena: (1) a change in the density of the space charges, (2) a change in the initial velocity of the electrons and (3) a change in the amplitude of the oscillations generated by the tube. We did not consider these phenomena and none of them is taken into account by formula (2).

The change in the density of the space charges is frequently used to explain the changes in the wave-lengths with changing heating current. Starting from the concept of the influence of the space charges on the motion of the electrons, H. G. Möller[4] has shown theoretically that a decrease in the emission current must produce an increase in the length of the generated waves. This does not contradict our observations on normal waves, for which the theory was devised. However, there are good reasons to maintain that in our case the change in the density of the space charges cannot have an appreciable influence on the motion of the electrons. In the first place, all of our observa-

[4] H. G. Möller, Electr. Nachr. Techn. **7**, 411–419 (1930).

tions were made at such grid voltages which lay far in the region of saturation current, even at the maximum values of the heating current used. Therefore the influence of the space charges on the motion of the electrons ought to be very small in our case. Furthermore, if the change of the space charges had any appreciable influence, its effect would be the same for all kinds of waves. Our results show, however, that with a change in the heating current the normal waves vary in a different way than the dwarf waves. For the same reason we must consider as unapplied to our case the explanation proposed by A. Rostagni[5] which is based on the possibility of the existence of a natural period of the space charges analogous to the natural period of an ionized gas, and which is dependent on the density of the space charges. There is still less ground to admit the possibility of an influence due to a change in the initial velocity of the electrons, in view of the fact that this velocity is relatively low. There remains the third factor—the effect of a change in the amplitude of the generated oscillations.

If there are oscillations in the plate and the grid currents of the tube then alternating potentials must appear on the electrodes of the tube, as on the plates of a condenser. If these potentials are not vanishingly small in comparison with the constant grid voltage, they necessarily must affect the character and the velocity of electronic motions and change the time the electrons take to pass from the filament to the grid. Thus the length of the generated waves will be changed. E. Gill and J. Morrell[6] had mentioned the possibility of an influence of the alternating potentials on the motion of electrons. H. E. Hollmann[7] was the first to make an estimate of the influence of these potentials on the time of passage of the electrons and on the length of the generated waves. The formula which he obtained shows that the wavelength must decrease as the amplitude of the oscillations is increased. The same conclusions were arrived at by N. Kapzov[8] and F. W. Sears[9] who made a graphical investigation of the electronic trajections within the tube, and also by H. G. Möller,[4] as a result of his theoretical investigations. All of these results refer to normal waves only and are in complete agreement with the results obtained for these waves, presented in Table II. From this table it is seen that the length of the normal waves decreases continuously, as the amplitude of the oscillations (or the current I_a) is increased. P. S. Epstein,[10] independently from the previous papers, made a theoretical investigation of the influence of the amplitude of the alternating potentials on the length of the normal and dwarf waves. He showed that for dwarf waves this influence must be opposite to that for normal waves.[11] To this difference he ascribed

[5] A. Rostagni, Atti della R. Acad. di Torino **66,** 123–130, 217–223, 383–395 (1931); see also Th. V. Ionescu, C. R. **193,** 575–577 (1931).

[6] E. W. B. Gill and J. H. Morrell, Phil. Mag. **44,** 161–178 (1922).

[7] H. E. Hollmann, Ann. d. Physik **86,** 129–188 (1928).

[8] N. Kapzov, Zeits. f. Physik **49,** 395–427 (1928).

[9] F. W. Sears, J. Frankl. Inst. **209,** 459–472 (1930).

[10] P. S. Epstein, Report at a Physics Research Conference, Pasadena, Mar. 5, 1931.

[11] According to his theory the above deduction is always true for dwarf waves of the 1st order. For dwarf waves of the second and higher orders this deduction depends on the dimensions of the tube.

our systematic discrepancy between the observed and the calculated wavelengths. So far we had no opportunity for a detailed verification of this theory. One of its results shows, however, that this theory not only explains the above discovered difference in the effect of the heating current on the normal and on the dwarf waves but also leads to quantitatively correct results.

We have seen above that the ratios const.$_0$/const.$_1$, const.$_0$/const.$_2$, const.$_0$/const.$_3$ must be equal to 4, 9 and 16 if Eqs. (1) and (3) are true. If the assumption of the influence of the amplitude of the alternating potentials is correct, then in comparing our observations it will be more correct to refer them to the same amplitude of oscillations and not to the same value of the

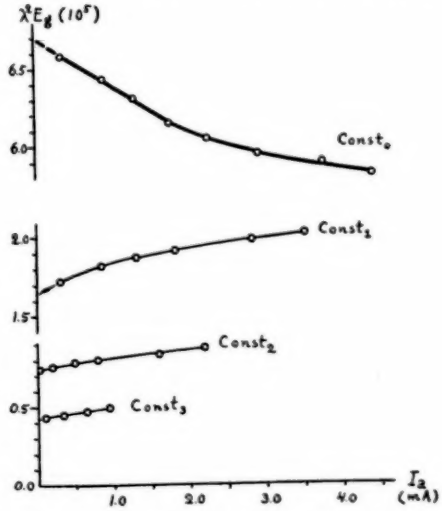

Fig. 3. Curves showing the dependence of the values of const.$_0$, const.$_1$ const.$_2$ and const.$_3$ on the amplitude of oscillations (amplitude of the alternating potentials which appear at the electrodes of the tube during oscillations).

heating current, as we have done it before. The ratios const.$_0$/const.$_1$, const.$_0$/const.$_2$, const.$_0$/const.$_3$ must be equal to 4, 9 and 16 at infinitely low amplitudes of the alternating potentials, i.e., in the limit at $I_a = 0$.

The values of const.$_0$, const.$_1$, const.$_2$, and const.$_3$ at $I_a = 0$ can be determined graphically from the data of Table II, by constructing curves showing the relations between these constants and the plate current which, as we have seen before (I, §6) approximately corresponds to the amplitude of oscillations and, which is more important, appears only when oscillations are present. For this last reason the condition $I_a = 0$ does really correspond to the condition of infinitely small amplitudes of alternating potentials. These curves are shown on Fig. 3. We find by extrapolation

$$\left.\begin{array}{l} \text{const.}_0 = 6.70 \times 10^5 \\ \text{const.}_1 = 1.65 \quad \text{“} \\ \text{const.}_2 = 0.735 \quad \text{“} \\ \text{const.}_3 = 0.43 \quad \text{“} \end{array}\right| \; I_a = 0$$

where the value 0.735×10^5 is taken directly from Table II. Hence we obtain

$$\left(\frac{\text{const.}_0}{\text{const.}_1}\right)_{I_a=0} = 4.1 \quad \left(\frac{\text{const.}_0}{\text{const.}_2}\right)_{I_a=0} = 9.1 \quad \left(\frac{\text{const.}_0}{\text{const.}_3}\right)_{I_a=0} = 15.6.$$

The discrepancy between these figures and the theoretical values does not exceed the limits of the possible errors. This proves that as far as can be seen from the above investigations, the difference between the observed and calculated wave-lengths is to be completely explained by the dependence of the length of waves on the amplitude of the alternating potentials which appear on the grid and the plate of the tube during oscillations.

Evidently it does not follow that the dependence of the wave-length on the heating current can *always* be explained as being due to the influence of alternating potentials alone. When observations are made in the region $E_g < E_s$ a greater influence can be exercised by the space charges of which we have spoken previously (II, §12). On the other hand, our results permit us definitely to deny the widely spread opinion, according to which a decisive importance is attributed to the space charges in all cases when explaining the dependence of the wave-length on the emission and heating current. This opinion is usually connected with the notion that the amplitudes of the alternating potentials are vanishingly small in comparison with the constant grid potentials and that the influence of the alternating potentials on the period of electronic oscillations is insignificant. This conception is erroneous.

The dependence of the wave-length on the amplitude of oscillations and the heating current enables us to explain some of the other phenomena observed. We shall mention as an example the displacement of the regions of oscillations with a change in the heating current (II, §13). Since to each point of the diagram corresponds its own wave-length it is clear that a change in the heating current and a consequent change in the wave-length must produce a displacement of the region of oscillations. Furthermore, the regions of normal waves will be differently displaced than the regions of dwarf waves; for their wave-lengths change differently with varying heating current, as we have just seen. The fact that for normal waves of low intensity, when they are mixed with the dwarf waves (II, §13), the values of $\lambda^2 E_g$ are greater than usual will also be readily understood.

§5

In the previous paper we have discussed the results of a graphic integration of the equations of motion of the electrons in the tube, performed by G. Kreutzer. As we saw, the electronic trajectories showed that the alternating potentials at the electrodes of the tube must decrease the length of the dwarf waves. On the other hand, we have found above, that the length of the dwarf waves increases with an increase in the heating current and the amplitude of the alternating potentials. As a matter of fact, these two results are not contradictory. The graphic integration of the equations of the motion of the electrons was performed for the case $E_0/E_g = 1/10$, E_0 being the ampli-

tude of the alternating potentials. Direct measurements of the amplitude of the alternating potentials, which we shall not discuss for the present, showed, however, that for our dwarf waves of the 2nd and 3rd order the maximum value of the ratio E_0/E_g is approximately equal to $1/30-1/45$, i.e., is considerably below the value assumed in our computations. For dwarf waves of the first order this ratio had a larger value being approximately equal to $1/14$, as a maximum. Fig. 1 shows that it is exactly for these waves that the curve showing the relation between the wave-length and the heating current has a maximum. Hence it follows that in the case of dwarf waves the alternating potentials at the electrodes of the tube have the following effect: the wave-length increases at first, reaches a maximum and decreases as the amplitude of oscillations is further increased. It is evident that no maxima are observed on the curves relating to dwarf waves of the 2nd and 3rd orders simply because the amplitudes of the alternating potentials are very small in this case. On the other hand, all the calculations were made for relatively large amplitudes of alternating potentials. This explains the apparent discrepancy mentioned above.

§6. On the Limiting Value of Const.$_0$

There are several formulas expressing the length of the waves in terms of the voltage at the electrodes and the dimensions of the tube. The simplest one is the well-known formula of H. Barkhausen

$$\lambda^2 E_g = d_a^2 \times 10^6 \tag{8}$$

which is easily obtainable from Eqs. (1) and (2). This formula claims no particular accuracy, since in deriving Eq. (2) plane electrodes were assumed for the sake of simplicity.

S. Zilitinkiewitch[12] and A. Scheibe[13] obtained more accurate formulas which take into account the cylindrical shape of the electrodes. The formula of S. Zilitinkiewitch is expressed in a function of two rather slowly converging series. It is therefore less convenient than the formula of A. Scheibe. The latter formula can be written as follows for the case when the plate potential are low or equal to zero:

$$\lambda^2 E_g = \frac{2c_0^2 d_g^2}{e/m \times 10^8}[f(\ln d_g/d_f)^{1/2} + g(\ln d_a/d_g)^{1/2}]^2 \tag{9}$$

where d_a, d_g and d_f are the diameters of the plate, grid and filament respectively, e/m is the ratio of the electronic charge to its mass[14] and the two functions in the brackets are:

[12] S. Zilitinkiewitch, Drahtl. Tel. u. Tel. (Russ) **18,** 2–22 (1923); **19,** 166–175 (1923); Arch. f. Elektrot **15,** 470–484 (1926).

[13] A. Scheibe, Ann. d. Physik **73,** 54–88 (1924).

[14] The constant coefficient $[2c_0^2/(e/m)\times 10^8] = 1.017\times 10^6$. Strictly speaking, formula (8) also ought to have this coefficient. It had been omitted, as this formula is only approximate.

$$f(\ln d_g/d_f)^{1/2} = f(x) = xe^{-x^2}\int_0^x e^{n^2}dn$$
$$g(\ln d_a/d_g)^{1/2} = g(x) = xe^{x^2}\int_0^x e^{-n^2}dn. \tag{10}$$

The numerical values of $f(x)$ and $g(x)$ can be obtained from the tables given in the paper of A. Scheibe[13] or from more detailed tables computed by N. Kapzov and S. Gwosdower.[15]

As to the accuracy of Barkhausen's formula, we have already mentioned that it gives wave-lengths which differ by approximately 15 percent from the observed values. Of course, this figure refers only to the observations described above. From what we have said, it follows that the discrepancy between the observed and the calculated lengths of normal waves must become greater at greater amplitudes of oscillations. As an example, we can mention our preliminary measurements made with two tubes working simultaneously (II, §3). During these observations the plate current was greater than the one given by a single tube, $\lambda^2 E_g$ was equal to 5.44×10^5 and the discrepancy between the observed length of normal waves and that given by formula (8) was approximately 20 percent, as could be readily shown by simple computations.

The formula of A. Scheibe has been verified experimentally several times. As could be expected, it was in better agreement with the observations than formula (8). Nevertheless, the values it gave differed by some 10 percent from the observed wave-lengths.

Approximately the same agreement with the experimental data is obtained using the formula of S. Zilitinkiewitch, judging from the data of his paper. It must be mentioned that the obtained wave-lengths (normal waves) are always shorter than those computed from formulas (8) and (9).

In deriving formula (9), as well as in deriving formula (8), the dependence of the length of waves on the amplitude of the oscillations has also not been taken into account and the electrode potentials were assumed to be constant. From the preceding it is clear that for this reason alone there could be no good agreement between these formulas and the observations.

In the limiting value of $(\text{const.}_0)I_a = 0$ the effect of the alternating potentials is eliminated. Hence, this value must be in better agreement with formulas (8) and (9) than the direct observations. We shall-verify this statement.

Let us consider formula (8). As we have seen previously (II, §4), for the tubes of the type R5 this formula gives:

$$\text{const.}_{\text{Barkh}} = 7.6\times10^5. \tag{11}$$

This value differs from our limiting value 6.70×10^5 by approximately 12 percent. This corresponds approximately to a 6 percent difference in the wave-lengths, since the constant contains the square of the wave-length.

[15] N. Kapzov u. S. Gwosdower, Zeits. f. Physik **45**, 114–134 (1927).

As previously this difference in the wave-length amounted to approximately 15 percent (the difference in the values of $\lambda^2 E_g$ being approx. 30 percent) it becomes evident that among the errors of this formula, the largest error is introduced by neglecting the effect of the alternating potentials. Of course, this statement refers only to waves of sufficient intensity, such as our normal waves. As the intensities of the waves falls off, there must be a decrease in the relative error due to the alternating potentials.

Using formula (9) we obtain:[16]

$$\text{const.}_{\text{Sch}} = 7.22 \times 10^5. \tag{12}$$

This value differs from the limiting value of $(\text{const.}_0) I_a = 0$ by approximately 7 percent, which corresponds to a difference in the wave-lengths of approximately 3.5 percent. It could be shown by computations that the difference between directly observed wave-lengths and formula (9) constitutes approximately 12 percent. By comparing this figure with the preceding one, we can see again how large is the error introduced by neglecting the influence of the alternating potentials.

Under the conditions of our experiments the possible errors in formulas (8) and (9) can roughly be estimated as thus: neglecting the alternating potentials at the electrodes introduces in the wave-lengths an error of about 9 percent; the simplification of the problem by assuming plane instead of cylindrical electrodes introduces an error of about 3 percent, finally, all the other possible causes,[17] including the effect of space charges and the initial velocity of the electrons, introduce an error of also approximately 3 percent.

Comparing the magnitudes of all these errors it can be seen that in developing a theory of the generation of ultra-short waves there is no particular need of taking into account the shape of the electrodes.

In order to simplify the problem, it is quite sufficient to assume the electrodes of the tube to be plane. At the same time, it is quite necessary to take into account the effect of the alternating potentials. This is true of all problems which aim at determining the length of the generated waves, the time it takes the electrons to pass inside the tube, etc. In other cases, for example, in deriving formulas determining the conditions of the appearance of oscillations, their energy, etc., the assumption of plane electrodes will be of greater importance.

§7.

In deriving formulas (8) and (9) the wave-lengths were determined from the time it takes the electrons to pass from the filament to the plate and back to the filament. The very small difference existing between the values of $(\text{const.}_0)_{I_a=0}$, $\text{const.}_{\text{Barkh}}$ and $\text{const.}_{\text{Sch}}$ shows that *the normal waves generated by the tubes do really correspond to the time of passage of the electrons from the*

[16] The tubes of the type R5, which we investigated, had d_a (internal) = 0.87 cm; d_g (middle) = 0.37 cm; d_f = 0.006 cm.

[17] The error introduced through experimental errors is very small. For example, for observations given in Table V of article II the calculations give for normal waves $\lambda^2 E_g = 5.78 \times 10^5 \pm 0.017$.

filament to the plate[18] *and back to the filament*, in other words, they correspond to a complete period of electronic oscillations about the grid of the tube. This conclusion is of a very great importance for the theory of the generation of ultra-short waves. There exists a number of papers,[19] in which the length of waves is calculated from the time it takes the electrons to pass from the grid to the plate and back to the grid. This tendency of using a shorter path is quite understandable in view of the fact that the observed wave-lengths are always shorter than those obtained from formulas (8) and (9), as we have mentioned before. The agreement between the theory and the observations can be improved thereby. The foregoing considerations show, however, that another way must be chosen in order to obtain a better agreement between the theory and the observations. Namely, the effect of the alternating potentials on the motion of the electrons within the tube must be accurately estimated. At the same time, it is necessary to preserve the fundamental idea of H. Barkhausen's theory, according to which the length of the normal waves, generated by the tube corresponds to a complete period of electronic oscillations. This idea is unquestionably correct. The only possible exception is the case when waves are generated by a tube with a very closely wound grid (close mesh). In such a case, as it was shown by H. Hollmann,[6] it is possible to obtain, together with the usual oscillations, the so called "oscillations of a higher frequency." They will correspond to the shorter path and to a shorter time of passage of the electrons, which in this case will be easily captured by the grid on their way from the plate to the filament.

In conclusion the author wishes to express his gratitude to the Carnegie Corporation of New York for the grant of a Fellowship and to Professor R. A. Millikan for the facilities of the Norman Bridge Laboratory.

[18] Strictly speaking to the point of reversal.

[19] See, for example, E. W. Gill and J. H. Morrell, Phil. Mag. **44**, 161–178 (1922), D. Pfetscher, Phys. Zeits. **29**, 449–478 (1928); E. W. Gill, Phil. Mag. **12**, 843–853 (1931).

The Hall Effect With Audiofrequency Currents

By LAWRENCE A. WOOD
Department of Physics, Cornell University

(Received May 16, 1932)

Hall e.m.f. in tellurium for currents of frequencies up to 25,000 cycles per sec.—The Hall e.m.f. in tellurium has been investigated with currents of frequencies up to 25,000 cycles per second, with particular reference to any effect of frequency on the magnitude of the Hall coefficient R_H, and on the phase of the Hall e.m.f. relative to the longitudinal current producing it. A Hartley-circuit vacuum-tube oscillator furnishes the current for the specimen, which is placed in a constant magnetic field of about 3000 gauss. The Hall e.m.f., amplified by a resistance-coupled vacuum-tube amplifier, is observed on a cathode-ray oscillograph. A general method of procedure is indicated for use in *comparing alternating e.m.f.'s* as small as a few millivolts or less with respect to magnitude and phase. The current drawn and the power consumed are entirely inappreciable. The results of a comparison method of this sort and a null method agree in the conclusion that in the range studied, the Hall coefficient for tellurium is constant to within about 2 percent for frequencies up to 10,000 c.p.s. and to within 7 percent for the complete range. This agrees with the results of Smith on bismuth. For the specimen used the value found for the Hall coefficient is $R_H = 481$. The two methods also agree in finding the frequency, wave-form, and phase of the Hall e.m.f. the same as those of the longitudinal current producing it. The phase difference, if any, is believed to be less than 2° at frequencies below 20,000 c.p.s. and less than 4° at 25,000 c.p.s.

ALTERNATING-CURRENT HALL EFFECT

THE usual equation for the Hall e.m.f.

$$E_H = R_H H I/d \tag{1}$$

(in which R_H is the Hall coefficient, H the magnetic field, d the thickness of the plate, and I the current) shows that the e.m.f. reverses direction with reversal of the current. The Hall effect may be regarded as a rotation of the equipotential lines in the plate, and it may be readily shown[1] that

$$R_H H = \rho \tan \theta \tag{2}$$

where θ is the angle of rotation and ρ is the resistivity of the material. The angle of rotation is thus seen to be independent of the magnitude and direction of the current.

The number of workers who have investigated the Hall effect with alternating currents is surprisingly small. All investigators[2,3,4,5] agree that the

[1] Campbell, Galvanomagnetic and Thermomagnetic Effects, Longmans, Green, and Co., 1923.

[2] Des Coudres, Phys. Zeits. **2**, 586 (1901).

[3] Von Traubenberg, Ann. d. Physik **17**, 78 (1905).

[4] Zahn, Ann. d. Physik **36**, 553 (1911).

[5] Smith, Phys. Rev. **35**, 81 (1912).

magnitude of the effect is the same as with direct current, but no further observations of its character seem to have been reported.

In the work described in the present paper, alternating current, furnished by an oscillating vacuum-tube circuit was maintained in a tellurium plate. A unidirectional magnetic field produced an alternating Hall e.m.f. which was then amplified by the use of a vacuum-tube amplifier and observed on a cathode-ray oscillograph.

An arrangement of this sort has two important advantages over those previously used for studying the a.c. Hall effect. In the first place, practically no current is drawn from the circuit for the purpose of measurement (observations indicating that even the d.c. grid current is less than 10^{-9} amp.), and thus we are able to deal with an actual Hall e.m.f. rather than with a Hall current, which may disturb conditions in the plate, and which in any case necessitates corrections for the inductive effects of leads and measuring instruments. Secondly, observations can be made of the frequency, wave form, and phase of the Hall e.m.f. as well as of its magnitude.

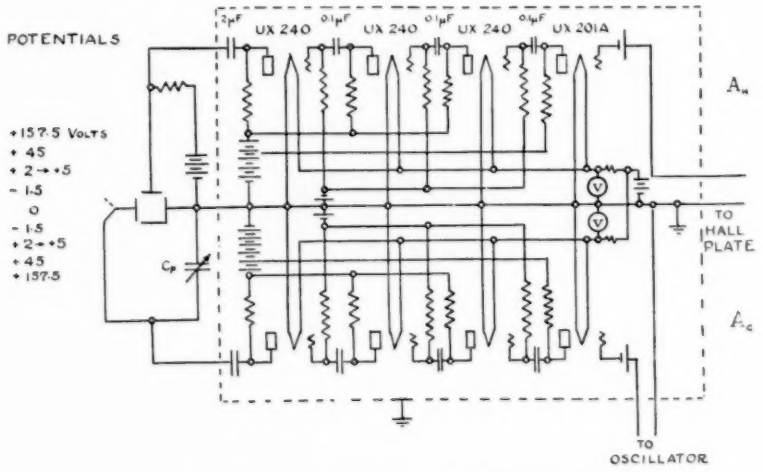

Fig. 1. Amplifier—oscillograph circuit diagram.

Tellurium was chosen because of its extremely large positive Hall coefficient. Bismuth, the material used in the high frequency work of Smith[5] (the only other observer to work at higher than commercial frequencies), has a negative coefficient of smaller magnitude.

Experimental Arrangement

Oscillator

The vacuum-tube oscillator was of the conventional Hartley circuit type, utilizing a UX 250 tube and giving a maximum power output of almost five watts. It was unshielded and was placed about twelve feet from the other apparatus, it being found by experiment that this distance was sufficient to prevent direct transfer of energy to the shielded amplifier and was more satisfactory than shielding. The inductance was a flat multilayer coil with air

core. For the purpose of electrostatic shielding a grounded strip of solid copper was placed around the coil, the lapped ends being insulated from each other in order to avoid electromagnetic shielding. Outside this, ten turns of wire formed a pick-up coil sufficient to maintain a half-ampere current in the tellurium plate.

The specimen was shielded from the oscillator and other electrical disturbances by being placed in a grounded copper box.

Hall plate and magnetic circuit

The tellurium plate itself, of dimensions $4 \times 2 \times 0.25$ cm, was cast in a rectangular hole cut in an asbestos plate and supported on a second asbestos plate rotated 45° with respect to the first, to give support to the lead wires. Platinum wires running through a groove between the asbestos plates were melted into the tellurium when the plate was cast. These made three fixed contacts with the plate—one at each end and one on one side.

A fourth contact P on the opposite side, was a movable pin which made contact with the upper surface of the plate. This pin was mounted on a carriage, similar to the tool-rest on a lathe, which gave by adjustment of micrometer screws two-dimensional motion in the plane of the specimen. The pressure of the contact at P could be adjusted by a thumbscrew.

The plate was mounted in the air gap of a magnetic circuit in which fields up to slightly more than 4000 gauss could be obtained.

Amplifiers

The two amplifiers, placed in a second large copper box, each consisted of a UX 201A tube followed by three stages of resistance-coupled amplification employing the "high-mu" UX 240 tubes. This gave a voltage amplification of 40,000 when needed. The amplification was controlled by varying the filament voltage.

One amplifier served to amplify the Hall e.m.f. or an ohmic p.d., while the other, merely in order to impress on the oscillograph a voltage of the same frequency as the first but of variable phase, amplified the voltage picked up by a single-turn coil about a foot away from the oscillator. This coil could be rotated to vary the amplitude. The variation of phase was accomplished by the use of a variable condenser C_P placed across the amplifier output. When this variation was not sufficient, a resistance was placed in series with the condenser and the potential across one or the other placed on the oscillograph.

It was not desirable to connect the oscillograph directly across the plate resistance of the last amplifier tube, because of the potential difference caused by the d.c. plate current. An output transformer did not prove satisfactory because of variations in magnitude and phase of the output with change of frequency and conditions of operation of the amplifier. Placing a two microfarad blocking condenser in the line to the oscillograph, however, accomplished the desired result without appreciable reduction of the a.c. voltage to be measured.

Oscillograph

The cathode-ray oscillograph, a Bedell-Reich Oscilloscope,[6] was used to examine the output of the first amplifier, either with the horizontal linear time axis or with the horizontal sinusoidal time axis provided by the second amplifier, or with no horizontal displacement at all. Amplified stabilization, as described by Bedell and Kuhn,[7] was employed with the linear time axis.

A method of frequency measurement[8] by means of a calibration of the current charging the condenser in the "sweep voltage" circuit of the linear time axis of the oscilloscope was employed.

In order to avoid the distortion[9] often produced in the oscillograph tube when the electric field across the vertically-deflecting plates is zero, a 45-volt B-battery in series with a resistance was placed across these plates. The spot was then brought back to the center of the screen by a permanent magnet above the tube. Experience showed that this eliminated the distortion and introduced no appreciable additional change in the beam.

Procedure

I. Comparison method

The first method consisted of the comparison of the Hall e.m.f. with an ohmic potential difference as nearly as possible in phase with the current in the tellurium plate and proportional to it. Comparison of the magnitudes of the two voltages was followed by a comparison of their phases. The magnitude comparison involved merely the measurement of the oscillograph deflections, first when the Hall e.m.f. was placed across the amplifier A_H and then when, by a switch, connections were shifted to place the ohmic potential difference across the same amplifier.

A similar plan was followed in the phase comparison, but in this case the second amplifier A_C was utilized. With the ohmic potential difference on the vertically-deflecting plates of the oscillograph, the phase of the comparison voltage E_C was varied by variation of condenser C_P until there was no phase difference. By the shift of connections already mentioned the Hall effect itself could now be amplified by the same amplifier and placed across the vertically-deflecting plates. By this means the phase of the Hall e.m.f. could be compared with that of E_C and thus with that of the ohmic potential difference. Any phase difference showed itself in an opening of the straight line into an ellipse. Measurements of the amplitude of the vertical and horizontal deflections separately and of the major and minor axes of the ellipse gave data for phase computations.

After several other methods of obtaining the ohmic potential difference had proved unreliable, it was realized that a potential difference E_B along the edge of the plate itself, obtained by displacing the movable pin contact P a fixed distance from its initial position P_1, was certain to be in phase with the

[6] Bedell and Reich, Journal Am. Inst. E. E. **46,** 563 (1927).
[7] Bedell and Kuhn, Rev. Sci. Inst. **1,** 227 (1930).
[8] Wood, Rev. Sci. Inst. **3,** 378 (1932).
[9] Bedell and Kuhn, Phys. Rev. **36,** 993 (1930).

current and proportional to it, providing only that the inductive reactance of the plate was negligible in comparison with its resistance. Calculation indicated that this was true.

II. Null method

The second or null method of observation, obviously suggested by the other method, employed the potential difference E_B along the side of the plate to balance out the Hall e.m.f. Accordingly with the amplifier A_H connected to terminals P and Q on an equipotential line as before, the magnetic field was impressed across the plate and the resulting Hall e.m.f. E_H was balanced out by a displacement of point P parallel with the edge of the tellurium plate from its former position P_1 to a new position P_2, so that P_2 and Q lay on the same new equipotential, as shown by zero vertical displacement of the oscillograph. No horizontal deflection whatever was employed. In the comparison method, E_B was made only approximately the same size as E_H; here they were made exactly equal by this adjustment for zero deflection. The amplifier and oscillograph were thus used here only as a potential-detecting instrument.

The location of P_2 should be dependent only on the angle of rotation of the equipotentials, and thus should be independent of the current and of the actual size of the Hall e.m.f. and consequently independent of the amplification. With P_2 left fixed, the frequency was varied in order to observe whether P_2 and Q still remained at the same potential.

RESULTS

A detailed summary of some of the experimental results obtained by each method will now be given.

In the first place, the production of ellipses and straight lines on the oscillograph screen showed that the frequency of the Hall effect was the same as that of the current in the tellurium plate. There was hardly any doubt that this result was to be expected, yet apparently no direct observations of this sort had been made previously. Furthermore the fact that the ellipses and lines were undistorted showed that the wave-form of the Hall e.m.f. was essentially the same as that of the current producing it.

Values obtained in the $E_H - E_B$ comparison are given in Table I. The numerical values of the oscillograph deflections recorded are of no particular

TABLE I. *Amplitude and phase comparisons at different frequencies. $I = 0.48$ amp. $H = 3100$ gauss.*

f (c.p.s.)	Magnitude			Phase			
	$2E_H$	$2E_B$	E_H/E_B	$2E_H$	$2E_e$*	$2b$	ϕ
750	7.63 cm	7.48 cm	1.02	7.5 cm	7.4 cm	<0.3 cm	<3° 20′
2750	7.34	7.19	1.02	7.8	7.6	<0.3	<3° 10′
5500	7.53	7.34	1.03	7.4	7.2	<0.3	<3° 20′
10000	7.27	7.25	1.00	7.2	7.2	<0.3	<3° 30′
19200	6.30	6.10	1.03	6.1	6.3	<0.3	<3° 50′
25000	2.75	2.70	1.02	2.9	3.0	<0.3	<8° 20′

* Adjusted to phase equality with E_B.

significance; it is the variation of their ratio with frequency that is of interest. The column headed ϕ gives the phase angle between E_B and E_H, as computed by the method given below from the experimental observations in the preceding three columns.

In the null method, when P was placed at the equipotential point P_2 at a given frequency by making the oscillograph deflection zero, it was observed that at each other frequency within the range studied the oscillograph deflection, if any, was too small to be measured. It could not have been greater than 0.2 cm. This held true even when the amplification (at all but the frequencies above 10,000 c.p.s.) was increased to a value which would have produced a Hall e.m.f. deflection three or four times those previously used (in the comparison method). At frequencies above 10,000 c.p.s. the full amplification obtainable was used at all times.

A similar test was also made without the magnetic field, and, to the same precision as before, the location of P_1 was also found to be unchanged with frequency.

The distance between P_1 and P_2 when a field of 2900 gauss was used was observed to be approximately 0.022 cm. This corresponds to an angle θ of rotation of the equipotentials of about 38′.

Interpretation of Results

Combining the Hall equation

$$E_H = R_H \cdot (H/d) \cdot I \tag{1}$$

with

$$E_B = IZ_B \tag{3}$$

where Z_B is the impedance between the two points P_1 and P_2 along the edge of the tellurium plate, we obtain

$$E_H/E_B = (H/d)(1/Z_B)R_H. \tag{4}$$

Thus the question of the constancy of Z_B with frequency is seen to be of importance here.

The inductance of the tellurium plate was calculated[10] to be 0.024 microhenry, corresponding to an inductive reactance of 0.0038 ohm at 25,000 c.p.s. The value of the resistance of the plate, measured directly, (2.5 ohms) is about 660 times this value, and hence Z_B should be independent of frequency within the precision of the measurements. The constancy of the E_H/E_B ratio as shown in Table I then indicates that there is no change in R_H with frequency.

The question of the determination of phase from measurements of a given ellipse has already been discussed elsewhere.[11] The formula developed there is

$$\sin \phi = ab/A_x A_y \tag{5}$$

[10] Bureau of Standards Circular No. 74 (*Radio Instruments and Measurements*), page 246.
[11] Wood, Rev. Sci. Inst. **2**, 644 (1931).

where a and b are the semi-axes of the ellipse, and A_x and A_y half the horizontal and vertical deflections respectively. Measurements of all four quantities were made, and the phase angle calculated by this formula. The four quantities are also connected by the relation:

$$A_x^2 + A_y^2 = a^2 + b^2. \tag{6}$$

This relation was used as a check on the measurements.

The phase angle ϕ_{BI} between E_B and the current I should be such that

$$\tan \phi_{BI} = X_B/R_B. \tag{7}$$

The argument to show that this ratio of inductive reactance X_B to resistance R_B along the edge of the plate is negligible has already been given in the discussion of the magnitude ratio E_H/E_B.

Thus the phase of E_B is negligibly different from that of I. From Table I it may be seen that ϕ the phase angle between E_B and E_H, if different from zero, is smaller than can be detected by this method.

In the null method the simple fact that the locations of P_1 and P_2 are unchanged with frequency variation, leads to the conclusion that both magnitude and phase of the Hall effect are independent of frequency.

Since the oscillograph deflection remained zero to within 2 mm in, say, 150 mm at frequencies of 10,000 c.p.s. or below, we may say that the Hall coefficient is constant (or proportional to the impedance, if our calculations in regard to the negligibility of inductive reactance should be in error) to within 1.5 percent. At a frequency of 25,000 c.p.s. we may say that it is constant to within 2 mm in 30 mm or 7 percent. Thus this method checks with greater precision the result of the comparison method in finding no change of Hall coefficient with frequency.

The very fact that it is possible to find a point P_2 at the same potential as Q, when the magnetic field is turned on, shows that there is no phase difference between the Hall e.m.f. and the current producing it. Calculations indicate that a phase difference of 2° could have been detected at frequencies below 20,000 c.p.s. and a phase difference of 4° at 25,000 c.p.s.

Magnitude of the Hall Coefficient

Although the primary object of this work was merely to observe changes in the magnitude and phase of the Hall effect with frequency, no particular attention being paid to making a careful measurement of the actual value of the Hall coefficient R_H, it is possible to make an approximate calculation of its value, from observations made in a comparison method similar to that already described, but which involved the use of the potential across a small series resistance.

The comparison with the small series resistance proved unsatisfactory only at the higher frequencies. Therefore, since the average low-frequency value of the E_H/E_R ratio was 1.115 and $Z_R = R_R = 0.005$ ohm, we are able to utilize an equation similar to that already derived for the E_H/E_B ratio, namely,

$$E_H/E_R = (H/dZ_R)R_H \tag{8}$$

in order to calculate R_H. Other numerical values are $H = 2900$ gauss, and $d = 0.25$ cm, the latter dimension being somewhat uncertain. Thus we find for the Hall coefficient

$$R_H = 481$$

in reasonable agreement with values reported by other observers working exclusively with direct currents, as given in Table II (taken from Campbell's monograph[1]).

TABLE II. *Tellurium Hall coefficient.*

Temp.	H	R_H	Observer
20°C	2800	530	Ettingshausen and Nernst
27.1°	Immaterial	784	Wold
65°	4000	430	Lloyd
—	—	500	Zahn
21.8°	8800	I 536	Smith
20.3°	8800	II 621	Smith

CONCLUSIONS

It would seem manifestly desirable to continue the work to higher frequencies. In view of the radical changes in technique rendered necessary at radiofrequencies, this was not attempted in the present investigation. The null method, in particular, would seem to lend itself readily to this extension, and work upon it is now in progress.

The combination of two amplifiers and oscillograph offers, it would seem, a powerful tool for the investigation at different frequencies, of the phase and magnitude of small voltages other than the Hall e.m.f. The comparison procedure here outlined could be followed with little change.

Finally, the author desires to express heartfelt gratitude to Professor Merritt, who suggested the problem and without whose continued interest it could not have been carried to completion, as well as to many other friends whose advice and suggestions have been extremely helpful.

Some Thermo- and Galvanomagnetic Properties of a Bismuth Crystal

By H. E. BANTA
The Rice Institute

(Received June 9, 1932)

The fractional changes, due to a magnetic field, in the electrical conductivity, in the thermal conductivity, and in the thermoelectric power of a single bismuth crystal are measured in these experiments. These changes are determined as a function of the field strength, of the direction of the field, of the direction of the crystal axis, and of the direction of the heat and electric currents through the crystal. An electric current sent through the crystal cools one junction and heats the other by the Peltier effect. The temperature difference thus produced gives rise to a thermal e.m.f. in the crystal circuit. Observations of this e.m.f. allow the calculation of the fractional changes produced in the thermal conductivity and in the thermoelectric power. The change of electrical conductivity is influenced much more strongly by the crystal structure than is the change of thermal conductivity. Crystal structure and orientation of the magnetic field both affect strongly the change in the thermoelectric power. The theory of electrons in metals in its present form does not give an adequate explanation of the results. If the magnetic field changes the free electron density in bismuth some of the results may be explained in a general way.

IN 1886 Nernst and Ettingshausen[1] discovered that if a copper-bismuth thermocouple were put in a magnetic field, the e.m.f. of the couple was changed. In their experiments the magnetic field was perpendicular to the direction of heat flow. They concluded that the effect varied with the square of the magnetic field strength and with the temperature, but was independent of the dimensions of the bismuth. Other investigators[2] have found that the effect exists for other orientations of the magnetic field, but that the magnitude of the effect depends on the direction of the field; that[3] if a single crystal is used, the magnitude of the effect depends also on the orientation of the crystalline axis.

The intimate connection between the thermoelectric power, thermal conductivity, and electrical conductivity (all three being supposed to depend on free electron concentrations) suggests that a study of their changes in a magnetic field and the relation between these changes and the position of the crystalline axis might add materially to the knowledge of the nature of galvanomagnetic and thermomagnetic effects. This paper contains an account of such a study with single crystals of pure bismuth.

Apparatus and Method

The method used was in general as follows:—an electric current sent through the crystal cools one junction and heats the other by the Peltier

[1] Nernst and Ettingshausen, Wied. Ann. **29**, 343 (1886).

[2] Hall and Campbell, Proc. Am. Acad. **46**, 625 (1911); A. W. Smith, Phys. Rev. **2**, 383 (1913); Lownds, Ann. d. Physik **4**, 776 (1901).

[3] C. W. Heaps, Phys. Rev. **31**, 648 (1928).

effect. This current is broken and a very short time afterwards the crystal is connected to a potentiometer which is set to balance the thermal e.m.f. produced by the temperature difference at the junctions. This same experiment is repeated when the crystal is in a magnetic field. It is then possible to calculate the fractional change of the thermoelectric power produced in the crystal by the field. This general method was first used by la Rosa.[4] He did not, however, make a necessary correction for a possible effect of the field on the thermal conductivity.

The arrangement of the apparatus is shown in Fig. 1. A single crystal of bismuth was immersed in oil between the poles of a large Weiss water-cooled electromagnet. The electromagnet could be rotated so as to vary the direction of the magnetic field. The crystal was soldered to copper wires with Wood's metal. Two Burgess vacuum relays were connected to these wires.

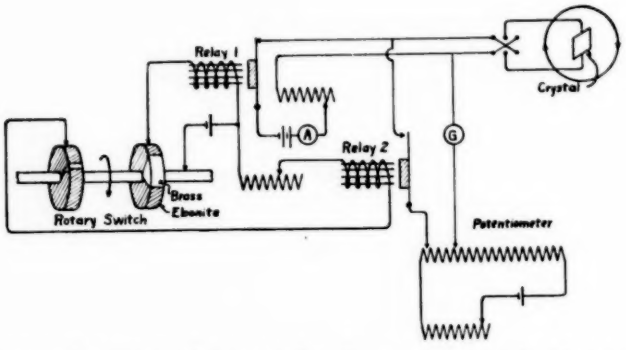

Fig. 1. Arrangement of apparatus for measuring change of thermoelectric power and thermal conductivity in a magnetic field.

The relays were operated by a rotary switch running at constant speed. They were so arranged that both were never closed at the same time. From Fig. 1 it is seen that relay 1 controlled the current through the crystal, and relay 2 connected the crystal across the potentiometer. The galvanometer used with the potentiometer, of the astatic moving magnet type, was adjusted to a sensitivity of about 300 mm per microvolt.

In the position shown the rotary switch allows a current i to pass through the crystal. This current, because of the Peltier effect, produces a temperature difference between the junctions on the crystal. Rotating the rotary switch cuts off this current by operating relay 1. At an adjustable time t later, by operating relay 2, the rotary switch connects the crystal to the potentiometer for a very short time. Farther rotation turns on the current i, and the cycle is repeated in the next revolution of the rotary switch. If the potentiometer is not adjusted to the e.m.f. of the crystal, the galvanometer will be deflected once during each cycle. By adjusting the potentiometer till the galvanometer is not deflected, the thermal e.m.f. in the crystal circuit could be measured. The rotary switch was arranged so that the e.m.f.'s E_1 and E_2

[4] La Rosa, Nuovo Cim. **18,** 26 (1919).

at two times t_1 and t_2 after the current was cut off could be determined. E_1 and E_2 were determined with and without the magnetic field. The apparatus was capable of measuring an e.m.f. to a tenth of a microvolt; but variable stray thermal and contact e.m.f.'s make the accuracy of observation somewhat less than this.

Theory of the Method

The heat generated at the hot junction, for example, raises the temperature of that junction, and is then conducted partly through the crystal to the cold junction and partly into the oil around the junction. If the electric current has been flowing long enough for the crystal junctions to reach an equilibrium temperature difference, the heat is conducted away as fast as it is liberated. If the heat conducted through the oil from one junction to the other be neglected, the heat conducted through the crystal will be equal to the Peltier heat liberated at the hot junction plus the difference between the Joule heats developed at the hot and cold junctions. Hence

$$i\pi + i^2(r_2 - r_1) = kBd\theta/dx \tag{1}$$

where i is the electric current, π the Peltier coefficient, r_1 and r_2 the resistances of the cold and hot junctions respectively, k the thermal conductivity, B a constant depending on the dimensions of the crystal, and $d\theta/dx$ the temperature gradient along the crystal. The term $i^2(r_2-r_1)$ is the difference between the Joule heats developed at the two junctions, which must be conducted through the crystal. Let $d\theta/dx=\Delta\theta/l$, l being the length of the crystal and $\Delta\theta$ the temperature difference between the junctions. In a magnetic field certain of these quantities will be changed. Denoting by a subscript H the values of these quantities in a magnetic field H, we have

$$i\pi_H + i^2(r_2 - r_1)_H = k_H B(\Delta\theta_H/l);$$

whence

$$\Delta\theta_H/\Delta\theta = k/k_H \frac{i\pi_H + i^2(r_2 - r_1)}{i\pi + i^2(r_2 - r_1)}. \tag{2}$$

When i is reversed the heat $i\pi$ is reversed in sign, but the heat $i^2(r_2-r_1)$ remains unchanged. It is thus possible by reversing i to estimate the magnitude of $i^2(r_2-r_1)/i\pi$. For example, E_1 was 76 microvolts; when the current was reversed E_1 was 84 microvolts. Thus the Joule heats developed at the two junctions contributed 4 microvolts to the observed e.m.f. In every case experiments gave $i^2(r_2-r_1)/i\pi$ less than 0.1. Thus to a good approximation

$$\Delta\theta_H/\Delta\theta = (k/k_H)(\pi_H/\pi). \tag{3}$$

Substituting $E=P\Delta\theta$ and $P=\pi/\theta$, where E is the e.m.f. of the crystal thermocouple and P its thermoelectric power, we get

$$\frac{E_H}{E} = \frac{P_H}{P}\frac{\Delta\theta_H}{\Delta\theta} = \frac{P_H}{P}\frac{k}{k_H}\frac{\pi_H}{\pi} = \frac{P_H^2}{P^2}\frac{k}{k_H}. \tag{4}$$

Putting $\Delta E = E_H - E$ and $\Delta k = k_H - k$ this relation gives

$$\Delta P/P = (1 + (\Delta E/E)_0 + \Delta k/k + (\Delta E/E)_0 \Delta k/k)^{1/2} - 1 \tag{5}$$

where $(\Delta E/E)_0$ is the value of $\Delta E/E$ at time $t=0$, immediately after the electric current is cut off, but before sufficient heat has been conducted away through the crystal to diminish $\Delta\theta$ appreciably. In order to calculate $\Delta P/P$ it is necessary to calculate $\Delta k/k$ and $(\Delta E/E)_0$.

Determination of $\Delta k/k$.

To determine $\Delta k/k$ we utilize the fact that $\Delta\theta$ is decreased after the electric current is stopped by conduction of heat through the crystal. Let $d/dt(\Delta\theta) = -Ak\Delta\theta$, A being a constant. This equation gives $\log(\Delta\theta/\Delta\theta_0) = -Akt$, where $\Delta\theta_0$ is the value of $\Delta\theta$ when $t=0$. Since $E/E_0 = \Delta\theta/\Delta\theta_0$, we have $\log(E/E_0) = -Akt$. It is impossible to observe E_0 experimentally. However, let E_1 and E_2 be the values of E at times t_1 and t_0 respectively. Then

$$\log(E_2/E_1) = -Ak(t_2 - t_1);\ \log(E_2/E_1)_H = -Ak_H(t_2 - t_1), \tag{6}$$

the H subscripts again denoting values obtained in a magnetic field. Dividing the second of these equations by the first and setting $\Delta k = k_H - k$ gives

$$\Delta k/k = \frac{\log(E_2/E_1)_H}{\log(E_2/E_1)} - 1. \tag{7}$$

Determination of $(\Delta E/E)_0$.

To determine $(\Delta E/E)_0$ we combine the two equations $\log(E_1/E_0)_H = -Ak_Ht_1$ and $\log(E_1/E_0) = -Akt_1$, getting

$$E_{0H}/E_0 = E_{1H}/E_1 e^{A(k_H - k)t_1} = E_{1H}/E_1 e^{Ak\Delta k/kt_1}. \tag{8}$$

A similar relation holds for t_2, which combined with (8) gives

$$(1/t_2 - 1/t_2)\log(E_{0H}/E_0) = 1/t_1 \log(E_{1H}/E_1) - 1/t_2 \log(E_{2H}/E_2). \tag{9}$$

This relation gives $(\Delta E/E)_0$, since $E_{0H}/E_0 = (\Delta E/E)_0 + 1$.

Thermal equilibrium must be reached in the crystal before the electric current is stopped if Eq. (1) is to apply. This condition was satisfied by increasing the time during which i flowed till further increase did not increase the values of the e.m.f.'s obtained. This made the time of one revolution of the rotary switch about 5 seconds. Then the e.m.f.'s were observed to be proportional to the current, as would be expected from equation (1) if the Joule heat be neglected. It was estimated from the magnitude of the observed e.m.f.'s that $\Delta\theta$ was about 1°C. P, π, and perhaps k are functions of the temperature, but it was assumed that the temperature changes during an experiment are so small that these quantities can be regarded as constant. A few observations were made with different currents; but within the limits of experimental error $\Delta E/E$, $\Delta k/k$, and $\Delta P/P$ were found independent of i.

With the direction of heat flow perpendicular to the crystalline axis and with a magnetic field of 8000 gauss perpendicular to both the crystalline axis and the heat flow, it was found that $E_1=85.0$ microvolts, $E_2=58.0$ microvolts, $E_{1H}=61.8$ microvolts, and $E_{2H}=45.3$ microvolts. If these values be substituted in Eq. (7), it is found that $\Delta k/k=-0.190$. From Eq. (9), with $t_1=0.129$ sec. and $t_2=0.662$ sec., it is found that $(\Delta E/E)_0=-0.285$. The variation of $\Delta E/E$ with the time is clearly seen here, since $(\Delta E/E)_{t_1}=-0.273$ and $(\Delta E/E)_{t_2}=-0.219$. If the above values be substituted in Eq. (5), $\Delta P/P=-0.245$ is obtained. These values are plotted in Figs. 4 and 6.

RESULTS

It was found much easier to determine accurately $\Delta E/E$ than $\Delta k/k$, since $\Delta k/k$ is calculated from the ratio of the logs of two quantities differing little from unity. Since the rate of cooling of the crystal couple depended on the physical dimensions of the crystal, it was found desirable for the crystal to have a cross-sectional area of about 1 mm^2; hence it was necessary to use two different specimens in order to secure all the desired orientations with

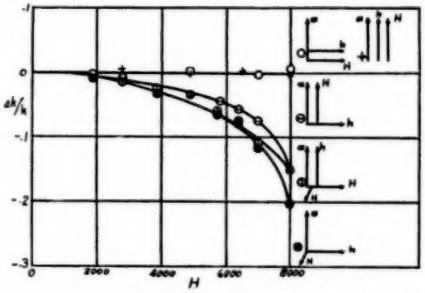

Fig. 2. Fractional change of thermal conductivity as a function of magnetic field strength.

respect to the crystalline axis. Both crystals were grown from the same very pure bismuth, supplied by Eimer and Amend. The direction of the crystalline axis was determined by observing reflections from cleavage planes by Bridgman's[5] method. The three-dimensional direction diagrams accompanying all the curves show the angles between the crystal axis a, the heat flow h, and the magnetic field H. The data for h parallel to a were obtained with one crystal, for h perpendicular to a with the other crystal.

The fractional changes in the thermal conductivity as a function of the magnetic field strength for several different orientations of the crystal axis a, heat flow h, and magnetic field H are shown in Fig. 2. It is of interest to note that the longitudinal effect, in which h is parallel to H (see the two top direction diagrams) is too small to measure.

It was found that when h was along a and H was perpendicular to both a and h, a rotation of H in this normal plane made no difference in the magnitude of the observed effects. This fact is indicated in the direction diagrams next to the bottom by showing H in two positions. The differences between

[5] Bridgman, Proc. Am. Acad. **60**, 305 (1905).

the curves for the cases in which the effect is measurable are about the same as the magnitude of the errors of observation. The values at 8000 gauss, however, are averages of several sets of observations, and it is believed that they show a real effect of the orientation of a on the value of $\Delta k/k$. In general it appears that the orientation of H with respect to the heat flow is of considerably greater importance than the orientation of H with respect to the crystal axis.

So far as is known to the author $\Delta k/k$ has not been measured before for a single crystal. If a bismuth plate consists of small crystals randomly oriented, the magnitude of the transverse effect should be the same as that shown here for the transverse orientations, (H perpendicular to h) which are approximately equal. The mean of two such values obtained for polycrystalline bismuth plates by Leduc[6] and Van Everdingen[7] at 6000 gauss is -0.0575. The mean of the values shown in Fig. 2 for this field is -0.056. The agreement is very good.

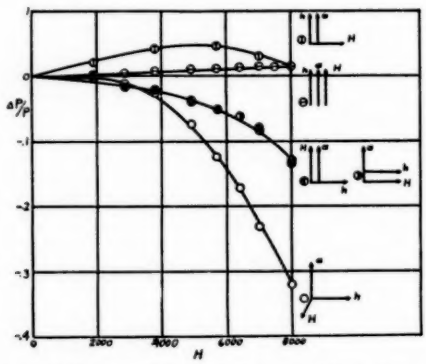

Fig. 3. Fractional change of thermoelectric power as a function of magnetic field strength.

As has been indicated, the fractional change in the thermoelectric power of the crystal couple can be calculated from the same four observations that gave $\Delta k/k$. The results obtained in this way are shown in Fig. 3. A similar set of results has been obtained by C. W. Heaps, who obtained $\Delta P/P$ by a more direct method. For h parallel to a, and H perpendicular to both a and h, his curve is almost a straight line rising to a value of 0.08 at 8000 gauss. The corresponding curve in Fig. 3 agrees with this up to about 4000 gauss. The lack of agreement between his curve and the one given here is probably due to a small angle between a and h, which would introduce components of all the negative values of $\Delta P/P$ shown in Fig. 3. A lack of uniformity in the evolution of heat over the ends of the relatively short crystals would result in a heat flow not strictly along the length of the crystal, which in this case was along a. Obviously a very small departure from parallelism of a and h would suffice to produce an appreciable decrease in the value of $\Delta P/P$. For the other curves of Fig. 3 the agreement with those of Heaps is as good as one might

[6] Leduc, Compt. Rend. **104,** 783 (1887).
[7] Van Everdingen, Jour. de Physique (3) **10,** 217 (1901).

expect, considering the difficulty of exact adjustment and the impossibility of securing crystals without flaws.

$\Delta P/P$ was observed to be a function of the temperature, but observations were only made between 18°C and 40°C. The results for $\Delta P/P$ are in general agreement with the experiments of A. W. Smith,[2] showing a decrease of $\Delta P/P$ with increasing temperature. The values of $\Delta P/P$, $\Delta k/k$, and the fractional changes of electrical conductivity given in this paper were all taken at 25°C.

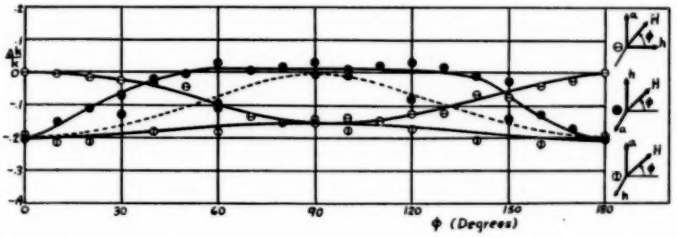

Fig. 4. Fractional change of thermal conductivity as a function of the varying angle ϕ shown in the three-dimensional direction diagrams.

Fig. 4 shows the effect on $\Delta k/k$ of rotating a constant magnetic field of 8000 gauss about h as an axis, about a as an axis, and about an axis perpendicular to both a and h. Maxima and minima are found where they would be expected from the curves of Fig. 2. The flat maximum of the curve with H perpendicular to a seemed peculiar, so the curve was repeated with another crystal and improved apparatus. All values obtained were negative; these results are shown by the dotted curve in Fig. 4. These last results are considered much more dependable than the first obtained. Hence no significance

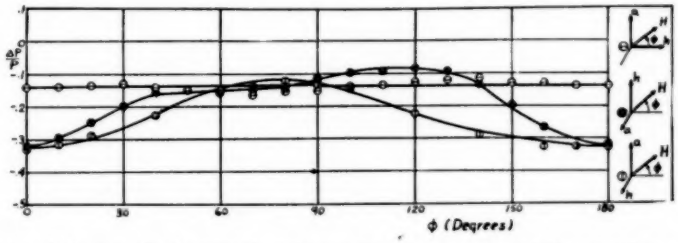

Fig. 5. Fractional changes in thermoelectric power as a function of the varying angle ϕ shown in the three-dimensional direction diagrams.

is to be attached to the small positive values of $\Delta k/k$ for the solid curve in Fig. 4, nor to the wide range through which they were obtained.

The values of $\Delta P/P$ were calculated from the data giving $\Delta k/k$ in Fig. 4. The results are shown in Fig. 5. For one direction of rotation the points fall approximately along a straight line. The outstanding feature of the other two curves is their lack of symmetry about 0° or 90°. The maxima and minima do not occur in the transverse or longitudinal positions, and one of the curves is not symmetrical about its maximum or minimum. It was found that

changing the direction of the magnetic field by 180° did not alter the magnitude of any of the effects observed, so all of these curves are repeated in the next 180°.

The curve through the black points was repeated with another crystal. The values of E_{0t_1}, E_{Ht_1}, and $\Delta P/P$ obtained are shown in the polar chart of Fig. 6. The variation in $\Delta P/P$ is not as large as that in Fig. 5, but the curve in Fig. 6 giving $\Delta P/P$ has the same general features as the corresponding one in Fig. 5.

Bismuth crystallizes in the dihexagonal alternating class of the hexagonal system. The plane of easy cleavage is parallel to the (111) planes and is per-

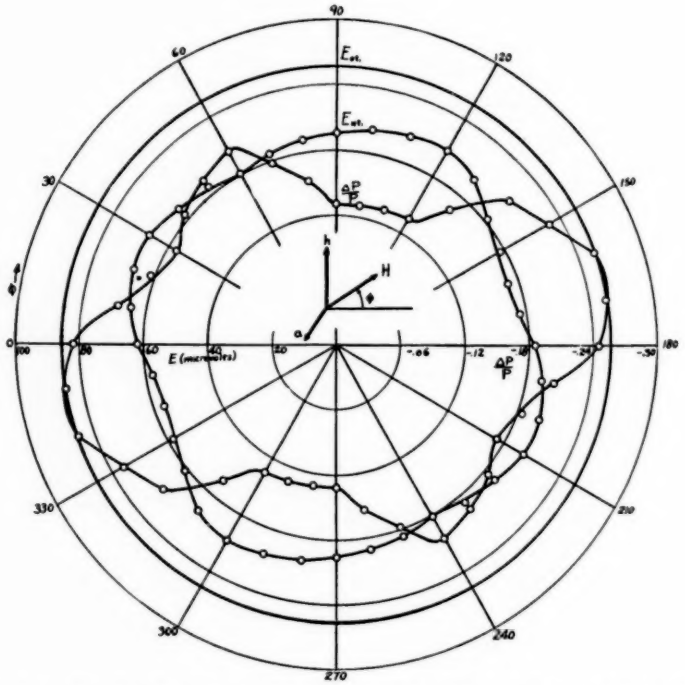

Fig. 6. Polar chart showing E_{ot_1}, E_{Ht_1}, and $\Delta P/P$ as a function of the varying angle 0 shown in the three-dimensional direction diagram.

pendicular to the trigonal axis. There is also fair cleavage parallel to the $(11\bar{1})$ planes. The crystal used to obtain Fig. 6 was found to have the magnetic field along the $(11\bar{1})$ planes as well as along the (111) planes at 165°. A maximum in $\Delta P/P$ occurs here. The $(1\bar{1}1)$ and $(\bar{1}11)$ planes intersect the (111) plane so that one is parallel to H at 105°, and the other at 45°. There is in Fig. 6 a minimum of $\Delta P/P$ at 105, but there is no similar feature at 45.

It appears from these considerations that the $\Delta P/P$ curve in Fig. 6 is not symmetrical about 0° or 90° because there are structure factors in the crystal which produce a distortion. The plane perpendicular to the crystal axis can thus not be considered as possessing circular symmetry about a. The separation in this plane of the two effects—namely, the structure effect and the

effect due to the direction of h with respect to H—appears to be impossible without a much more detailed investigation.

The fractional changes produced by the magnetic field in the electrical conductivity are shown as $\Delta c/c$ in Fig. 7. These results were obtained by soldering two more copper wires to the crystal where the current leads were soldered on, and by measuring with a potentiometer the potential drop V along the crystal. The current being held constant, the change ΔV produced in V by the field was determined, whence $\Delta c/c$ could be calculated. It was found that the temperature difference caused by the Peltier effect produced an appreciable error in these results; but since E_0 and $(\Delta E/E)_0$ could be calculated, the necessary correction could be applied.

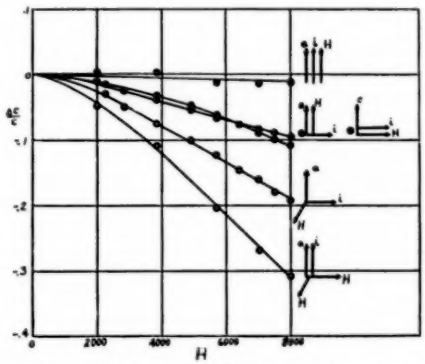

Fig. 7. Fractional changes of electrical conductivity as a function of magnetic field strength. Electric current direction is indicated by i, crystal axis by a, and magnetic field by H.

This effect is well known, and has been extensively investigated for polycrystalline bismuth. Lownds[8] gives two values of $\Delta c/c$ for a single crystal with different orientations in a magnetic field, and Borelius and Lindh[9] give several values which can be compared with the values of $\Delta c/c$ shown in Fig. 7. Their values were obtained at an average temperature of 18°C. The comparisons are made in Table I. The values given by Lownds, and by

TABLE I. *Values of $\Delta c/c$. Comparison with the results of others.*

Orientation	i ↑ a, H	a, H, i	a ↑ H, i	a, i, H	a ↑ i ↑ H	i ↑ a, H
Field H (gauss)	5000	5000	2300	2300	2300	2300
Lownds	-0.198	-0.143	----	----	----	----
Borelius & Lindh	-----	-----	-0.039	-0.053	-0.026	-0.085
Banta	-0.160	-0.103	-0.015	-0.015	-0.004	-0.055

Borelius and Lindh, are larger than the corresponding values found by the present experiments. Part of these differences can be explained as a tempera-

[8] Lownds, Ann. d. Physik (4) **9**, 677 (1902).
[9] Borelius and Lindh, Ann. d. Physik (4) **53**, 97 (1917).

ture difference, since Drude and Nernst[10] found that $\Delta c/c$ decreased rapidly with increasing temperature. As before, some of the differences may be due to imperfections in the crystals.

Conclusions

The results reported here are difficult to fit into any simple theory. There is at present no theory of electrons in metals which adequately accounts for all of the observed facts of thermoelectricity in crystals. Any theoretical result for $\Delta c/c$, $\Delta k/k$, or $\Delta P/P$ should be an even function of H, since the direction of H can be changed by 180° without affecting the magnitude of any of these quantities. Such a result has been obtained for $\Delta c/c$ with transverse fields by Sommerfeld[11] and Frank,[12] who get $\Delta c/c = -BH^2/(1+CH^2)$, B and C being positive constants. In obtaining this expression it is assumed that the magnetic field does not change the density of free electrons in the metal, but does disturb the distribution function. This equation has been found to fit the experimental results very well for ordinary polycrystalline metals. It is not, however, so successful in dealing with bismuth, which in many respects is abnormal; and it cannot be expected, in the form derived, to account for the important effect of crystalline structure. It might be expected that $\Delta c/c$ and $\Delta k/k$ would have their smallest values for H parallel to h and i respectively, since then the electron flow is along H. In general, this seems to be true. While the direction of the crystalline axis with respect to H or h is relatively unimportant for $\Delta k/k$, it is of decided importance for $\Delta c/c$.

Sommerfeld and Frank state that in the adiabatic case their calculations indicate that $\Delta k/k$ is only about two percent of $\Delta c/c$. Thus bismuth apparently has a much larger $\Delta k/k$ than can be accounted for by the Sommerfeld theory.

There is no satisfactory theory to account for the change in thermoelectric power in a magnetic field. If the classical result[13] $Pe = R \log (n_1/n_2)$ is assumed to hold approximately, then the only way to account for the change in P is to suppose that the density n of free electrons in bismuth is changed by the magnetic field. Possibly this change is indicated by the divergence of $\Delta c/c$ and $\Delta k/k$ from the values predicted by Sommerfeld's theory, which does not allow for a change of n. Suppose then that n_1 is the electron density in bismuth, and n_2 the electron density in copper. Then, since copper is a normal conductor and does not have its thermal e.m.f. affected by a magnetic field, $P_H e = R \log (n_{1H}/n_2)$.

Thus

$$P_H/P = \log (n_{1H}/n_2)/\log (n_1/n_2).$$

Let

$$n_{1H} = n_1 + \Delta n_1.$$

[10] Drude and Nernst, Wied. Ann. **42**, 568 (1891).

[11] Sommerfeld, Zeits. f. Physik **47**, 1 (1928).

[12] Sommerfeld and Frank, Rev. Mod. Phys. **3**, 1 (1931).

[13] O. W. Richardon, Electron Theory of Matter, p. 461.

Then

$$P_H/P = \frac{\log (1 + \Delta n_1/n_1) + \log (n_1/n_2)}{\log (n_1/n_2)}$$

$$= 1 + A \log (1 + \Delta n_1/n_1). \tag{10}$$

So $\Delta P/P = A \log (1+\Delta n_1/n_1)$, where $A = 1/\log (n_1/n_2)$.

From the curves of Fig. 3, Δn_1 is seen to be a function of both the magnetic field strength and the direction in the crystal. If we suppose that n_2 is greater than n_1 which seems a reasonable assumption in view of the relative electrical conductivities of the two metals, then A is negative. So, again from Fig. 3, Δn_1 is positive for three orientations of a, h, and H in the crystal, and negative for two orientations. The largest change in n_1 is for a, h, and H mutually perpendicular, and is an increase.

Classical electron theory[14] indicates that $k = Dn\lambda$ and $c = En\lambda$, λ being the mean free path of the electrons and D and E being constant at a given temperature.[15] It seems possible that a magnetic field, in addition to affecting n, may produce changes of molecular configuration which would alter λ. Changes of λ produced in this way would be distinct from any changes produced by such effects as curving of the free paths in the magnetic field, etc. Thus

$$\Delta c/c = \Delta n/n + \Delta\lambda/\lambda$$

and

$$\Delta k/k = \Delta n/n + \Delta\lambda/\lambda.$$

So $\Delta c/c = \Delta k/k$. According to Sommerfeld's theory, $\Delta k/k$ is only a small fraction of $\Delta c/c$. Thus the above result is more nearly in agreement with experiment than is Sommerfeld's theory. If it be assumed that the change in electrical conductivity c is due to a change in n and λ of the character indicated above, with the change predicted by Sommerfeld's theory in addition, then $\Delta c/c = \Delta n/n + \Delta\lambda/\lambda - BH^2/(1+CH^2)$. Since $\Delta k/k$ is very small according to Sommerfeld's theory, the whole effect may be given by $\Delta k/k = \Delta n/\lambda + \Delta\lambda/\lambda$.

Thus

$$\Delta c/c = \Delta k/k - BH^2/(1 + CH^2). \tag{11}$$

The experimental results indicate that this result is hardly satisfactory. According to Sommerfeld B is a positive constant; but if Eq. (11) is true, B must be negative for one orientation: namely, with H along a, and i and h respectively perpendicular to a. For these curves in Figs. 2 and 7, $\Delta k/k$ is less than $\Delta c/c$ at 8000 gauss. Another objection is based on the shape of the curves: it is hard to see how the addition of a square function of H to the curves of Fig. 2 could give the curves of Fig. 7. Also, the result of the theory of Sommerfeld and Frank is supposed to hold for transverse fields, and the quantity $BH^2/(1+CH^2)$ is thus zero for longitudinal fields—a result con-

[14] O. W. Richardson, Electron Theory of Matter, pp. 410–421.

[15] If Sommerfeld's formulae are used instead of the classical ones the results deduced are not essentially different from these above.

tradicted by these experimental results, although the longitudinal values of $\Delta k/k$ and $\Delta c/c$ are in general the smallest obtained.

Consideration of the results leads to the following conclusions: Theory indicates that $\Delta c/c$ should be negative for transverse fields. It is found negative, but the value is found to be dependent on the orientation of the crystalline axis with respect to the current and the magnetic field. The curves of Figs. 2 and 4 appear to indicate that there is some unrecognized but essential difference between the mechanisms of heat conduction and electric conduction in bismuth crystals. This conclusion is indicated by the fact that the $\Delta c/c$ curves are strongly influenced by crystal structure; the $\Delta k/k$ curves, on the other hand, appear to be roughly all the same for all cases where H is perpendicular to h. When H is parallel to h there is no measurable effect produced in $\Delta k/k$. There is some evidence that strong magnetic fields change the density of free electrons in the bismuth crystals.

The crystals used in this investigation were supplied by Professor C. W. Heaps, to whom the author is indebted for much valuable assistance and discussion. It is also a pleasure to thank Professor H. A. Wilson for generous advice on this problem.

Does Nickel Show a Positive Elongation in the Joule Magnetostrictive Effect?

By S. R. WILLIAMS
Fayerweather Laboratory of Physics, Amherst, Massachusetts

(Received June 4, 1932)

The question as to whether there is a positive Joule magnetostrictive effect in nickel has once more arisen. The following note points out that there is no positive elongation unless remanent magnetism or an extraneous field is present to give the sample of nickel a preliminary magnetization before the main field is applied. Even then, there is no positive elongation unless the preliminary magnetization is opposed to that of the main field.

THE above question seems to have cycles of recurrence. Not always does it take the form of the caption. In 1893–1904, Honda and Shimizu[1] carried on an extensive discussion with Heydweiler[2] concerning the presence or absence of a Villari reversal effect in nickel. If the Villari reversal effect occurs in nickel, then a positive elongation of nickel should also be found in the Joule magnetostrictive effect. This relation between the Villari and Joule effect seems to be very definitely established.[3]

Recently two papers[4] have appeared purporting to show a positive elongation for the Joule magnetostrictive effect in nickel and saying that it is an effect to be expected.

It is desired to point out that this may be misleading as these two papers state definitely that in the regular Joule magnetostrictive effect they did not find a positive elongation. They found a positive elongation only when the magnetizing force was reversed in observing a hysteresis curve for the Joule magnetostrictive effect. A positive elongation in nickel occurs only when there is remanent magnetism present in the specimen or an extraneous field is imposed, and then *only when the magnetizing field is opposed in direction to the remanent magnetization or the extraneous field.*

In Fig. 1 are shown continuous records of the changes in length of a nickel rod as the magnetizing force is increased from zero up to 71.2 gausses. The vertical lines in the photographs denote certain currents' strengths in the magnetizing coil. All of the photographs in Fig. 1 show six vertical lines and represent field strengths of 0, 14.2, 28.5, 42.7, 56.9, and 71.2 gausses respec-

[1] Honda and Shimizu, Ann. d. Physik **14,** 791 (1904); Phys. Zeits. **5,** 254 (1904); Ann. d. Physik **15,** 855 (1904); Phys. Zeits. **5,** 631 (1904).

[2] Heydweiler, Sitzungsber. d. Wurzb. phys. med. Ges. **11** Marz (1893); Phil. Mag. **35,** 469 (1893); Beibl. **17,** 1095 (1893); Ann. d. Physik **52,** 462 (1894); **15,** 415 (1904); Phys. Zeits. **5,** 255 (1904).

[3] Thomson, Applications of Dynamics to Physics and Chemistry, pp. 48–63, 1888. Williams, Proc. A.S.T.M. **19,** Pt. 2 (1919); School Science, and Math. **22,** 859 (1922); Phys. Rev. **10,** 129 (1917); Jour. Franklin Institute **203,** 843 (1927).

[4] Dietsch, Zeits. f. techn. Physik **12,** 380 (1931). Kersten, Zeits. f. Physik **72,** 500 (1931).

tively. In Fig. 2 the maximum field strength was carried up to 413 gausses. The constant of the magnetizing coil was 142.4 gausses per ampere.

The magnetizing coil in these experiments stood in a vertical position. In *a* the vertical rod was demagnetized by a decreasing a.c. in the presence of the vertical component of the earth's magnetic field. This shakes the rod

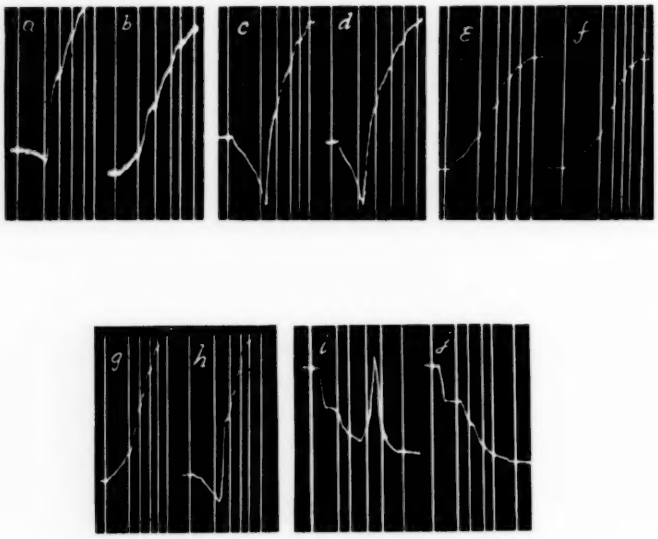

Fig. 1.

down and leaves it permanently magnetized in a direction with the north pole down. When the magnetizing field in the solenoid was applied to the rod, with the field of the solenoid directed upwards, a positive elongation occurred. In *b* the rod was again demagnetized, in the presence of the earth's magnetic field, but this time the magnetizing force in the solenoid had its

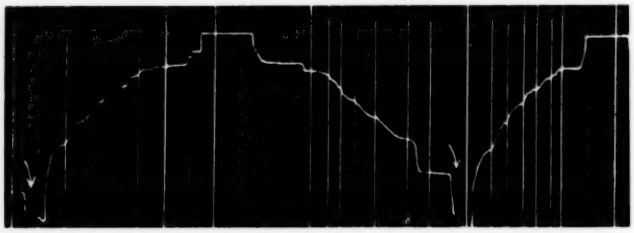

Fig. 2.

direction downwards. This time there is absolutely no positive extension of the rod.

In *c* and *d* no demagnetization occurs, but in both curves the magnetizing force is reversed to what it was in the preceding magnetization. The magnetizing force in both cases is opposed to the remanent magnetism of the nickel rod. This is the effect observed by Dietsch and theoretically discussed

by Kerstens. If no demagnetization occurs and the magnetizing force is applied each time in the same direction as the remanent magnetism of the nickel rods, then no positive elongation occurs. This is illustrated by the curves *e* and *f*, Fig. 1.

By means of a second coil surrounding the main magnetizing coil, one may apply an extraneous field and leave it on while the rod is being magnetized by the main coil. *g* and *h* show what occurs when the rod is demagnetized in the presence of this field and then the main magnetizing force is applied. This extraneous field had a value about three times as great as the vertical component of the earth's magnetic field. In *g* it will be observed that no positive elongation occurs since the main magnetizing force is in the same direction as the extraneous field. A positive elongation in the presence of this extra field occurs only when the main magnetizing force is opposed to the added field. This is shown in *h*, Fig. 1. It will be noted that the positive elongation in *h* is greater than in *a*.

One may apply any magnitude of extraneous field he chooses, and introduce it at any value of the main field desired and so get any form of curve one may select for the Joule magnetostrictive effect in nickel. In *i* and *j* are shown the queer changes in length which can be obtained for iron if one applies extraneous fields. In *i* there is an elongation then a shortening followed by a second elongation, while in *j* the change in length is wholly an elongation.

In Fig. 2 is shown a hysteresis curve of the Joule magnetostrictive effect in nickel. It is one continuous run in which the two points of positive elongation are indicated by arrows. These are the so-called positive elongations found by Dietsch and are of the same type of elongation as shown in *c* and *d*, Fig. 1. In the true sense of the word they are not positive elongations. Thus far we have no positive indications to show that either the Villari reversal effect or the Joule positive elongation occurs in nickel.

Particular attention is called to Fig. 2 to show how well the temperature changes are controlled. If temperature were affecting the length then the horizontal portions of the curve would not be parallel to the edge of the photographic film, but would be tilted up or down as the film progressed past the slit in the camera.

The inference has been made in a number of papers that the capacity-beat method is the only method by which these positive elongations may be detected. This inference is to be challenged. The mechanical-optical device with which the curves in Figs. 1 and 2 were made fifteen years ago did not begin to approach the limit to which it could have been pushed and yet it shows this positive elongation very plainly. Furthermore, since these photographs were made, a greatly improved extensometer has been constructed and will be described in a subsequent paper. The ability to secure a continuous record of the changes in length is a very desirable feature of any extensometer.

LETTERS TO THE EDITOR

Prompt publication of brief reports of important discoveries in physics may be secured by addressing them to this department. Closing dates for this department are, for the first issue of the month, the twenty-eighth of the preceding month; for the second issue, the thirteenth of the month. The Board of Editors does not hold itself responsible for the opinions expressed by the correspondents.

Electronic Structure of the a-X Band System of N_2

By using a powerful discharge in pure nitrogen it has been found possible to photograph certain bands belonging to this system[1] in the first order of a twenty-one foot Rowland grating. The nitrogen was prepared from prebaked sodium azide, and was allowed to stream through the discharge tube during the progress of a 48 hour exposure. Copper lines served as wave-length standards[2] and the very faint bands were measured using a cylindrical lens so as to eliminate the effect of plate grain. Every line was measured about twenty times in order to minimize error. The bands λλ2006.01 (3–11), 2023.48 (4–12), 2041.16 (5–13), 2059.04 (6–14), 2125.92 (5–14), 2143.95 (6–15), 2162.27 (7–16) were visible on the plates but only λ2041.16 and λ2125.92 were sufficiently developed to allow of measuring the branches.

The system is almost certainly a singlet transition to the ground state $^1\Sigma_g^+$ of nitrogen for it is the only strong system yet observed in absorption.[3] Accepting this idea, the experimental results are to be explained by the assumption that it is a $^1\Pi_u - ^1\Sigma_g^+$ transition. All the bands show in addition to the head measured by Hopfield and Birge a faint second head displaced towards longer wave-lengths by about 13 cm^{-1} though only sharp and clear in the case of λ2125.92 which is the best exposed band. In other bands it can however be made quite distinct by enlargement on contrasty film and subsequent superposition of the enlargements[4] so as to enhance the photographic contrast. It is natural to account for this as a Q head. Unfortunately, the resolving power is too small to allow one to measure the branches in the neighborhood of the head, and where the series are resolved, (at about the twentieth member of the Q branch) the R branch is so faint that it occurs only as a few stray lines very difficult to measure. A provisional analysis from the Q and P branches of (5–13) and (5–14) gives $B_5' = 1.5207 \pm 0.001\ cm^{-1}$, $B_{13}'' = 1.7625 \pm 0.001\ cm^{-1}$ and $B_{14}'' = 1.7424 \pm 0.003\ cm^{-1}$, neglecting the contribution due to Λ-doubling which must be very small, since the stray R lines lie in their predicted positions as far as the can be measured. This assignment of constants accounts for the positions of all measured lines and heads to within experimental error, and, by using an estimated effective temperature, for their intensity also. One may say therefore with some confidence that this system is indeed a $^1\Pi_u - ^1\Sigma_g^+$ transition.

To account for the existence of a $^1\Pi_u$ level in this position seems very difficult, as Mulliken,[5] has pointed out. If we assume with Hund[6] that it has the electronic structure $\sigma_u^2 2s\pi_u^4 2p\sigma_g 2p\pi_u 3p$ then the $\pi_u 3p$ electron should be strongly bonding in character since it has descended from the high energy atomic orbit $3p$. This, experimentally, appears not to be the case.

Two other bands with heads at λ2033.6 and λ2112.1 also show on the plates. They are obscured by members of the a-X system but

[1] Birge and Hopfield, Astrophys. J. **68**, 257 (1928).

[2] Burns and Walters, Allegheny Observatory Vol. **8**, No. 3. (Corrected by supplementary circular.)

[3] Hopfield (Phys. Rev. **31**, 1131, (1928)) has reported a progression of bands in absorption whose upper level lies below the 'a' level. This might be the $^3\Pi_u$ level corresponding to the $^1\Pi_u$ of this system; but the spacings of the vibrational levels appear unfavourable to this interpretation.

[4] Oldenberg, Zeits. f. Physik **58**, 722 (1929).

[5] Mulliken, Rev. Mod. Phys. **4**, 53 (1932).

[6] Hund, Zeits. f. Physik **63**, 749 (1930).

are strongly degraded to the violet; the best exposed shows strongly alternating intensities; hence it is certainly due to nitrogen or to ionized nitrogen. It has the appearance of a single branch whose spacing rapidly increases towards shorter wave-lengths. These bands appear not to have been observed before.

A more complete investigation of the *a-X* system is proposed in the near future using a large vacuum spectrograph.

E. T. S. APPLEYARD
Ryerson Physical Laboratory,
University of Chicago,
June 26, 1932.

Deposition of Chromium on Glass

R. Ritschl[1] has perfected a simple apparatus with which a uniform half-silvering can be done on Fabry-Perot interferometer plates. The film is put on by evaporation of silver from a hot tungsten filament in a vacuum; the silver having been tied to the tungsten with platinum.

The writer has extended this process to chromium, with an idea to its use for astronomical reflectors. As is well known, the present silver-on-glass surfaces tarnish quickly, and do not reflect a usable fraction of incident light beyond 3350A. To remedy this defect, other metals have been deposited by evaporation, but chromium seems to excel in reflectivity and permanence. The chromium was electroplated about a millimeter thick on a tungsten filament and was evaporated *in vacuo* very quickly. The resultant surface is firm, and can be dissolved only by HCl. The reflectivity of a test surface has been determined as: 60 percent at 4200A; 68 percent at 3450A; and 62 percent at 2900A. The adaptation of the process to large surfaces is now in progress.

ROBLEY C. WILLIAMS
Physical Laboratory
Cornell University,
June 27, 1932.

[1] *Half-Silvering Interferometer Plates*, Zeits. f. Physik **69**, 578–585 (1931).

Note on Molecular Structure

Hund[1] and Mulliken[2] in recent papers have considered the structure of polyatomic molecules, treating each electron as if it moved in a wave function which was a solution of a problem of many centers—a molecular orbital, as Mulliken happily names such a function. The writer[3] and Pauling[4] on the other hand have treated the same problem from a starting point in which each electron moves as in a single atom, or as Mulliken would say in an atomic orbital. It is the purpose of this note to point out the relation between the two methods. This has already been done to some extent in a paper on metallic cohesion;[5] there the method used by Hund and Mulliken has an analogue in the treatment of Sommerfeld and Bloch, whereas the other method, used by Pauling, the present writer, Heitler and London, resembles more closely Heisenberg's treatment of ferromagnetism. In that paper, the connections between the two methods were brought out, and it was shown that if treated in the proper way both methods necessarily led to the same answer, so that a choice between them must be made on the basis of convenience rather than correctness. Essentially the same situation holds in the molecular case.

A first simple calculation by either method will be incorrect, and it is necessary to go to a considerable refinement to secure good results. First we shall describe these refinements necessary in the method of Pauling and the writer. One can start by assuming covalent bonds, and taking these bonds to be located between definite pairs of atoms. Then the writer has shown how to set up wave functions, correctly taking account of antisymmetry and of spin, describing this situation. But now to improve this we must (1) take account of other possible ways of drawing the valence bonds. This can be considered in one way as the correct perturbation treatment for spin degeneracy. Or it can be considered as taking account of *shared valence*, a common phenomenon, and the one which Mulliken

[1] F. Hund, Zeits. f. Physik **73**, 1 (1931); **73**, 565; **74**, 1 (1932).

[2] R. S. Mulliken, Phys. Rev. **41**, 49 (1932). I am indebted to Professor Mulliken for sending me a copy of the latter paper before publication.

[3] J. C. Slater, Phys. Rev. **38**, 1109 (1931).

[4] Linus Pauling, Journ. Am. Chem. Soc. **53**, 1367 (1931).

[5] J. C. Slater, Phys. Rev. **35**, 509 (1930).

evidently has in mind when he does not wish his molecular orbitals to indicate bonds definitely between pairs of atoms, but to have them more diffused. In a metal, this phenomenon is of major importance, as the writer showed in the paper above quoted. It is also of major importance in the study of chemical reactions, as Eyring and others[6] have pointed out. (2) We must take into account the various possible ionic states. The importance of this step has been emphasized both by Pauling and by the writer; many structures are just intermediate between the covalent and the ionic cases, and without considering both it is not possible to get accurate results. Both these corrections (1) and (2) are to be made by setting up separate wave functions describing the various possible structures, computing the matrix of the energy with respect to them, solving the resulting secular equation, and using the resulting coefficients, making the best combination of the various wave functions to describe the resulting state.

To get a correspondingly accurate result with the method of Mulliken and Hund, we first set up the molecular orbitals, and assign electrons to the suitable orbitals. This is essentially as far as Mulliken and Hund go. But then we must set up antisymmetric combinations, taking account of spin. We must ordinarily consider several such assignments of electrons, taking into account some antibonding orbitals, and must solve the secular problem between these, finally resulting in the correct function as a linear combination. It should be pointed out that this process is particularly necessary if one is to get correct results at large distances of separation, which is very important in considering energies of dissociation of the various bonds. When this is done, as shown by an extension of the method used in the paper on metals, the results are essentially the same by either method.

There is one respect in which the method of Pauling and the writer can be made definitely better than that of Mulliken and Hund, when carried to the point described. It takes definite account of the ionic states. Hence it can use as the wave function for these states a wave function in which shielding of one electron by another is properly taken into account. The method of Mulliken and Hund, however, treats the ionic state rather as the accidental overlapping of electrons in molecular orbitals, resulting in fluctuations of electron density with an increase or decrease of the charge on an atom, with respect to the mean charge. Thus it cannot separate the ionic from the covalent cases, and cannot take account of the variation of shielding from one state to the other. On account of these ionic terms, the method of Pauling and the writer really contains, in its final wave function, a dependence of the wave function on the relative coordinates of the electrons, and it is well known that this is essential for a satisfactory representation of the correct wave functions, and is definitely lacking both in the treatment of atomic structure by the conventional method, and in the corresponding method of Mulliken and Hund as applied to molecules. This advantage of the method was not brought out in the paper on metals quoted above.

Aside from the point just mentioned, the two schemes are equivalent. We then discuss their relative merits from the standpoint of convenience. For a qualitative discussion, in which the calculations are not carried to the point just described, but are rather broken off at the earliest possible point, the writer believes the method of Mulliken and Hund to be at least as valuable as the one which he and Pauling have used. The best procedure, and one which he is accustomed to follow, seems to be to carry through a discussion of a problem qualitatively by both methods, checking them against each other to find their real relationship. For instance, in discussing a metal, even if using the method of atomic orbitals, no one would think of not comparing with the method of Sommerfeld and Bloch constantly, for better orientation and understanding of the problem if for no other reason. On the other hand, even for qualitative discussion, the method of the writer and of Pauling seems to have some advantages in that the various separate effects, as valence bonds between different pairs of atoms, states which are partly covalent and partly ionic etc., seem to have some physical significance, and it seems worth while to bring them explicitly into the picture. Further, the method of Pauling and the writer is more convenient for considering the limiting case of infinite atomic separation.

[6] Eyring and Polanyi, Zeits. f. Physik Chem. **B12,** 279 (1931); forthcoming papers by Eyring in J. Am. Chem. Soc.

When it comes to numerical application of the methods, the situation is somewhat altered. The writer has seen no general mathematical method of treating the molecular orbitals which does not rest on writing them as combinations of atomic orbitals. It goes without saying that the atomic orbitals are not to be taken as the same as electronic orbits in single atoms, but are to depend on the molecular structure. The recent calculation of Rosen[7] on H_2 is an excellent illustration of this; he allowed his atomic orbitals both to change scale, and to be polarized, in the presence of the other atom, and similar changes should surely be made in general. But when that is done, the calculation reduces to one in which atomic orbitals are used, in any case. Thus one can reduce either method, if carried through in detail, to the same integrals, and it is unimportant which scheme is used. The writer has been more inclined to use the atomic orbitals from the beginning, for the reason that it seemed an unnecessary waste to build these up into molecular orbitals, carry through a calculation in the manner of Mulliken and Hund, and eventually have to break up again into atomic orbitals for the calculation of the integrals. There are, however, important advantages which should be emphasized in the method of Mulliken and Hund, as far as numerical calculation goes. The advantage rests in the fact that the molecular orbitals are orthogonal to each other, while the atomic orbitals are not. The factors S, which come into the method of Heitler and London in the process of solving a secular equation between non-orthogonal states, come into the method of Mulliken and Hund in the process of normalization alone. For many purposes this is more convenient, and the writer is seriously of the opinion that this advantage, with complicated systems, may be a deciding factor in favor of the molecular orbital method; at least, it can well be used as a stage in the calculation.

In conclusion, it is the object of the present note to point out again that the method of Mulliken and Hund, and that of Pauling and the writer, are complementary, not antagonistic. The writer is quite sure that there are no facts explainable by the scheme of Mulliken and Hund which could not be equally well treated by his method, interpreting it in a suitable way. On the other hand, he would be the last to question the great power of the method of Mulliken and Hund, particularly for qualitative discussion, and welcomes the treatments of molecular structure which are being made by that method.

JOHN C. SLATER
Massachusetts Institute of Technology
Department of Physics,
June 28, 1932

[7] N. Rosen, Phys. Rev. **38**, 2099 (1931).

BOOK REVIEWS

Annual Tables of Constants and Numerical Data, Chemical, Physical, Biological and Technological—published under the authority of the International Research Council and the International Union of Pure and Applied Chemistry. Index for Volumes I to V (1910–1922)—Price $16.00 also Vol. VII—Years 1925–1926, inclusive; Part I, pp. i–xxxv, 1–946 (1930)—Price (including Part II); cloth $25.00—McGraw Hill Book Company, Inc. (New York).

Two extracts from Volume VII can be purchased separately: "Spectroscopy—Emission and Absorption Spectra, Electro and Magneto-Optics" (Numerical Data) by L. Bruninghaus, V. Henri and F. Wolfers. I Vol. 4–to, pp. xviii–514. Price: Cloth, Frs. 190; Paper, Frs. 170; "Electricity, Magnetism, Electrochemistry" (Numerical Data) by A. Buffat, G. Durand, G. Foex, R. L. Fortrat, N. Marinesco, N. Thon. I Vol. 4–to, pp. xviii–136. Price: Cloth, Frs. 90; Paper, Frs. 80. Publishers: Gauthier-Villars et Cie, 55, quai des Grand-Augustins, Paris 6°.

One should not attempt to use these tables without first consulting the directions given at the beginning of the volume. These are found to be very clear and explicit, so explicit that the uninitiated should have no trouble thereafter in using the tables. The newly adopted policy of stressing English so that little or no French is required will be helpful to a large group of American students.

The reviewer has found the General Index to Volumes I to V to be of considerable aid in the use of the tables. It contains three types of indexing which occupy space not in the order of their usefulness. First and most important is an Analytical Index of 38 pages in four languages. Without losing too much in conciseness it often offers somewhat more than a bare reference to volume and page. The arrangement of subjects is reasonable, the detail is sufficient, and there is some cross referencing. The wide range of subject matter covered by the Tables is brought out by a glance at this index. Then follows the Alphabetical Index of 63 pages. This gives references to those things treated in the Tables which are commonly known by name. When it is necessary, a German, English, or Italian name is listed with its French equivalent under which the references are listed. Thus—Dachshund s. Basset; Perch s. Perche; Perca v. Perche. The third index is the Formula Index—319 pages. It has an arbitrary but convenient arrangement described in the Introduction. Of course, most of this Index is devoted to organic compounds. References are given up to $C_{264}H_{176}$. At the end of each reference appropriate errata to Volume I to V are recorded. It is proposed that in addition a separate list of all errata and omissions be published. Only French is used in this part and the frequent occurrence of abbreviations makes it difficult to get along without recourse to the list of abbreviations at the beginning of the volume.

Volume VII of the Annual Tables contains the data for 1925–1926 with the exception of those data on Photography and Geophysics. Chapters on these subjects will not be published annually. The next issue to contain data on them will probably be Volume X. Two chapters appear for the first time—Explosives and Explosion in Gaseous Mixtures. The text accompanying the data is given in French and English. The English in the translation is quite satisfactory. The custom of including a bibliography of papers containing data not easily tabulated, and brief summaries of related qualitative or theoretical work is continued. These summaries often provide pleasant and sufficient substitutes for the original papers. Sometimes the assignment of space to these notices is a trifle extravagant. Thus on page 739 the same research of one author published in two places is listed under two separate headings and most of his data are given twice. Again on page 755 there are two headings for a single paper.

If the compilation is to appear four years after the data are published, the reader is entitled to a somewhat critical presentation. There is no apparent effort in this direction but on the other hand the committee promises to produce up to Volume IX (1929) (now published) and then to resume annual publication of the Tables. Such promptness should outweigh all considerations of criticism. But this is not to be taken to excuse the laxity, which, apparently

because the original author was careless, permits the recording of numerical data without indicating the units used. For example, on page 921 it is impossible to find whether Verdet's constant is given in terms of radians or degrees. While this would scarcely inconvenience a worker in the field, it is most baffling to students and most annoying to the instructor who is trying to teach them how to locate data.

Instead of attempting to describe in detail the important applications of these unique Tables or to emphasize the special features of Volume VII, Part I, which is here under review, it might be useful to remark that almost every page provides some interesting reading and as a practical primer for the study of foreign languages it is excellent. As a by-product one learns a great deal of physics and chemistry and gets a vivid panorama of the development of the exact sciences.

The importance and value of the Annual Tables becomes obvious to one who merely turns over the pages and perhaps another subscriber is made thereby. The committee in charge seems hesitant in advertising their prices. In general one has to make special inquiry by mail. The prices are, however, by no means exorbitant, although unfortunately high enough to keep the Tables out of the personal collections of the average student. Perhaps the cost in the future may be reduced as the committee has announced its intentions of lowering the price if the subscription list grows.

R. M. LANGER
University of Minnesota

The New Conceptions of Matter. By C. G. DARWIN. Pp. 224+xi. Figs. 46. The Macmillan Company, New York. 1931. Price $3.00.

Professor Darwin has undertaken, and carried out with rare skill, the difficult and oft times thankless task of expressing in non-mathematical, and indeed to an unusual degree non-technical language, the newer conceptions of modern physical theory.

Beginning with the "*building materials*"—electrons, protons, and photons,—the first lecture outlines with brief yet lucid strokes the modern ideas of the essential characteristics of these, together with a section dealing with the "*building site*,"—space and the ether. The two following lectures are devoted to the discussion of the essentials of wave propagation, and the notions of wave-velocity and group-velocity together with the diffraction of waves, leading thus naturally to the diffraction of electrons, and of atoms.

The Uncertainty-Principle is then developed in a manner which,—clear and simple as the author's style is,—still calls for close and considered concentration in its reading. Following lectures treat the wave-atom, the polarization characteristics of electrons and protons, the collisions of alpha-rays, protons, and electrons, and finally the exclusion principle of Pauli with charming simplicity of language, although simplicity of conceptions is not so readily possible.

These lectures do not,—could not reasonably be expected to,—contain adequate detail of the essential experimental bases of these newer conceptions of physics; so the volume can hardly serve as a text of modern physics, but most certainly Professor Darwin may be assured that his is a valuable contribution towards the result that "surviving readers may no longer speak of the mysteries of science" but rather "of the naturalness of Nature."

The volume contains a number of excellent illustrations of alpha-ray tracks and diffraction effects. It is regrettable that the negative of the Stern-Gerlach experiment got inverted in the plate, so that the accompanying legend will confuse the reader unacquainted with the phenomenon, (a blunder which,—curiously enough,—appears also in Gerlach's English edition of "Matter, Electricity, Energy").

JOHN E. ALMY
University of Nebraska

Hydro- und Aeromechanik nach Vorlesungen von L. Prandtl Bd. II. O. TIETJENS. Pp. 299+viii. Figs. 238, (Springer 1931). 28 tafeln. Berlin. Price RM 23.

This second volume, written as was the first by Dr. Tietjens, and based in part on Professor Prandtl's lectures, is devoted to the study of the motion of non-viscous fluids and to technical applications. The early chapters contain a summary of the theory of fluid flow, a treat-

ment of the principle of similarity, and a critical discussion of flow, both laminar and turbulent, in tubes and canals including the early work of Hagen, Poseuille, and Reynolds, together with that of more recent investigators. Formulas are given for the resistance to flow in the various turbulent regimes. Particularly interesting is the discussion of the incidence of turbulence with gradually increasing velocity of flow.

There follow three important chapters treating respectively Prandtl's boundary layer theory, the resistance encountered by a solid moving in a fluid, and the theory of lift as applied to aeroplane wings. These chapters contain a systematic presentation of the results of recent investigations. In Prandtl's boundary layer theory that has proved so valuable in the study of viscous fluid motion, the effect of viscosity is neglected except in a thin layer of fluid in contact with a solid boundary. Aside from its use in connection with turbulent flow in tubes, it plays an important rôle in the theory of the resistance suffered by a body moving through a fluid as treated in the next chapter. In addition to the purely frictional resistance encountered by such a body, there is the resistance that results from the alteration of the velocity field from that of irrotational flow and the consequent change in the pressure distribution. In a chapter that occupies about one-fourth of the book, the theory of the lift of aeroplane wings and its technical applications are fully set forth.

The last chapter is devoted to instruments and methods of experimentation including wind tunnels, devices for rendering fluid motion visible, and measurements of pressure, velocity, and resistance. At the end there are some seventy excellent photographs of fluid motion illustrating the motions of solids in water, turbulent flow in canals, and the formation of vortices.

The book is a clear and authoritative exposition of fundamental theories and experimental results in a field that has developed very rapidly in recent years.

H. W. March
University of Wisconsin

PROCEEDINGS OF THE AMERICAN PHYSICAL SOCIETY

MINUTES OF THE PULLMAN MEETING

JUNE 17–18, 1932

The 178th regular meeting of the American Physical Society was held at the Washington State College, Pullman, Washington, room 110 Mechanical Arts Building, in affiliation with the Astronomical Society of the Pacific, and the Pacific Division of the A. A. A. S., on June 17th, 1932.

The sessions began at 9:30 in the morning, extended until noon, and resumed in the afternoon at 2:00 o'clock, terminating at 4:30. There were twenty-five members of the Physical Society in attendance, covering institutions from San Diego to the University of British Columbia.

It was moved, seconded, and voted to hold the 181st meeting of the American Physical Society on the Pacific Coast, on December 16–17th, 1932, at the California Institute of Technology, Pasadena. No other business was transacted.

The members of the Physical Society enjoyed a joint luncheon at noon, June 17th, and a joint dinner on the evening of June 17th, with some twenty-five members in attendance.

In spite of its small size, the meeting was highly successful in the renewal of contacts which it gave between members of the Society in the Pacific Northwest and those from other portions of the Pacific area.

LEONARD B. LOEB, *Secretary for the Pacific Coast*

ABSTRACTS

1. The energy distribution of electrons in field current emission. JOS. E. HENDERSON, R. K. DAHLSTROM, FRANK R. ABBOTT. *University of Washington.*—The energy distribution of electrons extracted from a cold tungsten filament by means of a high electrical field was obtained by using an arrangement of three cylinders with the filament as the common axis. The two inner cylinders were grids. The potential which produced the field necessary for emission also accelerated the electrons through the first grid. By connecting the second grid directly to the filament except for a small variable accelerating potential these electrons were then decelerated. With various magnitudes of field currents the current to the second grid was measured as a function of this small accelerating potential. From these data the energy distribution of the electrons was obtained. The most striking feature of the distribution was that the largest number of electrons had energies only slightly below the maximum. The relative numbers having lower energies increases with the magnitude of the field currents. The range of energies extended over approximately thirty volts. The outer cylinder provided a means of determining the effect of secondary electrons, which effect was found to be small.

2. Mobilities of sodium ions in helium measured in short time intervals. LEONARD B. LOEB. *University of California.*—Extending the mobility measurements of sodium ions in various gases (Phys. Rev. **38**, 549, 1931), as a function of time to helium using an improved oscil-

lator designed for the writer by the Bell Telephone Laboratories and using a new baked-out glass chamber, the following results were obtained. In intervals of 2×10^{-5} sec. and 5×10^{-4} sec., the sodium ion has the astonishingly high mobility of about 30 cm/sec. per volt/cm. Below 5×10^{-4} sec., the mobility has a value of about 23 cm/sec. In the old metal chamber with a directly heated Kunsman source, rather uncertain values indicated the presence of ions of mobilities 30 cm/sec., 23 cm/sec., 17 cm/sec., and 13 cm/sec. on progressive aging. The latter values are somewhat in doubt and the more exact values in the new chamber are open to an uncertainty of the order of magnitude of 5 percent owing to the inadequate knowledge of the temperature correction to be applied in the new chamber.

3. Electroscope of high charge sensitivity. E. J. WORKMAN, *National Research Fellow* and H. B. DEVORE, *California Institute of Technology.*—Electroscopes for use in ionization measurements have been developed to combine a high voltage sensitivity over a limited range with a very small capacity. Bearing in mind that the character of the voltage calibration curve is determined by the rate of variation of capacity with deflection, instruments have been designed to have this vary abruptly in the voltage range in which it is desirable to work. This modification of the calibration curve has been achieved by electrically shielding the deflecting element by placing it in a small metal trough or slot. The size, shape, and position of the trough can be adjusted to give the desired sensitivity at the collecting voltage required. This principle has been applied to the deflecting fibre type in which a heavy quartz fibre, fixed at one end, is used, and to the torsion types where the deflecting element consists of a short quartz fibre fixed at the center to the torsion member. A deflecting instrument has been used which gave a full scale deflection of 100 divisions for 350 volts, but from 80 to 100 divisions the sensitivity was uniform at 10 divisions per volt. In other instruments higher sensitivities have been observed with characteristics indicating that the sensitivity may be made several times that given above. These instruments are, by nature, extremely rugged and simple of construction.

4. Photoelectric currents in gases between parallel plates as a function of the potential difference. NORRIS E. BRADBURY. *University of California.*—If one of two parallel plate electrodes in a gas emits photoelectrons, the current received at the collecting electrode is a function of the potential difference, the gas pressure, the initial velocity of the photoelectrons, and the mobility of the carrier. In the experiments reported here, a quartz mercury arc and a plane zinc electrode were used as the source of photoelectrons. Current-potential difference curves were obtained for different gas pressures in hydrogen and nitrogen, and the ratio of the current, i, to the saturation current, I_0, obtained in each case. A theoretical equation of J. J. Thomson gives the relation

$$i = [I_0(6\pi)^{1/2}kx]/[c + (6\pi)^{1/2}kx],$$

where X is the field strength, k the mobility of the carrier, and c its random velocity. Adopting the suggestion of Loeb that c is the average velocity of photoelectric emission of the electrons from the plates, the validity of this equation is established by the experimental data which permit the values of the electron mobility k to be determined as a function of X/p. Values so obtained agree well with those obtained by Loeb and by Townsend and Bailey. An equation recently given by Langmuir (Phys. Rev. **38,** 1656, (1931)), is shown to be applicable only at low pressures where it yields a satisfactory value of the mean free path of the electron.

5. On the specific heats of ferromagnetic materials. PAUL S. EPSTEIN. *California Institute of Technology.*—A theory of ferromagnetism developed by the author leads to the result that, at very low temperatures, the specific heats of ferro-magnetic substances follow the law $c=0.208sR(T/\theta)^{3/2}$, where R is the gas constant and s the number of valency electrons per atom. The constant θ is closely related to the Curie point T_0 being of the order of magnitude of $\frac{1}{2}T_0$. The available experimental data do not go to sufficiently low temperatures to permit a test of this law but they are encouraging as far as the order of magnitude is concerned.

6. Mobilities of gaseous ions in mixtures of hydrogen and nitromethane and hydrogen and methyl cyanide. ELIZABETH A. HIGLEY AND CAROLYN C. THORSEN. Introduced by L. B. LOEB. *University of California.*—In continuation of the investigations of L. B. Loeb on ionic mobilities in mixtures of various gases, it seemed worthwhile to investigate the action of nitro-bodies and cyanides. Owing to the toxic and unstable nature of these substances it was decided to study the simplest organic derivatives of the two radicals. The mobilities of the positive and negative ions in Kahlbaum's methyl cyanide were 0.237 cm/sec. and 0.234 cm/sec. respectively, and the values in Kahlbaum's nitromethane were 0.221 cm/sec. and 0.221 cm/sec. respectively. The addition of traces of both of these gases to hydrogen caused an abnormal decrease of the mobility on both ions, and cause a deviation from Blanc's law indicating the formation of a definite addition product with ions of both signs. The effect in nitromethane was distinctly greater than the effect in methyl cyanide. These measurements were made keeping the auxiliary field equal to the driving field, and therefore represent the mobilities on the new standard absolute scale.

7. Determination of the coefficient of ionization by collision using large plate distances and higher pressures. FREDERICK H. SANDERS. Introduced by L. B. LOEB. *University of California.*—The coefficient of ionization by collision, α, was measured in dry air at a pressure of 380 mm over a range of field strengths varying from $X=13{,}680$ $(X/p=36)$ to $X=7{,}600$ $(X/p=20)$. The ionization chamber used was of such dimensions as to make the investigations possible at plate distances ranging from one to five centimeters. With these large plate distances it was possible to evaulate α for values of X/p as low as 20. It was found that instead of the coefficient being equal to zero at $X/p=30.1$ as shown by Paavola (Archiv. für Elektrotechnik **443,** 22 (1929)). α actually has a measurable value at $X/p=20$. Plotting α/p as a function of X/p, the curve approaches the zero axis asymptotically. The highest value of X/p attained was 36.5, which is within two percent of the sparking potential at a plate distance of 2.5 centimeters. At this field strength no increase in current with plate distance was noted beyond that given by the simple Townsend relation $i=i_0e^{\alpha d}$. (Laboratory equipment for this research was made possible through a grant-in-aid from the National Research Council.)

8. The distribution of electrons in the photo-effect by Roentgen rays, classically treated. JAKOB KUNZ. *University of Illinois.* (*To be read by title.*)—Several treatments of this effect by means of wave mechanics have been given. If a beam of Roentgen rays passes through a gas, most of the electrons are not given out in the direction of the electric force E, but in a more forward direction. If the direction of observation makes an angle θ with c, the velocity of light, the component of E is $E \sin\theta$ and the intensity of light is $CE^2 \sin^2\theta$ and is proportional to the number of electrons emitted in the direction θ. Moreover, I have shown in a previous article, (Phys. Rev. **6,** 413, (1915)), that in the Roentgen pulse the electric force

$$E_t = \frac{ev \sin\theta}{\delta\rho(c - v\cos\theta)}$$

where the thickness

$$\delta = l(2c - v\cos\theta)/v.$$

The intensity of the beam is again equal to

$$CE_t^2 = \frac{Ce^2v^4\sin^2\theta}{\rho^2l^2}(c - v\cos\theta)^{-2}(2c - v\cos\theta)^{-2}$$

$$= \frac{Ce^2v^4c^2 2}{\rho^2l^2}\left(1 + \frac{5}{2}\frac{v}{c}\cos\theta\right)\sin^2\theta$$

a formula deduced in wave mechanics with different constants.

9. A theory of the Raman rotation spectra. WILLIAM V. HOUSTON, *California Institute of Technology.*—The Raman spectrum may be treated as due to variable polarizability, as has been done by Placzek for the vibration lines. If the tensor of polarizability is transformed, by means of the Eulerian angles, to axes which are fixed with reference to the incident beam of

light, the periodic change of these angles gives the Raman lines of the rotation spectrum. It is thus possible to evaluate the relative intensities of the lines, as well as their polarization, without any knowledge of the electronic levels of the molecule. This method of treatment explains very nicely why a spherically symmetric molecule, such as methane, shows no rotation spectrum, although it does show a rotation-vibration spectrum.

10. Secondary effects in the ionization by hard gamma-rays. E. J. WORKMAN, *National Research Fellow, California Institute of Technology.*—The author has previously reported concerning the increase of the ionization in a metal electroscope, as produced by increasing the wall thickness of the chamber. Another arrangement has been used in which a canalized beam of gamma-rays from the radium, filtered by as much as 3 cm of lead, was directed along the axis of a cylindrical ionization chamber (10 cm long and 9 cm diameter) containing air at atmospheric pressure. Various thicknesses of cellophane, graphite, aluminum, iron, tin, and lead were placed on the front and then on the back of the chamber and the ionization studied. Lead, placed on the back end of the chamber, causes an increase of approximately 60 percent in the ionization when a filter of 3 cm of lead is used. For other materials the increase is nearly proportional to the atomic number. A large part of the increase is doubtless due to scattering of electrons from the back wall. Equivalent electron thicknesses of the materials on the front end of the chamber may either increase or decrease the ionization according to whether the material is of low or high atomic number. The order in which the materials arrange themselves with respect to the effect they produce on the ionization, as well as the magnitude of the effect for a given material, depends upon the thickness of the filter.

11. Absorption bands in the infrared spectrum of Venus. W. S. ADAMS AND THEODOR DUNHAM, JR. *Mt. Wilson Solar Observatory.*

12. The absolute magnitudes of the O5 to B2 stars determined from the interstellar lines. J. A. PEARCE. *Dominion Astrophysical Observatory.*

13. On the temperatures of Wolf-Rayet stars and novae. C. S. BEALS. *Dominion Astrophysical Observatory.*

14. Further details ascribable to bands of the carbon isotope C_{13} in stars of spectral classes R. and N. R. F. SANFORD. *Mt. Wilson Solar Observatory.*

15. An investigation of the hydrocarbon bands in the solar spectrum. R. S. RICHARDSON. *Mt. Wilson Solar Observatory.*

AUTHOR INDEX TO ABSTRACTS OF PULLMAN MEETING

Abbott, Frank R.—see Henderson
Adams, W. S. and Theodore Dunham, Jr.—No. 11
Beals, C. S.—No. 13
Bradbury, Norris E.—No. 4
Dahlstrom, R. K.—see Henderson
DeVore, H. B.—see Workman
Dunham, Theodore, Jr.,—see Adams
Epstein, Paul S.—No. 5
Henderson, Jos. E., R. K. Dahlstrom and Frank R. Abbott—No. 1
Higley, Elizabeth A. and Carolyn C. Thorsen—No. 6
Houston, William V.—No. 9
Kunz, Jakob—No. 8
Loeb, Leonard B.—No. 2
Pearce, J. A.—No. 12
Richardson, R. S.—No. 15
Sanders, Frederick H.—No. 7
Sanford, R. F.—No. 14
Thorsen, Carolyn C.—see Higley
Workman, E. J.—No. 10
———and H. B. DeVore—No. 3

CURRENT LITERATURE OF PHYSICS

Extracts from the Tables of Contents of Some of our Contemporaries

PROCEEDINGS OF THE ROYAL SOCIETY

SERIES A. VOL. 136, No. A830 — JUNE 1, 1932

Discussion on the Structure of Atomic Nuclei. **By Lord Rutherford** 735
Ship Waves: their Variation with certain Systematic Changes of Form. By **T. H. Havelock** 465
Molecular Structure and Physical Properties of Prussic Acid. Part I.—Refractive Dispersion of Prussic Acid and its Homologues. By **T. M. Lowry and S. T. Henderson** 471
Note on the Theory of Rectification. By **A. H. Wilson** 487
Radio Transmission Problems Treated by Phase Integral Method. By **T. L. Eckersley** .. 499
Theory of some Electron-levels in H_2. By **J. K. L. MacDonald** 528
Reproducibility and Rate of Coagulation of Stearic Acid Smokes. By **H. S. Patterson and W. Cawood** 538
Motion of Electrons in the Static Fields of Hydrogen and Helium. By **J. McDougall** 549
Electron Polarization. By **G. O. Langstroth** 558
Ionic Diamagnetic Susceptibilities. By **W. R. Angus** 569
Diamagnetic Susceptibilities of some Beryllium Compounds. By **W. R. Angus and J. Farquharson** 579
Fine Structure in the Arc Spectra of Bromine and Iodine. By **S. Tolinsky** 585
Anomalous Scattering of α-Particles by Hydrogen and Helium. By **H. M. Taylor** 605
Experiments with High Velocity Positive Ions.—(1) Further Developments in the Method of Obtaining High Velocity Positive Ions. By **J. D. Cockcroft and E. T. S. Walton** 619
On some Close Collisions of Fast β-Particles with Electrons, Photographed by the Expansion Method. By **F. C. Champion** 630
On the Polarization of Electrons by Scattering. By **E. G. Dymond** 638
On the Photographic Action of Slow Electrons. By **R. Whiddington and J. E. Taylor** 651
Nature of the Interaction between Gamma-Radiation and the Atomic Nucleus. By **L. H. Gray and G. T. P. Tarrant** 662
Existence of a Neutron. By **J. Chadwick** 692
Collisions of Neutrons with Nitrogen Nuclei. By **N. Feather** 709
Attempts to Detect the Interaction of Neutrons with Electrons. By **P. I. Dee** 727

NATURE

VOL. 129, No. 3267 — JUNE 11, 1932

Differential Equations of Physics. By **E. T. Whittaker** 850
Short Reviews:
Electrical Conductivity of Metals at the Lowest Temperature 858
Letters to the Editor:
Resonance Spectrum of Hydrogen. By **K. R. Rao** 869
Photochemical Dissociation of Carbonyl Sulphide. By **W. Lochte-Holtgreven, C. E. H. Bawn, and E. Eastwood** 869
Rotation of Molecules in Crystals. By **J. D. Bernal** 870
Heat of Dissociation of Nitrogen. By **Arun K. Datta** 870
Decomposition of Hydrogen Peroxide by Catalase. By **Derek Richter** 870
Electrochemical Periodicities. By **Ernest S. Hedges** 870

NATURE

VOL. 129, NO. 3268 — JUNE 18, 1932

Principles of Modern Physics 886

Letters to the Editor:

Origin of the Coronal Lines. By **R. Frerichs; Herbert Dingle** 901

Attack of Oxygen Molecules upon Highly Crystalline Graphite. By **E. N. Greer and B. Topley** 904

NO_3 Frequency in Organic Nitrates. By **A. S. Ganesan and V. N. Thatte** 905

Displacement in the N Lines of Tungsten and Tantalum. By **Dr. F. C. Chalklin and Mrs. L. P. Chalklin** 905

NATURE

VOL. 129, NO. 3269 — JUNE 25, 1932

Letters to the Editor:

Theory of Induced Polarities in Benzene. By **E. Hückel and W. Hückel** 937

Adsorption of Weak Electrolytes on Charcoal. By **R. A. Peters and H. J. Phelps** 939

Mechanical Hardness Influenced by Magnetization. By **S. R. Williams** 939

Specific Heat of Gases at High Temperatures. By **W. T. David** 942

Relative Excitation of the Three X-ray *L*-Levels with Cathode Rays of Different Velocities. By **D. Coster and J. van Zuylen** 942

ZEITSCHRIFT FÜR PHYSIK

VOL. 76, NOS. 3 AND 4 — MAY 31, 1932

On the Cohesion Limits of Synthetic Potassium Halide Crystals. By **Willi Schütze** 135

Dependence of the Cohesion Limits of Synthetic Potassium Chloride Crystals on Orientation. By **Willi Schütze** 151

On the Meaning of Relative Humidity Especially at High Temperatures. By **H. Ebert** ... 163

On the δ-Rays and the Relation between Range and Velocity for Slow Electrons. By **Tikvah Alper** 172

Multiplex Interference Spectroscope in Comparison with Other Interference Spectroscopes. By **Ernst Lau and Erich Ritter** 190

Measurements with the Help of Liquid Helium. XVIII. On the Behavior of Superconducting Zinc to Bombarding Slow Electrons. By **W. Meissner and K. Steiner** 201

Formation, Detection and Absorption of Slow Neutral Rays. By **H. Kallmann, W. Lasareff and B. Rosen** 213

Calculation of Potential Curves for Diatomic Molecules with the Help of Spectral Terms. By **O. Klein** 226

Intensity Measurements in Raman Spectrum. By **A. Carrelli and J. J. Went** 236

Ionization and Excitation through Ion Collisions. By **W. Weizel and O. Beeck** 250

Excitation of Noble Gases through Collision of Noble Gas Ions. By **W. Weizel** 258

Plasmic Oscillations and Selective Optical Reflection by Metals. By **Max Steenbeck** .. 260

On the Cause of a Forbidden Line in the Spectrum of the Hg II. By **S. Sambursky** ... 266

Investigations of Hardening of Zinc Aluminum Alloys having the Composition Al_2Zn_3 By **Herbert Meyer** 268

Becquerel Effect of Copper Oxide as Contact Layer (Sperrschicht) Photoeffect. By **F. Waibel** 281

ZEITSCHRIFT FÜR PHYSIK

VOL. 76, NOS. 5 AND 6 — JUNE 7, 1932

On the Scattered (Seitiche) Radiation and the Nature of the Coloring Substance in Blue Rock Salt. By **Marya Kahanowicz** 283

Retardation Formula for Electrons with High (Relativistic) Velocities. By **H. Bethe** 293

Wave Mechanical Calculation of the Polarization Energy of Water Molecules. By **Bernhard Mrowka** 300

On the Pressure Effect in Radiationless Dissociation. By **K. Wurm** 309

Second Spark Spectrum of Sodium, Na III, in the Extreme Ultraviolet. By **Jonas Söderqvist** 316
Remarks on the Liberation of Electrons from a Negative Probe by Excited Atoms or Positive Ions. By **F. Lüdi** 319
On the Ultraviolet Transmission of Thin Blown Window Glass. By **Hans Klumb and Th. Haase** 322
On the Dependence of the Piezoelectric Constant of Quarts on Temperature. By **V. Freedericksz and G. Michailow** 328
On Quantum Theory of Electrodynamics. Invariant Formulation of the Dirac Dispersion Theory. III. By **W. Wessel** 337
Röntgenographic Investigations on Solid Nitrogen and Oxygen. By **Martin Ruhemann** .. 368
Augmentation of Predissociation by Collisions and Beers' Law. By **V. Kondratiew and L. Polak** 386
Demonstration of the Focusing and Resolving Properties of the Field of a Cylindrical Condenser on Cathode Rays. By **Helmut Voges** 390
Remarks on the Form of Diaphragms in Work with Electron Rays in Gases. By **Hellmut Seyfarth** 395
Excitation Process and Ion Motion in Arcs. By **R. Mannkopff** 396
Reflection of Sound Waves at Anisotropic Thin Lamina. By **Alfred Seiffert** 407
On the Permeability of a Pure Coulomb Barrier for α-Particles. By **W. Alexandrow** 415

DIE NATURWISSENSCHAFTEN

VOL. 20, NO. 25 — JUNE 17, 1932

Remark on the Radius of Electron. By **E. Guth** 470
Crystal Structure of Gallium. By **F. Laves** 472
On the H-Isotope of Mass 2. By **H. Kallmann and W. Lasareff** 472

ANNALEN DER PHYSIK

VOL. 13, NO. 5 — MAY 13, 1932

Measurements with the Help of Liquid Helium. XIV. Systematic Investigation on a Series of Alloys with Regard to Their Superconductivity. By **W. Meissner, H. Franz and H. Westerhoff** 505
Measurements with the Help of Liquid Helium. XV. Resistance of Barium, Indium, Thallium, Graphite, Titanium at Low Temperatures. By **W. Meissner; H. Franz and H. Westerhoff** 555
Contribution to the Theory of Electrical Resistance and Superconductivity of Metals. By **E. Kretschmann** 564
Absorption Spectra of Carbon Dioxide, Carbon Monoxide and Water Vapor in the Region 600–900 AE. By **Hans Joachim Henning** 599
On the Question of Regular Solutions of Einstein's Gravitation Equation. By **Cornel Lanczos** 621
Reply to Remarks of Mr. M. Wien on My Paper "On Permeability at High Frequency." By **W. Arkadiew** 636

ANNALEN DER PHYSIK

VOL. 13, NO. 6 — MAY 21, 1932

Measurements with the Help of Liquid Helium. XVII. Resistance of Lead in Magnetic Fields Below the Transition Temperature. By **W. Meissner** 641
Electric Behavior of Boundary Layers. By **Horst Teichmann** 649
Sound Absorption Measurements in Gases at High Frequencies. By **E. Grossmann** 681
Photocell and "Lightelement." By **F. v. Korösy and P. Selenyi** 703
h/e Determination by Means of Electron Diffraction. By **R. von Meibom and E. Rupp** ... 725
On the Ignition of Glow Discharge. By **Giorgio Valle** 732
On the Measurement of Coherence Length (of Light) with the Multiplex Interference Spectroscope of Gehrcke and Lau. By **P. H. van Cittert** 753

ANNALEN DER PHYSIK

VOL. 13, NO. 7 — JUNE 2, 1932

Photoelectric and Thermoelectric Effects in Palladium-Silver and Palladium-Gold Alloys with Absorbed Hydrogen. By **Joseph Schniedermann** 761
Transport of Slow Positive Particles by Canal Rays. By **J. Koenigsberger** 780
Investigation of the Action of Mechanical and Electrical Force Fields on the Double Refraction of Quartz. By **Norbert Günther** 783
On the Range of Measurement of the Knudsen Monometer. By **Ernst Fredlund** 802
Voltage Effect on the Conductivity of Strong and Weak Acids. **By Josef Schiele** 811
Outer Photoelectric Effect in Liquids. Determination of the Long Threshold Wave-Length of Water. By **P. Görlich** 831
Dependence of the Degree of Ionization on the Field Strength and the Mean "Ionization Field Strength" in Fluids. By **Alexander Nikuradse** 851

ANNALEN DER PHYSIK

VOL. 13, NO. 8 — JUNE 11, 1932

Effective Absorption Spectrum of "Lenardphosphore." By **Richard Kühner** 873
On the Theory of Absorption of Solid Bodies. By **R. Peierls** 905
New Sounding Method for Investigation of the Process in Gas Discharges. By **Jürg Johannesson** 953
Measurements with the Help of Liquid Helium. XIX. Investigations on the Alloy Series Lead Pb-Tl and Pb-Bi in Relation to Their Superconductivity. By **W. Meissner, H. Franz and H. Westerhoff** 967

COMPTES RENDUS

VOL. 194, NO. 22 — MAY 30, 1932

On the Movements of Infinite Liquids. By **J. Leray** 1892
Calculation of an Upper Limit to the Duration of the Detonation in the Gas Engine and the Explanation of the Presence of a Break in the Diagrams Furnished by Certain Electric Manometers. By **Max Serruys** 1894
Bands and Emission Lines in the Spectrum of the Night Sky. By **J. Dufay** 1898
Example of a Multiple Harmonic Function Furnished by the Theory of the Newtonian Potential. By **R. Wavre and P. Dive** 1901
On the Existence of Oscillations at High Frequencies in the Secondary Current of High Tention Magnetos. By **Jean Jaffray and Pierre Vernotte** 1902
On a Method of Comparison of Small Capacities. By **Michel Durepaire** 1902
On a Radiometer Sensitive to the Hertzian Waves. By **G. A. Beauvais** 1904
On the Properties of Gas Ions at High Frequencies. By **Antonio Rostagni** 1906
Theory of the Diffusion of Neutrons, Coefficient of Absorption and Ionization. By **Jean-Louis Destouches** 1909
Anomalies in the Absorption of X-rays by Lead up to 210 KV. By **M. E. Nahmias** 1911
On the Fluorescent Spectrum of I_2. By **I. I. Agarbiceanu** 1913
On the Compton Effect of Very Hard γ-Rays from ThC″. By **D. Skobelzyn** 1914
Electrolytic Deposit of Polonium on Various Metals. By **M. Haïssinsky** 1917
Absolute Measurements of Velocities of the Principle Groups of α-Rays. By **S. Rosenblum and G. Dupouy** 1919
Diffusion of Hydrogen through Palladium. By **Victor Lombard and Charles Eichner** 1929

REVUE D'ACOUSTIQUE

VOL. 1, NO. 1 — MARCH, 1932

Suggested Acoustical Vocabulary. By **F. Canac** 1
Acoustical Receivers. By **Jean Perrin** 9
Absolute Measurements of the Fundamental Magnitudes in Acoustics. By **Z. Carriere** 28
Measurement of the Coefficient of the Absorption of Sound in Tubes. By **F. Canac** 52

BUREAU OF STANDARDS, JOURNAL OF RESEARCH

VOL. 9, NO. 2 — AUGUST, 1932

Vacuum Tube Amplifier for Feeble Pulses. By **L. F. Curtiss** 461

Infrared Spectra of Helium. By **William F. Meggers and G. H. Dieke** 462

Tests of Cellular Sheet-Steel Flooring. By **J. M. Frankland and H. L. Whittemore** 463

Influence of Temperature on the Evolution of Hydrogen Sulphide from Vulcanized Rubber. By **A. D. Cummings** 464

Some of the Factors which Affect the Measurement of Sound Absorption. By **V. L. Chrisler and Catherine E. Miller** 465

Reciprocal Spherical Aberration of an Optical System Including Higher Orders. By **H. F. Bennett** 466

Attachment for Turning Approximately Spherical Surfaces of Small Curvature on a Lathe. By **I. C. Gardner** 467

Wave-lengths and Zeeman Effects in Lanthanum Spectra. By **W. F. Meggers** 468

Note on the Freezing Point of "Iso-octane" (2, 2, 4-Trimethylpentane). By **J. H. Bruun and Mildred M. Hicks-Bruun** 469

Twin-Bomb Method for the Accurate Determination of Pressure-Volume-Temperature Data and a Simple Method for the Accurate Measurement of High Pressures. By **E. W. Washburn** 470

NATIONAL ACADEMY OF SCIENCES

VOL. 18, NO. 6 — JUNE, 1932

On the Scattering of Light by Supersonic Waves. By **P. Debye and F. W. Sears** 409

Additivity of the Energies of Normal Covalent Bonds. By **Linus Pauling and Don M. Yost** 414

Geometry of the Heat Equation: First Paper. By **Edward Kasner** 475